



University of Évora

ARCHMAT

(Erasmus Mundus Master in Archaeological Materials Science)

Mestrado em Arqueologia e Ambiente (Erasmus Mundus-ARCHMAT)

Materials and production methods in 17<sup>th</sup>-century Portuguese illuminated cartography: a study of the maps in António Bocarro's "Book of the Plans of all Fortresses, Towns and Villages of the East Indies"

Sima Krtalic – m38415

Cristina Maria Barrocas Dias, Universidade de Évora  
(Supervisor)



Catarina Miguel, Universidade de Évora  
(Co-Supervisor)



Antónia Fialho Conde, Universidade de Évora  
(Co-Supervisor)



Évora, October 2018



## ACKNOWLEDGEMENTS

I would like to first thank my supervisors, Professor Cristina Dias, Dr. Catarina Miguel, and Professor Antónia Conde for sharing my curiosity and for giving me the tools and guidance to take on this project. I have been lucky to have three advisors who at once value creativity and rigorous research, who are passionate about their subjects, and who are all equipped with an excellent sense of humor. It has been a privilege to study these maps and a pleasure to learn from these scholars.

My sincere thanks as well to all of HERCULES Laboratory, and in particular Mafalda Costa, Tânia Rosado, Sara Valadas, Ana Manhita, José Mirão, and Teresa Ferreira. I would also like to thank the researchers who generously gave their time to field questions and discuss the project, especially Milene Gil, Henrique Leitão, and Catherine Delano-Smith.

I give my gratitude to the staff of the Public Library of Évora. Their kindness and support made this research possible.

Finally, I thank all my friends and family. In particular, I thank Tina and Sophia Bessias, my mother, my husband, and Masya.



## ABSTRACT

This thesis presents an interdisciplinary, multianalytical investigation of the early 17<sup>th</sup>-century illuminated maps of Pedro Baretto de Resende in the Antonio Bocarro's *Livro das plantas de todas as fortalezas*, a codex made in Goa and currently housed at the Biblioteca Pública de Évora in Portugal. The work addresses previously unexplored aspects of the maps, including issues of authorship, the possibility of cross-cultural collaboration during their production, and the way their design and use of map signs depict late-stage empire. Using technical photography, FORS, h-XRF, Raman microscopy,  $\mu$ -FT-IR, LC-DAD-MS, and vp-SEM-EDS, the maps' materials and production methods were revealed and contextualized. The results are relevant to research concerning the connections between decorative cartography, economic and social history, and fine art. In addition, the findings contribute to the small but growing literature on the material characteristics of cartographic works. Finally, the work suggests a more holistic approach to the study of maps.

## RESUMO

Nesta tese é apresentada uma investigação interdisciplinar e multi-analítica dos mapas iluminados datados do início do século XVII de Pedro Baretto Resende no *Livro de plantas de todas as fortalezas* de António Bocarro, um códice produzido em Goa e que pode ser encontrado na Biblioteca Pública de Évora. O trabalho aborda aspectos anteriormente inexplorados destes mapas, incluindo questões de autoria, a possibilidade de colaboração intercultural durante sua produção e a forma como o design e o uso de sinalética são influenciados por um império em decadência. Usando técnicas de fotografia, FORS, FRX, microscopia Raman, micro-IV-TF, LC-DAD-MS e MEV-EDS, os materiais e métodos de produção dos mapas foram revelados e contextualizados. Os resultados são relevantes para o estudo das relações entre a cartografia decorativa, a económica e a história social, e as belas artes. Esta tese sugere ainda uma abordagem mais holística ao estudo de obras cartográficas.

## LIST OF ABBREVIATIONS

BSE	Backscattered electron
FORS	Fiber optic reflectance spectroscopy
GC-MS	Gas chromatography-mass spectrometry
h-XRF	Handheld X-ray fluorescence spectroscopy
LC-DAD-MS	Liquid chromatography-photodiode array detector-mass spectrometry
MALDI-MS	Matrix-assisted laser desorption/ionization mass spectrometry
μ-FT-IR	Micro-Fourier transform infrared spectroscopy
PDA	Photodiode array
SERS	Surface-enhanced Raman spectroscopy
SIM	Single ion monitoring
SRM	Single reaction monitoring
UVF-IV	Ultraviolet fluorescence induced in the visible
UV-Vis-NIR	Ultraviolet-visible-near infrared
VP-SEM-EDS	Variable pressure scanning electron microscopy and energy dispersive X-ray spectroscopy
XRD	X-ray diffraction

## IN-TEXT REFERENCES FOR MAP COLLECTIONS

Note: Manuscript maps are noted with the prefix MS, engraved maps with the prefix E.				
In-text Reference	Author of Maps	Title of Manuscript or Book	Location (for manuscript maps)	Access (book or web address)
MS c.1635 Teixeira Albernaz I	J. Teixeira Albernaz I	<i>Livro das plantas de todas as fortalezas...</i>	Biblioteca Nacional de España (R. 202)	<a href="http://bdh-rd.bne.es/viewer.vm?id=0000044154&amp;page=1">http://bdh-rd.bne.es/viewer.vm?id=0000044154&amp;page=1</a>
MS 1600-1650 Teixeira Albernaz I	J. Teixeira Albernaz I	<i>Plantas das cidades, portos, e fortalezas da conquista da Índia Oriental</i>	Bibliothèque Nationale de France (Collection Klaproth, 0168)	<a href="https://gallica.bnf.fr/ark:/12148/btv1b55007625f">https://gallica.bnf.fr/ark:/12148/btv1b55007625f</a>
MS 1622 Erédia	M. Godinho de Erédia	<i>Atlas-Miscellany</i>	Collection of Dr. C.M.C. Machado Figueira, Lisbon	Reproduced in part in <i>Portugaliae Monumenta Cartographica, Vol. 4</i>
MS 1636 Anon.	Anonymous	<i>Breve tratado ou epilogo de todos os visorreyes que tem havido no estado da Índia...</i>	Bibliothèque Nationale de France (MSS Fonds Portugais n.º 1)	<a href="https://gallica.bnf.fr/ark:/12148/btv1b10033419k">https://gallica.bnf.fr/ark:/12148/btv1b10033419k</a>
MS 1639 Carneiro	A. de Maris Carneiro	<i>Descripçam da fortaleza de Sofala, e das mais da Índia...</i>	Biblioteca Nacional de Portugal (IL n.º 149)	<a href="http://purl.pt/24313/1/index.html#/1">http://purl.pt/24313/1/index.html#/1</a>
MS 1646 Resende	P.B. de Resende	<i>Livro do Estado da Índia Oriental</i>	British Library (Sloane MS 197)	Reproduced in part in <i>Portugaliae Monumenta Cartographica, Vol. 5</i>
MS 1635 Resende	P.B. de Resende	<i>Livro das plantas de todas as fortalezas...</i>	Biblioteca Pública de Évora (BPE COD. CXV/2-X)	<a href="http://purl.pt/27184">http://purl.pt/27184</a>
E 1729 Child	G. Child	<i>The Universal Traveler</i>	N.A.	<a href="http://www.columbia.edu/itc/mealac/pritchett/00maplinks/mughal/salmonmaps/salmonmaps.html#madras">http://www.columbia.edu/itc/mealac/pritchett/00maplinks/mughal/salmonmaps/salmonmaps.html#madras</a>
E 17C. Machado	D.B. Machado	<i>Mappas do Reino de Portugal e suas conquistas collegidos</i>	Biblioteca Nacional (Brasil) (Col. Real Bibliotheca: Diogo Barbosa Machado)	<a href="https://bdib.bn.gov.br/acervo/handle/123456789/45705">https://bdib.bn.gov.br/acervo/handle/123456789/45705</a>

## NOTE ON IMAGES OF MAPS

All images from MS 1600-1650 Teixeira Albernaz and MS 1636 Anon. are © Bibliothèque Nationale de France.

All images from MS c.1635 Teixeira Albernaz are © Biblioteca Nacional de España.

All unaltered, visible light images of Évora codex maps are © Biblioteca Pública de Évora.

All handheld digital microscopic images, NIR images, and UVF-IV images of the maps of the Évora codex are © Biblioteca Pública de Évora and Laboratório HERCULES.

The sources of all map images are provided in the table entitled 'In-Text References for Map Collections' on page iii.

## LIST OF FIGURES

Figure 1: Left, map of 'Manar' (Évora codex). Right, map of 'Moro de Chaul' (Évora codex).....	1
Figure 2: Flow chart illustrating relationship between similar maps.....	4
Figure 3: Flow chart describing research design.....	9
Figure 4: Example of early Rajput Chaurapanchasika-school painting.....	15
Figure 5: Example of Mughal painting.....	15
Figure 6: Maps of 'Cranganor.' Top, MS c. 1635 Teixeira Albernaz. Bottom, Évora codex.....	17
Figure 7: Left, map of 'Gale' (MS. C 1635 Teixeira Albernaz). Right, map of 'Guale' (Évora codex).....	18
Figure 8: Maps of 'Mada.' Top, MS 1636 Anon. Bottom, Évora codex.....	20
Figure 9: Actual and Évora codex scale of fortress of Mombasa.....	20
Figure 10: Left, Évora codex map of 'Iafanapatam' (detail). Right, Évora codex map of 'Solor' (detail).....	21
Figure 11: Details from the Évora codex maps. Left, 'Quelba.' Middle, 'Matara.' Right, 'Coriate'.....	21
Figure 12: Fortress design with convergent versus divergent perspective.....	22
Figure 13: Vegetation signs in the Évora codex maps.....	24
Figure 14: Rock signs in the Évora codex maps.....	26
Figure 15: Lake and pond signs in the Évora codex maps.....	26
Figure 16: Ship and boat signs in the Évora codex maps.....	27
Figure 17: Typical church signs in the Évora codex maps.....	28
Figure 18: Atypical church signs in the Évora codex maps.....	29
Figure 19: Map of 'Cochin' (E 1729 Child).....	30
Figure 20: Temple and mosque in 1596 illustrated <i>Itinerario</i> of J.H. van Linschoten.....	30
Figure 21: Mosque signs in the Évora codex maps.....	31
Figure 22: Details of 'Negapataõ.' Left, MS c.1635 Teixeira Albernaz. Right, MS 1636 Anon. ....	32
Figure 23: Left, drawing by C. de Sá Noronha. Middle and right, Évora codex maps of 'Triquilimale' and 'Dio' (details).....	32
Figure 24: Pillory and gallows signs in the Évora codex maps.....	33
Figure 25: Administrative structure signs in the Évora codex maps.....	33
Figure 26: Housing distribution patterns in the Évora codex maps.....	34
Figure 27: Map of 'Malaca' (Évora codex).....	35
Figure 28: Maps of 'Mangalor'. Top, Évora codex. Bottom, MS 1600-1650 Teixeira Albernaz.....	36
Figure 29: Examples of pink fortifications in Mughal and Rajput painting.....	38
Figure 30: People signs in the Évora codex maps. Left, map of 'Libedia' (detail). Right, map of 'Guale' (detail).....	39
Figure 31: 'Nomadic Encampment,' c. 1540 (Harvard Art Museums).....	39
Figure 32: Undeciphered map signs in Évora codex.....	39

Figure 33: Location of selected Portuguese fortresses and cities in India.....	40
Figure 34: Annotated Évora codex map of ‘Damaõ’ .....	47
Figure 35: Annotated Évora codex map of ‘Dio’ .....	48
Figure 36: Left, Google Earth image of Diu. Right, Jalandhar Dada temple.....	49
Figure 37: Annotated Évora codex map of ‘Chaul’ .....	51
Figure 38: Annotated Évora codex map of ‘Cochim’ .....	52
Figure 39: Annotated Évora codex map of ‘Baçaim’ .....	53
Figure 40: Materials study research design.....	55
Figure 41: Overview of analytical methods used to study maps.....	57
Figure 42: Chain and laid lines in Évora codex map of ‘Chaul’ .....	59
Figure 43: Laid mold with watermark stamp (Robert C. Williams Paper Museum).....	59
Figure 44: Preferential cracking of green regions (Évora codex map of ‘Sera de Aserim’). .....	59
Figure 45: Preferential cracking of green regions (Évora codex map of ‘Moro de Chaul’). .....	59
Figure 46: $\mu$ -FT-IR spectrum of paper microsample from Évora codex map of ‘Damaõ’ .....	60
Figure 47: EDS elemental map of paper microsample from Évora codex map of ‘Damaõ’ .....	61
Figure 48: BSE image of glue-like substance in paper microsample from Évora codex map of ‘Damaõ’ .....	61
Figure 49: BSE image of granules in paper microsample from Évora codex map of ‘Damaõ’ .....	62
Figure 50: BSE images of fibers in in paper microsample from Évora codex map of ‘Damaõ’ .....	63
Figure 51: Fort of ‘Sam. Irm.’ in Évora codex map of ‘Damaõ.’ Left, illuminated from below. Right, from above.....	64
Figure 52: Digital restoration of original composition of the Évora codex map of ‘Dio’ .....	65
Figure 53: Handheld digital microscopic images of fortifications in Évora codex maps of ‘Dio’ (left) and ‘Cochim’ (right)....	66
Figure 54: Handheld digital microscopic images of selected cannons of Évora codex maps.....	66
Figure 55: Handheld digital microscopic images of selected white houses of Évora codex maps .....	67
Figure 56: Handheld digital microscopic images of selected <i>cruzeiros</i> in the Évora codex map of ‘Cochim’ .....	67
Figure 57: Handheld digital microscopic images of selected thatched houses of Évora codex maps.....	67
Figure 58: Handheld digital microscopic images of selected rocks of Évora codex maps.....	68
Figure 59: Handheld digital microscopic images of selected trees of Évora codex maps.....	69
Figure 60: Hypothesized coloring sequence of the subset of Évora codex maps.....	70
Figure 61: Handheld digital microscopic images from the Évora codex map of ‘Cochim’ showing coloring sequence.....	70
Figure 62: Digital restoration of an altered bastion in the Évora codex map of ‘Dio’ .....	71
Figure 63: Colorimetric coordinates in CIE L*a*b* color space by map feature.....	73
Figure 64: Left to right, images of Évora codex map of ‘Sera de Aserim’ with visible light, UVF-IV, NIR.....	74
Figure 65: Images of Évora codex fort of ‘Sam. Irm’. Left, UVF-IV. Right, visible light.....	74
Figure 66: Stratigraphy of Évora codex maps.....	77
Figure 67: Edge painting on text portion of Évora codex.....	77
Figure 68: Left, FORS spectra of beige and tan regions. Right, FORS spectra of light brown and tan regions.....	78
Figure 69: FORS spectra of medium and dark brown regions compared with tan regions.....	79
Figure 70: FORS spectra of light and dark pink regions.....	80
Figure 71: FORS spectra of light, dark, and yellow-green regions.....	80
Figure 72: FORS spectra of light, medium, and dark blue regions.....	81
Figure 73: FORS spectra of red regions compared with mockups.....	84
Figure 74: $\mu$ -Raman spectrum of red region (Di.R.7).....	84
Figure 75: EDS maps showing distribution of selected elements in red microsample (Da.S.3).....	85
Figure 76: BSE images of red microsample (Da.S.3).....	85
Figure 77: FORS spectra of overpainted tan regions compared with non-overpainted tan regions (map of ‘Dio’).....	86
Figure 78: FORS spectra of tan regions compared with mockups.....	86
Figure 79: $\mu$ -Raman spectrum of a tan region (Di.S.4).....	87
Figure 80: $\mu$ -FT-IR spectrum of a tan microsample (Di.S.4).....	87
Figure 81: FORS spectra of green regions compared with mockups.....	88
Figure 82: $\mu$ -FT-IR spectrum of a green microsample (Di.S.3).....	89
Figure 83: Digital microscopic image of a green region from the Évora codex map of ‘Cochim’ .....	89
Figure 84: FORS spectra of blue regions.....	90

Figure 85: Flowchart of indigo processing with molecules relevant to discussion of Maya blue.....	91
Figure 86: $\mu$ -Raman spectrum of a blue region (map of 'Dio,' 1) .....	92
Figure 87: $\mu$ -FT-IR spectrum of a blue microsample (Di.S.3), 1800-600 $\text{cm}^{-1}$ .....	93
Figure 88: $\mu$ -FT-IR spectrum of a blue microsample (Di.S.3), 3800-2800 $\text{cm}^{-1}$ .....	93
Figure 89: EDS map of distribution of sodium, aluminum, iron, and lead in blue microsample (Da.S.2).....	94
Figure 90: EDS map of distribution of magnesium, silicon, potassium, and calcium in blue microsample (Da.S.2) .....	94
Figure 91: FORS spectra of dark pink region compared with mockups.....	95
Figure 92: Top, anthraquinone skeleton structure. Bottom, laccaic acid A molecular structure.....	95
Figure 93: EDS maps of distributions of aluminum (left), calcium (right) and lead in pink microsample (Di.S.5).....	96
Figure 94: $\mu$ -FT-IR spectrum of a pink microsample (Di.S.5).....	97
Figure 95: PDA chromatogram of pink combined sample (Co.S.5 and M.S.2) at 500 nm.....	97
Figure 96: MS chromatogram in SIM mode of pink combined sample (Co.S.5 and M.S.2).....	97
Figure 97: PDA chromatogram of lac dye standard at 500 nm.....	98
Figure 98: MS chromatogram in SRM mode of lac dye standard.....	98
Figure 99: $\mu$ -Raman spectrum of a white region (Di.R.6).....	99
Figure 100: $\mu$ -Raman spectrum of a white region (Da.R.6).....	99
Figure 101: $\mu$ -FT-IR spectrum of a white microsample (Di.S.2).....	100
Figure 102: EDS map of a white microsample (Di.S.2) showing distributions of lead and calcium.....	101
Figure 103: EDS map of a white microsample (M.S.3) showing distributions of lead, calcium, and aluminum.....	101
Figure 104: BSE image of a white microsample (Di.S.2).....	101
Figure 105: $\mu$ -Raman spectrum of a black region (Co.S.3).....	102
Figure 106: $\mu$ -FT-IR spectrum of black microsample (Co.S.3).....	102
Figure 107: EDS map of a black microsample (M.S.1) showing distributions of carbon, phosphorus, and calcium.....	102
Figure 108: EDS map of a black microsample (Co.S.4) showing distributions of carbon and phosphorus.....	102
Figure 109: Native cinnabar from the Almadén district of Spain.....	105
Figure 110: Botanical illustration by Ehret & Trew of <i>Indigofera</i> plant.....	106
Figure 111: Details of maps of 'Dio' from MS c.1635 Teixeira Albernaz, MS 1639 Carneiro, and Évora codex.....	107
Figure 112: Illustration of <i>Kerria lacca</i> life cycle by Maxwell-Lefroy.....	108

## LIST OF TABLES

Table 1: Analyses, questions, and maps.....	56
Table 2: Use of preparatory sketch by map and feature.....	66
Table 3: Summary of technical photography observations.....	75
Table 4: Summary of occasional colors and their constituent pigments as hypothesized by FORS and XRF.....	81
Table 5: Summary of recurring colors and their constituent pigments as hypothesized by FORS and XRF.....	82
Table 6: Microsamples and analyses.....	83
Table 7: Some morphological criteria for cinnabar/vermilion differentiation.....	85
Table 8: Expected infrared absorption bands for egg, hide glue, and gum Arabic, and shellac.....	103

# TABLE OF CONTENTS

Acknowledgements.....	i
Abstract .....	ii
Resumo.....	ii
List of Abbreviations.....	iii
Note on Images of Maps.....	iii
Table of In-Text References for Map Collections.....	iii
List of Figures.....	iv
List of Tables.....	vi
1. Introduction.....	1
1.1 Setting the stage.....	1
1.2 How to study a map: a survey.....	5
1.3 Research design.....	8
2. The Maps in Historical and Artistic Context.....	10
2.1 Key figures surrounding the maps.....	10
2.2 The Portuguese in India, early 17 <sup>th</sup> century.....	11
2.3 Artistic context.....	13
2.3.1 Authorship.....	13
2.3.2 Artistic exchange.....	14
2.3.3 Rajput painting.....	14
2.3.4 Mughal painting.....	15
3. Formal Aspects of the Maps.....	15
3.1 Overview.....	17
3.1.1 Format.....	18
3.1.2 Regions and toponyms.....	18
3.1.3 Fortification typology.....	18
3.2 Style.....	19
3.2.1 Scale.....	19
3.2.2 Perspective and vantage point .....	20
3.2.3 Line.....	22
3.2.4 Color.....	22
3.2.5 Labels.....	22
3.3 Map signs.....	23
3.3.1 Vegetation.....	23
3.3.2 Rocks.....	25
3.3.3 Water, ships, and coastlines.....	26
3.3.4 Churches and monasteries.....	27
3.3.5 Crosses ( <i>cruzeiros</i> ) .....	39
3.3.6 Non-Christian religious architecture.....	30
3.3.7 Administrative structures.....	33
3.3.8 Houses.....	34
3.3.9 Fortifications.....	36
3.3.10 People.....	38
3.3.11 Unidentified map signs.....	39
4. Maps of India.....	40
4.1 Introducing the fortresses and towns.....	41
4.1.1 'Damaõ' (Daman).....	41

4.1.2 'Dio' (Diu).....	42
4.1.3 Chaul.....	42
4.1.4 'Moro de Chaul' (Korlai).....	43
4.1.5 'Cochim' (Kochi).....	43
4.1.6 'Baçaim' (Vasai).....	44
4.1.7 'Salsete' (Salcete).....	45
4.1.8 'Mangalor' (Mangaluru).....	45
4.1.9 'Sera de Aserim' (Asherigad).....	46
4.2 Locating specific buildings.....	46
4.2.1 'Damaõ' (Daman).....	47
4.2.2 'Dio' (Diu) .....	48
4.2.3 Chaul.....	51
4.2.4 'Cochim' (Kochi).....	52
4.2.5 'Baçaim' (Vasai).....	53
4.3 Closing remarks.....	54
Investigation of artistic materials and their use.....	55
5. Paper support.....	58
5.1 Lightbox examination.....	58
5.2 Sizing and fillers.....	60
5.3 Fibers.....	62
6. Observing artistic technique.....	64
6.1 Alterations to the maps' design noted using the lightbox.....	64
6.2 Use of preparatory sketch (by feature/map).....	65
6.3 Sequence of painting, within features.....	66
6.4 Sequence of painting major features.....	69
6.5 Alterations to the maps' design noted by handheld digital microscopy.....	71
6.6. Pigment characteristics and possible mixtures/overlays.....	71
7. Searching for pigment variations.....	73
7.1 Colorimetry.....	73
7.2 Technical photography.....	74
8. Pigment and binder identification.....	77
8.1 Same pigments, different colors? Defining the core palette.....	78
8.1.1 Beige, tan, and brown.....	78
8.1.2 Light pink and dark pink .....	79
8.1.3 Dark green, light green, and yellow-green.....	80
8.1.4 Light blue, dark blue, medium blue.....	80
8.1.5 Occasional colors.....	81
8.2 The core palette in detail.....	83
8.2.1 Red (cinnabar).....	83
8.2.2 Tan (yellow ochre).....	86
8.2.3 Green (copper proteinate).....	87
8.2.4 Blue (indigo + ?).....	90
8.2.5 Pink (lac lake).....	94
8.2.6 White (basic and neutral lead carbonates).....	98
8.2.7 Black (bone or ivory black, with possible addition of iron gall ink or vine black).....	101
8.3 Binder.....	103
8.4 Materials in context.....	104
Final remarks and future research.....	110

Bibliography.....	112
Appendix I: Toponyms and reproductions of Évora codex maps.....	126
Appendix II: Materials and methods.....	136
Appendix III: Expanded results, organized by instrumental technique.....	145



## Chapter I: Introduction



**Figure 1:** Map of 'Manar' (left) and 'Moro de Chaul' (right). From Pedro Barreto de Resende's collection, included in Antonio Bocarro's *Livro das plantas de todas as fortalezas* (*Book of the plans of all the fortresses....*). Copyright Biblioteca Pública de Évora.

### 1.1: Setting the Stage

"...Even the great labor which it cost me was not sufficient to perform it in the manner which I intended and desired, with the plans oriented and measured out, and drawn to scale, which was not possible for the great lack of persons skilled in these arts within this State, and the fortresses being so many, and I have attempted to make good their defects in the description, which may be fully trusted, while no more is to be expected from the Plans of the Fortresses and Cities than their form and figure, since in some the measurements are uniformly taken in proportion, while in others they have been less precisely determined; nor is the number of cannon painted in the plans to be accepted unless it is confirmed by the text..."

(Antonio Bocarro, letter 17 Feb 1635 to Count-Viceroy Miguel Linhares de Noronha)

"[Bocarro said that]...the plans could not be made unless I gave them to him, since I already had the greater number of them; wherefore, the Count my lord having commanded me to do so, I abandoned certain purposes which I had and gave them to him, on the condition that he gave me their description..."

(Pedro Barreto de Resende, introductory letter to the *Book of the State of Oriental India*, Bibliothèque Nationale de France, MSS Fonds Portugais n.º 1)

In early 1635, after much pestering from the monarch in Madrid, Antonio Bocarro's *Livro das plantas de todas as fortalezas, cidades, e povoações do Estado da Índia Oriental* (*Book of the plans of all the fortresses, cities, and towns of the State of Oriental India*) was completed and shipped off in two copies for a year-long journey from Goa to Lisbon. For its leading collaborators, Bocarro (Chronicler of the State of India) and Barreto de Resende (Secretary to the Viceroy of India), this would-be celebratory moment was marred by a central component of the project: its maps (see figure 1 for examples).

Bocarro had taken great pains to compile his text—a fact both he and Resende underscore in their correspondence. Though pressed for time, Bocarro's work would have been an impressive testament to his assiduousness and efficiency. For

his service, he could look forward to considerable perks (Newitt 2005, pp. 172-173). But far away in Spain, King Felipe IV of Spain (III of Portugal) needed an up-to-date picture of the Portuguese footprint in India. He wanted maps alongside Bocarro's written description. The problem was that most of Portugal's truly qualified cartographers had, by this time, been allocated to the imperial efforts in Brazil (Alegria et al. 2007). Resources were spread thin for the Portuguese kingdom, and by the early 17<sup>th</sup> century difficult choices were being made about where to concentrate forces and consolidate power.

The solution to the king's demand was one that neither Resende nor Bocarro would like: Resende would have to hand over his own growing collection of cartography to Bocarro. Resende's displeasure with the arrangement is evident in the letter quoted above. After all, it was only at Count-Viceroy Linhares de Noronha's command that he "abandoned" his own intentions for the maps. Nor was Bocarro overjoyed with the compromise: while he doesn't deign to credit Resende for supplying the maps, he spares no ink lamenting their inadequacy before assuring the monarch that his own work, the text, is utterly reliable.

Bocarro's poor reception of Resende's contribution betrays his desire for a different sort of map entirely. A system for indicating latitudes had been introduced into Portuguese nautical charts in the early 1500s (Alegria et al. 2007). Aware of such developments in cartography, Bocarro wants strictly plotted maps, to scale, with meridians. He also notes discrepancies between the actual and pictured quantities and types of artillery in the Resende maps. He leaves off any critique of their artistic merit and frames them as "illustration."

In the years following their arrival in Europe, the maps of Bocarro's *Livro das plantas* were reproduced by numerous authors, breeding great confusion as to which of the iterations were the originals sent from Goa and intended for the King. Cortesão and de Mota have hypothesized that the codex at the Biblioteca Pública de Évora<sup>1</sup> represents one of the two copies created by Resende and Bocarro in India (Cortesão & de Mota 1960b). Officials in Lisbon, they suggest, did not find the maps suitable for delivery to the monarch, and renowned cartographer João Teixeira Albernaz I was enlisted to produce substitutes. The Bocarro text and replacement maps were then bound together and presented to the king. This codex, currently at the Biblioteca Nacional de España in Madrid, was completed within a year of 1635. It is referred to in this thesis as MS c.1635 Teixeira Albernaz. Cortesão and de Mota's theory explains both Teixeira Albernaz's rush to complete his set of maps and the ultimate locations of the respective codices. The flowchart in figure 2 (page 4) is provided to clarify the connection between various copies and the maps of the Évora codex.<sup>2</sup>

---

<sup>1</sup> As the maps of this codex are the subject of the present thesis and will be mentioned many times, we will refer to the work as the Évora codex throughout the text.

<sup>2</sup> The relationship between the maps described in figure 2 is based on the *Portugaliae Monumenta Cartographica, Volume 5* (Cortesão and de Mota 1960). In most cases, the phenomenal work undertaken by the authors still stands today. A few updates and comments are nevertheless in order. Although the Bibliothèque Nationale de France continues to attribute the maps in the MS 1636 Anon. (figure 2, no. 8) to Resende, I agree with Cortesão and de Mota that these are the work of an anonymous artist. Some of the colors are changed (such as the walls of 'Damaõ') and the washes on the terrain around the fortress are far more delicate. They display a tendency not shared with the maps of the Évora codex to avoid any overdrawing on the fortresses. More significantly, the scale of almost all the map signs (from fortress walls, to houses, to trees) is much smaller, giving the territories depicted an uncluttered, underpopulated appearance. These are unlikely to represent an evolution of Resende's style, because in the London codex (MS 1646 Resende; figure 2, no. 7) from ten years later we encounter drawings of almost identical design to the Évora codex. Cortesão and de Mota ascribe the four uncolored plans in the MS 1646 Resende codex (figure 2, no. 7a) to Resende, albeit with some skepticism. A careful study of these four maps casts doubt on the attribution. In the maps of the Évora codex, Resende consistently strives for uniform scale of trees and

The maps of the Évora codex polarized the opinions of its contemporaries. Modern scholars are similarly divided, with some dismissing the maps as “mediocre and [of] limited cartographic value” (Cortese & de Mota 1960b) or “so heavily illuminated that certain details become almost illegible” (Alegria et al. 2007), and others praising their fresh and ingenious design (Cid 1992, p. 53). It is hard to know what to make of these works. Before describing the methodology adopted for the study of these unusual maps, a fuller picture of their cartographic context is in order.

The maps of the Évora codex belong to one of the best-studied periods in Portuguese cartography, but have not been the subject of much scholarly research; perhaps because India was the periphery of Iberian cartography by the 1600s, and Resende was not a mapmaker by trade. By the 17<sup>th</sup> century, crown-sponsored mapmaking had increased in volume and significance to such an extent that a bureaucratic infrastructure had been built up around it. In the Portuguese case, the institution of the *Armazem* functioned as a repository and lending library of maps. The *Armazem* of India dealt largely with two categories of maps: navigational charts and plans of fortresses (Alegria et al. 2007). Resende’s maps belong to the second group. Such works tend to employ multiple vantage points and do not typically depict inland regions unless they are strategically relevant (*ibid.*). These characteristics are manifested at the level of design (or drawing) and do not relate to the color. For painted maps like Resende’s, the distinction between design and coloring is important. The maps’ design seems to have been uncontroversial. The maps of João de Castro<sup>3</sup> and of Gaspar Correia<sup>4</sup> predate Resende’s work but demonstrate comparable priorities and approaches. Where Resende breaks away from de Castro and Correia are in his generalization and concern with aesthetics. Both de Castro and Correia attempt to bring out the specifics of the places they document; their works more closely resemble well-finished sketches than decorative objects. Resende’s maps, at first glance, seek to homogenize and beautify. The complicated interplay between standardization and communicating region-specific information will be discussed in Chapter 3. The use of color in Resende’s maps also separates it from its antecedents and indeed from the colored maps of its followers. Among these followers, comparison will be frequently drawn with Erédia’s and Teixeira Albernaz’s works. Their maps are uniquely relevant to the maps of the Évora codex because they represent “professional” cartographic output both from direct experience with the regions depicted (in the former case), and by compilation from secondary sources (in the latter case).

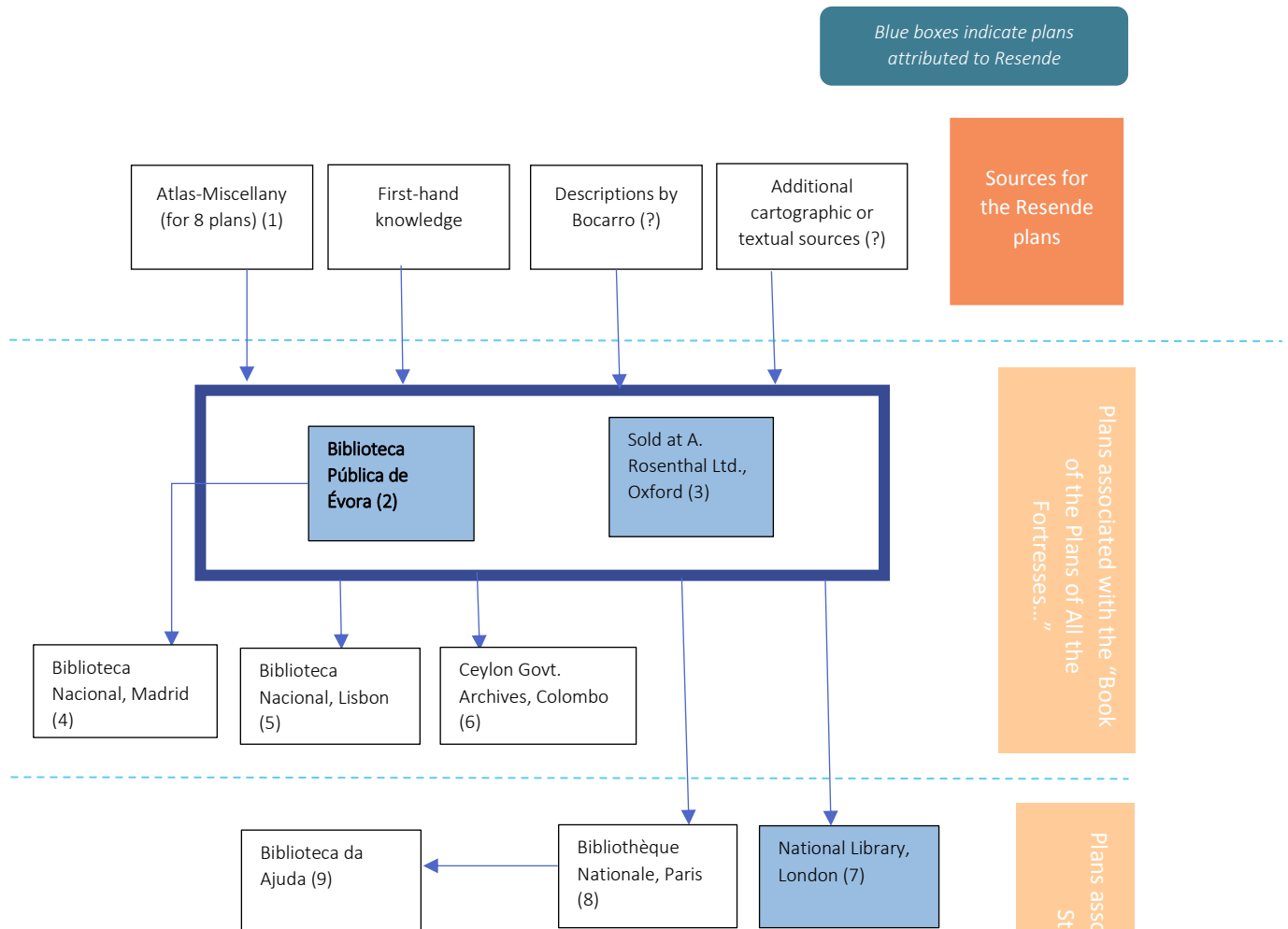
To better comprehend the maps of the Évora codex it may be helpful to outline how 17<sup>th</sup> century maps were made and what training this entailed. Astengo characterizes 16<sup>th</sup>-17<sup>th</sup>-century mapmaking as either a workshop activity, or

---

buildings. The features of these uncolored maps, in contrast, are drawn in a wild range of sizes. Resende’s colored maps depict vegetation homogeneously (according to a few well-defined types); here, a variety of plants are encountered. Resende almost always uses overdrawing on both interior and exterior fortress walls, and draws his fortresses with low, long walls so that the area inside the fort is visible. Here the interior space of the fortress is almost completely concealed, and the inside walls are free of ornamentation. The maps of codex no. 6 in figure 2, formerly housed at the Ceylon Government Archives, have been impossible to locate in the online catalogue of the present-day Sri Lanka Department of Archives. I was likewise unable to locate digitalization of any Tinoco maps (figure 2, no. 9), or any of the Resende maps sold at A. Rosenthal, Ltd. (figure 2, no. 3). Reproductions from the Erédia Atlas-Miscellany (MS 1622 Erédia; figure 2, no. 1) are accessible in the *Portugaliae Monumenta Cartographica*, Vol. 5. More recent scholars have declared this codex to be lost. Cortese and de Mota, viewing it in the private collection of Machado Figueira, commented on its poor conservation state. If it remains in the Machado Figueira collection, I have found no evidence of digitalization or any update on its status.

<sup>3</sup> Particularly in the *roteiro* from Goa to Diu [1538-1539] which survives in a copy from the late 16<sup>th</sup> century; reproduced in part in Alegria et al. 2007, p. 1016.

<sup>4</sup> See the map of Diu from Correia’s *Lendas da Índia* of the mid-16<sup>th</sup> century; reproduced in Alegria et al. 2007, p. 1020.



1) "Atlas-Miscellany" (c. 1615-c. 1622). 137 leaves with charts, plans, and cartographic drawings by Manuel Godinho de Erédia and an unknown artist. Dimensions of leaves: 275 x 200 mm. Collection of Dr. C.M.C. Machado Figueira, Lisbon.

2) "Book of the plans of all the fortresses, cities and towns of the State of Oriental India..." (1635). 48 illuminated plans (originally 52) by Pedro Barreto de Resende. Dimensions of plans: 406x604 mm. COD. CXV/2-X.

3) "Book of the plans of all the fortresses, cities and towns of the State of Oriental India..." (1635). 48 illuminated plans (originally 52) by Pedro Barreto de Resende. Dimensions of plans: 410x600 mm. Sold at A. Rosenthal Ltd., Oxford.

4) "Book of the plans of all the fortresses, cities and towns of the State of Oriental India..." (c. 1635). 52 colored plans by João Teixeira Albernaz I. Dimensions of plans: 412x560 mm. Mss. 1190 (text), R.202 (plans).

5) "Description of the Fortress of Sofala, and other [fortresses] of India" (1639). 48 (originally 52) colored

plans by António de Maris Carneiro. Dimensions of plans: 455x690 mm. Iluminados n.º149.

6) "Book of the plans of all the fortresses, cities and towns of the State of Oriental India..." (17<sup>th</sup> century). 52 uncolored plans by unknown artist. Ceylon Government Archives, Colombo.

7) "Book of the state of Oriental India..." (1646). 62 colored plans by Pedro Barreto de Resende, 4 uncolored plans by an unknown artist (a), 1 colored plan by another unknown artist (b), 9 uncolored plans by Pedro Berthelot (1635). Dimensions of plans: (Berthelot) 365x535 mm, (Resende and anonymous) 365x535 mm. Sloane MS 197.

8. "Brief treatise or epilogue concerning all the Viceroyes who have been in the State of India..." (1636). 70 colored plans by unknown artist. Dimensions of plans: 282x422 mm. MSS Fonds Portugais n.º 1.

9. "Book of the Strongholds of Portugal..." (1663). 70 plans (7 colored) by João Nunes Tinoco. Dimensions of plans: 233x365 mm. 46-XII-10.

Figure 2: Flowchart illustrating the relationship between similar maps.

as the occasional work of individuals (Astengo 2007). The latter category may include pilots like Erédia, while the former might include cartographic families like the Teixeira Albernazes, whose fame could have enabled the hire of assistants and colorists, with the leading mapmaker providing quality control. The maps produced by Resende seem to belong to the sometime-mapmaker group, although possibly with some outsourcing of labor. Had there existed in Goa a dedicated cartographic workshop, one would not expect the personal pleading required by Bocarro in order to secure the maps, and some crediting of the leading cartographer might have been evident. Rather, the maps seem to be a one-off production, compiled from sources both known and unknown.

The training received by professional mapmakers is difficult to reconstruct; for occasional mapmakers it is even harder. Delano-Smith points to informal personal directives as a means by which map sign use was guided but notes that while some certification might have been required for maritime chart makers, there is no indication of an analogous training for topographical charts and their signs (Delano-Smith 2017). If we presume Resende to have been the draughtsman of the maps, we must not expect a rigorous indoctrination in terrestrial cartography for the reasons cited by Delano-Smith, and for the fact that mapmaking was not his primary occupation. Instead, his approach to mapmaking would have been influenced by the maps he accessed in his career as Secretary, and by a general “map literacy” imparted by his education up to that point. The patronage system by which important offices were assigned in the Estado, as described by Newitt, implies that Resende would have come from an elite background (Newitt 2005, pp. 172-174). This makes it likely that he would have had a comprehensive education involving the use of maps as pedagogical aids (Woodward 2007; Cormack 2007). Access to copies and written descriptions, consciousness of how maps work, and a good eye may have been enough for Resende to produce the drawing of the maps of the Évora codex himself.

## I.2: How to study a map: a survey

At first glance, old maps amuse. The strange distortions of continents seem ludicrous, and the mind and eye collaborate to identify all the inaccuracies and wonder at the solemn backwardness of people from the past. This impulse can, and has, been translated into serious scholarly research on maps. As the science of cartography developed, the ways in which mapmakers erred can be insight into the evolving methods used to generate maps (for an example of maps used to study the history of science and maritime charting, see for example Gaspar and Leitão 2017). The specificity and accuracy of a map can also be a record of exploration, where from missing, mangled, or myth-based geographies we can infer a lack of first-hand information sources (Alegria et al. 2007).

Alternative interpretations of terrestrial maps (like the ones of the Évora codex) must be added in light of the actual use of terrestrial maps at the time. Throughout the Renaissance, maps took a backseat to written information (Woodward 2007). This is clearly the case with the maps of the Évora codex, where not even compass orientations are provided, but the Bocarro text supplies both navigational directions and an abundance of fine-grained information about the fortresses and neighboring towns. We are safe, therefore, to assume that these maps were meant to serve another purpose than helping a traveler to the region find their way around or providing scientific geographical information. Their ability to function as defensive military maps may be considered within the parameters put forth by Hale (Hale 2007). To some extent,

the priorities evidenced by the maps in question align with those of defensive military mapping: bridges, wells, and fortifications are studiously recorded. However, the maps lack many crucial details needed to develop defensive strategies, including well-defined terrain, indication of roads, information about adjacent populations who could play a part in battles, and trustworthy portrayal of fortress scale and weaponry. We must also bear in mind that communication with the king in Madrid took over a year, and that his direct involvement in responding to threats would have been minimal. The best way the maps could affect military strategy is by illustrating the condition of fortresses so that funding for improvements could be allocated.

If not navigational or military (in any meaningful way), another angle from which to examine the maps is as artistic objects to be admired. The concept of a “nonutilitarian” function for maps is well-established. Of Charles V’s cartographic patronage, for instance, Kagan and Schmidt note that “[the king] collected them in a way that implies the aesthetic value of these prized princely artifacts” (Kagan & Schmidt 2007). Treating maps as works of art has produced interesting studies on perspective in maps (Cosgrove 1985), the evolution of ornamentation in maps (Welu 1987), and the sometimes-shared lineages of cartography and fine art (Rees 1980). Map signs can also be studied systematically, as Delano-Smith has brilliantly endeavored in a manner owing less to Panofsky and more to linguistics (Delano-Smith 2007).

But perhaps the most holistic and appropriate paradigm through which to examine the maps of the Évora codex is offered by the so-called “New History of Cartography,” whose proponents and tenets have been summarized by Delano-Smith and Kain (Delano-Smith & Kain 2009). This “New History” seeks to look at the map “as artifact, as image, and as vehicle of communication fashioned in the image of the society which created it” (*ibid.*). More concretely, this includes increased attention to the function of a map and questioning the attitudes behind what maps record, how they record them, and what they leave unsaid (see Harley 1988b). Expanded interrogation of maps also enables investigation of the way maps were compiled and how they can represent a dialogue between the new arrivals to a region (explorers) and the experts (locals), as Barbara Mundy has demonstrated in her study of New Spain (Mundy 1996). In this way, the map is accurately perceived as a highly informative response to a specific set of requirements.<sup>5</sup> It is under this framework that we will attempt to understand the maps in the first part of the research.

For the second part of the research, we will turn an inquisitive eye to the map as an object. Materials studies on maps have followed at least three lines of questioning, with various instrumental methods. The first is to exploit imaging and elemental mapping strategies to improve the legibility of faded maps or document changes to the maps over time (see for instance Bai, Messinger, & Howell 2017). The second is a general identification of pigments. This sort of investigation is usually applied to maps and globes of conspicuous artistic value, or during a conservation intervention (Lewincamp & McNaught-Reynolds 2010). A third issue addressed by materials study has been provenance/cultural background, as deduced from materials used to produce the map (Kogou et al. 2016). Although maps have not been the subject of much materials research, useful approaches can be borrowed from elsewhere. The methods applied to the study of illuminated

---

<sup>5</sup> While this paradigm seems to leave behind the pedantry of older ways to study cartography, its conclusions can only be made once a study of the “accuracy” of the map is undertaken as well as possible. It is not possible, for example, to conclude that one settlement was exaggerated to inflate its leader’s prestige until the actual scale of the settlement has been compared with that of the map.

manuscripts are an excellent starting point. Manuscripts, like maps, frequently demand *in situ* analysis with noninvasive techniques. Manuscripts also share features with maps from a materials perspective, in that they are executed on paper or parchment support, and therefore have constraints on their scale and paint formulations.

Characterization of a manuscript or painting on paper can include identification of materials and their production method (paper fiber source, paper sizing and fillers, pigments, binders), uncovering how those materials are wielded by the artist, and identifying any alterations to the materials or work of art as a whole. While a comprehensive survey of these methods is beyond the scope of this section, a brief introduction will provide context to the research design.

Establishing broadly the homogeneity of the paint formulations can be achieved by carefully-designed point analysis, or by techniques that allow comparisons of the materials by various proxies across the whole work. Spectrophotometry (colorimetry and FORS) and portable XRF can be useful tools for point analysis, as both are nondestructive, rapid, and can be performed *in situ*. Spectrophotometry has been used since the late 1930s to record reflectance spectra of pigments in various binders (Barnes 1939), and with portable fiber optic devices and the growth of spectral databases, it has become increasingly useful to researchers for pigment identification and monitoring changes to paint films. It may also be helpful for identifying mixtures of pigments (Cavaleri, Giovagnoli, & Nervo 2013). Portable or handheld XRF deliver data on the elemental composition of the analyzed area and can give a broad assessment of the homogeneity or heterogeneity of the paints used, if analysis points are selected judiciously. However, in a reversal of the issues with spectrophotometry (in which altered surfaces can impair identification of pigments), *in situ* XRF results can be difficult to interpret, as underlying paint can contribute to the spectra and make it difficult at times to discriminate between pigments, mixtures, and overlays.

To ensure that point analyses performed *in situ* are representative, visual inspection and technical photography are indispensable, as they allow observation and comparison across the entire work. Technical photography involves documentation of the artwork using modified cameras and specific lighting conditions and filters. These can include raking light to locate *giornate* in frescos, the use of ultraviolet illumination to identify new and aged varnishes on oil paintings, and capturing only the near-infrared region of reflected light to visualize carbon-based underdrawings. When several wavelengths are used, the term multispectral imaging may be applied, and it is sometimes possible to identify pigments (Cosentino 2014b). Recently, hyperspectral imaging has gained traction as a means of mapping binders (Ricciardi et al. 2012) and pigments (Mounier et al. 2014). A comparison of its performance relative to Raman spectroscopy has been described by Maybury et al. (Maybury et al. 2018).

More fine-grained data on the pigments and binders can necessitate analysis with non-portable equipment, or the use of microsamples. These techniques include LC-MS, Raman microscopy, FT-IR, GC-MS, SEM-EDS, and XRD. Since Jan Wouters' work on anthraquinone dye identification using liquid chromatography (Wouters 1985), LC-MS has been used to identify madder, cochineal, brazilwood, and lac lakes (Degano et al. 2009). Raman spectroscopy and FT-IR spectroscopy are vibrational techniques whose spectra are related to the molecular structure of the pigments and can offer complementary data to each other and to the findings of FORS and XRF analyses. A review of Raman spectroscopy's applications to cultural heritage can be accessed in Smith & Clark 2001 and Clark 2003. SERS is especially suited to the investigation of painting

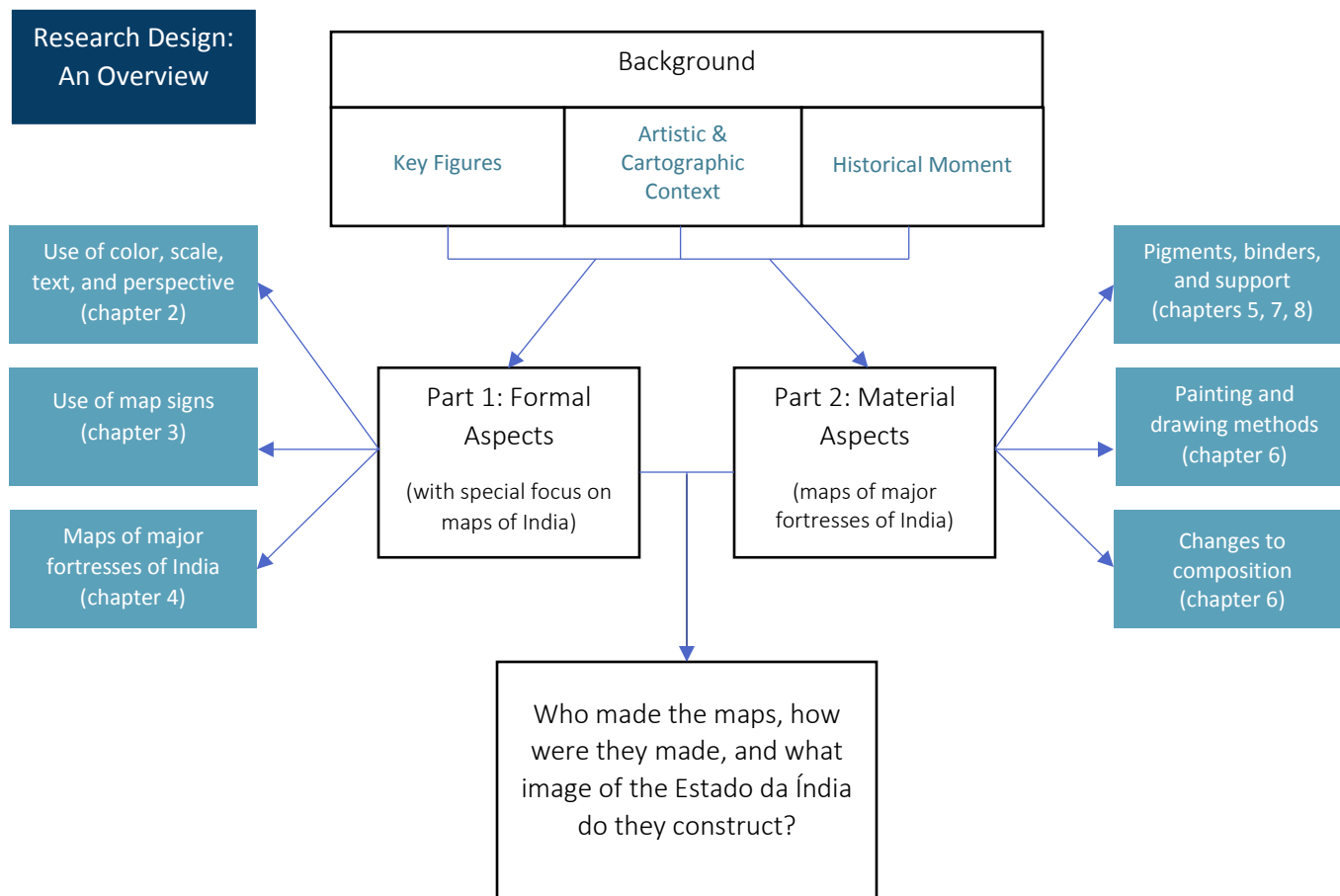
lakes and dyes. It was first used to study anthraquinone dyes by Guineau and Vichard, and in recent years has been applied to the study of wide variety of dyes and lakes (Guineau & Vichard 1987; Leona 2009). Besides helping to identify the pigments and binders themselves, FT-IR can give insights into the relationship between pigments and binders (Scott et al. 2001; Centeno et al. 2004) or dyes and substrates (Ovarlez et al. 2006). An alternative to FT-IR for binder characterization is GC-MS. Some notable uses have been to build a database of new and degraded plant gums (Lliveras-Tenorio et al. 2012) and to identify egg as the binding material in German manuscripts (Scott et al. 2001). MALDI-MS was also successfully employed for binder identification on an illuminated manuscript for the first time in 2017 (van der Werf et al. 2017). Variable pressure SEM-EDS can allow visualization of elemental distribution on microsamples or entire artifacts with almost no preparation and has an advantage over portable XRF in detection limit and elements that can be recorded. Lastly, XRD can be used to determine the degradation state of papers due to changing in crystallinity (Manso et al. 2011) and distinguish between minerals with the same elemental composition but different crystal structure, such as calcite and aragonite. It has also been helpful for the identification of mineral pigments (Duran et al. 2009). The paper support can be characterized by spectroscopic techniques (see Manso & Carvalho 2009 for a survey), by GC-MS, or by optical or scanning electron microscopy for fiber identification (Espejo et al. 2010).

The analytical approach selected by researchers will depend on questions they hope to answer, the equipment accessible, and the nature of the materials under study. In the research design presented below, only the aims of the materials study will be presented. At the beginning of Part 2 a breakdown of the instrumental techniques to be applied and their respective goals will be provided.

### I.3: Research Design

Very little information on the maps of the Évora codex exists, and the first step of this thesis will be to lay out what we already know and fill in some gaps. Following this, we will move towards a holistic characterization and interpretation of selected maps. They will be treated as the product of a specific cultural moment with specific political, economic, and artistic features. The attitudes embedded in the maps will be explored in terms the maps' formal aspects, with special attention to enhancements and erasures of the world they purport to document. The way the maps fit into an artistic context will be endeavored through study of the materials and production methods of the maps, as well as their stylistic features. In doing so, the research will not only provide information on the maps of the Évora codex, but supplement the literature concerning the materials used in cartographic works. Synthesizing this information, we hope to provide new information about the mapmaker(s) and how cartography depicted empire in the twilight years of the Estado da Índia (see figure 3). Although this work is preliminary and cannot always go into great depth, it hopes to lay solid groundwork for future studies. Perhaps more importantly, the work strives to demonstrate that the study of maps requires an interdisciplinary approach, and that materials characterization can be a key part of a cartographic investigation.





**Figure 3:** Research design.

## 2: The Maps in Historical and Artistic Context

### 2.1: Key figures surrounding the maps

**Antonio Bocarro:** Chronicler of the *Estado da Índia*, author of the text in the Évora codex, and a major source for Resende's *Book of the State of Oriental India* (Cortesão & de Mota 1960b).

**Pedro Barreto de Resende:** Secretary to the Viceroy, supplier and presumed creator of the maps of the Évora codex. As Resende played a central role in the maps' production, we will endeavor a more comprehensive description of his activities and character.

The life of Barreto de Resende comes to us in bits and pieces that are often contradictory. The correspondence quoted in Chapter 1, for example, raises more questions than answers about his cartographic proclivities. On the one hand, Resende claims he had accumulated the maps out of "curiosity" (Cortesão & de Mota 1960b). Then later in the same letter he hints at "certain purposes" he had had in mind for them. There is also the fact that Resende produced a book very similar to Bocarro's about a decade after the Évora codex was completed (*The Book of the State of Oriental India*, referenced in this text as MS 1646 Resende; see figure 2). It seems probable that Resende had begun collecting or producing maps with the intention of compiling a book of his own to ingratiate himself with the king.

Biographical information on Resende is scant and derives mainly from the dedication page in the 1646 London copy of *The Book of the State of Oriental India* in which the author identifies himself as "Captain P.o Barreto de Resende, professed knight of the Order of St. Benedict of Avis, Native of Pauia (Pavia?)" (Cortesão & de Mota 1960b). In 1629, Resende traveled to Goa to serve as Secretary of State under the Count-Viceroy Linhares de Noronha, and on ending his term there in 1635 he moved to Lisbon, where he died in 1651. He was buried in the Igreja do Carmo in Lisbon (Machado 1752, p. 563). He fathered two daughters (from the first of his three marriages) and authored four books<sup>1</sup>.

The diary of Count-Viceroy Miguel Linhares de Noronha proved an ally in research about Resende. The remarks of the Viceroy give an indication of the responsibilities with which Resende was charged during his tenure in Goa and provide a less-than-flattering performance review. As far as the Viceroy was concerned, Resende's two main jobs were to advise and to deal with correspondence (reading and replying to letters from the many fortresses of the far-flung empire). This second task should have ensured that Resende had up-to-date knowledge of projects and problems across the *Estado*. That being said, on February 6, 1634, the Viceroy writes that "I saw the letters that the Secretary of State brought written, and to some of them I added a lot, to others corrected a lot..." (de Noronha 1937, p. 4), on April 28 that "the Secretary of State, who is a good man, is not good for this service as he does not solve anything and does not even know about it" (*ibid.*, p. 85) and on May 1 that "the Secretary of State on his own is not able to write a letter with substance" (*ibid.*, p. 91) (translation from the Portuguese by Dr. Catarina Miguel). Modern scholars have argued against Resende's authorship of the maps on

---

<sup>1</sup> Besides the one already listed, he wrote *Tratado dos Vizo Reys da India* (1635) (Raczynski 1847, p. 244), *Noticias de todas as Praças que os Portuguezes tinhaõ na India...*, and *Relaçã da Familia dos Sylveiras Lobos...* (Machado 1752, p. 563).

the grounds that a Secretary of State would not have had time for cartography (Alegria et al. 2007). Perhaps it was the reverse - he was too preoccupied with his maps to be much of a Secretary.

**Count-Viceroy Miguel Linhares de Noronha:** Viceroy of the Portuguese *Estado da Índia*, Resende's superior, "project manager" for the Bocarro *Livro das plantas* who brokered the agreement between Resende and Bocarro that led to the former's maps being included in the latter's book.

**Felipe III of Portugal, IV of Spain:** the monarch at whose order the Évora codex was created, and who expected maps to be included.

**Manuel Godinho de Erédia:** pilot, cosmographer, and author of numerous cartographic works, including the Atlas-Miscellany of 1615-1622 (the source of models for Resende's maps of 'Cochim,' 'Dio,' 'Cananor,' and perhaps 'Manar') (referred to in this work as MS 1622 Erédia; see figure 2). Considered by some to be the last great Portuguese cartographer active in India (Cortesão & de Mota 1960a; Alegria et al. 2007).

**João Teixeira Albernaz I:** son of acclaimed cartographer Luis Teixeira, creator of many maps of Brazil, producer of at least two groups of maps based on Resende's models. One set was made sometime in the first half of the 17<sup>th</sup> century and is referred to in this work as MS 1600-1650 Teixeira Albernaz<sup>2</sup>. The other is a group directly adapted from Resende's work and included in the version of Bocarro's *Livro das plantas* presently housed in Madrid. It is referred to here as MS c.1635 Teixeira Albernaz (see figure 2; Cortesão & de Mota 1960b).

## 2.2: The Portuguese in India, early 17th Century

Over the past century, a diverse body of scholarship has taken on the many facets of the Portuguese *Estado da Índia*, with more discoveries to come as the archives of Goa are mined. This thesis makes no pretense at adding to the historical literature; rather, it hopes to bring together key data from primary, secondary, and cartographic sources to assist in interpreting the maps of the Évora codex as a gestalt. To that end, the merest introduction to the history of the *Estado* is essayed below, with the goal of opening a window into the mindset of the mapmaker. The focus of this section will be on India. If knowingly, necessarily superficial, the summary hopes to be fair to the topic.

The *Estado da Índia* refers to a network of fortresses strung together across Africa and Asia - the subject of the maps under study. Its origins may be traced to the Portuguese capture of Ceuta in Morocco in 1415, after which, with the ever-increasing means and momentum provided by innovations in navigation, the Portuguese steadily laid claim to coastal territories stretching from Brazil to Japan (Newitt 2005, p. 1). The motivations for empire varied over time. On the one hand, a crusade mentality was central to the Portuguese justification of conquest. However well they wielded it, the Portuguese had been granted the nominal right to direct missionary efforts in many regions of the world and fiercely defended their monopoly (Boxer 1973, p. 230). On the other hand, economic aims dictated the physical contours of the empire and the

---

<sup>2</sup> This collection (MS 1600-1650 Teixeira Albernaz) is part of a codex entitled *Plantas das cidades, portos, e fortalezas da conquista da Índia Oriental* and is housed at the National Library of France in Paris. Access: <https://gallica.bnf.fr/ark:/12148/btv1b55007625f>

territories it would come to encompass. The goal, as articulated by Afonso de Albuquerque, was to corner the spice trade to Europe by choking off the usual land routes, and to oversee and tax commerce in Asia. This meant controlling the straits of Mecca (by capturing Aden), the straits of Basra (by seizing Hormuz), and ruling India from Goa and Diu (Pearson 1987, p. 31). The plan, in its perfect form, meant upending the *mare liberum* that had governed trade for centuries.

The Portuguese were neither the first Europeans to make contact with India (Pearson 1987, p. 10), nor its first would-be emperors. Though the Portuguese generally stuck to their coastal fortresses, great powers with equally great visions of dominion stirred inland and struck whenever the newcomers' presence became too bothersome. In the early 16<sup>th</sup> century, these included the Hindu Vijayanagara empire in the south (Sinopoli 2000) and the Muslim Mughal empire that had swept in from the north and established a base in Delhi (and to which the Rajasthani central kingdoms would eventually become vassals) (Kossak 1997, p. 8). More than a century after the Portuguese arrived in India, the largest cities in the subcontinent remained Delhi, Lahore, and Agra: the metropolises of rival powers (Pearson 1987, p. 93). The trade routes that the Portuguese would attempt to control were already bustling with Muslim ships full of Gujarati merchandise (*ibid.*, p. 23), and the *cartaz*<sup>3</sup> system's untenable ambition guaranteed its failure (Pearson 1998, p. 135). Perhaps more than by meddling in trade and occasional abuses of power at sea, the Portuguese provoked conflict with local rulers by overzealous proselytizing and seizure or construction of fortresses (regarding evangelism, see for example Boxer 1973, pp. 243-245; regarding fortification as bad diplomacy, see Disney 1996, discussion of Cambolim).

In the space of about a century, the *Estado* had transformed: the handful of key fortresses needed to anchor a largely maritime empire had become a sprawling assemblage of footholds across multiple continents. The reasons for the change were several: a will to conquer (Pearson 1987, p. 74), a need to secure tradeable goods to keep the *carreira*<sup>4</sup> going and Goa fed, and the very system of privileges that characterized the official empire. Being the captain of a fortress in the *Estado* could be tremendously lucrative. Captaincies were granted as a reward for service to the king but one had to pay a hefty fee to the Crown to exercise a monopoly on trade from one's fortress. By the 17<sup>th</sup> century, important posts in India had long waiting lists, making a strategic reduction in the size and cost of the *Estado* diplomatically difficult (Newitt 2008, p. 174). By the time Pedro Barreto de Resende reached Goa and assumed his secretarial duties, the empire had probably overstretched itself. Problems that had plagued it since its inception were escalating. Resende himself reports that from 1629 to 1635, only 5228 men had headed for India from Portugal, of which less than half arrived (Pearson 1987, p. 93). Shipping losses in approximately the same period had amounted to 155 ships, 1499 men, and 7,500,000 *xerafims* in goods (Subrahmanyam 2012, p. 177). The region around Goa had suffered a devastating famine from 1630-1632, leading to heavy mortality and increased outbreaks of plague among the enfeebled population (Disney 1996). The effects of the famine were felt well outside of Goa; in Surat, there were even reports of cannibalism (Winters, Hume, & Leenstra 2017). To top it off, by the 1630s the English and Dutch challengers to Portuguese power were becoming savvier; they would not rest until the *Estado* had been reduced from over fifty fortresses at the start of the 17<sup>th</sup> century to a mere nine by 1666 (Pearson 1987,

---

<sup>3</sup> The *cartaz* was a kind of maritime passport issued by the Portuguese which supposedly made trading safer, and stipulated the merchants call at Portuguese forts to pay customs duties and abstain from trade with Portugal's enemies (Pearson 1998, p.131).

<sup>4</sup> The *carreira (da Índia)* refers to the maritime trade route running between Goa and Lisbon starting in the 15<sup>th</sup> century (Boxer 1960).

p. 142).

It is difficult to understand how Resende would have looked upon the *Estado* from his vantage point. Secured with a job that allowed him to seek personal enrichment and privileges from the Crown, did he feel the anxieties of an empire on the precipice? Or did he, like so many Portuguese abandoning the “official system” for private trade (Pyrard 1887/1611, p. 334), find the finances and future of the *Estado* irrelevant? The 1630s would be a turning point for the Portuguese in India. As Newitt astutely notes, “[...] it is significant that one of the commonest responses of Goa to any threat, whether from Asian rulers or the Dutch, was to plan the construction of further fortresses [...] It is no coincidence that one of the last great descriptive works inspired by the *Estado da Índia* should be a lavishly illustrated description of its fortresses” (Newitt 2005, p. 194). This description is the Bocarro *Livro das plantas*.

## 2.3: Artistic Context

### 2.3.1: Authorship

Before we look into the artistic context of the maps, some disputes about their authorship should be addressed. There is no doubt that Resende gave maps to Bocarro. The issue is that Resende’s possession of the maps does not necessitate his direct involvement in their production; as others have pointed out, he could have commissioned them, hiring artists in Goa to produce the works (Alegria et al. 2007). But between the extremes of “Resende did everything” and “Resende did nothing,” there exists a very plausible intermediate: that Resende drafted the maps and hired others (possibly local artists in Goa) to color them.

That Resende drafted the maps is likely for several reasons. First is the use of Erédia models. It is far more probable that Resende would have access to these models than that a local artist would have encountered them (particularly since they were manuscript maps, not printed maps). Secondly, the church signs in the maps follow a distinctly European cliché. The distillation of a church into this form might not have occurred to a native artist, who would have had far fewer examples of churches from which to generalize. A last piece of evidence in favor of Resende as the draughtsman is the breadth of knowledge required to make such maps. Resende may not have had the ability to visit all the fortresses, but he had the connections needed to get information. In his job as Secretary, he was practically awash in news and complaints and suggestions from the network of fortresses. While Resende could have personally dictated all the aspects of each fortress (as he knew them) to a hired draughtsman, it is equally or more likely that Resende simply did the drawings himself.

That Resende also colored the maps is more doubtful. Painting in the early 16<sup>th</sup> century was not for the casual hobbyist. Artists at this time had to secure and maintain an assortment of supplies and were responsible for preparing their own paints. The time and skill required of the artist before even picking up a paintbrush was not trivial. Beyond logistical considerations, there are aspects of the maps’ color that hint at influence from non-European painting traditions. These include the unusual use of pink for the fortresses, the absence of wash technique and tendency to use flat, unshaded color, and the organization of space into horizontal bands. The way that the rocks and herbs are painted is also tangentially suggestive. The rocks of the Évora codex bear a striking resemblance to the rocks in the 16<sup>th</sup> century codex Casanatense 1889 (accessible at <http://opac.casanatense.it/Record.htm?idlist=&record=19917226124917354089>). The European

pedigree of the codex Casanatense 1889 has increasingly been called into question, with scholars suggesting that the artist was Indian (Archer 1992, pp. 12-13; Losty 2012).

Alternatively, the maps could have been colored by a European artist accustomed to working in a smaller format and pushed outside their comfort zone by the demands of the large pages in the Évora codex. Or finally, perhaps Resende did color the maps, but without the rigorous training of a professional artist was more receptive to influences from outside European painting traditions.

### 2.3.2: Artistic exchange

European influences on Indian miniature painting are easy to pinpoint and are supported by primary sources (particularly in the case of the Mughal emperor Akbar). The possibility of local Indian traditions affecting European art-even the art of cartography-has been less fully examined. The line between Hindu and Muslim, Rajput and Mughal art, is sometimes blurred. To avoid conflation of “Indian” with “Hindu,” we will first set the stage with some examples of artistic collaboration between Indian and European artists, and then summarize some major aspects of Hindu and Muslim art separately.

That Portuguese (and later British) colonists in India employed local artists to execute various projects is well-documented. In the British case, the “Company painting” became a kind of genre, whereby Mughal artwork adapted for European tastes were produced to satisfy at once a sincere admiration and attraction for the exotic (Eaton 2006; see also Kossak 1997 for examples and Archer 1972 for a detailed discussion). In the Portuguese case, Hindu painters of the 17<sup>th</sup> century made and sold paintings of Christ, the Virgin, and various saints, as well as executing commissions for altarpieces (Pearson 1998, p. 123). It was an Indian artist who colored 13 of Gaspar Correia’s portraits of the Viceroy (now in the Archaeological Museum of Old Goa) (*ibid.*, p. 116), and an Indian artist who compiled the botanical drawings for Garcia da Orta’s *Coloquios dos Simples* (Archer 1992, p. 12). The output of local artists was not always to European tastes, however. Thevenot remarks that “one may see a great many pictures in the Indies upon paper and paste-board, but generally they are dull pieces...however, since those of Agra represent lascivious postures, there are but few civil Europeans that will buy them” (Thevenot & Careri 1949/1656, p. 55). Referring to painters in Delhi, he goes deeper, saying that artists “apply themselves to the representing of histories, and in many places, one may meet with the battles and victories of their princes, indifferently well painted. Order is observed in them, the personages have the suitableness that is necessary to them, and the colors are very lovely, but they make faces ill. They do these things in miniature pretty well...[but] all their care is to do as much work as they can, for present money to subsist on” (*ibid.*, p. 65). The simultaneous appreciation and skepticism of local Indian artistic conventions makes collaboration (rather than pure patronage) on important projects all the more likely. By collaborating, one assumes, European tastes could be satisfied while labor costs were reduced.

Who were these local artists? And which artistic traditions might Resende have encountered in India? While this thesis cannot presume to provide a full picture of the painting traditions of India in all their regional and temporal permutations, a very sketchy overview to orient the reader may be attempted. For the sake of brevity, by the early 17<sup>th</sup> century, Indian art can be divided into two powerful movements, both based in royal courts. The first is Rajput art, which drew on and elaborated indigenous pictorial traditions. The second is Mughal art, which by the 17<sup>th</sup> century had moved



beyond its Persian roots to become a distinctive Indian style. We will start with some background on Rajput art, and then turn to Mughal work.

### 2.3.3: Rajput painting

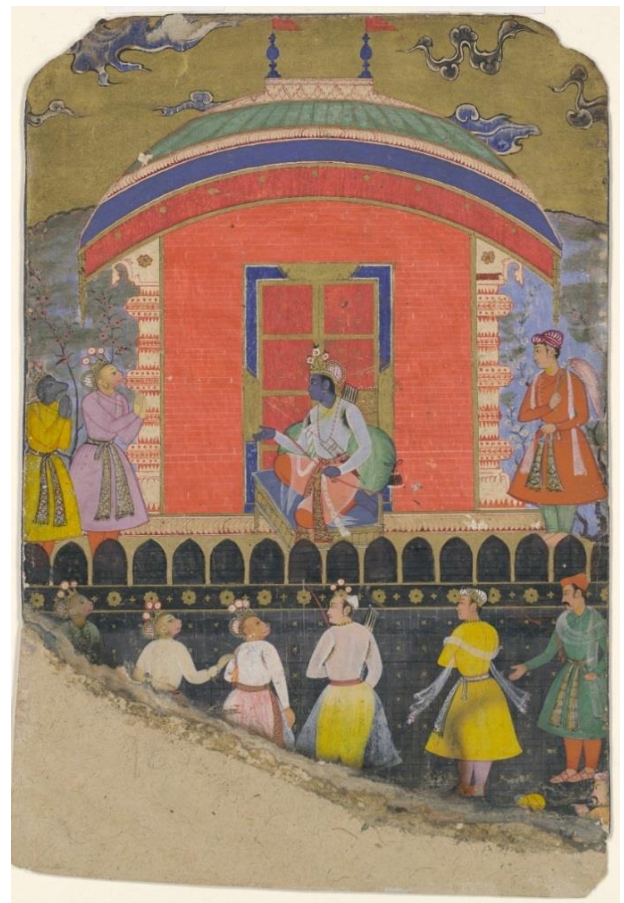
Rajput painting, a catch-all term for a number of schools that developed in the royal courts of Rajasthan in Western India, is inextricably connected with a rich folk art tradition (Beach 1975). This indigenous style was developed to fulfill devotional needs, and some of the earliest surviving painting from India pertains to the Buddhist, Hindu, and Jain scriptures (Beach 2008, pp. 4-14 for an overview; for a detailed history of Jain painting, see Moti 1919; for an early but wide-reaching treatment of Buddhist art in India, see Grünwedel 1901)<sup>5</sup>. The works were initially executed on palm leaves and tended towards stereotyped scenes in a predominantly white, red, green, yellow, and bluish-black palette (Kossak 1997, p. 6). By the mid-1500s, a new format had emerged in Hindu painting: illustrations that dominate full pages. One manifestation of this change is seen in the paintings of the *Chaurapanchasika* school<sup>6</sup>. Possibly emerging from Jain pictorial traditions, this school can be treated as emblematic of a Hindu art that remained true to its roots despite increasing competition with Mughal paradigms. The shallow pictorial space, flat fields of evocative color, and concern with line and pattern that characterize this school are hallmarks of traditional Hindu art prior to the 17<sup>th</sup> century (see figure 4). By the time the maps of the Évora codex were created, evidence exists for a spectrum of Rajput styles, ranging from more conservative schools in regions that did not feel the Mughal impact as strongly, to profoundly Mughal-influenced work (Kossak 1997, p. 16; Welch 1985, p. 335).

### 2.3.4: Mughal painting

Although periodically drawing on Indian folk traditions, the roots of Mughal art are in the Islamic courtly workshops of Persia. The Mughal empire's history in India starts with Babur's



**Figure 4:** Example of early Rajput *Chaurapanchasika*-school painting. Nanda and Vasudeva (page from a dispersed *Bhagavata Purana*, c.1520-1530). Ink and opaque watercolor on paper. Metropolitan Museum of Art.



**Figure 5:** Example of Mughal painting of a Hindu subject. "Rama receives Sugriva and Jambavat, the Monkey and Bear Kings" (folio from a *Ramayana* manuscript, c. 1605). Ink, opaque watercolor, and gold on paper. Metropolitan Museum of Art.

<sup>5</sup> Since much of early Hindu painting was wall painting and has survived poorly, even the most detailed description of Hindu painting will remain incomplete.

<sup>6</sup> The name means "Fantasies of a Love Thief." The school is named after an illustrated version of this text produced in 1550.

conquest of Delhi in 1526. His son Humayun was expelled from the region, and during his exile in Persia was exposed to the traditions of manuscript painting in the Muslim courts. The painters of these Persian schools emphasized jewel-like color and ornate patterning, but with components of the painting clearly delineated from each other and an absence of deep space, producing an effect almost like opus sectile work (Soudavar 1999). When Humayun recaptured Delhi in 1555, he brought Persian painters with him and set up an atelier. His son Akbar was similarly passionate about miniature painting and prided himself on his connoisseurship. Akbar's rule marked a move away from the Persian miniature tradition, as artists now worked on larger pages and called on both Hindu and European conventions to create dynamic scenes with myriad subjects (Welch et al. 1987, p. 16; Dimand 1953). When Akbar's son Jahangir took over in 1605, the size of studios was reduced, with the (also art-loving) ruler keeping on only the "best" artists (Dimand 1944). The unneeded and newly unemployed artists could have set themselves up in less prestigious provincial ateliers, or sought work elsewhere, even among Europeans (Kossak 1997, pp. 12-13). The production of miniatures, incorporating ever-changing blends of influences, continued under Shah Jahan, whose early reign overlaps with Resende's arrival to Goa. See figure 5 for an example of Mughal painting from the early 17<sup>th</sup> century.

The heights of Mughal or Hindu artistry would have been concentrated at locations far outside of Resende's Goa. It is with the itinerant artists whose income had been disrupted by suppression of religious practice, or whose place in a major atelier could not be secured, with which we are concerned. While remaining careful not to jump to conclusions, we will approach the maps with their potential involvement in mind.



## Chapter 3: Formal Aspects of the Maps

### 3.1: Overview

Moving toward a formal description of Resende's maps, a pause to compare the cartography of a professional (MS c.1635 Teixeira Albernaz) with those of the Évora codex is warranted. In doing so, we can begin to see how Resende's maps stylistically deviate from the norms of European decorative terrestrial cartography from the early 17<sup>th</sup> century and make more room for the possibility of local artists' involvement.

Perhaps the most obvious way in which the maps of the two codices differ is in color. Teixeira Albernaz's soft, wash-driven technique imparts delicacy and realism to the landscape (figure 6, top). His "correction" towards naturalism extends to the coloring of the fortresses as well. The illustrious cartographer has done away with Resende's codified use of two shades of pink (figure 6, bottom) and renders the majority of the fortresses in a sandy beige tint.<sup>1</sup> Teixeira Albernaz I does not attempt to improve on Resende's perspective or composition, perhaps due to time constraints and lack of information about the actual layouts of the cities in question. His efforts to achieve greater naturalism are instead expressed through a program of "prettification" mostly affecting the terrain around the fortresses. He puts shadows underneath trees and strives for consistent lighting effects on mountain ranges, insisting on three-dimensionality where Resende's maps had been flat but vivid. Additionally, where Resende's use of line is limited to fortresses and houses, Teixeira employs linework to integrate architecture and landscape, using careful hatching to suggest the contours of hills.

If we assume that part of the maps' functions was conveying important information, Teixeira Albernaz's adaptation is in some ways a damning indication of misplaced priorities. While of arguably greater artistic merit, the cartography of MS



**Figure 6:** (top) MS c.1635 Teixeira Albernaz map of 'Cranganor' (copyright Biblioteca Nacional de España), (bottom) Évora codex map of 'Cranganor' (copyright Biblioteca Pública de Évora). Note the different approaches to coloring the terrain and vegetation and the alteration of the water and fortification colors.

<sup>1</sup> The ways in which this move decision may have rendered the maps *less* realistic (i.e., less representative of the fortresses' aspect in reality) and less informative will become apparent in a discussion of the two shades of pink used by Resende, and his use of pink in general.



**Figure 7:** (left) MS c.1635 Teixeira Albernaz map of 'Gale' (Copyright Biblioteca Nacional de España), (right) Évora codex map of 'Guale' (Copyright Biblioteca Pública de Évora).

c.1635 Teixeira Albernaz disregards potentially useful details embedded in the Évora codex maps. One of these has already been referenced (the systematic use of pink on fortifications). Teixeira Albernaz I is also casual in reproducing the construction types presented in Resende's maps, and does not hesitate to replace thatched houses with stone houses where it suits him (figure 7).

### 3.1.1: Format

The BPE *Livro das plantas* contains a total of 48 maps, each measuring about 406x604mm. The regions depicted are listed in full in Appendix I.1. Four of the maps that were originally included in the codex have since been lost or intentionally removed: 'Goa,' 'Honawar,' 'Colombo,' and 'Negapatam.' Their general design can be inferred by examining the Teixeira Albernaz I maps (MS c.1635 Teixeira Albernaz) or Maris Carneiro maps (MS 1639 Carneiro). The four maps were probably removed as recently as the late 19<sup>th</sup> century; Raczyński reports in 1847 that there are two versions of the Bocarro *Livro* (one of which is presumably the Évora codex), each with 52 maps (Raczyński 1847, p. 244).

The support for the maps is paper. In her analysis of the codex and excellent transcription of the text, Isabel Cid detected at least 6 different watermarks on the papers of the BPE *Livro das plantas*. The recourse to multiple paper suppliers in the execution of a royal mandate may be indicative of supply-chain and funding issues for the Goan government. Citing viceregal complaints of paper deficits in 1631, Cid interprets this aspect of the BPE codex as a sign that the problem persisted (Cid 1992, p. 38). She reports that the paper of the maps and text is similar: medium press, with a weight of about 32 g, and brownish in color (*ibid.*, p. 53). Regarding the watermarks on the map papers, Cid reports the following:

- **Watermark 1** (archbishop's hat): plans of 'Matara,' 'Quelba,' 'Mada,' 'Tana' (perhaps), 'Caliture,' 'Solor'
- **Watermark 2** (flag or flower with letters): plans of 'Borca,' 'Mada'
- **Watermark 3** (hat or flower with letters): plans of 'Doba,' 'Sera de Aserim,' 'Baçaim'

### 3.1.2: Regions and Toponyms

The toponyms inscribed on the maps do not always correspond to the modern names of the locations in question. To avoid confusion, especially while discussing areas which are not presently centers of habitation, throughout this text we refer to

the regions using the names listed on the map, changing only the “v” to a “u” where needed, and periodically recalling the modern name where applicable.

### 3.1.3: Fortification Typology

In Appendix I.2, reproductions of all the maps of the BPE codex are provided, permitting the reader to easily appreciate the diversity of fortifications that the mapmaker documents in the *Estado da Índia*. Following Cid’s schema, we can summarize the geometry of the fortresses as follows:

- **Square:** ‘Sofala,’ ‘Monsambique,’ ‘Coriate,’ ‘Matara,’ ‘Quelba,’ ‘Mada,’ ‘Tana,’ ‘Salsete,’ ‘Mombaim,’ ‘Cambolim,’ ‘Barçalor,’ ‘Mangalor,’ ‘Cais dos Elefantes,’ ‘Jafanapatam’
- **Triangular:** ‘Sibo,’ ‘Borca,’ ‘Corfacam,’ ‘S. Irm.,’ ‘Tarapor,’ ‘Triquilimale’
- **Rectangular:** ‘S. Tome,’ ‘Libedia,’ ‘Solor’
- **Irregular polygons with five or more sides:** ‘Batecalou,’ ‘Negumbo,’ ‘Malaca’
- **Star:** ‘Mombaça’
- **Regular polygons with five or more sides:** ‘Samges’
- **Combination:** ‘Soar,’ ‘Cochim,’ ‘Damaõ,’ ‘Baçaim,’ ‘Agoada,’ ‘Bardes,’ ‘Cranganor,’ ‘Dubo,’ ‘Doba,’ ‘Cananor’
- **Irregular:** ‘Mascate,’ ‘Dio,’ ‘Sera de Aserim,’ ‘Moro de Chaul,’ ‘Chaul,’ ‘Coulam,’ ‘Guale,’ ‘Macao’
- **Other:** ‘Sirgao,’ ‘Maim,’ ‘Ilha das Vaças,’ ‘Manora,’ ‘Tana,’ ‘Manar’

(Cid 1992, p. 52). The variability among the fortresses has several causes, among which are the technological innovations imported by visiting architects from Spain and Italy (Luengo 2017) and the seizure and use of already-existing fortresses, such as the fort at Sibó, which Bocarro states is “already old, made by the Arabs” (Bocarro 1992, p. 54, author’s translation). Some of the fortresses drawn in the plans represent a transitional period between medieval and early modern fortification (see the forts in the maps of ‘Cranganor,’ ‘Mangalor,’ and ‘Cochim’) (Cid 1992, p. 52). The most obvious sign of changing fortification designs can be seen in the shape of the bastions. By the middle of the 16<sup>th</sup> century, the Portuguese had begun to employ the angle bastion in their fortresses abroad (Arnold 2001, p. 45). The goal of angle bastions was to reduce “dead zones” (areas where enemies could evade the line of fire emanating from the gunners within or atop the bastion) (Lynn 1991). For maximal effectiveness, the bastions had to be close enough to one another that no length of wall was outside the firing range of the two closest bastions. The fortress of Baçaim shows an enthusiastic attempt to satisfy this parameter (Appendix I.2).

## 3.2: Style

### 3.2.1: Scale

Most of the maps in the Évora portray a single fortress with a pattern-like suggestion of the surrounding terrain. The fortress usually occupies a central position and takes up much of the page. Two maps of the codex are exceptions to this tendency, adopting a distant vantage point and encompassing much more territory: the map including ‘Bardes,’ and the map of ‘Salsete’ (Appendix I.2). The effort to cover more ground (so to speak) in these maps has a rather chaotic effect, and the author seems to struggle with the task of condensing all the same information (churches, vegetation, fortifications, towns, etc.) into a much more compact space.

The relative sizes of the objects within the maps distinguish Resende’s maps from some of their antecedents and



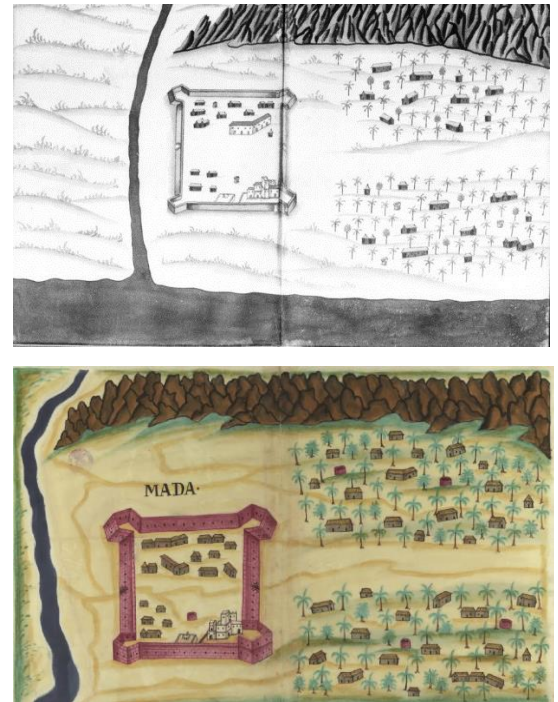
followers. We have already alluded to Manuel Godinho de Erédia's cartographic output. In most instances where Resende used Erédia's models, he followed them rather closely. It is impossible to contrast the work of these two authors in every aspect (since color plays an important part in Resende's plans), but a notable difference between them comes on the level of drawing and specifically of scale. In Erédia's plans, churches are consistently drawn much larger than houses, almost at the height of fortresses. In Resende's plans, on the other hand, churches are much more modest, often on the same scale as houses and sometimes only identifiable by the tiny cross on their rooftops.

Another demonstration of the subtlety with which scale can be manipulated is found in the MS 1636 Anon. (figure 8, top). The scale of the landmasses depicted is identical to the Évora codex maps (figure 8, bottom). The scale of buildings and fortresses, however, is much more diminutive. This drastically alters the impression the maps make on the viewer. Where Resende's maps seem to portray a well-populated world with empty edges urging further expansion, the MS 1636 Anon. maps give a sense of sparsity. The presence of the Portuguese in these maps seems frailer, and the world much more expansive than the fortresses and towns can hope to rein in and control.

Scale is not applied uniformly in the Évora codex maps. That is, different features of the maps are selectively magnified or diminished, so that the above-stated principle of filling the page with fortifications can be achieved. This has been noted by others in the case of 'Damaõ' (present-day Daman), where Sam Jeronimo (maps: 'S.Irm.', English: St. Jerome) fortress is magnified (see for example dos Santos & Mendiratta 2011, discussing the analogous map in MS 1646 Resende). 'Mombaça' provides another example (see figure 9). Insofar as the maps regularly enhance the fortresses, scale is uniformly distorted.

### 3.2.2: Perspective and vantage point

The perspective employed in the maps is in some ways quite conventional for 17<sup>th</sup>-century terrestrial cartography and in others intriguingly idiosyncratic. Overall the maps utilize a dual perspective system (a typical technique). The shape of landmasses is depicted as if seen from far overhead, whereas fortresses and towns are seen more obliquely. Within this latter category, the draughtsman experiments with several solutions. Aerial perspective is completely absent. One of the more interesting strategies the draughtsman adopts is related to vantage point. The vantage point often shifts throughout



**Figure 8:** (Left) MS 1636 Anon. map of 'Mada' (detail; decorative border has been excluded for easier comparison). (Right) Évora codex map of 'Mada'.



**Figure 9:** Comparison of actual and map scale of the fortress of 'Mombaça' (Mombasa). Aerial images courtesy of Google Earth.

the map, as if to provide an image of each area as it appears to a person approaching it. This becomes an issue in maps with multiple fortresses, where one struggles to figure out which way is “right side up” (see for example the map of ‘Mombaim’ in Appendix I.2). An analogous tactic is sometimes adopted in the treatment of streets within cities. Rather than choose one vantage point, a collection of



**Figure 10:** Details from maps of Évora codex showing different strategies from drawing houses. (Left) moving vantage point (map of ‘Iafanapatam’). (Right) one vantage point (map of ‘Solor’).

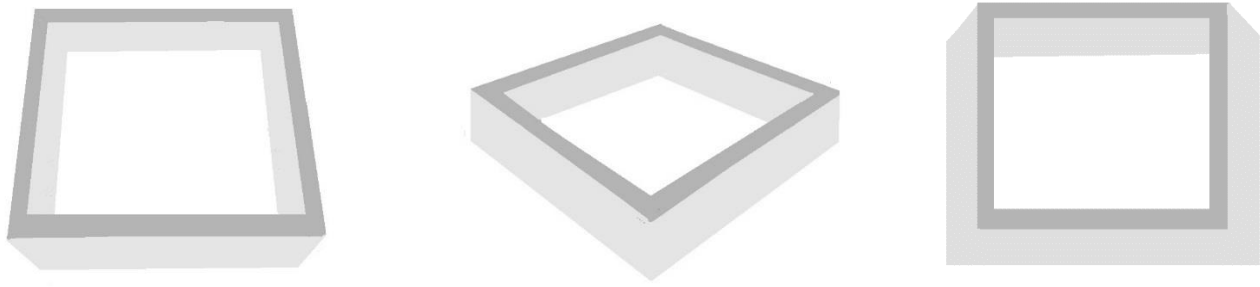
perspectives are taken, allowing the viewer to “walk around” within a city (figure 10 left). The vantage point for rows of houses is variable, however (figure 10 right); the draughtsman seems to struggle with the problem of informatively but plausibly depicting this aspect of the urban landscape.

The complicated contours of fortresses also lead to a perspective system unfamiliar to the modern eye. The pervasiveness of non-linear perspective can be examined in the maps by restricting ourselves to one fortress geometry: rectangular (figure 11). Figure 12 (next page) illustrates the expected forms a rectangular fortress should take when depicted from an elevated oblique position. Where the fortress is viewed head-on, three internal walls and one external wall should be visible. When viewed from a corner, two internal and two external walls are anticipated. This is due to what is termed “orthogonal convergence.” It is a central feature of a larger system of describing three dimensional space on a two dimensional plane. That system has been called linear, rational, or scientific perspective, and took root in its familiar form in the 16<sup>th</sup> to 17<sup>th</sup> centuries (Elkins 1994). When orthogonals diverge, the terms divergent, reverse, or Byzantine perspective are often encountered. There are 24 cases of rectangular fortresses in the maps, if we treat maps with corner bastions such as the examples in figure 10 as rectangular. In only ten cases is the ratio of visible internal to external walls compatible with linear perspective. In one of these ten cases (the map of Libedia), 3 internal walls are shown, and one external wall; however, the angle of the fortress would make us expect 2 internal and 2 external walls (Appendix I.2).

The use of divergent perspective may be due to problems with drawing complex forms. All of the rectangular fortresses using divergent perspective have intricate open bastions at their corners. When we assess the nine forts (putting



**Figure 11:** Details from Évora codex showing non-linear perspective in the maps of ‘Quelba’ (left), ‘Matara’ (middle), and ‘Coriate’ (right).



**Figure 12:** Approximate expected aspect of rectangular fortresses with minimal foreshortening versus map perspective. On the left, the fortress is viewed from a point elevated above the middle of a stretch of wall. Three internal walls are visible, and one external wall is visible. In the middle, the fortress is viewed from a point elevated above a corner. Two internal walls are visible, and two external walls. On the right, the perspective sometimes used in the maps. Under linear perspective systems, assuming the vertical walls are parallel, it is never expected to have three external walls visible, because receding orthogonal planes converge.

aside ‘Libedia’) that are drawn with “proper” perspective, we find that only 3 of them have complicated open bastions. The rest have closed towers. This makes for a simpler drawing process, and could explain the less convoluted perspective witnessed on some maps. Modern research on drawing and perception support the notion that the distortions are due to the artist’s difficulty with complex three-dimensional forms (possibly owing ignorance of the latest discoveries in perspective). In a set of particularly relevant experiments, Howard and Allison found that untrained artists had a tendency to draw a cube with slightly divergent perspective, just as we see in the maps (Howard & Allison 2011). This is not to say that artists working before the entrenchment of convergent perspective were unskilled. Rather, the point is made that this distortion is not necessarily culturally significant or symbolically relevant. For a more contemplative and in-depth treatment of perspective in landscape and maps, see Cosgrove 1985.

### 3.2.3: Line

A fine black line with variable thickness is used across the maps to outline both thatch and white houses, crosses, and artillery. A fine maroon line outlines pink fortifications and embellishes their surfaces. These lines are fairly neat and homogeneous. On maps featuring rocky terrain, very heavy lines applied with a brush separate individual boulders. There is a notable absence of line when it comes to terrain, trees, and coastlines, which are established purely by chromatic means. The exception to this rule is the map of ‘Macao.’

### 3.2.4: Color

The colors in the maps are consistent. Water is typically rendered in a very deep, unmodulated blue. Terrain is described using including mid-tone green, tawny yellow, light brown, and beige. Vegetation is usually drawn in a darker version of the green used for grassy terrain, with black or brown for trunks of trees. Buildings are completed in white, brown, red, and sometimes pink. Fortresses are pink or white. Rocks are filled in with brown or black. The labels on all the maps are black.

### 3.2.5: Labels

Labels are written in black ink and delightfully wobbly capital letters, and in a few instances enclosed in a box (‘Sofala,’ ‘Mombaim,’ ‘Bahia de Beligãõ’). Text is generally restricted to toponyms, sometimes including those of non-Portuguese settlements. The hand of the all the labels appears to be the same, although the orientation of the label on the page is flexible; sometimes a toponym swoops down the side of a hill, other times it is nestled within the fortress walls, and in other

cases it is crammed wherever space remains. Numbers (related to the depth of water?) are inscribed in the water of the maps of 'Sofala,' 'Guale,' 'Bahia de Tanavare,' 'Bahia de Beligaõ,' and 'Triquilimale.' In only one case is a written explanation of the fortress provided<sup>2</sup>. In the maps of 'Quelba' and 'Mombaim,' for reasons which remain unclear, the toponym has been scrubbed out and moved to another position (to the detriment of the map's appearance, as the erasure was never perfect). From the dearth of labels, we may assume that the maps were meant to be presented with a companion text even before Bocarro's requisition request.

### 3.3: Map Signs

Though our focus will be on a subset of maps, their comprehension would be limited without an understanding of the cartography in the Évora codex as a gestalt. We have already surveyed the maps in terms of their format and general characteristics. Now we will turn to their use of signs. Moving category by category, we will examine the priorities of the mapmaker, explore the meaning of the signs he employed, and attempt to understand the ways the maps do or do not correspond to historical fact. We will see that color in the maps is used systematically and may provide valuable information. We will also consider the way the maps present Portuguese relations with local populations. Finally, we will see that Resende is not illustrating. Illustration would imply an effort to bring across what is individual to each place, to record the peculiarities of every region. Instead, Resende works towards a system of symbols, breaking down the chaos of the ramshackle empire and distilling its cities into orderly sets of objects from well-defined iconographic categories.

The sources drawn on to elucidate the maps' iconography were varied, and included the Bocarro text accompanying the plans, primary sources describing the fortresses and towns, modern and archival photographic documentation of the sites, and maps of the sites produced by other artists and cartographers in the fifty years before and fifty years after the Resende maps were completed. For the moment, we will not attempt to comprehensively correlate the structures on each map with extant buildings; extant buildings will only be called on to illustrate the sources for map signs and underscore the symbolic, rather than naturalistic, approach to portraying the cities and fortresses.

#### 3.3.1: Vegetation






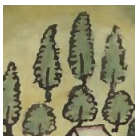
A visual summary of the vegetation signs included in the maps is provided in figure 13.<sup>3</sup> Vegetation on the scale of grasses is suggested broadly by the terrain washes referred to above. Trees and herbs tend to follow the contour of terrain washes and are distributed with uniform density within a given zone, rather than scattered across the landscape. Fields of crops are typically drawn from high oblique or plan view but prove a consistent problem due to the already complicated perspective scheme used in the maps. Trees include palms and a generic broadleaf. The vegetation signs may of the maps surely please

---

<sup>2</sup> This is the map of 'Manora,' where the author has labeled a church, a convent, and written among the houses the following: "Asy tem aqui 20 portuguezes cazados e 23 homens camezma 5 ha [?]. De prezidio e 80 gentios e mouros frexeiros e 20 [illegible] espingard [illegible]," giving the viewer of the map an awareness of the population of the town, its ethnic composition, and its readiness for armed conflict. The hand of this label appears different from the hand of the toponyms; moreover, the ink used is different (here a brownish ink).

<sup>3</sup> The region listed beside each image is merely an indication of the map from which the detail was taken. This does not imply that it is the only region to have a certain vegetation sign, nor even that the vegetation sign shown dominates in the map. Salsete's fields, for example, are mostly of the same type as Bardes and Agoada.



Palm Trees	Generic Broadleaf	Herbs	Gardens and Fields
 Borca	 Bardes and Agoada	 Barçalor	 Doba
 Corfacam	 Guale	 Borca	 Guale
 Soar	 Bahia de Tanavare	 Sera de Aserim	 Jafanapatam
 Tarapor	 Caliture	 S. Tome	 Bardes and Agoada
 Cambolim	 Coulam	 Moro de Chaul	 Mascate
 Doba	 Macao	 Chaul	 Salsete

**Figure 13:** Details of vegetation in the Évora codex maps.

the eye, but do they also encode clues about significant crops and natural resources of the region in the maps?

Rice took on life-or-death significance in the Portuguese cities of the *Estado*. This was particularly true of Goa, which imported most of its food and had been hit by a widespread famine during the years just prior to the completion of the maps (Pearson 1987, p. 154). The Count-Viceroy Linhares de Noronha only left the capital once during his stay in India, and it was for rice.<sup>4</sup> The crop had become a staple in the Goan Portuguese diet, to the chagrin of leaders like Albuquerque (*ibid.*, p. 105) and the wonderment of visitors from other European countries, who noted the deliciousness of the bread made of rice<sup>5</sup> eaten in ‘Damaõ’ (Daman) (Thevenot & Careri 1949/1656, p. 161). In the early 1600s, most of the rice consumed in Goa came from northern India (including Baçaim), southern India (including Barçalor and Mangalor), some interior regions, and the so-called Old Conquests of Bardes and Salsete (Disney 1996). After the famine of 1629-1632, the significance of this

<sup>4</sup> The voyage lasted 2 months. The security of supply routes had been threatened by the un-diplomatic decision of the Viceroy to build up the fort at Cambolim, leading to a dispute with local powers. Famine was on the horizon after bad harvests in several key regions. After buying up as much rice as possible, the matter of distribution remained. The disastrous mismanagement of this responsibility, and Linhares’ own possible role in rice profiteering, is discussed in detail by Disney (Disney 1996).

<sup>5</sup> A discussion of the strategies the Portuguese in India employed to recreate leavened wheat bread can be found in Collingham 2006, pp. 60-61.



humble crop would have been undeniable. Yet on this point the maps are unemphatic. Nothing like rice paddies can be seen in the maps of 'Mangalor,' 'Barçalor,' or 'Baçaim,' despite the fact that all three of these regions had been taken specifically to supply rice to Goa (Subrahmanyam 1984; Subrahmanyam 2012, p. 79). Rice paddies may be depicted on the Goa-adjacent territories of 'Bardes' and 'Salsete.'

Palm trees are drawn on all the maps in the codex except 'Dio,' 'Damaõ,' 'S. Tome,' 'Macao,' 'Solor,' 'Sera de Aserim,' and 'Moro de Chaul.' Palm trees had been exploited by local populations for many purposes, enumerated ecstatically by French visitor to the region François Pyrard (who considered palm trees "one of the great marvels of the Indies"). The palm, he relates, was used for paper, thatch, buildings; for its milk; to make black dyes (by steeping the sawdust of the nut in honey and water in the sun); to make paintbrushes; and to produce an oil which the Portuguese too used as an unguent and fuel for lamps (Pyrard 1887/1611, pp. 376-383). The Portuguese produced a sweet wine by combining palm-derived liquor with Persian raisins (*ibid.*, p. 383). If Careri is to be believed, the Portuguese also used palm fronds, borne aloft by slaves, as parasols when strolling (Thevenot & Careri 1949/1656, p. 160). The versatility of this crop and its capacity to impress Europeans may be part of the reason for its ubiquity in the maps.

The drawing of the fronds shows two patterns: simple, and with articulated individual leaves on each frond. The latter kind of palm can be found in the maps of 'Sibo,' 'Mada,' 'Soar,' 'Corfacam,' 'Quelba,' 'Matara,' 'Borca,' and 'Caliture.' It is only on the palms with articulated leaves that one can find fruits or trunks drawn with hatched details (although not all of them have this feature). Combining this with the geographical restriction of such palms to the Arabian peninsula (with the one exception of 'Caliture,' in present-day Sri Lanka), some hypotheses can be generated. It is possible that the artist randomly varied the style of palm tree. It is also possible that the different approaches to palm trees is caused by the collaboration of multiple painters with different preferred working style, and that the regional character of the variation is due to chance or to the maps being produced in batches, by region. A final option is that the artist intends to differentiate these trees from the other trees. The palm trees with articulated leaves (and sometimes fruits) may stand for date palms. Careri notes that the palm trees of India "produce no fruit, but they draw *nira*<sup>6</sup> from them" (Thevenot & Careri 1949/1656, p. 200). Date fruits, according to Tomé Pires, were brought in from Ormuz, in the Arabian peninsula (Pires 1949, p. 45). The distinction between two kinds of palms, meaningful or not, is obliterated in the maps of MS c.1635 Teixeira Albernaz and MS 1636 Anon. but retained in the maps of MS 1639 Carneiro.

A last case in which vegetation may be informative, rather than decorative, can be found in the map of 'Mascate.' The white fields (figure 13, right column) could represent cotton crops. Bocarro writes that "in [Mascate] there is some cotton, although not much, and for food they harvest wheat, barley, and some vegetables, but not in such quantity that rice is unnecessary..." (Bocarro 1992, p. 52, author's translation).

### 3.3.2: Rocks

Rocks in the maps take a variety of curious forms. On coastlines, they tend to be diminutive and of dark color. Inland, they take many forms but share a rhythmic, undulating repetitiveness (figure 14). The mutability of rock forms can be explained

---

<sup>6</sup> A sweet liquid that can be turned into toddy.

by the participation of multiple painters with personal approaches, an effort to individualize regions, or a single artist who is unsure how to portray the geology of regions he may not have seen.

### 3.3.3: Water, ships, and coastlines

Coastlines and riverbanks are marked by the abrupt meeting of land and flat dark water. Opaque white is frequently sponged along the water's edge, probably to demonstrate areas where waves break.<sup>7</sup> Water known to be shallow (significant for maritime transit between fortresses) is indicated with zones of black stippling, sometimes difficult to see in the dark water. The stippled zones seem to first be outlined by a tight line of dots, and then filled in less precisely (as in 'Mangalor') or washed over in a darker blue and then filled in with black dots (as in 'Mombaça'). Dangerous rocks in water are depicted in several ways: as crosses (in 'Tanavare'), as crosses with white sponging, pictorially (i.e., as rocks), and as a combination ('Coulam'). Anchors are drawn in the maps of 'Mascate,' 'Matara,' and 'Beligaõ.' See Appendix 1.2 for images of maps referenced.

Fluvial and marine water are rendered identically. Inland enclosed bodies of water (ponds, lakes) are outlined in or white, and sometimes include fine white overdrawn ripples on their surface (figure 15). Using satellite images, the relation of some of the maps' inland bodies of water to present-day lakes was investigated. This information would have been useful in understanding the scale at which the artist depicts this feature of the landscape. For 'Triquilimale' (Trincomalee) this was not feasible because the coastline depicted in the map departs radically from the coastline today. The same was true of 'Manar' (Mannar). In 'Ilha de Carania' (now the site of several cities on the landmass south of Mumbai) the river Resende included is partly discernable, but none of the small bodies of water in satellite images of the region can be definitively identified as those in the maps. In 'Cranganor,' the inlet included on the map seems to be Vijayan Thodu (a small river), but the lake in the map could not be matched to any specific extant body of water as several exist in the area.



Figure 14: Details of rocks in the Évora codex maps.



Figure 15: Details of inland water in the Évora codex maps.

<sup>7</sup> This sign is largely omitted in MS c.1635 Teixeira Albernaz possibly because of his use of a lighter tint for water, against which white would have shown up poorly. It is used in a neatened form (less like sponging, more like rows of white dots) in the maps of MS 1636 Anon. For an example of this technique in Resende's maps, see the plan of 'Salsete' in Appendix 1.2. 'Macao' is an exception to this tendency; instead of white sponging, it has overlapping black waves drawn over zones of white.

## Rowboats



Sofala



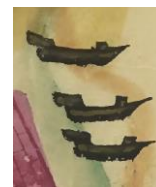
Macao



Chaul



Dio



Baçaim

## Large ships



Sofala



Guale



Bahia de Tanavare

**Figure 16:** Details showing all boat and ship signs in the Évora codex maps.

One water feature deserves special comment: the river that makes a left-turn to surround the fort of ‘Malaca’ (Appendix I.2). The elaborate game of telephone between mapmakers led to considerable confusion about the waterways of the region (for an in-depth discussion, see Wheatley 1954). This river is absent from the current landscape and absent from maps by Godinho de Erédia, who had spent time in the area and would know its details better than most European mapmakers. Following in Resende’s footsteps, Teixeira Albernaz I and Maris Carneiro (MS c.1635 Teixeira Albernaz and MS 1639 Carneiro) include the river. It is possible that this water feature is meant to represent a moat, rather than the mysterious river that Wheatley describes. It wasn’t until the Dutch rule more than 25 years after the maps were made that a moat was built around the fortress walls, although digging ditches around fortress walls was a common practice (Irwin 1962). Perhaps Resende was trying to compensate for the “work in progress” appearance of the fortress by including some defensive features not currently in place or was misled by his sources.

Rowboats outnumber ships in the maps (see figure 16). They would have provided a practical means of traveling along inland waterways or suitable craft for leisure boating. They are also depicted in the first edition illustrations of Linschoten’s *Itinerario*. The rowboats in the maps appear too small to be *fustas*, a hybrid rowing and sailing boat used in the *Estado*. The ships appear to be *naus* or carracks, given the characteristic u-shape of their bodies caused by high fore- and stern castles, their lack of elongated beak, and the way they sit high in the water. Ships of this kind could have been built in Asia; indeed, the availability of excellent timber in the many parts of the *Estado* allowed ever-larger cargo ships to be built (Rei 2011). The large ships are excluded in the MS c. 1635 Teixeira Albernaz maps, possibly because the fortresses at which they are stationed seem very random.

### 3.3.4: Churches and monasteries

Churches abound in the Évora codex maps. Although their scale and complexity would have been equivalent to or greater



**Figure 17:** Details from the Évora codex maps showing typical church signs.

that of houses, the artist draws them three-dimensionally. This may be because the churches tend to stand apart from other buildings, making it easier to draw them. The three basic types of churches are seen in the figure 17. More unusual churches can be grouped into four categories: (1) minorly atypical because of different building material or design, (2) Arabian peninsula regional variant, (3) pink churches, (4) and cylindrical churches.<sup>8</sup> With the exclusion of these atypical churches (figure 18), the core concept of a church is stable across the majority of the maps: single nave, topped with a cross, with or without cloisters and steeple. Differences between typical churches amount to little more than variations on a very familiar theme.

This convenient idiom bears a historical relation to the churches of the *Estado*. In contrast to the churches of New Spanish territories, so-called “hall churches” were common across Portugal’s strongholds in Asia and the Philippines (Luengo 2017). The map sign that Resende uses mirrors the actual geometry of most churches in the *Estado*, but the lack of embellishment on this sign reflects a severe simplification. The most cursory survey of extant churches dating to Resende’s period indicate a decadence and diversity that is utterly absent in the maps. The churches of the maps are many, but they are presented as humble, pious constructions. Drawing churches so plainly could have been a tactic for speeding up the production time for the maps or may have been a deliberate ploy. By offering up such unassuming churches, perhaps Resende tried to undermine claims that the Portuguese missionary effort was too focused on grandeur and show.

<sup>8</sup> The cylindrical style does have surviving examples, such as the Capela de Nossa Senhora de Candelária in Divar (1763) and the Church of Nossa Senhora da Conceição (second half of 17<sup>th</sup> century) in Mandapeshwar. The cylindrical church in the map of ‘Choraõ’ may represent the Hermitage of San Jeronimo, built in the mid-16<sup>th</sup> century (Mattoso 2010, p. 225). Bocarro does not reference this hermitage or the seminary that preceded it. Among extant cylindrical churches dating to Resende’s time and in the regions he depicted, this is the only example I have been able to locate.



The abundance of churches in the maps would seem to attest to a strongly implemented and well-organized messianic plan. The reality on the ground, however, was more complicated. Although the *Padroado* had at times functioned creditably and the Jesuit mission had expanded between 1580 and 1620 (Newitt 2005, p. 184), by the 17<sup>th</sup> century Portuguese leadership of evangelical work in Asia and Africa was frequently criticized (Boxer 1973, p. 247). The upkeep of a sound religious infrastructure was costly, and funding to maintain churches was often insufficient, misused, or flagrantly allocated to festivals and pageantry (*ibid.*, pp. 235-237). In some regions, clergy were unavailable to Portuguese residents. Writing in the early 1670s, Abbé Carre remarked on the beautiful churches of Chaul, but noted that most of them were deserted (Carre 1947, p. 189). Speaking of ‘Damaõ’ (Daman), he adds “There are so few priests now that there are not enough to serve the churches; and the two outside the town [...] have no services for want of clergy” (*ibid.*, p. 167). Whether this was the case during the early 17<sup>th</sup> century is not certain. If we consider the same cities two as described by Bocarro, in the 1630s there were at least 32 *religiosos* in ‘Damaõ’ (although his numbers fluctuate throughout the text), and in Chaul more than 80 (Bocarro 1992).

For all the emphasis Bocarro lays on the clerical apparatus in India and its breakdown by religious order, no information about confessional affiliation is given in the maps, although the edifices in the maps of India do seem to represent real churches (as will be seen in the next chapter). Silence on religious order is typical of maps from this period. Discussing the signs used on printed maps between the 1470-1640, Delano-Smith notes that “despite an acute interest in matters of confession during and after the Reformation, only a few mapmakers showed confessional allegiance on their maps” (Delano-Smith 2007).

Cylindrical churches may indicate personal knowledge of the architecture of a region; in the case of ‘Choraõ,’ the cylindrical church may be the Hermitage of Saint Jerome and its seminary (Mattoso 2010, p. 225). Any trace of a cylindrical church in ‘Maim’ (modern day Mahim) is now undetectable due to the former fortress’s state of ruin (*ibid.*, p. 140). It is likewise impossible to identify the building represented by the atypical church from the map of ‘Tana’ (Thane).

### 3.3.5: Crosses (*cruzeiros*)

Freestanding are typically found in front of the entrance to churches. They are drawn homogenously and simply, probably

Atypical Construction  
Material or Style



Macao



Baçaim



Sera de Aserim

Arabian Peninsula  
Regional Variant



Mascate



Soar



Doba

Pink



Guale



Batecalou

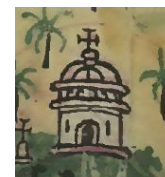


Manar

Cylindrical



Maim



Choraõ



Tana

**Figure 18:** Details from the Évora codex maps showing atypical church signs.

because of their minute size and enormous quantity in the maps. *Cruzeiros* are included in modified form in several subsequent maps of the regions (including MS c.1635 Teixeira Albernaz, MS 1636 Anon., and MS 1639 Carneiro).

In later engraved maps not connected with Bocarro's or Resende's text (but based on Resende's models), the number of *cruzeiros* is frequently reduced. In G. Child's map of "Cochin" (E 1729 Child), Resende's composition is freely utilized, but the 13 *cruzeiros* are gone (figure 19).

### 3.3.6: Non-Christian Religious Architecture

**Buddhist Temples:** Buddhist temples could not be located on the maps, although the map of 'Caliture' (Kalutara) in Sri Lanka gives us an example of what, until recently, had been the site of a temple (Appendix I.2). The map portrays a fortress on a hill, with four stone towers at its corners and a rudimentary wooden stockade running between them to form a square. Half of the houses are white-walled and red-roofed, and half are thatched, and the two are mixed amongst each other both inside and outside of the fortress. The fortress, constructed in 1622, was built on the site of the ancient Gangatilaka Vihare after it had been demolished (de Silva 1988, p. 203).

**Mosques:** In a few cases mosques can be recognized in the Évora codex maps (see figure 20 for a non-cartographical depiction of a mosque and Hindu temple and figure 21 for a complete inventory of mosques identified in Évora codex maps). Geographically, clearly-indicated mosques can be found in maps from the southwest Indian subcontinent, and in Sri Lanka. The clarity of this symbol to Resende's contemporaries is apparent in later maps, which record the same structures but add labels. Given the strained relationship between Portugal and the "Moors," the inclusion of these buildings in maps should not be taken as a sign of religious acceptance and harmony, but as a signifier of a population loyal to a rival sovereign; a warning sign and a grudging acknowledgement of the failures of conversion efforts on Muslims within and adjacent to the *Estado*.



Figure 19: E 1729 Child map of 'Cochin' ('Cochim,' present-day Kochi)

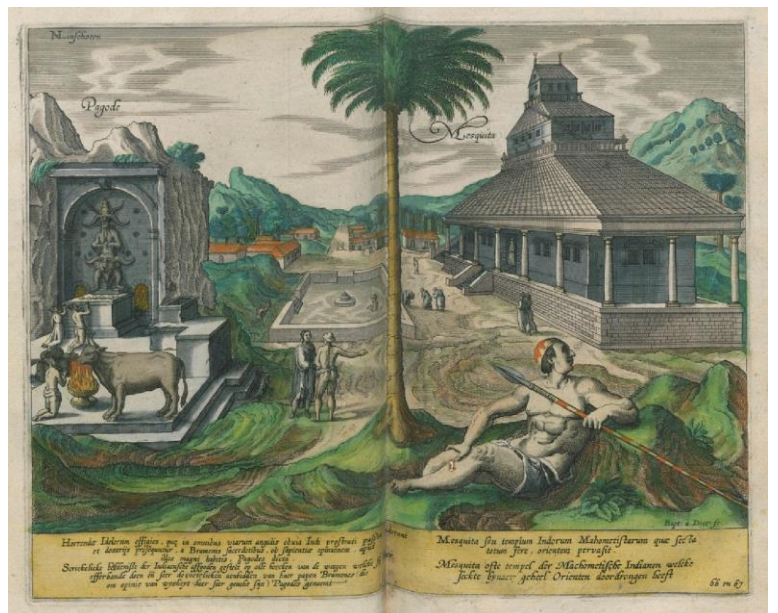


Figure 20: Depiction of "pagode" (left) and mosque (right). From 1596 illustrated first edition of Linschoten's *Itinerario*, digitalized by the University Library of Utrecht ( <http://bc.library.uu.nl/key-east-jan-huygen-van-linschoten-s-itinerario.html>)



Barçalor de Cima



Cambolim outskirts



Manar



Near Banguel (map of Mangalor)



Olala (map of Mangalor)

**Figure 21:** Details of mosques in the Évora codex maps.

Besides the instability of the pictorial sign used for mosques across the maps, a few additional features should be noted. First is the frequent use of pink, a color typically associated with fortifications. This may hint at the military relevance of Muslim-identified regions. The pink tower in 'Manar' is labeled *Alcoran* (mosque) in MS 1636 Anon, but in the Évora codex and the MS c.1635 Teixeira Albernaz it is topped with a cross (figure 21). What to make of this structure is uncertain. It was not possible to correlate it definitively to any extant structure in the region of present-day Mannar in order to establish its identity and history.

**Hindu temples:** Hindu temples are more difficult to pinpoint than mosques. It is probable that large temple complex had been drawn on the lost map of 'Negapatam,' since the maps of MS 1636 Anon. and MS c.1635 Teixeira include and label such an enclave (figure 22). As the drawing of the MS c.1635 Teixeira Albernaz follows closely that of the Évora plans, we can infer that the lost map's temples were drawn with a fair amount of heterogeneity but were united by their deviation from the rectangular prism form taken by most other buildings. Temples of this kind should be easy to distinguish from cylindrical bastions because of their location and lack of crenellation. Periodic campaigns to demolish temples adjacent to Portuguese fortresses might explain the apparent absence of temples on the maps. In 1540, Goa's temples were destroyed. The temples of 'Bardes' met the same fate in 1573, and 'Salsete' between 1583 and 1587. King Felipe III wrote of plans to pillage the great temple of Tirupati for profit in 1610, indicating cognizance at the highest echelons of Portuguese governance of the architectural riches held by Hindu rulers. Nonetheless, as late as 1623 the Portuguese in Goa complained of a huge population of Hindus in their midst, presumably with places of worship (Subrahmanyam 2012, pp. 242-243). In the second half of the 17<sup>th</sup> century, Thevenot references great temples on the river running from 'Cochim' to 'Cranganor' and in the outskirts of 'Cochim' (Thevenot & Careri 1949/1656, p. 124) as well as many in 'Salsete' (*ibid.*, pp. 173-178) and in the environs of Goa (*ibid.*, p. 171). If temples continued to proliferate in the areas in and around Portuguese forts, where are they in the maps?

One possibility concerns Portuguese reluctance to venture inland, allowing sacred images to be surreptitiously removed from temples in imminent danger and placed in ad-hoc temples just outside of Portuguese control (Axelrod and Fuerch 1996). For the same reason, inland temples would have survived unscathed but not feature in the coast-centric maps. Another cause of their seeming absence could be their repurposing as churches. Careri visits an underground church beneath a Franciscan college and monastery that had originally been a rock-cut Hindu temple (Thevenot & Careri



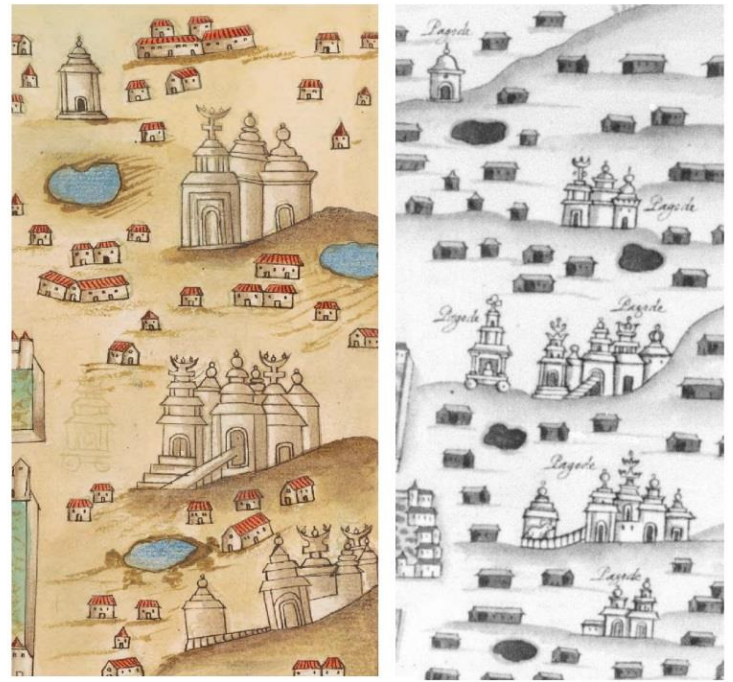
1949/1656, p. 172). This opens up the possibility that some of the more unusual churches on the maps could have originally been temples (such as the one in the map of ‘Tana,’ figure 18 bottom right).

The omission of temples may relate as well to limitations of Resende’s knowledge, and to the fact that these maps are not unbiased documents. The map of ‘Triquilimale’ can shed light on this issue. It has been suggested that the group of three atypical buildings on the map correspond to the three classical-medieval Koneswaram temples, which were destroyed in 1622 by Portuguese general Constantino de Sá Noronha to make room for fortifications (Sivaratnam 1964, pp. 255-256) (figure 23, middle). Luckily for us, the general made sketches of the “pagodes” before demolishing them (figure 23, left). If the structures in Triquilimale are taken to be temples, then we may find temples in other maps, including Dio (figure 23, right).

If we take the opposite tack, finding examples of sites where Hindu temples did exist but are not depicted is straightforward. ‘Ilha do Elefant,’ on the map of ‘Mombaim’, is drawn as a hilly little island with a white flag and a tower (Appendix I.2). In reality this island is and was the home to a series of Hindu rock-cut temples (now called the Elephanta Caves) dating to the 5<sup>th</sup>-6<sup>th</sup> centuries CE and currently registered as a Unesco World Heritage Site (for more information, see the report at <https://whc.unesco.org/en/list/244>). That the Portuguese were aware of the temples is obvious. Bocarro describes them as follows:

“There is on said island a pagoda, which is called Elephant, a work extraordinarily grandiose because [...] [it] was cut from a hill entirely of stone with pickaxes [...] with columns of the same stone with figures chiseled with great perfection” (Bocarro 1992, p. 119, author’s translation).

How the Portuguese dealt with these temples is less certain. One Dr. John Fryer wrote in 1673 that the monuments had been defaced by the Portuguese, and a Captain Pyke wrote at the start of the 18<sup>th</sup> century that a bored fidalgo had used



**Figure 22:** Left: detail, MS c.1635 Teixeira Albernaz plan of ‘Negapataõ’ (Biblioteca Nacional de España). Right: MS 1636 Anon. detail of the same region (Bibliothèque Nationale de France).



**Figure 23:** (left) drawing of a ‘Triquilimale’ shrine by Constantino de Sá Noronha (from *Plantas das fortalezas, pagodes, & ca. da ilha de Ceilão*. 1687); (middle) the same shrines in the Évora codex map of ‘Triquilimale’ (?); (right) unidentified structure in the Évora codex map ‘Dio.’



the pillars for shooting target (Ramaswami 1979, p. 47). Whether this account is accurate or was fabricated to impugn the conduct of the Portuguese nobility is unclear.

For all the ambiguity we have encountered, two points are patently evident. The first is that the draughtsman struggled to develop a consistent map sign for Hindu and Muslim places of worship. The second is that his sparing use of these signs systematically minimizes or conceals the presence non-Christian populations in the *Estado*.

### 3.3.7: Administrative Structures

**Pillories and gallows:** The *forca* (gallows) is seen in the maps of ‘Monsambique,’ ‘Mombaça,’ ‘Damaõ,’ and ‘Malaca’ (figure 24). Their identification was made through cross-referencing with labeled maps and with historical texts. Pillories can be identified definitively in Chaul, ‘Moro de Chaul,’ ‘Mangalor,’ ‘Manar,’ and ‘Damaõ’ (figure 24). Their identification was based on cross-



**Figure 24:** Details from the BPE maps showing pillories and gallows. (Top, left to right) Map of ‘Damaõ,’ ‘Monsambique,’ ‘Malaca,’ ‘Mombaça.’ (Bottom, left to right) ‘Manar,’ ‘Mangalor,’ ‘Moro de Chaul,’ Chaul (not pictured: pillory of ‘Cochim’). (Far right) ‘Damaõ.’

reference with MS 1600-1650 Teixeira Albernaz, with extant pillories (Mattosa 2010, p. 239), and by recognizing their repeated elements across maps (pediment, column, two spheres at the top). The presence or absence of these signs in the maps does not necessarily correspond to reality. In the map of ‘Baçaim’ for example, there are neither pillory nor gallows, but Bocarro attests that a pillory did exist, even specifying the location (Bocarro 1992, p. 109). In ‘Cochim,’ where no gallows is painted, Pyrard says that near St. John’s Square (in the center of the city, on the mainland) “[the Portuguese] showed us a gallows tree, whereupon two or three Hollanders had been hung” (Pyrard 1887/1611, p. 500). Although there is a pillory in ‘Cochim,’ there is no gallows (unless the unidentified map sign in figure 28 is a strange gallows sign). Gallows are usually placed on the edges of settlements (Delano-Smith 2007), although the one in ‘Malaca’ is rather centrally located, and in a suburb that was notoriously crowded. The suburb’s demographics will be discussed below; that this symbol of Portuguese law and power came to reside there is interesting.



Câmara (Baçaim)

Warehouse (Borca)

Prison (Mombaça)

Well (Corfacam)

Cistern (Camolim)

**Figure 25:** Representative images of administrative structures.

**Câmara (municipal council):** To the extent that *câmaras* can be identified in the maps, they are drawn as large buildings with flags, usually near the center of the town (figure 25, far left).

**Warehouses:** Bocarro describes several solutions for the storage of food and munitions at the fortresses, not all of which would have been amenable to pictorial record. Nonetheless, several maps of fortresses on the Arabian peninsula ('Sibo,' 'Quelba,' 'Libedia,' 'Mada,' and 'Doba') include what appear to be locked magazines (figure 25, second from left).

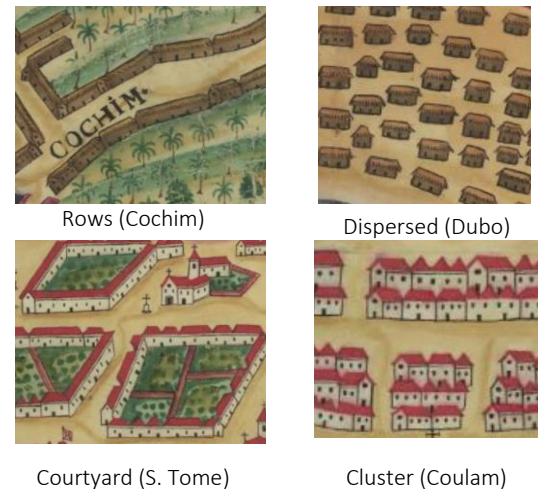
**Wells and cisterns:** Wells are plentiful in the maps. They are drawn with extreme uniformity, with a base color of light pink and darker pink bricks outlined on top. Some maps include dark blue within the well to show water (such as at 'Samges'); others do not ('Solor' for example). Five maps include rectangular water tanks ('Sera de Aserim,' 'Moro de Chaul,' 'Cambolim,' 'Barçalor,' 'Mangalor'). These may be the ablutions tanks and bathing pools used by local populations and described in the accounts of Pyrard, Thevenot, and Linschoten (Pyrard 1887/1611, pp. 125, 402; Thevenot & Careri 1949/1656, p. 114; Linschoten 1885/1596, p. 283) (figure 25, far right and second from right).

**Prisons:** Although it is possible to determine the location of several prisons in the *Estado* by consulting primary sources, only once does Resende use a pictorial sign (figure 25, middle).

### 3.3.8: Houses

With rare exceptions,<sup>9</sup> the houses in the maps fall into three categories: completely white, white-walled and red-roofed, pink, and brown-walled with thatch roofs. The spatial arrangement of the houses follows 4 patterns: dispersed, rows, courtyards, and clusters (see figure 26), with thatched roof houses generally following the dispersed pattern and houses with white walls and red roofs either clustered, arranged around gardens, or forming long chains and rows. The all-white houses are mostly restricted to the Arabian peninsula (an area where several regional variations on the map signs can be found); the pink houses can be found in some cities of present-day Sri Lanka where the Portuguese town is located on a cape which is fortified against the inland ('Guale,' 'Triquilimale'). Considering the difficulty the Portuguese had in securing their presence in Sri Lanka, this color use may not be accidental. As we will see, the color of the maps may be a kind of map sign in and of itself, and pink is deeply connected with the maps' iconography of defense.

It is tempting to assume that the white and red houses indicate Portuguese settlements, while the thatched houses mark indigenous populations. An in-depth treatment of the way demographic distributions are depicted in maps of this period will be the subject of further work; for the moment, a word of warning will suffice. Although it is beyond the scope of the current research to comprehensively address the cartographic portrayal of demographic distributions in the *Estado*, 'Malaca' provides a cautionary tale against hasty conclusions. At first glance, Resende's map offers us a clear dichotomy:



**Figure 26:** Housing distribution patterns

<sup>9</sup> See the houses of 'Olala' on the map of 'Mangalor,' which are an unusual warm pale pink (Appendix I.2).

pink stone fortress walls with white and red houses inside, and in the surrounding country, fortifications in wood with thatched earthen houses (figure 27). The illusion of a well-defined Portuguese zone and indigenous zone begins to erode when one notes the presence of a Portuguese banner and *forca* on the settlement at the far left of the map. The churches in the thatched house settlement provide ambiguous evidence for Portuguese habitation in these areas, given the fact that Jesuit missionaries were known to sometimes live among the native populations, speak in their language, and wear their attire. Although Erédia wrote about ‘Malaca’ earlier and his map does not seem to be the model for Resende’s, his depiction of the area is illuminating. The settlement with two churches and a *forca* on the left of Resende’s map correspond to the suburb of Upé on Erédia’s 1604 sketch entitled ‘Fabrícia da Cidade de Malaca Intramuros’ (reproduced in Loureiro 2008). Of this settlement, Erédia says:

“This suburb [of Upé] is divided into two Parishes: St. Thomas and St. Stephen...in [St. Thomas] live the Chelis of Coromandel who must be the ‘Chalinges’ of which Pliny writes in Chapter XVII of Book VI. The other parish, St. Stephen, is called Campon China...[and here live] the ‘Chincheos’ descendants of the ‘Tocharos’ of Pliny, foreign merchants and natives occupied in fishing. The two parishes...contain 2500 Christians, men, women, and children, beside the other heathen inhabitants. The houses are all built of timber and are cover’d with tiles to preserve them from the risk of war. Stone buildings are, for reason of defense in case of war, not allowed.” (Maxwell 1911)

Before the Portuguese arrived, the suburbs of Upé had been the dominion of Hindu traders from the Coromandel coast, as well as a sizeable Chinese and Javanese community. The wooden palisades, however, were a Portuguese addition (Maxwell 1911), and by the end of the 16<sup>th</sup> century, Upé was also home to a number of Portuguese married men who lived in “thatched houses, which are risky in case of a fire” (Bocarro 1992, p. 251, author’s translation).

The colors of the houses in the maps signal differences in construction method. Across the *Estado*, the methods and materials used in building were determined by a variety of concerns. To begin with, many of the areas the Portuguese would capture already contained established populations and fortifications. The housing arrangements in some of these regions were described by Bocarro and other European travelers. These could include



Figure 27: Évora codex map of ‘Malaca.’ Copyright Biblioteca Pública de Évora.

earth-walled, palm-thatched houses (see Thevenot & Careri 1949/1656, pp. 160 and 179 for example), wood houses (Pyrard 1887/1611, p.118), or stone houses (Linschoten 1885/1596, p. 286; Pyrard 1887/1611, p. 403). Of course, different regions had different ways of constructing houses, but even where the homes were made of stone, European visitors were often unimpressed, complaining that the local populations lived in dark houses and cramped neighborhoods (CITE). The white buildings seen on the maps, where they really existed, represent an effort of the Portuguese to hold onto something familiar. The means by which this normality was achieved resulted in what Luengo has termed “architectural hybridity”

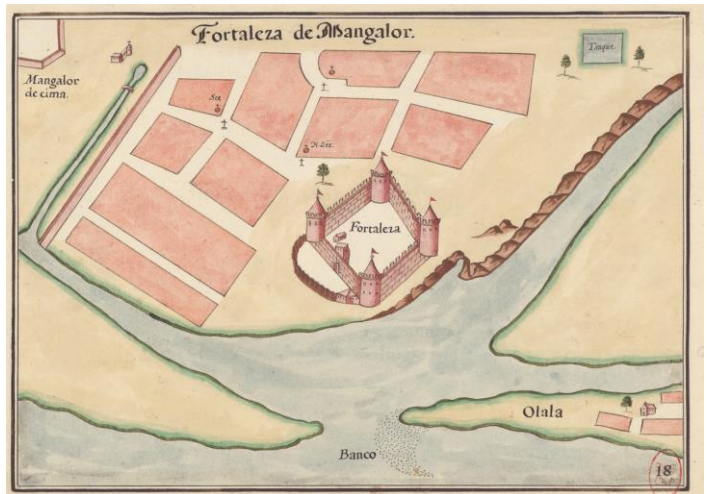


(Luengo 2017). Well-known manifestations of such hybridity include exploitation of oyster shells to fashion windowpanes similar to the glass used in Europe, and whitewashing buildings with lime made from crushed, burned shells (rather than the familiar rock lime) (Thevenot & Careri 1949/1656, p. 158; Luengo 2017). The Portuguese did not necessarily, as Silveira asserts, import their lifestyle whole-cloth into the far reaches of the empire (Silveira 1957, p. 21). But where it mattered, they did their best to approximate it.

### 3.3.9: Fortifications

We have already touched upon the design of their fortresses in discussing the use of perspective and scale in the maps, and the shape of the fortresses under Cid's typology. We will now consider an aspect peculiar to Resende's maps, and up to now not well understood or described: the color of the fortresses.

A striking feature of the maps is the use of the color pink for fortresses. There are two pinks used in the depiction of military architecture: rose pink, and orangeish pink. Fortifications in rose pink include detailed overdrawing in maroon. On the external faces of walls and towers, individual stones are drawn in a precise and painstaking manner. The internal faces of walls, in contrast, are ornamented with dashes.<sup>10</sup> Orangeish pink walls are left without any overdrawing and merely outlined in maroon. Orangeish pink walls can be found on military structures in six of the forty-eight maps: 'Monsambique,' 'Salsete,' 'Barçador' and 'Barçador de Cima' and 'Cambolim,' 'Mangalor,' 'Cananor,' and 'Cranganor' (see Appendix I.2). Using the number of pages of accompanying text by Bocarro as a very rough proxy for importance (or availability of information), all of these places except for 'Mangalor' fall into the "highest importance" category,



**Figure 28:** (top) BPE map of Mangalor; (bottom) MS 1600-1650 Teixeira Albernaz map of Mangalor (copyright Bibliothèque Nationale de France). The Texeira Albernaz map is clearly based on the map of the same region by Godinho de Erédia, *Lyvro de Plantaforma das Fortalezas da India*, Fortaleza de S. Julião da Barra, Oeiras, c. 1620.

<sup>10</sup> It is unclear whether these two textures indicate anything more than internal and external faces of walls. Given the comparative difficulty of drawing individual stones versus rows of dashes, one might expect that very small forts on very large-scale maps would tend to have dashes. This is not the case: the miniscule plans of the fortresses of 'Bardes' and 'Agoada' on the large-scale map of 'Salsete' have individual stones. Meanwhile, the fortress at 'Tarapor' includes one section with external walls overdrawn with dashes, and one section with individual stones. Last, on the map of 'Barçador' and 'Barçador de Cima,' the fortress of the former is drawn with in the usual way (external walls with individual bricks, internal with dashes), and the latter with dashes exclusively. In this case, the difference in the surface texture between the two fortresses may function as a visual cue of a social distinction. 'Barçador' proper was a Portuguese base, and 'Barçador de Cima' was the territory of the *gentios* (non-Christian local people), according to Bocarro (Bocarro 1992, p. 185).

with 'Mangalor' in the second-highest category. This may be related to their location: other than 'Monsambique,' all of these fortresses lie in close proximity to each other and are found on the western side of the Deccan peninsula just south of Goa (the capital of the *Estado*). With the significant caveat that Resende's knowledge of the state of all of the fortresses was imperfect, what can we deduce from this chromatic polymorphism?

There are some indications that the occasional rendering of walls in orangeish pink served a communicative purpose: specifically, it functioned to indicate walls constructed such that they were not capable of withstanding significant battery. Various versions of the map of 'Mangalor' can illustrate this point. The map of MS 1600-1650 Teixeira Albernaz (figure 28, bottom) does not include orangeish pink walls. The building connected to the outer bottom left wall of the fortress is also absent in this map, with a timber fence in its place. A likely explanation for these differences is that the Teixeira Albernaz modeled this map of 'Mangalor' on an earlier depiction of the region by Manuel Godinho de Erédia included in *Lyvro de Plantaforma das Fortalezas da India* (Fortaleza de S. Julião da Barra, Oeiras, c. 1620; reproduced in Cortesão & de Mota 1960b) which is compositionally and informationally identical. The maps of MS c.1635 Teixeira Albernaz are modeled on the map of the Évora codex. Though the walls of 'Mangalor' in MS c.1635 Teixeira Albernaz are all the same color, those that were orangeish pink in the Évora codex map lack overdrawn stones in the Teixeira Albernaz map. Taking also into consideration the timber (not stone) towers on Resende's map (figure 28, top), we can theorize that these orangeish pink walls are temporary, weaker constructions (perhaps made of wood and packed earth), which over time, section by section, could be replaced with sounder stone works. This gradual approach to fortification has been described with regard to several fortresses in the *Estado* (see, for example, Mattosa 2010, p. 102 regarding 'Damaõ' (Daman), or Irwin 1962 on Malacca).

An analogous example can be found in the case of 'Barçalor' (Appendix I.2). In the Erédia map from 1620 (in *Lyvro de Plantaforma das Fortalezas da India*, Fortaleza de S. Julião da Barra, Oeiras; reproduced in Cortesão & de Mota 1960b), there is a timber construction extending from the bottom left fortress wall to the water, and no sign of the orangeish pink wall and its wood bastions that Resende records. It is probable that either from letters sent to the Viceroy, or through encounters with other unknown maps or with the fortress itself, Resende updated Erédia's depiction to reflect the reality of the fortifications as he knew them.

In the instances above, the orangeish pink walls seem to signify new constructions that have not yet been properly fortified. In other cases, we cannot determine whether the walls are dilapidated or merely unfinished, but the Bocarro text underlines their inadequacy. Describing 'Cranganor' (another city with orangeish pink walls; see Appendix I.2), he says: "All the said town [...] is encircled with a wall that doesn't exceed a *braça* and a half [approx. 3.3 meters] in height, very homely and broken [...] [and which] cannot suffer any battery" (Bocarro 1992, p. 187, author's translation).

The choice of pink to begin with may be connected with the geology of Goa, where Resende spent most of his time in the *Estado*. The soil and stone in the area is an iron-rich laterite material that has a deep reddish hue. Given the wide swath of territory across which the Portuguese fortresses were strewn, multiple materials were employed to construct fortresses and walls. Bocarro notes that the forts at 'Borca,' 'Quelba,' 'Doba,' and 'Coriate' were made of adobe, adding that this material is commonly used by the "Moors" in Arabia (Bocarro 1992, p. 43). Nonetheless, for purposes of uniformity



**Figure 29:** Pink fortifications in Mughal and Rajput art. (Clockwise from right) ‘Mesbah the Grocer Brings the Spy Parran to His House’ (c. 1570), Metropolitan Museum of Art. ‘Assad Ibn Kariba Attacks the Army of Iraj Suddenly by Night’ (c. 1570), Metropolitan Museum of Art. ‘Khambavati Ragini of Malkos’ by Nasir ud-Din (1605), San Diego Museum of Art.

(and since Resende did not personally see each fortress) pink is the default for military architecture throughout the maps. The notable exception to this rule (‘Damaõ’) will be discussed in the chapter to follow.

It is worth noting that Resende’s maps are not the only paintings to use this shade of pink: among the miniatures produced by artists in Mughal courts, the color is frequently encountered. It can also be found in the output of some Rajput workshops. In using pink, these Indian artists may have brought a stylized realism to their works. See figure 29 for examples of pink fortifications in Mughal and Rajput art.

### 3.3.10: People

Only two maps in the Évora codex include people or animals. These are the maps of ‘Libedia’ and ‘Guale’ (figure 30). The figures on the map of ‘Libedia’ ride camels and their attire resembles the costumes of Arab traders depicted in the codex Casanatense 1889. The style of turban the figures wear is akin to those in Persian manuscripts from the Safavid period (figure 31), and to those in Ottoman miniatures. Although it is not possible to precisely identify the nationality of these characters, the mapmaker seems to want to represent sojourners from the Middle East.

The figures in ‘Guale’ wear the topknots documented in the codex Casanatense 1889 in the illustrations of Sinhala women and Sinhala warriors. The figure with the long skirt may be a women; writing in the late 17<sup>th</sup> century, Robert Knox comments that the women of “Ceylon” wore “necklaces of Beads or Silver, curiously wrought and engraved, gilded with Gold, hanging down so low as their breasts [*sic*]” (Knox 1681, p. 90). Centuries earlier, Marco Polo had remarked on the habit of both men and women to go uncovered above the waist (Polo 1993/c.1300, p. 312). A transitional period seems to



have been underway by the 17<sup>th</sup> century, possibly caused by increasing contact with Europeans. Knox states that women covered their chests when outside the house, but indoors dressed however they felt comfortable (Knox 1681, p. 90). Queyroz, writing in the same century, is more specific, stating that “the common women folk wear a piece of cloth white, red or striped, twelve cubits of the hand in length and two in breadth, half of which they gird round the waist and the other half above the shoulders when they go to work” (Queyroz 1930, p. 82). The female (?) figure on the map may be bare-chested to highlight the un-Europeanness of the people of ‘Guale.’

In short, the figures in the maps do not seem to be pure fantasy, but are attired in fashions compatible with the regions in which they are depicted (albeit perhaps with a touch of anachronism). It is unclear, however, whether these figures were part of the original composition that left Goa in the 1630s or were added sometime later. The fact that the MS c.1635 Teixeira Albernaz, MS 1636 Anon., and even MS 1639 Carneiro maps have no such figures is suspicious. Future research on a larger subset of the maps is needed to grapple with this question.

### 3.3.11: Unidentified map signs

Figure 32 provides details of map signs whose form or meaning raised questions that could not be answered.



Figure 32: Undeciphered map signs.



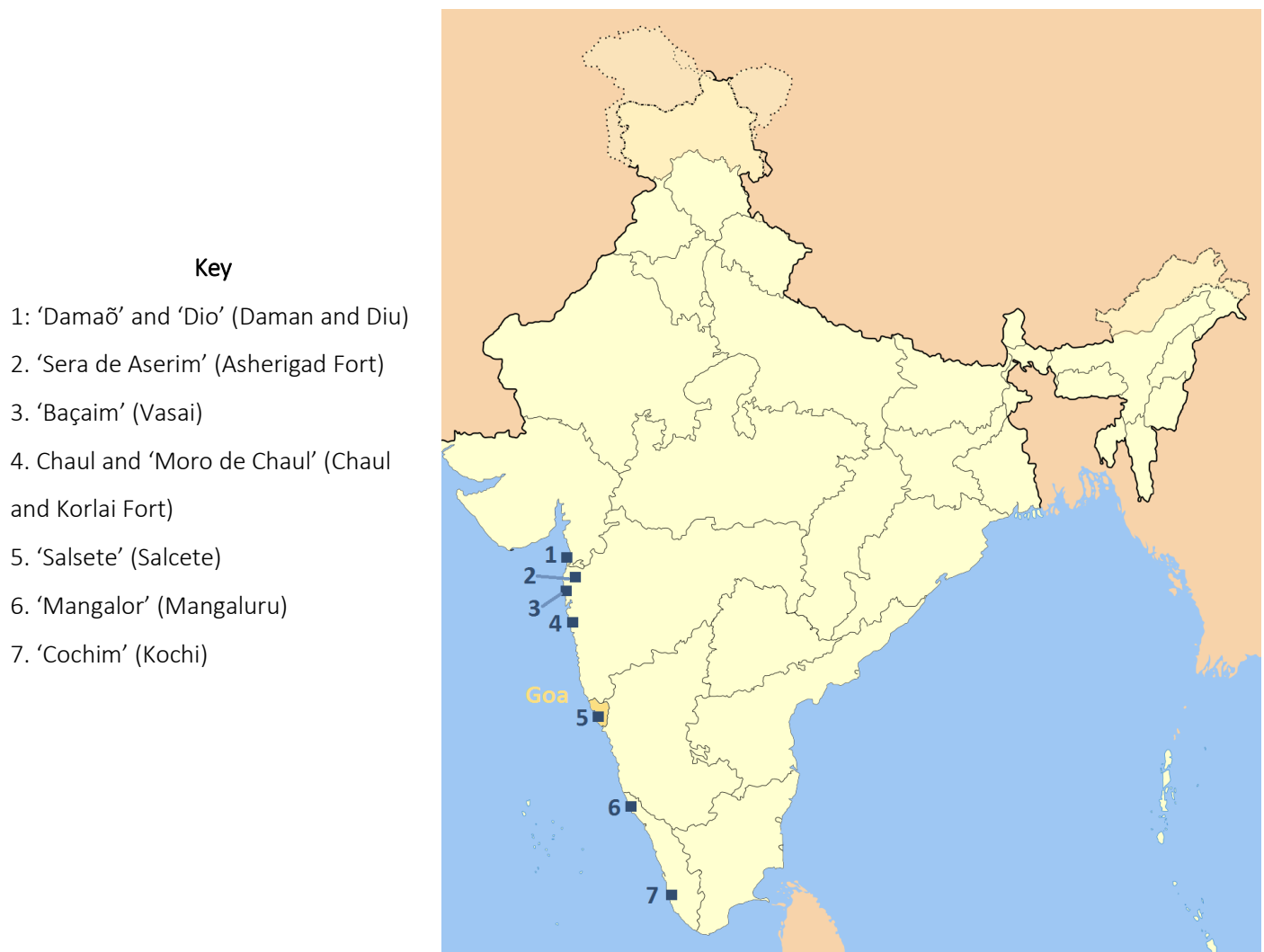
Figure 30: People in the Évora codex maps. (Left) map of 'Libedia' (detail), (right) map of 'Guale' (detail).



Figure 31: 'Nomadic Encampment,' Iran, c. 1540. Opaque watercolor with gold and silver on paper. Harvard Art Museums/Arthur M. Sackler Museum, Gift of John Goelet, formerly in the collection of Louis J. Cartier.

## Chapter 4: Maps of India

Due to the time constraints of the present work, it has been necessary to restrict production methods and materials characterization to a subset of the maps. Several groupings of maps could have been made according to various parameters. The maps of a geographical region could have been chosen for investigation (for example, the maps of the Arabian Peninsula, including 'Quelba,' 'Corfacam,' 'Borca,' 'Sibo,' 'Coriate,' etc.). Alternatively, a subset containing one major fortress from each geographical region could have been constructed ('Monsambique' for Africa, 'Malaca' for Malaysia, 'Macao' for China, 'Mascate' for the Arabian Peninsula). Another approach would have been to investigate a grouping in which a "control" map having the most typical stylistic and iconographic features is compared with "irregular" maps (with 'Barçalor' as a control, and 'Macao,' 'Corfacam,' 'Bahia de Tanavare,' and 'Moro de Chaul' as atypical).



**Figure 33:** Selected Portuguese fortresses and cities in India.



We have chosen to focus on the maps depicting important fortresses of India (see figure 33). The primary reason behind this decision is that as Secretary of State, Resende was stationed in Goa and was probably more familiar with the fortresses and cities of India than those of farther-flung territories. The maps of this region may therefore offer richer and more informative depictions of the *Estado*. Additionally, the maps of India have features roughly typical of the *oeuvre* on a whole, and the colors employed therein are diverse enough to explore a large part of the overall chromatic palette. Last, several maps of Indian fortresses have revisions and erasures, which can offer insights into the maps' production process and the sources that informed the cartographic design.

We will begin with some history, aiming to sketch out the role of each fortress in the *Estado* and the issues facing it in the 1630s. These introductions will focus less on fortification technologies and more on the human factor for each site, seeking to see within and beyond the walls to the people who inhabited the maps. Next, we will draw on outside sources to locate and describe the specific features recorded in the maps of five famous fortresses and provide an annotated version of each map. The reader is welcomed to jump ahead to the annotated map after reading the background for a given fortress city or read the chapter in the order in which it is presented.

## 4.1: Introducing the fortresses and towns

### 4.1.1: 'Damaõ' (Daman)

The site was captured in 1559 with the aim of tightening control over trade across the Gulf of Cambay (Pearson 1987, p. 31), but Portuguese Catholics remained a small minority in the city throughout its post-conquest history (Mattoso 2010, p. 100). This does not mean that the Portuguese lived among the locals of the region. In the late 1600s, Abbé Carre remarked that "the town is inhabited by Christians, both Portuguese and half-castes. They will not allow Moors, or Hindus, or people of any other heathen religion to dwell there. The latter dwell in the outskirts and neighboring villages, so that in Daman one can hardly find two hundred men who bear arms. Most of the houses are filled with women, who make dainties and sweets, and with troops of slaves who have hardly any food but rice and fish" (Carre 1947, p. 168). This observation is seconded by Careri, who says that "on the north side of the city is a small suburb, consisting of cottages cover'd with palm-tree-leaves, and inhabited by Christian Blacks; and a small distance from it, a village of Gentils, with a Bazar" (Thevenot & Careri 1949/1656, p. 159).

The eventual layout of the city set it apart from other Portuguese fortress towns: it followed a strict grid rather than an informal "medieval" pattern (Silveira 1957, p. 25; Mattoso 2010, p. 104). Careri described it as "[...] ill peopled, [but] beautiful enough, and built after the Italian manner" (Thevenot & Careri 1949/1656, p. 158). Its special status within the *Estado* is highlighted by the fact that it was accorded the same municipal privileges as Évora during the 1560s. It is also implied by a deal struck with the Mughal emperor Akbar in the late 1500s: the emperor promised not to strike Daman if the Portuguese consented the use of his name in Diu mosques and the replacement of old Gujarati coins with his coinage (Newitt 2005, p. 185). The fortress of 'Sam Irm.' (Saint Jerome) seen on the map was completed in 1627; the city walls were still in progress when Resende's map was produced (Mattoso 2010, pp. 105-106). Portuguese rule of Daman would end only when it was reclaimed by India in 1962 (Jayasuriya 2008, p. 6).

#### 4.1.2: 'Dio' (Diu)

When the Portuguese arrived at Diu, local rulers assumed they were just one more trading outfit hoping to get rich on the hitherto free waters (Pearson 1998, p. 140). The tenor of relations changed when Portugal's plans became apparent. The city was ceded by Sultan Bahadur of Gujarat in the mid-1530s, and fortified shortly after (Subrahmanyam 2012, pp. 79-84). The defenses proved timely; in 1538 Diu would be the site of an epic standoff between the Portuguese and the Ottoman Empire. After four months of siege, the Portuguese drove off the Turkish forces. The *Estado's* problems with rival rulers were far from over, but the glow of heroism over Diu would live on in legend for generations to come.

As the dust settled and outright challenges became scarcer, Diu illustrates the compromises to be struck between a zero-tolerance messianic policy and the necessity of tact to continue profitable trade. In the 1590s, the Portuguese king pressed the viceroy to do something about the number of temples in and around key cities of the *Estado*. In response, the viceroy stated flat-out that it "couldn't be done" in Diu because all the *vaniyas* (rich Gujarati traders) would abandon the city and commerce at the port would grind to a halt (Pearson 1987, p. 122). Bocarro remarks that the city was shared with "Gentiles, mostly Gujarati, and some white Jews, and Moors, in houses of stone and mortar...in the Moorish fashion, dark and with very small doors and windows and very narrow streets" (Bocarro 1992, pp. 75-76). The racial makeup of the city could be unsettling to viceroys: Linhares de Noronha pled the king to dispatch more Portuguese to the area because of the (to soften the viceroy's language) increasingly dark-skinned appearance of the garrison there (from the 'Documentos remetidos,' vol. XXXI, of the Archivo Nacional da Torre do Tombo; quoted in Pearson 1987, p. 95). By the 1630s, the effects of abusive governance and increasing European competition were undeniable. The Portuguese city was being abandoned. It would nonetheless be one of the nine forts left of the *Estado* by the late 1660s.

#### 4.1.3: Chaul

In 1508, Chaul was the site of the first Portuguese naval defeat in India (at the hands of the Muslim governor of Diu, Malik Aiyaz). The Portuguese commander in charge of the fleet (Lourenço de Almeida, son of Francisco de Almeida) perished in the clash (Mattoso 2010, p. 92). After this inauspicious start the territory was taken slowly, beginning with Sultan Nizam ul-Mulk de Ahmednagar's permission in 1516 to build a *feitoria* (factory) on the location that would become known as Lower Chaul. Clearance to construct a fort came five years after (Jayasuriya 2008, p. 89). In the decades to come, the Portuguese presence in Chaul would not go unchallenged. Chaul was sieged from 1570-1571 by Nizam Shah, by the Mughals in 1612, and faced threats to its trade following the British seizure of Ormuz in 1622 (Flores 2015, p. 93; da Cunha 1876, pp. 61-66). In the 1630s, the Imams of Oman emerged as a new worry for the Portuguese at Chaul (Subrahmanyam 2012, p. 185). During the same period, the defeat of the Ahmadnagar sultanate by Mughal and Bijapur rulers led to the flight of many Chaul merchants and prompted a decline in commerce to the port city (Barendse 2002, p. 57). The story of Chaul serves as another example of the complicated position of the Portuguese in India, where an ever-changing political environment required constant renegotiation.

Over time the fortress grew from a modest square nucleus into the complicated form depicted on the maps (Mattoso 2010, p. 94). It was tasked with reducing Gujarati trade between the west coast of India and enemy ports (Subrahmanyam 2012, p. 79), a motivation connected to the original Portuguese vision of a maritime trading monopoly

cemented by a network of fortresses. The vigorous commerce through Chaul allowed its Portuguese population to become one of the richest in the *Estado* and garnered the city comparisons with Venice (Barendse 2002, p. 57). Relations with powerful Hindu locals are illustrated in the story of a wealthy *vaniya* who died at Chaul in the late 1500s. Of his great fortune, he willed a pittance to Christian charities operating in the region, while the majority was bequeathed to a bird hospital in Cambay (sanctuaries for animals being a common Jain institution) (Pearson 1987, p. 122). Nearly 100 years later, Indo-Portuguese tensions persisted: Portuguese officers remarked, presumably proudly, that they had “never allowed Hindus or heathens among their Christians in the town” (Carre 1947, p. 187). The allegiance of the Portuguese captains to official institutions was also suspect: in the same period, the king decried their brazen (and illegal) sales of iron and steel to East African enemy powers for personal profit (Pearson 1998, p. 137). For all its troubles the fortress town of Chaul endured. It was lost not in battle, but as part of a treaty guaranteeing cessation of hostilities in 1740, making it one of the longest-lived Portuguese strongholds in Asia (Mattoso 2010, p. 96).

#### 4.1.4: ‘Moro de Chaul’ (Korlai)

‘Moro de Chaul’ is not often recalled in histories of the *Estado*. The strategic promontory had attracted the attention of Portuguese leaders from the mid-16<sup>th</sup> century but was only captured in the 1590s (Sohoni 2013). Although a partially-finished fortress had existed on the site, the fighting of the late 16<sup>th</sup> century necessitated a total rebuilding (Clements 2015). A small town eventually grew up around the foot of the fortress, possibly peopled by Indian Christians keen on trading with the local garrison (Clements 1991). Just across the river from Chaul, the fortress of ‘Moro’ was a foreboding reminder to the Portuguese to exercise constant vigilance. It remained in Portuguese hands until 1739 (Naravane 1998, p. 59).

#### 4.1.5: Cochim (Kochi)

‘Cochim’ has the distinction of being the first fortress constructed by the Portuguese in present-day India (Pearson 1987, p. 30). Its earliest defenses were a wooden stockade, which were rebuilt in stone following Almeida’s arrival in 1505 (Subrahmanyam 2012, p. 65). The fortress’s strategic value was established early on. It would later play host to the “Cochin coterie,” a group of *casado* (married male) traders with significant economic and political power (*ibid.*, p. 73). By 1523, the behavior of the Portuguese in ‘Cochim’ augured a troubling trend for the official *Estado*: they wanted to stay in India and make their own fortune outside the system of rewards and privileges set up by the king. This is documented in a letter reporting that wood for shipbuilding was in deficit because Portuguese residents of the area had bought it up to make their own vessels for private trade (Pearson 1987, p. 82). By the year 1540, approximately 400 out of the roughly 6500 Portuguese living in Asia could be found in this city (Subrahmanyam 2012, p. 79). Its importance increased in the late 1500s and early 1600s, when it became a hub of the “New Christian” trade networks<sup>1</sup> (*ibid.*, p. 125). Writing in the second half of the 16<sup>th</sup> century, Linschoten states that the city is “almost as great as Goa [...] and well-built with fair houses, churches, and cloisters [...] [And across the river] lies a place called Cochin Dacyma [De Cima; Upper], which is in the jurisdiction of the Malabars, who as yet continue in their own religions: there the king keeps his court: it is very full and well built [with houses] after the Indian manner, and has likewise a market every day, where all kinds of things are to be bought, as in Cananor, but in greater

---

<sup>1</sup> The term “New Christian” refers to Portuguese Jews who had at least nominally converted to Christianity, often due to the pressure of the Inquisition.

quantities.” Linschoten also notes the multinational Jewish population outside the city and its various Hindu and Muslim residents. If Linschoten is to be believed, relations between religions and ethnicities are harmonious. He remarks that “these three nations do severally hold and maintain their laws and ceremonies by themselves, and live friendly together keeping good policy and justice” (Linschoten 1885/1596, pp. 69-71). Pyrard’s description of the situation at ‘Cochim’ (from the early 1600s) may explain this unusual tranquility. He relates that there is a strict division of jurisdiction, where the Portuguese make the law in their territory, and the local king in his adjacent land, and these zones are so well demarcated that the Portuguese are not permitted to pursue their own criminals and extradite them for punishment if they cross into the local king’s territory.<sup>2</sup>

Bocarro paints a positive picture of the town, saying that it was “one of the richest and most populous cities of the world” (Bocarro 1992, p. 198, author’s translation). He gives facts about the pepper weights, the captain’s house, the customs house, the prison,<sup>3</sup> and the *câmara* (municipal council hall). Resende was ordered to deal with correspondence from ‘Cochim’ several times in 1634 (de Noronha 1937, p. 154). The early 1600s marked a decrease in revenues for the city, which spurred new fortification work (Subrahmanyam 2012, p. 163).

#### 4.1.6: ‘Baçaim’ (Vasai)

Vasai (‘Baçaim’) came into Portuguese possession after it was ceded by Sultan Bahadur of Gujarat in 1534. Its fortification was likely gradual: a preliminary perimeter that incorporated elements of the existing Indian defenses, then construction of houses, isolated towers, and religious structures, and finally the construction of a true fortress (Mattoso 2010, pp. 74-75). Its intended functions were to feed Goa and to reward fidalgos (who were given estates<sup>4</sup> here and elsewhere called *prazos*) (Subrahmanyam 2012, p. 79). Like Kochi (‘Cochim’), it was a center for fully-transplanted Portuguese who had no intention of returning to the motherland and every reason to seek private profit. Jesuit missionaries in the late 1500s found themselves baptizing increasing numbers of Eurasian women and boys in this region, a clear result of this tendency (Pearson 1998, p. 105). By 1588, the political sway of the church in this city was made manifest by the expansive and expensive estates held by the Jesuits<sup>5</sup> and the fact that over half of government expenditure for the fortress was dedicated to religious activities (*ibid.*, 142-149). In the early 1600s, the farmlands encircling the fortress contributed a major share of the rice consumed in Goa (Disney 1996). The crop was “cultivated by Christians, Mohometan, and pagan peasants, inhabiting the

---

<sup>2</sup> A curious story regarding the concord in Kochi is related in Linschoten. He reports that there was a dispute over who ranked higher in (the Portuguese or the Naires) and should be given way to during a meeting on the street. Nobody could decide, and it was resolved that the matter would be settled by combat. A Portuguese and Naire representative were selected, and after the Portuguese won the fight, the Portuguese were accorded higher rank (Linschoten 1885/1596, pp. 281-282). François Pyrard’s version differs slightly. He describes a compromise where in one neighborhood the Portuguese must yield the path to Naires, and in another, the reverse (Pyrard 1887/1611, p. 436).

<sup>3</sup> Pyrard gives a vivid account of the prison as he experienced it in the early 1600s. His description of the layout of the city corresponds closely to Resende’s depiction. He says the prison is called *Tronco* (as were many prisons abroad, nicknamed in reference to a famous prison in Lisbon), and “is built in the form of a large and lofty square tower, and high above, in the middle of the floor, is a large square hole, like the very trap or the hatches of a ship, which is closed and locked; there they let down the prisoners in a scale or wooden table [...] like a well [...]” (Pyrard 1887/1611, p. 429).

<sup>4</sup> These estates outside the city were also used as refuge from the plagues that would periodically afflict the region (Thevenot & Careri 1949/1656, p. 169).

<sup>5</sup> Some of these estates and monasteries grew European fruits (*ibid.*).

villages thereabouts” (Thevenot & Careri 1949/1656, p. 169). The city’s agricultural infrastructure was dealt a blow by a natural disaster in 1618, which commentators in Lisbon interpreted as divine punishment for immoral behavior (Mattoso 2010, p. 162). The damage was speedily repaired and ‘Baçaim’ was one of only nine forts to remain in Portuguese possession after 1666 (Pearson 1987, p. 137). At the close of the 17<sup>th</sup> century, Abbé Carre wrote that the city was “larger than Daman, very well-built in the European style, with broad streets, a fine square in the center, and several lovely churches [...] [And besides the Portuguese, there are] Portuguese half-castes, and they even allow Hindus and other indigenous people to stay in the town, because of its large trade” (Carre 1945, p. 178). One peculiarity of Baçaim that is omitted in the maps relates to its streets: it was the only fortress city in the Portuguese *Estado* with paved roads (Mattoso 2010, p. 161).

#### 4.1.7: ‘Salsete’ (Salcete)

The region of Salcete was one of a few parcels of territory ceded to the Portuguese by Bijapur in 1542 on the condition that the Portuguese allow trade to the Red Sea (Pearson 1987, p. 70). The agreement indicates an early shift in the overall vision of empire put forth by the assorted Iberian monarchs overseeing the *Estado*. Control of Red Sea trade had been an essential component of the Portuguese plan for economic domination. These sorts of deals were struck in response to the everyday exigencies of maintaining a coastal military presence, and perhaps a new realism about improbability of Red Sea dominion without a fortress at Aden. Throughout the 16<sup>th</sup> century, Salcete was mostly ignored (with the exception of some religious programs like the destruction of Hindu temples between 1583 and 1587) (Županov 2005, pp. 216-218). In the early 1600s, Salcete’s role in the *Estado* had come into focus: it would be an agricultural region in service to Goa and an enclave for missionary efforts (Disney 1996). Careri is skeptical of the clerics’ motives, writing in the second half of the 17<sup>th</sup> century that “the Jesuits are possessed of the best part of this island [...] and it is reported for a certain truth, that they have more revenues in India than the king of Portugal.” He continues his account, lavishing praise on the fruitful soil and heaping disapprobation on the settlement’s living conditions, saying “[...] there are several villages of poor wretched Gentiles, Moors, and Christians, living in houses built of wattles crusted over with mud, and covered with straw, or palm-tree leaves [...] the peasants are worse than vassals to the lords of the village” (Thevenot & Careri 1949/1656, p. 179).

The island’s profusion of Hindu temples had been a point of contention between the Portuguese and local population, but also served as an example of the unreliable conclusions resulting from European received historiography. Careri’s narrative indicates that even in the decades after the Évora codex was completed, a folk belief persisted in Salcete and Goa that the Pagoda of the Elephant was commissioned by Alexander the Great (*ibid.*, p. 180).

#### 4.1.8: ‘Mangalor’ (Mangaluru)

‘Mangalor’ was taken after much bloodshed (along with ‘Onor’ and ‘Barçalor’ [Honawar and Basrur]) in 1568-1569. It was meant to function as yet another granary for Goa (producing coarse red and black varieties of rice) and as a check on Kanara pepper trade (Subrahmanyam 1984; Disney 1996). According to Bocarro, the fortress was founded by Viceroy Dom Luis de Taide in 1579. By the 1660s it was back in the hands of the local king of Bangel and decried by one European as a “little ill-built town” (Thevenot & Careri 1949/1656, p. 123). Bocarro has relatively little to say about the site, but mentions that the city is ancient, and remarks that some of the walls are becoming ruined, and should be repaired when convenient, since rebuilding is not possible (Bocarro 1992, p. 187). The town of ‘Mangalor’ was said to have houses of stone and lime, covered

in tile (*ibid.*, p. 184). In contrast to ‘Barçalor’ to the north, ‘Mangalor’ maintained a powerful Jain contingent until the seventeenth century (Subrahmanyam 1984).

#### 4.1.9: ‘Sera de Aserim’ (Asherigad)

Lying between Vasai (‘Baçaim’) and Daman (‘Damaõ’) and practically impregnable thanks to its mountaintop position, ‘Sera de Aserim’ served as a key defense for sites such as ‘Maim’ and ‘Tarapor’ (Mattoso 2010, p. 89). The stockade at its feet and the fortress on the height were taken in 1556 and remained under Portuguese control until 1739. At the time of the preparation of the Évora codex, 120 men served at the fort (*ibid.*, p. 90). Writing in the late 1600s, Abbé Carre described the fortress, writing that “[it is] one of the curiosities of India. On its summit is a platform, on which there is a town resembling a fortress, inaccessible on every side. A very large spring rises at the top of the mountain and flowing down in several streams forms a river which irrigates the plains below” (Carre 1947, p. 178). The numerous cisterns depicted on Resende’s map bear witness to this fact.

#### 4.2: Locating specific buildings

Arguably the five most important fortresses of India to be found in the Évora codex are ‘Dio,’ ‘Damaõ,’ ‘Baçaim,’ Chaul, and ‘Cochim.’ We will now look at these maps and attempt to refine our understanding of the cities they depict. Using cartographic depictions, primary sources, secondary sources, and satellite images, we will endeavor to draw out the specificities of each city from the generalizations recorded by Resende. We will also begin to appreciate the extent to which Resende’s maps are “reliable.” The references for each identification are provided alongside each map.



#### 4.2.1: 'Damaõ' (Daman)

References: (1-11) MS 1636 Anon; Bocarro 1992.



1. (see box at right)
2. Church of S. Paulo
3. Church of S. Francisco
4. Church of S. Augustinho
5. Church of the See
6. Misericórdia
7. Gallows
8. Pillory
9. Bulwark of S. Tiago (?)
10. Bulwark of the field
11. Bulwark of Sam Francisco Xavier (?)

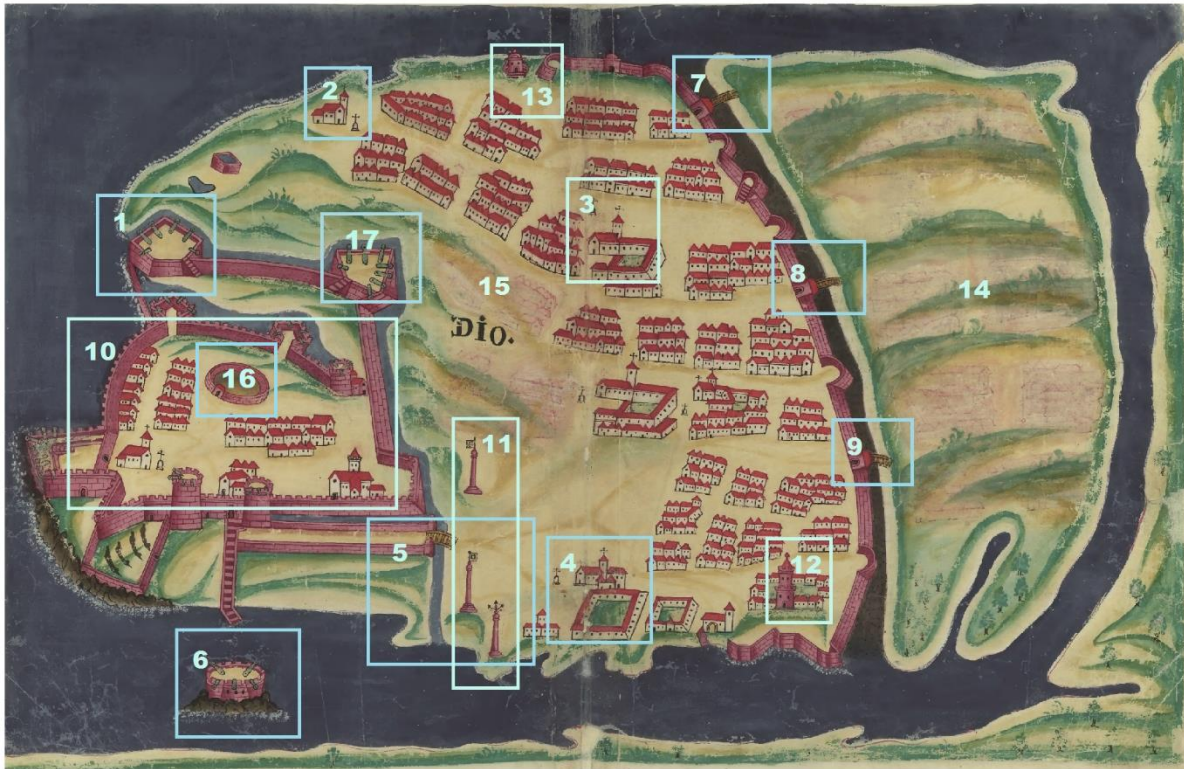
1. Bocarro on the fortress (Bocarro 1992, p. 86, author's translation):

"Inside the city, almost in the middle, is a fortress in which the captain lives, which is surrounded by square walls, with four bulwarks [...]. However, it is made of baked clay bricks, made by the Moors who inhabit this city, making in this place the residence of their *Divão*, which is like our Governor, and so it is very ruined [...] The Captain of this city and fortress lives inside [these walls], in houses attached to the walls, enough for himself and his family. Inside these walls are also the Church and College of St. Paul run by the fathers of the Company [of Jesus; i.e., Jesuits], and attached to that a prison where they take the miscreants, and a house of the *feitoria* [factory]."

Figure 34: Annotated map of 'Damaõ.'

#### 4.2.2: 'Dio' (Diu)

References: (1) Shokoohy & Shokoohy 2003; Bocarro 1992. (2-9) MS 1600-1650 Texiera Albernaz 1; MS 1636 Anon. (10) Bocarro 1992. (11) E 1729 Child. (12) Shokoohy & Shokoohy 2010. (13) Google Earth, iconographic inference (see Chapter 3). (14) MS 1636 Anon.; MS 1622 Erédia. (15) Dos Santos & Mendiratta 2011. (16) E 17C. Machado. (17) Shokoohy & Shokoohy 2003.



1. Bulwark of S. Philip (see discussion below)
2. Church of Nossa Senhora da Esperança
3. Church of S. Pedro
4. Hospital
5. "Jogo de Bolos" (ball game)
6. Bulwark of the Sea
7. Gate of the Abaxis
8. Gate Out ("Porta fora")
9. Field gate
10. (see box at right)
11. Flags with crosses, and three arrows
12. Tower is drawn and unlabeled MS 1622 Erédia, MS 1636 Anon., and MS 1600-1650 Teixeira Albernaz. It is absent in E 1729 Child. Some scholars identify it as the remains of the old Muslim citadel (Shokoohy & Shokoohy 2010).
13. Jalandhar Dada temple (?) (see discussion below)
14. (see discussion below)
15. (see discussion below)
16. (see discussion below)
17. St. Nicholas bulwark

10. Bocarro on the structures inside the fortress (Bocarro 1992, p. 70, author's translation):

"Inside the walls of the fortress are great ruins of many houses, very noble and beautiful, of two or three stories, where in the past there lived many Portuguese casados with their families, which, by their vicinity to the captains of the fortress and their servants and relatives, they will leave the said houses and move outside the fortress, letting them fall into such a state. There are also inside the walls a Church of the See, another of Misericórdia, a hospital of Your Majesty, a beautiful hermitage of Sanctiago [St. James] and a public prison, and a cistern, which draws 24000 pipas of water, very good and well-maintained..."

*For more detail on the form of the fortress in this plan and its inaccuracies, see dos Santos & Mendiratta 2011.*

Figure 35: Annotated map of 'Dio.'



1. This bulwark and the bulwark of St. Nicholas are part of a western wall that was built in 1546, incorporating new Italian concepts in fortification design. The impetus for the changes in shape of bulwarks is related to the increased use of heavy artillery. The irregular form of the fortress of 'Dio' is due to additions and updates to the origin Indo-Islamic fort, as well as to the latter's tendency to follow the contour of the landscape (rather than adhere to an arbitrary geometrical shape) (Shokoohy & Shokoohy 2003).



**Figure 36:** Location and appearance of Jalandhar Dada temple in Diu. Images courtesy of Google Earth.

13. Based on the existence and form of an extant temple at the approximate geographical location of this map sign (according to the matching of the map to the actual territory by dos Santos & Mendiratta 2011) and the iconographic evidence discussed in chapter 3, this feature may be very tentatively identified as the Jalandhar Dada temple (figure 36). However, in the absence of information regarding the date of this temple's construction, the idea must remain conjecture, and welcomes further evidence to confirm or discredit it. The continued existence of a Hindu shrine within the walls of the Portuguese city seems remarkable, but historical and textual evidence point to its possibility. Bocarro mentions that within the walls are Portuguese casados and their families (with their enslaved servants), black Christians, and "a large population of Gentiles [i.e. Hindus], mostly of the Guzarat caste, and some white Jews, [and] Moors..." (Bocarro 1992, p. 75, author's translation).

14. The presence or absence of buildings on this region follows a fascinating pattern. Buildings are drawn on the Erédia Atlas-Miscellany (MS 1622 Erédia), on the Paris anonymous codex (MS 1636 Anon.), and on the London Resende codex (MS 1646 Resende). Buildings are absent on the Madrid Teixeira-Albernaz maps (MS c.1635 Teixeira Albernaz), on the mid-1600s Teixeira-Albernaz maps (MS 1600-1650 Teixeira Albernaz), and on the Maris Carneiro maps (MS 1639 Carneiro). On the Évora codex, they seem to have been drawn according to the same layout seen in the London Resende codex (MS 1646 Resende), following the Erédia model, but have been erased. Those authors who used the Évora codex as a model, therefore, understandably exclude the houses; while those modeled after Erédia, or in whose construction Resende was closely involved, continue to have them. This pattern may indicate that the revisions occurred before the map was sent to Europe. The map of 'Dio' in MS 1646 Resende captions the area "Moorish City." Dos Santos and Mendiratta, possibly

working from the impression that houses had never been included in the Évora map, theorize that the settlement in zone 14 is omitted on the Évora codex map due to its strategic insignificance, since the Portuguese would have had “a more tenuous control” over its residents (dos Santos & Mendiratta 2011). This theory (of economy of labor in mapmaking and attempts to only include settlements strictly subject to the Crown) would be more plausible were it not for the facts that Resende did take time to draft the contents of this zone, and moreover included regions outside of Portuguese control in several other maps (such as ‘Olala’ in the map of ‘Mangalor’ and ‘Barçalor de Cima’ in the map of ‘Barçalor’).

Viewing the map over the lightbox, an intriguing structure can be seen in the center of this erased town. It is cylindrical, with what resembles Baroque scrollwork running up its sides. The same building can be found in the Paris anonymous codex (MS 1636 Anon.) and in the Erédia Atlas-Miscellany (MS 1622 Erédia). In the maps of the latter codex, the building is labeled as a mosque<sup>6</sup> and has a slightly simpler design.

The erased settlements at zones 14 and 15 of the Évora codex map had reached a high degree of completion before being deleted, and traces of the former composition were clear enough to enable a digital reconstruction of the original map design (see chapter 6).

15. Several clusters of houses were drawn and erased in this region. A possible explanation is proposed by dos Santos and Mendiratta. They observed that in this area, MS 1646 Resende has three fewer clusters of houses than the map of the Évora codex. They suggest that this is connected to an inspection of the fortress ordered by the Count-Viceroy Linhares de Noronha in 1634, which resulted in an order that the buildings closest to the fort be destroyed to clear lines of fire in case of an attack on the fortress. It is possible that the erasure of buildings from the Évora codex after they had already been drafted has the same cause.

16. The map of ‘Dio’ from *Mappas do Reino de Portugal e suas conquistas collegidos* by Diogo Barbosa Machado (E 17C. Machado) labels this structure as a cistern. Bocarro’s description of a fantastically productive cistern within the walls of the fortress would appear to confirm this identification. However, given the fact that there is so little corroboration of this fact, and bearing in mind the peculiarity of the feature’s design, its identity remains uncertain. Shokoohy and Shokoohy conjecture that it may have been a bull-fighting ring (Shokoohy & Shokoohy 2010).

---

<sup>6</sup> The presence of a mosque is also noted in the G. Child engraving of ‘Dio’ included in T. Salmon’s 1752 *The Universal Traveler*, but the design of this map and its handling of perspective are so different that a direct comparison of symbols is impossible.

#### 4.2.3: Chaul

References: (1-13) MS 1636 Anon.; E 17C. Machado. (14) iconographic inference. (15-20) MS 1636 Anon.; E 17C. Machado.



1. Fortress and houses of the captain
2. Church of the See
3. Bulwark of S. Felipe
4. Bulwark of S. Cruz
5. Bulwark of S. Tiago
6. Bulwark of S. Pedro and S. Paulo
7. Bulwark of S. Dionis
8. Bulwark of S. Francisco
9. Bulwark of S. Domingos
10. Church of S. Domingos
11. Church of S. Francisco
12. Church of Nossa Senhora da Graça
13. Church and college of S. Paulo
14. Pillory
15. Church of S. Sebastião
16. Fish market
17. Church of Madre de Deos
18. Chaul de cima (B), Chaul de arriua (E); see box at right
- 19-20. See discussion below

18. Bocarro on 'Chaul de cima' (Upper Chaul) (Bocarro 1992, pp. 125-126, author's translation):

(In reference to the Portuguese collection of tributes from local towns) "[...] the tributes from Upper Chaul are very poorly paid today because, as this kingdom of Melique is taken almost completely by the Mughal, and, when they are angry, there is no one to ask for said tributes. The other rents have their highs and lows, as is usual, but now they are mostly low, because of the lack of navigation and commerce in this State, since the Hollanders dominate the seas."

"Upper Chaul [...] is a town of Moors that is a quarter of a league away from our town, on the east side [...] in which there live many journeymen, weavers of silk, of which they have all kinds in this town, woodworkers who make desks and marquetry, of which there is great abundance, and other crafts. And there live [in Upper Chaul] many Moors of arms. And it is a town with three thousand residents, but without a wall or any kind of fortification."

Figure 37: Annotated map of Chaul.



19-20. The depiction of Chaul in E 17C. Machado includes Upper Chaul (albeit under another name). The town is drawn as dense blocks of houses, in the center of which one can find the label “Mesquita” (mosque). This mosque may be the building found at 19 on the Évora codex map. In the maps of the MS 1646 Resende, the structures at 19 and at 20 are included, but unlabeled. They are drawn in a nearly identical manner. It may be hypothesized that both buildings are mosques.

#### 4.2.4: ‘Cochim’ (Kochi)

References: (1-26) MS 1600-1650 Teixeira Albernaz I; MS 1636 Anon.



1. Church of S. Thomé
2. Church of Nossa Senhora da Graça
3. Bazaar
4. Church of S. Augustinho
5. Anunciada
6. Church of S. Sebastião
7. *Caixeiros* (Boxmakers?)
8. Pillory
9. Church of the See, Municipal Council
10. Misericórdia
11. Hospital
12. Church of S. Bartolomeu
13. Church of Nossa Senhora da Guadalupe

14. *Sapateiros* (Shoemakers)
15. Church of S. Frederico (?)
16. Church of S. Barbara (?)
17. Church of N. S. dos Anjes
18. Church of S. Domingos (?)
19. Church of S. Paulo
20. *Bazarinho*, Fish Bazaar
21. Church of Nossa Senhora do Amparo
22. Church of S. Lazaro
23. Church of Nossa Senhora da Guia de Milagre
24. House of the Bishop
25. Church of Nossa Senhora da Esperança
26. Pepper weight

Figure 38: Annotated map of ‘Cochim.’

#### 4.2.5: 'Baçaim' (Vasai)

References: (1-21) MS 1636 Anon; Mattoso 2010. (22) Bocarro 1992.



1. Bulwark "Cavaleiro"
2. Bulwark of S. Sebastião
3. Bulwark of S. Paulo
4. Bulwark of S. Pedro
5. Bulwark "Elefante"
6. Bulwark of S. João
7. Bulwark of Madre de Deos
8. Bulwark of S. Gonçalo
9. Bulwark of Sanctiago
10. Bulwark of Reys Magos
11. Bulwark of N. Senhora dos Remédios
12. Church of S. Francisco
13. Hospital
14. *Câmara* (municipal council)
15. Misericórdia (see also box at right)
16. Church of S. Domingos
17. Church of the See
18. Poor people's hospital
19. Church of S. Paulo
20. Church of S. Augusto
21. Fort of S. Sebastião
22. (see box at right)

15. Bocarro on the Misericórdia (Bocarro 1992, p. 109, author's translation):

"This city of Baçaim has inside it, attached to the Church of Misericórdia, some houses where the Captain lives, with an old adobe wall around it, which seems like the Moors made it, with a rounded stone bastion next to the pillory, a little thing [...] already in ruins."

22. Bocarro on the population outside the fortified town (*ibid.*):

"The people in these parishes, which are in Upper Baçaim and in the suburbs of the city, are mostly Christians, craftsmen (like carpenters), and those who serve to harvest the coconuts from the palms, and serfs who work the earth, whom the Captain of Baçaim has already enlisted and who make two thousand men of arms [...]."

*Alternatively, this area might be the country houses of Portuguese casados (Bocarro 1992, p. 109).*

Figure 39: Annotated map of 'Baçaim.'

### 4.3: Closing remarks

The frequency with which structures depicted in the maps can be verified and specified indicates careful compilation. This is particularly evident when considering the churches of the maps. Although the author took pains to depict the fortresses correctly (the fortress of S. Jerome, for example, shows signs of corrections), authors such as dos Santos and Mendiratta have pointed out errors (dos Santos & Mendiratta 2011). The maps betray a constant struggle between the desire for accurate representation and the need to depict the cities in a manner palatable to its audience. Both concerns occasionally supersede aesthetic considerations. The stage at which the erasures and corrections were made will be addressed in the next chapters.

The Portuguese relationship with local populations is glossed over in the maps. The use of the thatched house sign in these maps would appear to suggest clearly demarcated zones of European and non-European rule, with the non-European zones depicted as peripheral and defenseless. Some hints at porous boundaries come in the possible detection of non-Christian architecture within the “European” zones of the maps. However, the maps are never explicit. They offer multiple levels of reading and walk a fine line between acknowledgement and exclusion.

The fortresses of India ran the gamut of functions. Their economic and political stability by the 1630s was also variable, as discussed in 4.1. The maps do not seek to indicate the role of any fortress in the Estado, despite the existence of cartographic means to do so, such as the addition of human figures employed in one task or another, the depiction of ships coming to harbor, or even the use of labels. Rather, the maps present an image of permanence and invariability; the shape of fortress walls may change, but the colors and signs are constant. The world outside the fortress walls is glimpsed only on the margins of the maps.



## Part Two: Investigation of the Artistic Materials and their Use

The portion of our investigation involving instrumental techniques will seek to answer questions about the maps that historical and stylistic research cannot address. A slight shift in tone is to be expected as we move between methodologies, but the spirit of both parts remains the same: to understand the maps as objects, artworks, and artifacts. An overview of the investigation is provided in figure 40.

Overview of analytical strategy					
Chapter		Objectives	Techniques		
5		Recording features of paper support	Lightbox	μ-FT-IR	VP-SEM-EDS
6		Observing artistic technique	Lightbox	Digital Microscopy	
7		Establishing consistency of palette and generating hypotheses	Colorimetry	Technical Photography	
8			FORS	h-XRF	
		Refining pigment hypotheses	μ-Raman	FT-IR	LC-DAD-MS
		Clarifying pigment production method	VP-SEM-EDS		
		Identifying the binder	μ-FT-IR		

**Figure 40:** Research design of materials study. Note that the chapters in Part 2 are organized thematically and do not necessarily reflect the sequence in which analyses were performed.



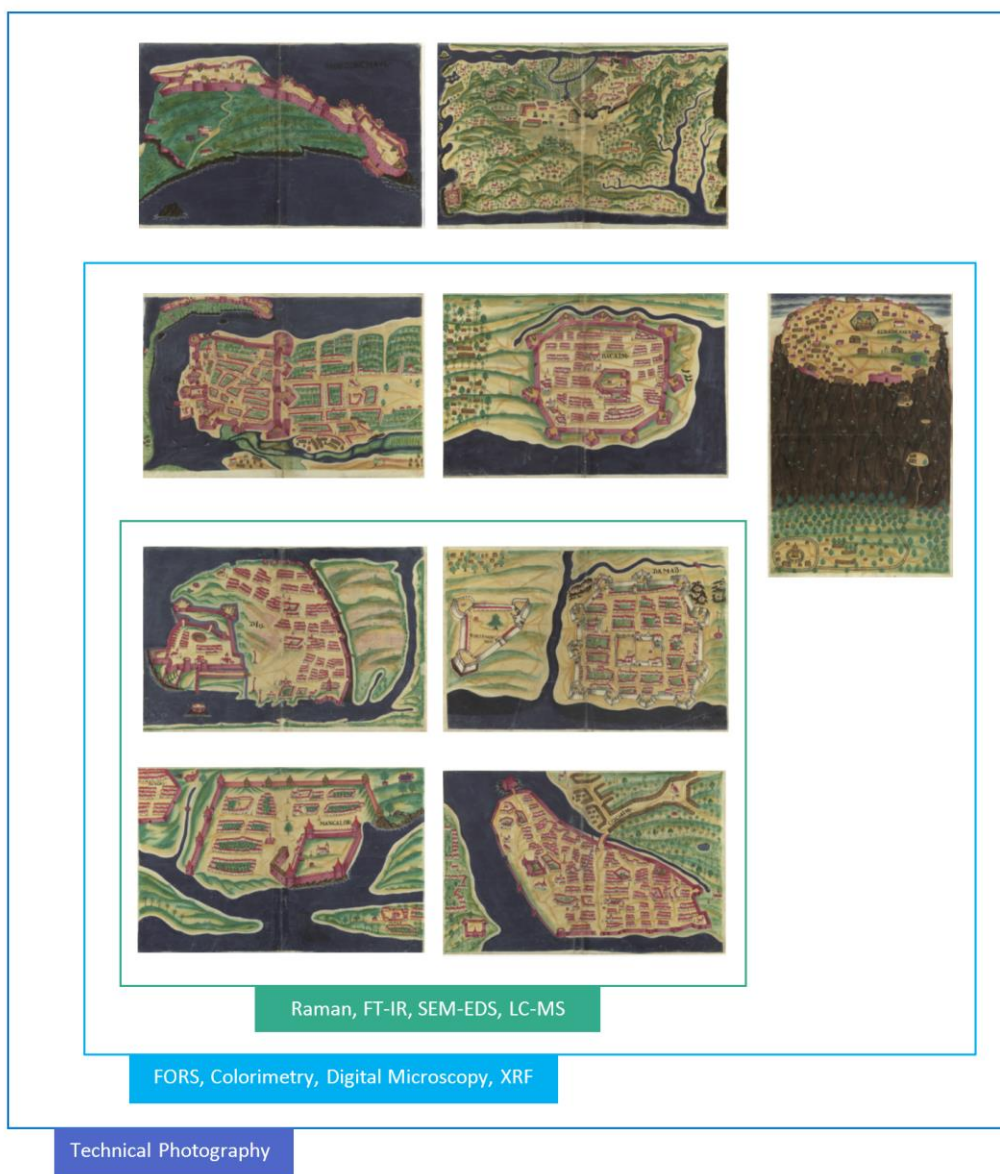
**Table 1:** Analyses, questions, and maps. An asterisk indicates analysis on microsamples. An asterisk in parentheses indicates analyses performed both *in situ* and on microsamples.v

Instrumental Method	Objectives in Detail	Maps studied		Additional Considerations
Observation of maps illuminated by lightbox	<ul style="list-style-type: none"> <li>-To confirm the presence of the watermarks described by Isabel Cid (Cid 1992)</li> <li>-To search for additional watermarks</li> <li>-To learn more about the paper production method</li> <li>-To evaluate the extent of cracking and paint loss in the maps</li> <li>-To record changes to the composition</li> </ul>	Baçaim Chaul Cochim Damaõ Dio	Mangalor Moro de Chaul Salsete Sera de Aserim	Non-invasive, non-destructive
Handheld digital microscopy	<ul style="list-style-type: none"> <li>-To determine the sequence in which features of the map were painted and whether that sequence is consistent across the maps</li> <li>-To study the behavior and texture of the paints used</li> <li>-To record changes to the composition</li> <li>-To observe the extent to which an underdrawing is employed in the creation of the maps</li> </ul>	Baçaim Chaul Cochim Damaõ	Dio Mangalor Sera de Aserim	Non-invasive, non-destructive
Colorimetry	<ul style="list-style-type: none"> <li>-To capture the chromatic palette in objective terms</li> <li>-To evaluate the consistency of colors between maps in terms of chromatic coordinates</li> </ul>	Baçaim Chaul Cochim Damaõ	Dio Mangalor Sera de Aserim	Non-invasive, non-destructive
Technical Photography	<ul style="list-style-type: none"> <li>-To attempt improved visualization of the underdrawing (NIR)</li> <li>-To begin to evaluate homogeneity of pigment use across the maps and spot possible restoration interventions (UVF-IV, NIR)</li> <li>-To begin to theorize which pigments may be present (UVF-IV, NIR)</li> </ul>	Baçaim Chaul Cochim Damaõ Dio	Mangalor Moro de Chaul Salsete Sera de Aserim	Non-invasive, non-destructive
FORS	<ul style="list-style-type: none"> <li>-To continue to test the homogeneity of the paints used between the maps</li> <li>-To continue building hypotheses as to the pigments and mixtures used</li> </ul>	Baçaim Chaul Cochim Damaõ	Dio Mangalor Sera de Aserim	Non-invasive, non-destructive
h-XRF	<ul style="list-style-type: none"> <li>-To continue to test the homogeneity of the paints used between the maps</li> <li>-To continue building hypotheses as to the pigments and mixtures used</li> </ul>	Baçaim Chaul Cochim Damaõ	Dio Mangalor Sera de Aserim	Non-invasive, non-destructive
μ-Raman (*)	-To confirm or disprove hypotheses generated so far regarding pigments identification	Cochim Damaõ	Dio Mangalor	Non-invasive, non-destructive ( <i>in situ</i> ); microinvasive (on microsamples)
μ-FT-IR*	<ul style="list-style-type: none"> <li>-To confirm or disprove hypotheses generated so far regarding pigments identification</li> <li>-To identify the binding medium and any surface treatments</li> <li>-To characterize sizing and fillers of paper</li> </ul>	Cochim Damaõ	Dio Mangalor	Microinvasive, non-destructive
LC-DAD-MS*	-To confirm the colorant in the pink lake pigment used on fortifications	Cochim	Mangalor	Microinvasive, destructive
VP-SEM-EDS*	<ul style="list-style-type: none"> <li>-To identify the inorganic substrate used for the lake pigments</li> <li>-To elucidate the production method of the red pigment</li> <li>-To describe paper fiber morphology and sizing</li> </ul>	Cochim Dio	Mangalor Damaõ	Microinvasive, destructive (samples cannot be recovered)

The analytical strategy was designed to be adaptive, such that each step was informed by the findings of the step prior. The analyses were also structured such that they moved in scale from large to small (whole map → grain analysis) and only when necessary involved invasive techniques (table 1). Although the complete set of analyses was only performed on four maps, the previous analyses allow for cautious extension of these findings to all seven maps that were study by FORS, h-XRF, and

colorimetry (figure 41). While it may impossible to apply these conclusions to the two maps that were studied only by technical photography and on the lightbox ('Moro de Chaul' and 'Salsete'), the choice to record images of these maps allows a more complete photographic documentation of the paintings of major cities of India in the Évora codex and may be of use to future conservators and researchers.

The chapters to follow will continue the story begun in the first four chapters. To keep the focus on the research questions while still giving space to important information on instrumental parameters, sampling strategy, and data processing, a separate appendix on materials and methods has been created (Appendix II). Another appendix provides expanded results organized by analytical technique (Appendix III).



**Figure 41:** Analyses and maps.

## Chapter 5: Paper Support

The paper support used for the maps has received little study so far. A serious impediment to its investigation is the fact that the original papers have been glued to modern Japanese tissue. Although in-depth study of the papers was outside the scope of this thesis, a combination of observation over the lightbox,  $\mu$ -FT-IR, and VP-SEM-EDS generated new information on the support of the maps. As the  $\mu$ -FT-IR and VP-SEM-EDS analyses and imaging were restricted to one microsample from one map, all findings (even as they pertain to the map in question) are preliminary.

Paper has been defined as “a random or felted sheet of isolated vegetable fiber produced by sieving macerated vegetable fiber from a watery slurry” (Ward 2008, p. 447). This definition encapsulates the two key features of papermaking: soaking and beating plant fibers and collecting them on a screen called a mold to dry. Although paper’s origins are placed in 1<sup>st</sup>-century China, by the time of the maps’ creation the technology of papermaking had enjoyed a wide dissemination, leading to novel production methods, niche uses and varieties, and growing brand recognition (of which watermarks are symptomatic). Fingerprinting the ingredients in historical papers can be useful, since several distinctive regional papermaking traditions had developed by the 17<sup>th</sup> century (*ibid.*, pp. 447-453). The papermaking process has several crucial steps which can leave their mark on the final process. Among these are the fibers used, the drying process, and the sizing process. As these features are encountered, their connection to paper production will be described. It should be noted that prior to 1850, wood pulp was not used for paper; rather, so-called rag was employed, which is characterized by longer fibers and leads to a typically more durable paper (Manso & Carvalho 2009).

Although we will look to the maps for signs of region-specific papermaking practices during this preliminary investigation of the map support, it is worth noting that by 1630, industrially-produced European paper had left Europe and was beginning to flood the markets of Islamic countries, leading to a decline in Arabic papermaking (Bloom 2001; Baker 1991). Historical records also describe the import of paper to the *Estado*. We will therefore consider the possibility that the paper was produced closer to Goa, but not expect it.

### 5.1: Lightbox Examination

Examining the papers on the lightbox, the use of a laid mold was instantly apparent (figure 42). A laid mold is a kind of screen for collecting macerated paper fibers that is characterized by closely-spaced “laid” wires (figure 43). The horizontal wires give rise to the laid lines in paper; the vertical wires produce the chain lines. European papers from the 13<sup>th</sup>-18<sup>th</sup> centuries, when illuminated from below, show signs of drying on a laid mold (Ward 2008, p. 250). Laid and chain lines are also found in papers from other regions. Chinese papermakers used laid molds, albeit fashioned from different materials (bamboo and thread, rather than metal wires) (Craddock 2009; Bloom 2017). The laid lines of these papers are reportedly much fainter than in European papers (Ward 2008, p. 252). The molds used by Arabic papermakers are poorly understood, but it has been suggested that a flexible organic material was used to form the screen of the molds. This is based on the observation that the chain and laid lines on these papers tend to be wavier than on European papers (Bloom 2017). The maps of the Évora codex show the typical pattern of chain and laid lines for papers made in European molds.

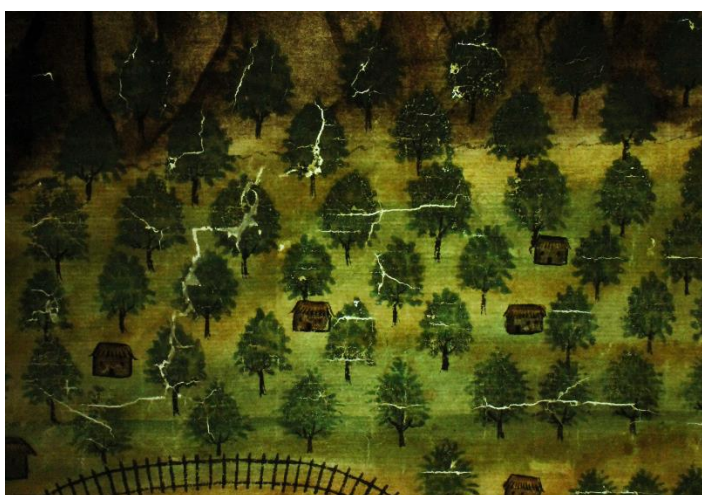




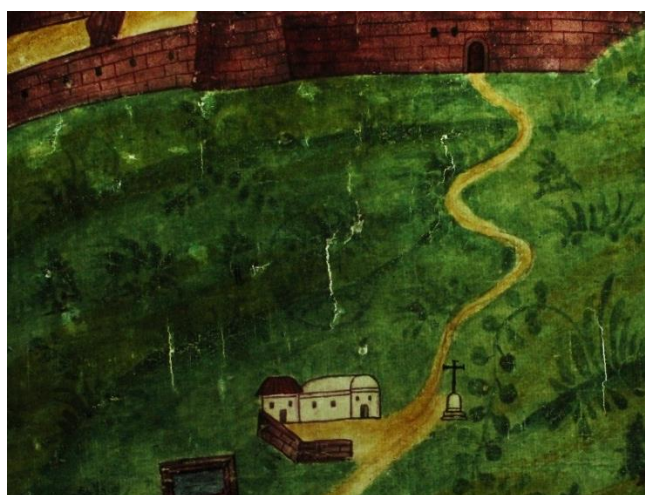
**Figure 42:** Chain (vertical) and laid (horizontal) lines ('Chaul').



**Figure 43:** Laid mold with watermark stamp (Holland, displayed in the Robert C. Williams Paper Museum; Wikipedia Commons).



**Figure 44:** Preferential cracking of green regions ('Sera de Aserim').



**Figure 45** Preferential cracking of green regions ('Moro de Chaul').

Two of the watermarks first identified by Isabel Cid were also apparent (see Appendix III.1), but no others could be detected. By the 17<sup>th</sup> century, watermarks were ubiquitous in European papers; figures for the total number of watermarks in use reach into the thousands (Hunter 1978). They were originally created by shaping wires into the desired design, and then lacing them onto the screen of the mold. A diversity of watermarks within a single book appears to have been a widespread feature of codices created in this period and could be a consequence of paper shortages. Indeed, paper deficits were reported as early as the 12<sup>th</sup> century (Ward 2008, p. 448). Watermarks are also reported on Islamic papers from at least the 15<sup>th</sup> century, possibly signaling the influence of European papermaking practices (Espejo et al. 2010). Although the design of the watermarks suggests that the papers were imported from Europe, the specificity and authenticity of the information they provide regarding paper mill should not be overstated. It would be easy enough for a forger to reproduce the watermarks of a company of good repute (Hunter 1978).

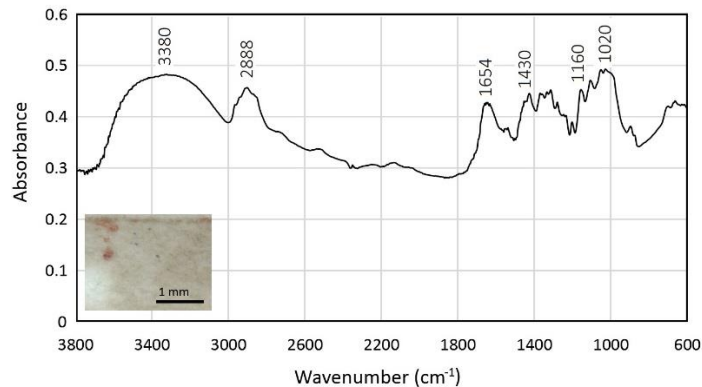
The integrity of the original paper support and the paint layers was also clarified by the lightbox. Minute tears throughout the maps were plainly seen, as well as preferential cracking and paint loss in the green, white, and some blue regions (figure 44-45).

## 5.2: Sizing and fillers

$\mu$ -FT-IR was used to investigate two more aspects of the paper: its sizing and fillers. Sizing is a surface treatment that reduces the paper's porosity and absorbency (Craddock 2009). This improves the crispness of lines, which would otherwise bleed into the paper and lose their sharpness. At the time of the maps' production, European papers were typically sized with gelatin (Espejo et al. 2010; Manso & Carvalho 2009). An added step in which the paper was soaked in an alum solution could also be performed, particularly for watercolor painting, as it allegedly imparted a brighter surface (Cohn 1977, p. 21). Islamic and East Asian papermakers preferred vegetable starches as a sizing (Ward 2008, pp. 452-453; Espejo et al. 2010; Bloom 2017). Islamic papermakers occasionally added white chalk to their starch sizing (Bloom 2017). Some Chinese papers did not require any sizing at all (Ward 2008, p. 452), since for some calligraphic traditions ink absorptiveness is a desirable characteristic in papers.

Fillers are additives introduced while the fibers are still part of a watery slurry, before they are captured on the mold. Their introduction to the paper before it is dried distinguishes it from a coating, although the materials used for coatings and fillers can overlap (Beazley 1991). Fillers include chalk, gypsum, calcite, dolomite, and kaolin (Craddock 2009; Manso et al. 2011). The function of fillers, apart from cheapening the paper manufacture, is to affect the appearance, acidity, and behavior of papers.

$\mu$ -FT-IR was performed on a microsample of the paper extracted from the top margin of the map of 'Damađ' (Da.S.1; for location of the sample, see Appendix II.1; for instrumental parameters, see Appendix II.9). Extension of the findings to other maps may not be possible. Future research on the materials used in the maps should exploit the possibility of *in situ* infrared spectroscopy for more detailed comparative questions, which was beyond the scope of this work. Additionally, for any future work *in situ*, the contribution of the Japanese tissue and modern glue to any attenuated total reflectance infrared spectra must be defined. As our current work centers around questions of artistic cultures (rather than conservation state),  $\mu$ -FT-IR was employed chiefly for investigation of sizing and fillers in the paper.



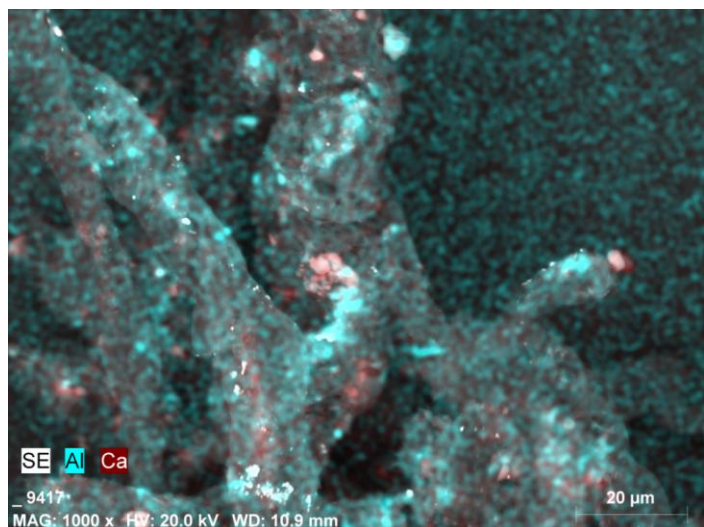
**Figure 46:** Infrared spectrum of the paper microsample (Da.S.1; for location of sample on map see Appendix II.1)

The infrared spectrum of the microsample is provided in figure 46. The cellulose content of the paper is indicated in the spectrum by broad band centered at  $\sim 3335\text{ cm}^{-1}$  (OH stretching). The band with shoulders centered at  $2888\text{ cm}^{-1}$  shows the combined absorbances of the cellulose's C-H stretching mode ( $\sim 2900\text{ cm}^{-1}$ ) and  $\text{CH}_2$  symmetrical stretching mode ( $2850\text{ cm}^{-1}$ ). However, the profile of the OH stretching band as well as the relative intensities of the OH and  $\text{CH}_2$  stretching bands do not correspond with typical infrared spectra for cellulose (compare, for example, with the infrared spectra of papers presented in Nunes et al. 2015 or Garside & Wyeth 2003). These features, along with the altered relative intensities of the C-O stretching bands between  $1160\text{ cm}^{-1}$  and about  $1100\text{ cm}^{-1}$ , suggest that cellulose is not the only carbohydrate

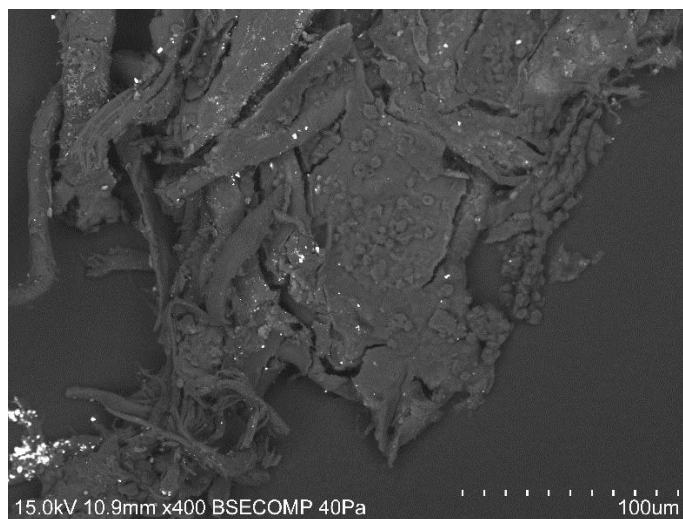


material in the sample. Another carbohydrate whose spectral features may explain the absorbance pattern of the paper microsample is plant starch, either related to the glue used to attach the map to the Japanese paper, a sizing, or a surface treatment (for a starch infrared spectrum, see for example Derrick, Stulik, & Landry 1999, p. 180). As expected for papers of the 1600s, no lignin could be detected, as identified by its C=C in-plane aromatic vibration ( $1595\text{ cm}^{-1}$  and  $1505\text{ cm}^{-1}$ ) (Garside & Wyeth 2003) which is compatible with the use of rags with a high cellulose-to-lignin ratio, such as cotton or flax.

The use of a gelatin sizing is most evident in the regions of the amide I and II absorptions, where we see bands at  $\sim 1650\text{ cm}^{-1}$  (C=O stretching) and  $\sim 1530\text{ cm}^{-1}$  (C-N-H bending). The C-H bending of the gelatin may be reflected by the absorption at  $\sim 1430\text{ cm}^{-1}$  on the spectrum (Derrick, Stulik, & Landry 1999, p. 182).



**Figure 47:** EDS elemental distribution map of paper microsample (Da.S.1; see Appendix II.1 for location of microsample on map) showing aluminum (blue) and calcium (dark red) distribution.



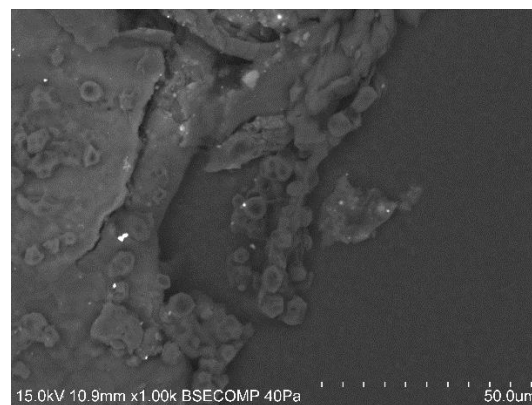
**Figure 48:** BSE image of paper microsample (Da.S.1; see Appendix II.1 for location of microsample on map) showing glue-like material.

Variable pressure SEM-EDS was also used to probe the elemental content of the microsample and detect fillers or surface treatments. Several features were noted. First, small grains of lead-rich and mercury-rich particles were observed (see Appendix III.10.2 and III.10.3 for EDS spectra). Their presence is not surprising, considering the heavy use of lead white throughout the maps and the red cinnabar edge painting on the map pages (to be discussed in Chapter 8). The lead grains were not distributed at a density suggestive of a heavy preparatory layer in this peripheral region of the paper support. Calcium was detected in both very thin, film-like layers, and in heavier accretions (see Appendix III.10.4). The fine layers could be calcium carbonate formed by a reaction of lime (CaO, often used during the maceration of the rag fibers) with atmospheric carbon dioxide (Dąbrowski & Simmons 2003). The regions with bulkier particles may be the result of the use of a calcium-based filler, such as chalk or gypsum (Beazley 1991). If such a filler was added intentionally, its quantity must have been minor, given the sparsity of such particles and the lack of unambiguous bands related to either material in the infrared spectrum for the sample. Particles of aluminosilicates were also detected in the sample (see Appendix III.10.6-7). In addition to aluminum and silicon, these grains had variable amounts of iron, titanium, sodium, potassium, and magnesium. These particles may relate to contamination or the light addition of a clay filler to the paper slurry during its



production. One grain of silicon with very minor quantities of aluminum and calcium was found, which could be a grain of impure quartz (Appendix III.10.5). Its presence can be explained by either of the two theories proposed above for the aluminosilicates. See figure 47 for an EDS elemental distribution map showing aluminum and calcium on part of the microsample.

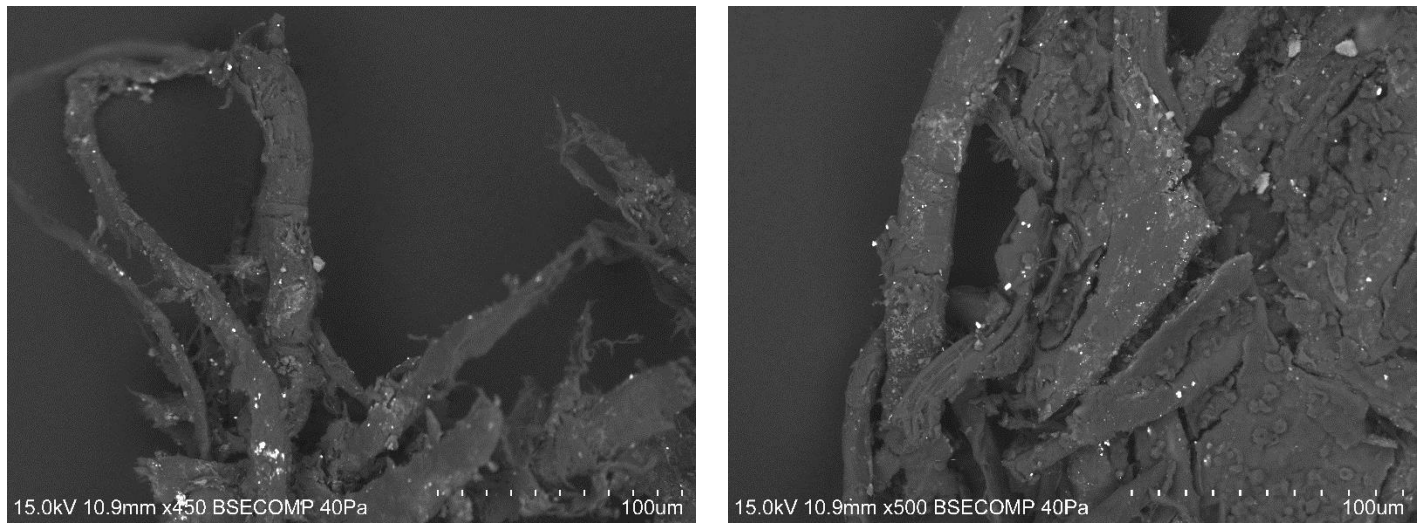
One region of the microsample seemed to be glued together (figure 48). The “glue” was composed primarily of carbon and oxygen, with some calcium and very minor quantities of iron, copper, sodium, magnesium, aluminum, silicon, phosphorus, sulfur, chlorine, and potassium (see Appendix III.10.10-11). The exact function and nature of this material is unclear. It could be a starch-based glue with a minor calcium carbonate or gypsum content, possibly the adhesive attaching the original map support to the Japanese paper below. It could equally be a surface treatment applied by the artist of the maps. Associated with this material were nodules with a diameter of approximately 50  $\mu\text{m}$  with a similar elemental composition to the plate-like “glue” material (figure 49). Morphologically, the nodules resemble the raw starch granules of several plant species (Jane et al. 1994). The dimensions of the grains are similar to those of wheat starch granules, a heated paste of which has been used as a gentle adhesive in paper conservation (Sanderson 2007). Although fresh wheat starch granules have a less angular aspect than the particles observed in the sample, it is important to note that heating can affect starch granule size and morphology (Patel & Seetharaman 2006). Though the complete characterization of fillers and consolidants of the paper has not been possible, several avenues for future inquiry have been opened.



**Figure 49:** Granules in paper microsample (Da.S.1).

### 5.3: Fibers

The fibers used in historical paper manufacture are myriad. European papers of the 17<sup>th</sup> century would have been made of rag (scraps of textile fibers patiently sorted by quality and color). The plant sources of the rags were typically hemp, flax, and cotton, although cotton usually formed a minor part of the overall blend until the 1800s (Collings & Milner 1984). The use of rag, with its high ratio of cellulose to lignin and its longer fibers, has been credited with the durability of antique papers compared with modern pulp paper (Manso & Carvalho 2009; Ward 2008, p. 441). Islamic papermakers used rags from ropes and fabric scraps as well, but with reportedly less cotton than in Western European production (Espejo et al. 2010), relying instead on hemp and flax. Arab papermakers also utilized bast fibers (Bloom 2017). East Asian papermakers availed themselves of materials inaccessible to the previous two cultures, and bamboo, jute, rattan, and paper mulberry (as well as hemp and flax) may be encountered in papers from this region (Craddock 2009, p. 315). The history of Indian papermaking is difficult to reconstruct given the poor survival of paper artifacts in warm, humid regions. In the 17<sup>th</sup> century, Tavernier reported that paper was commonly used in India to wrap tobacco and drugs, saying that “it is for this reason that so much paper is used in Asia, and it is the principal article of trade of the people of the provinces, who send theirs even to Persia” (Tavernier 1889/1676, p. 231). How and of what this paper was produced is not obvious. As far as writing papers



**Figure 50:** Fibers tentatively identified as linen.

Is concerned, Eastern and Western India followed different traditions. At least until the close of the 15<sup>th</sup> century, Eastern Indian papers were made of pulverized and retted tree fibers and a starch sizing. Western Indian papers seem to have been more connected with Islamic papermaking practices and utilized rags (Ramaseshan 1989). Some authors extend this Islamic influence further, suggesting that papermaking in India is a direct result of contact with Arab culture. This argument relates to the fact that palm leaves were long used as a portable support for religious texts and images, possibly making Arab introduction of papermaking technology more likely than indigenous development (Bloom 2017).

The identification of plant sources for the fibers of the microsample is still tentative. Future research using optical microscopy with stains to improve legibility of the fiber features will be essential. The use of variable pressure scanning electron microscopy allowed a tentative establishment of flax as a constituent of the rag mix, based on the nodes along the length of the fibers (see figure 50; Rahman & Sayed-Esfahani 1979). These fibers would have been common in European, Arabic, Western Indian, and Chinese papers.

While this preliminary work is suggestive, the case is far from closed on the papers of the maps. At the moment, the evidence supports the hypothesis that the papers were imported from Europe. Investigation of the paper of the maps also highlighted the compromises made when restorations occur. On the one hand, lightbox examination showed that the papers are very fragile and probably required the intervention. On the other, the restoration repeatedly impeded definitive interpretation of analytical results.

## Chapter 6: Observing Artistic Technique

Using a lightbox and handheld digital microscopy, the way the artist(s) worked was brought into focus. The goals of this part of the investigation were several: to observe the texture and behavior of the paints used in the map, to attempt to identify areas where colors are created by mixture of pigments, to note alterations to the maps' design, to track the use of preparatory underdrawings, and finally, to reconstruct the sequence in which the features of the maps were colored.

### 6.1: Alterations to the maps' design noted using the lightbox

Observation over the lightbox gave invaluable information about the artistic technique. The first discovery was the dual character of the various white regions of the maps. Most of the white areas were highly translucent, suggesting the absence of paint or the use of a very thin wash. However, regions where compositional changes had occurred showed signs of a heavier-bodied white. The map of 'Damað' is an edifying example (figure 51). When the form of the fortress of 'S. Irm.' (St. Jerome) was altered, the colorist had to use dense white to cover up the already-painted surrounding terrain. The artist's apparent reluctance to use this paint to define white regions is notable; it is only used in this subset of maps as a kind of



**Figure 51:** Alteration to a fortress (from the map of 'Damað'). (Left) map over the lightbox. (Right) map illuminated from above. The use of opaque white is evident in the areas appearing muddy brown on the image on the left.

correcting fluid for concealing mistakes.

Using the lightbox, the significant compositional amendment found in the map of 'Dio' could be better understood. It had already been apparent that the map had been dramatically altered, leading to the erasure of an entire settlement. The improved visibility of underlying layers offered by the lightbox gave an early indication of when that erasure had happened (one that would be confirmed by the subsequent h-XRF analysis of the overpainted areas). This enhanced visibility also made it possible to perform a digital restoration of the former design (figure 52). It seems that the map

had reached a high degree of completion when the erasure and overpaint were performed. This raises several questions. Why was such a huge alteration necessary? Who made the revision? And with such a big change required, why wasn't the map remade from scratch? It is likely that the first question has a political answer, and the last a logistical or financial one. We will attempt to tackle the second question in the pigment identification chapters, when we will strive to establish whether the materials used on the overpaint are the same as those used on the rest of the map.





**Figure 52:** Digital reconstruction of erased houses and settlement on the map of ‘Dio.’ Using Adobe Illustrator CC 2018, the outlines of deleted buildings were traced on top of a photograph of the map illuminated from below by the lightbox. The outlines were subsequently imported into Adobe Photoshop CC 2018 and overlaid in their correct locations on a digitalized image of the map with normal illumination. Then, using brush tools and color matching tools, the colors and line qualities of the reconstructed buildings were matched to the extant buildings. A hypothetical original landscape was also reconstructed, according to the usual approach in the maps of this region. The contours of buildings in the reconstruction have been placed with high confidence; the landscape, some of the windows, and the left side of the mosque have some uncertainty, since their original design were difficult or impossible to see using the lightbox.

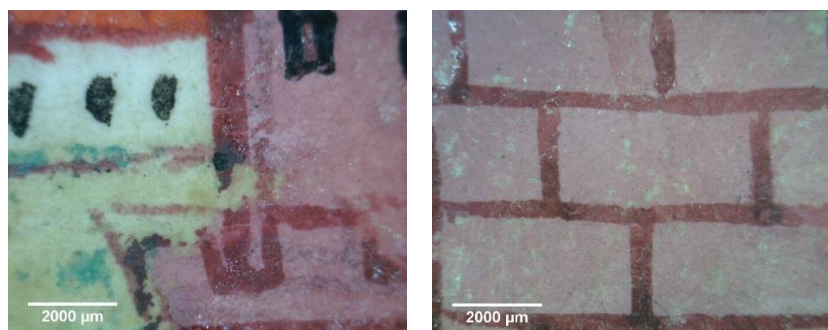
## 6.2: Use of preparatory sketch (by feature/map)

Preparatory drawings serve to guide colorists and are often examined in the context of easel and panel paintings for their insights into attribution and workshop practices (Ainsworth 1989; Wolters 2012; Valadas et al. 2016). Evaluating their use in these cartographic works may provide information on the distribution of labor during the creation of the maps and the features which the draughtsman considered essential. Underdrawing use in the subset of seven maps is recorded in table 2. Although the preparatory drawing is extensive, terrain and flowers are seldom underdrawn. If the colorist and draughtsman are different people, this may imply that these aspects are of low priority to the draughtsman. The fact that thatch on houses is often underdrawn would, on the other hand, suggest that the distinction between the two housing types was significant to the draughtsman.

**Table 2:** Preparatory drawing use by map sign. Presence of a preparatory drawing for a given feature is indicated by a plus sign (+), the absence of preparatory drawing for a feature by a minus sign (-). Mixed use is indicated by a plus and minus (+/-). NA (not applicable) means that the feature does not occur within the map.

	Dio	Damaõ	Baçaim	Sera de Aserim	Chaul	Mangalor	Cochim
Fortifications	+	+	+	+	+	+	+
Walls of buildings	+	+	+	+/- (some thatch houses painted on top of landscape)	+/- (some thatch houses seem to lack)	+	+
Thatch on roof	NA	+/-	+	+	-	+/-	-
Broadleaf trees	-	+		+ (once), otherwise -	+	+/-	-
Palm trees	NA	NA	-	NA	-	-	-
Rocks	+	-	NA	+	+	+	-
Hills	-	-	-	-	+/-	-	-
<i>Cruzeiros</i>	+/-	+	+	+	+	+	+/-
Crosses on churches	+/-	+/-	-	+/-	-	+	-
Flags	+	NA	-	NA	-	NA	+/-
Cannons	-	-	-	-	-	NA	-
Coasts/banks	+	+	+	NA	+	+	+
Flowers/grasses	-	NA	-	-	NA	-	-
Non-stone towers	NA	NA	NA	NA	NA	+	NA

### 6.3: Sequence of painting, within features



**Figure 53:** handheld digital microscopic images showing fortification painting sequence. (Left) 'Dio' fortification. (Right) 'Cochim' fortification. Note on the handheld digital microscopic image from 'Cochim' the darker appearance of the vertical lines toward the bottom. This probably signifies a heavier deposition of a translucent paint in these areas. This could result from painting these lines starting at the top and then moving to the bottom, or from painting with the paper held at an angle so that wet paint dripped downward.



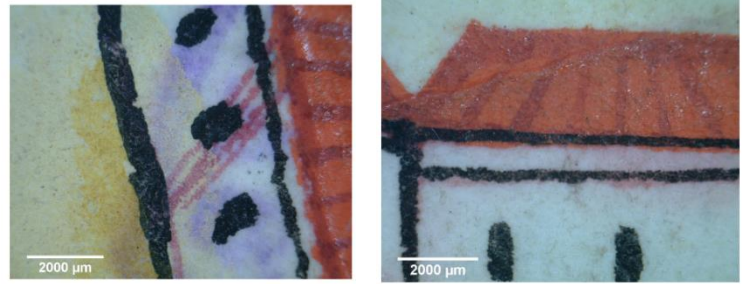
**Figure 54:** Cannons are an afterthought in the Évora codex maps. (Left to right) digital handheld microscopic images of cannons in 'Damaõ,' 'Mangalor,' 'Dio.' Note the sequence of painting, the execution of cannons on top of finished fortifications, and the incomplete cannon in 'Mangalor.'

**Pink fortifications** were first underdrawn and then filled in with an opaque pink (which appears to be mixed with white). On top of this base layer, individual stones were indicated using darker pink lines (figure 53). Black was then applied for windows. White highlights (sometimes used to accentuate gateways) were the final element to be added.

**Cannons** appear to have been painted after the fortress coloring was complete, using a combination of black and opaque gray (figure 54). No underdrawing was detected for any of the cannons. This is notable in light of Bocarro's complaints that the artillery is not correct in number, and may indicate that cannons were not part of the original composition.

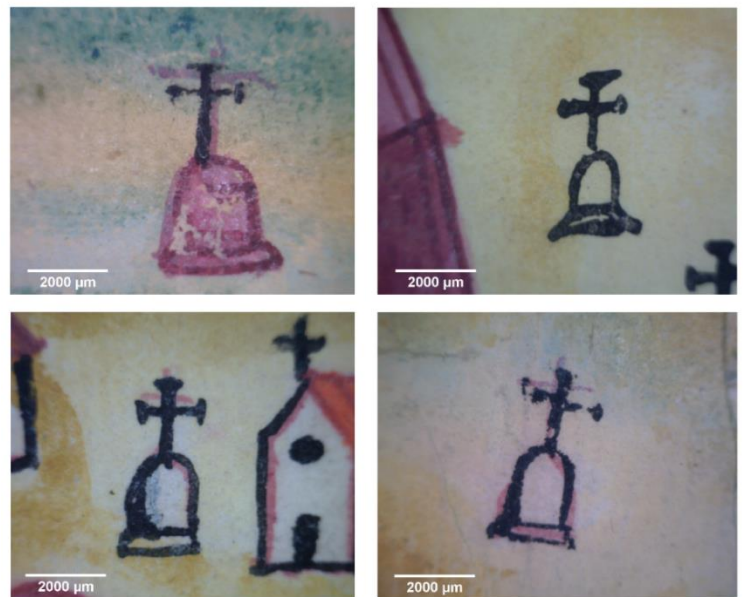


**White-walled, red-roofed buildings** were first underdrawn in dark pink. Terrain was then painted around them (so that the buildings' walls retained the white of the paper). The roof was subsequently filled in with bright red and sometimes embellished with vertical or diagonal lines of dark pink. Last, the lower walls of the building were delineated (and the underdrawing largely concealed) by black ink, and windows and doors were added (figure 55).



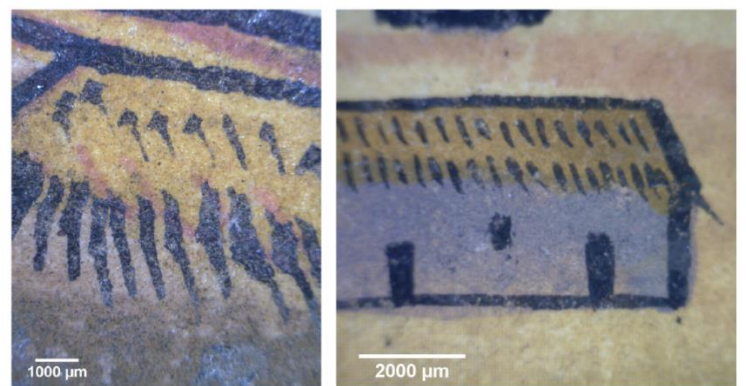
**Figure 55:** Digital handheld microscopic images showing painting sequence of white-walled, red-roofed houses. (Left) 'Cochim.' Note the encroachment of the terrain wash into the unpainted house and the underdrawing separating the house into two sections that has been disregarded in the final design. (Right) 'Baçaim,' showing that black is the last color to be added.

**Cruzeiros** are highly stable in design but show some variability in coloring. This is most apparent in the map of 'Cochim' (figure 56). The *cruzeiros* of 'Cochim' are painted both with and without an underdrawing. They can be left unpainted (to appear white), painted pink, or drawn on top of existing beige terrain and either painted over with opaque white or left beige. The inconsistent handling of the crosses in 'Cochim' may indicate that this was one of the earlier maps to be produced, before a system for coloring was decided on and effected. This theory also makes sense from the point of view of collecting maps: one starts with the most important regions, and then begins adding in lesser locales. Chaul also features several approaches to coloring *cruzeiros*.



**Figure 56:** Digital handheld microscopic images of selected *cruzeiros* of 'Cochim.' Note the variable approach to their design.

**Thatched buildings** were underdrawn with variable degrees of detail; sometimes the texture of the thatched roof was specified, other times just the general areas of roofs were blocked in. As with the white houses, the underdrawing was not always rigorously followed. The first color to be applied was the brown of the walls. Afterwards, the roof was filled in with a lighter yellowish brown. Finally, black was used to outline walls, doors, windows, and the thatched roof (see figure 57).

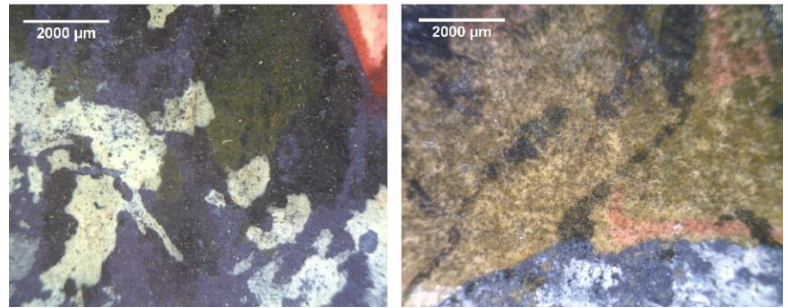


**Figure 57:** Digital handheld microscopic images demonstrating the sequence of coloring thatched houses. (Left) 'Baçaim,' showing underdrawing on thatch roof (and the relative translucency of the light yellow paint). The black appears to be added using a pen. (Right) 'Cochim,' showing a lower-velocity, stubbier line on the thatch, a lack of underdrawing on the thatch, and the overlapping of the two shades of brown used to color the house.

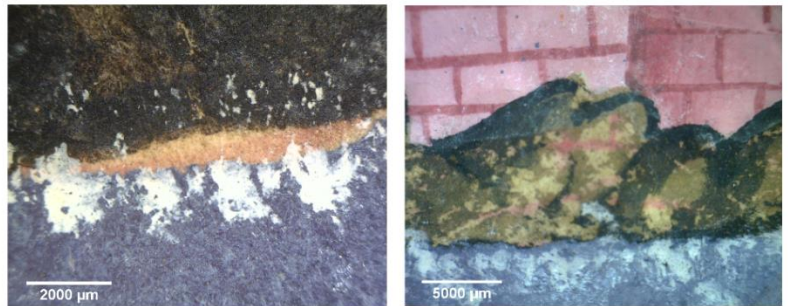
**Coastlines** are always sketched in before painting. The meeting area of the blue of the sea and beige of the landscape is typically underscored and tidied-up with a band of opaque white. Coastlines in the maps are one of the more tortured subjects in terms of establishing and adhering to a design, as evidenced by frequent occasions of multiple underdrawings and a final design following none of them exactly.

**Rocks** were sometimes very loosely underdrawn (figure 58, top right). There are two primary ways of drawing rocks in these maps:

- Filling in the area in with dark brown and then accentuating contours with overpainted dark brown or black ('Sera de Aserim,' 'Mangalor,' 'Dio,' 'Chaul'). This kind of rock often shows signs of underdrawing.
- Alternatively, rocks can be painted in very dark black or blackish brown, with overlays of an opaque reddish or yellowish color ('Cochim,' 'Damaõ,' 'Chaul' top right rocks) (figure 58, top left).



(Left) 'Cochim.' (Right) 'Dio.' The rocks of 'Dio' demonstrate a different technique, seen also in 'Sera de Aserim,' 'Mangalor,' and 'Chaul.'



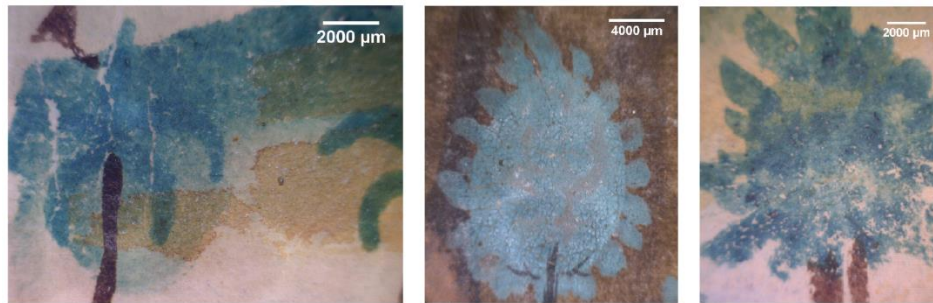
(Left) 'Chaul.' The gap between the water and rock, and the evident underdrawing, show that this rock was part of the original design. (Right) 'Mangalor.'

**Figure 58:** Handheld digital microscopic images showing ways of painting rocks.

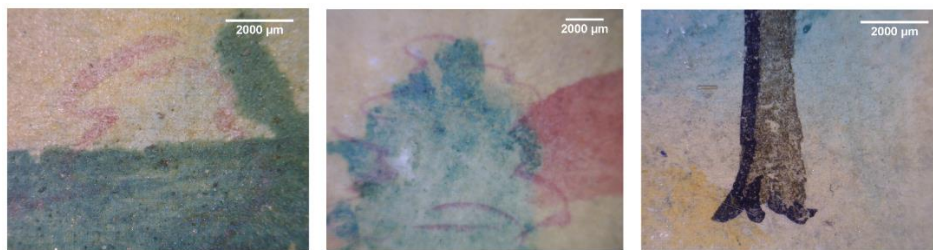
Sometimes the rocks are planned components of the composition, as can be seen on the image from 'Chaul' (figure 58, bottom left). Here, it is possible to discern the underdrawing for a rock in the water, and the gap remaining as the sea was painted such that it avoided covering the rock. Other times, whether the rock was part of the original design is harder to determine. 'Mangalor' provides an example; we can see that the rocks are painted over an area with a preparatory sketch of fortress walls (figure 58, bottom right).

**Trees** are drawn differently depending on type (figure 59). They are always painted after the surrounding terrain. The palm trees in this group uniformly lack underdrawings and are painted on top of the surrounding terrain. Broadleaf trees are occasionally underdrawn and are colored by first painting an oval of green, and then (using the same green) describing the foliage with horizontal rows of dots (see figure 59, top middle and right). This is most visible in the maps of 'Sera de Aserim,' 'Damaõ,' and 'Baçaim,' but is not incompatible with the trees on the remaining maps in this group. When needed, the green is mixed with white to enable painting over already-painted dark zones (see figure 59, top middle, 'Sera de Aserim'). The trunks of trees are executed in either brown, or black, or brown overpainted with black. It is interesting to note the disconnect between the underdrawing of broadleaf trees and the actual coloring process (figure 59, bottom left and middle). Where the underdrawing is fluid and organic, the painting is executed in a rather mechanical way based on a

simplified geometric form with surface embellishment. While supporting the hypothesis that the draughtsman and colorist were separate people, the consistency of this coloring strategy suggests that the colorist (at least of the foliage) was one person across this group of maps.



Left to right: 'Baçaim,' 'Sera de Aserim,' 'Cochim.' Note the *pentimento* on the image from 'Baçaim,' where the underpainted oval for a generic broadleaf was ultimately ignored and a palm tree was placed. Note also the consistent use of the oval underpainting between the trees of 'Cochim' and 'Sera de Aserim' even as the design of the tree trunks varies.



Left to right: 'Mangalor,' 'Chaul,' 'Mangalor.' In some cases, an underdrawing was used for the broadleaf trees in addition to the oval underpainting. Trunks were drawn flexibly; here, a brown trunk with black overlay is used.

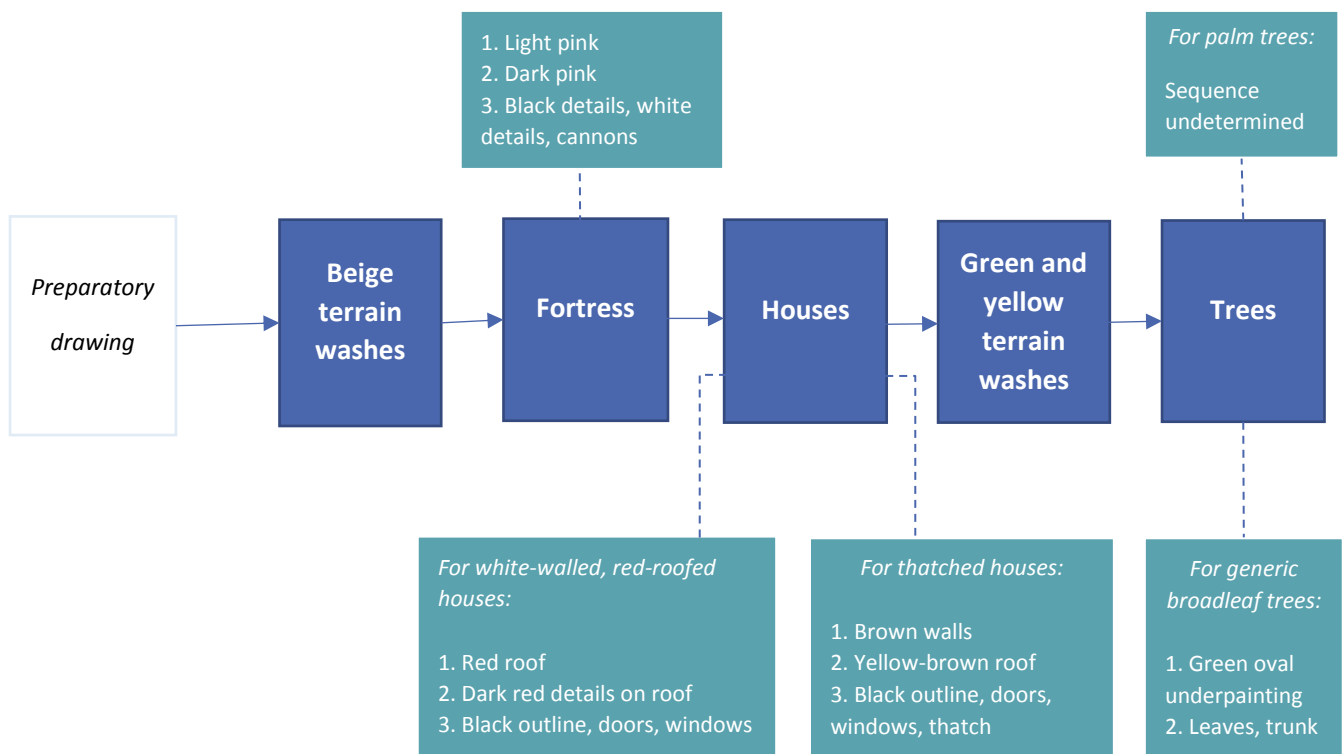
**Figure 59:** Handheld digital microscopic images showing techniques for painting trees.

#### 6.4: Sequence of painting major features

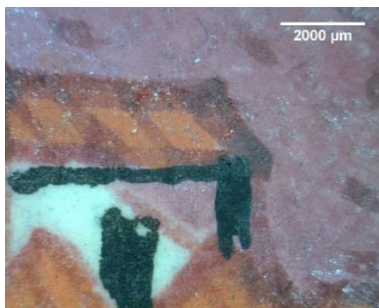
Using handheld digital microscopy, it was possible to sketch out the workflow for coloring of the maps of this subset (figure 60). The sequence was determined by searching for places in which there is overlap between two features (for instance, the edge of a fortress and a flower), and figuring out which is on top (i.e., which was painted later). While not included in the figure, miscellaneous details (bell towers, flowers, gallows) seemed to have been completed late in the process, and the gardens in the courtyards of houses were usually painted at the same time as the greens of the surrounding landscape. Figure 61 provides an illustration of the deductive process using handheld digital microscopic images from the map of 'Cochim.' One limitation of this approach to defining the workflow was that it hinged on the opacity and body of the paints. When features were colored with paints of poor hiding power it was sometimes impossible to discern which color (or feature) came first. These ambiguities have been accounted for in the hypothesized workflow in figure 60.

The proposal of a unitary workflow for the entire subset of was only feasible because the sequence in which different features were painted was largely consistent between the maps. The unvarying order in which the map features were colored is significant: it suggests the participation of either a single colorist, or the production of the maps in a tightly-controlled workshop setting.

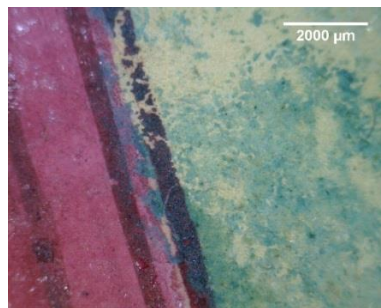




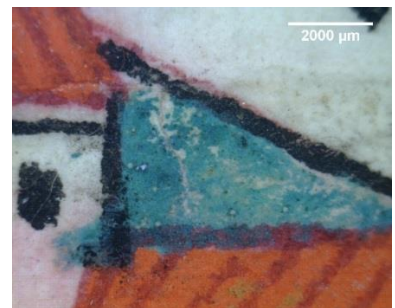
**Figure 60:** Hypothesized coloring sequence, summarized.



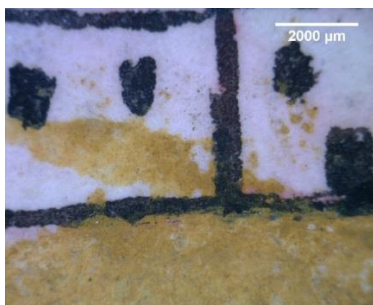
Houses are painted after fortresses.



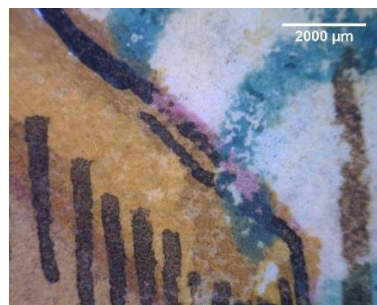
Green terrain is painted after fortress, beige terrain is painted before fortress.



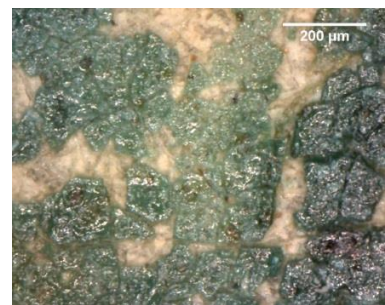
Gardens are painted after houses.



Yellow terrain is painted after houses.



Trees are painted after houses.



Trees are painted after beige terrain.

**Figure 61:** Handheld digital microscopic images providing evidence for proposed coloring sequence (from the map of 'Cochim').

## 6.5: Alterations to the maps' design noted by handheld digital microscopy



**Figure 62:** Digital restoration of the original fortress design ('Dio'). (Left) map of fortress at present. (Right) proposed reconstruction of leftmost bastion based on observations made at x57 digital microscopy, using Adobe Photoshop CC 2018.

Numerous changes to the maps' composition were evident using handheld digital microscopy. Deviation from the underdrawing is a common feature of the maps, and the instances of altered coastlines are obvious enough that microscopy is unnecessary. Major *pentimenti* were seen in the maps of 'Dio' and of 'Damaõ.' In the case of 'Dio,' the leftmost bastion was originally conceived as less angular. Handheld digital microscopy permitted close observation of the initial form of the bastion and a hypothesized reconstruction of the earlier design (figure 62). Microscopy of the map of 'Damaõ' confirmed that the whites in the map were sometimes due to absence of paint or a translucent wash, and other times implemented with a heavy-bodied opaque white paint.

An amusing minor change is found in the map of Chaul, where a house that was at first painted with white walls and a red roof was painted over and converted into a thatched-roof house. This alteration lends further support to the notion, introduced in Chapter 3, that the distinction between the two housing types was significant for the artist.

## 6.6: Pigment characteristics and possible mixtures/overlays

Following the spots used for colorimetry (Appendix II.1), 432x magnification handheld digital microscopic images were taken of the paints used in the maps. These images are provided in full in Appendix III.2. In some cases, colors could not be included in colorimetric measurements because they occupied a space smaller than the colorimeter's aperture. In such instances, the spots for high magnification digital microscopy do not correspond to the colorimetric spots.

Several observations about the paints' characteristics can be made based on these images. First, overall, the coherence and texture of different colored paints (red on roofs, dark green on trees, etc.) is consistent across the maps. The red, blue, green, light pink, and white paints are relatively thick and prone to cracking. The green and blue paints frequently flake off altogether. The shininess of painted surfaces is variable. In all cases (except for the white walls, which



are either unpainted or brightened with a diluted white paint), it is possible to find impurities. The size of these heteroparticles is generally greatest in the blue pigment, suggesting a less intense grinding procedure for the pigment preparation (or contamination/adulteration). The reds and light pinks are notable for their excellent hiding power, while the coverage provided by brown and beige paints is poor. Finally, on the areas where blue paint has flaked off, the underlying paper has been stained blue.

Deliberate mixtures were difficult to conclusively identify using handheld digital microscopy alone because of possible accidental impurities. Rather, microscopy has been used as supporting evidence during the determination of the core palette in Chapter 8. These supporting images can be found in the table in Appendix III.7.

The material used for the underdrawing were slightly elucidated during this part of the investigation. Based on the coherency of its line and its tendency to bleed and soak into the paper, it seems likely that a wet medium was used, such as a colored ink.

## Chapter 7: Searching for pigment variations

Considering the lack of chronology for the maps' creation and absence of definitive identification of their colorist, an analysis of the materials used must not assume homogeneity across the maps. Colorimetric and technical photography results are grouped together as they represent the first attempt to understand the similarities or variabilities of artistic materials used in the maps. See Appendix II.2 for methods used for technical photography and Appendix II.4 for colorimetry.

### 7.1: Colorimetry

The consistency in painting sequence observed during digital microscopy had suggested that the maps were colored by a single artist or in a tightly-controlled workshop. This hypothesis leads one to expect a degree of continuity in types of painting materials between maps as well. The colorimetric data, as expressed in CIE  $L^*a^*b^*$  coordinates, supports this theory (figure 63). The red of roofs, or blue of water, is highly consistent between the maps. On colors such as beige and tan unvegetated terrain, or green vegetated terrain, far more spread is observed. This variability is easily understood as the result of mixing, dilution, or overlays of colors, and does not necessarily imply the use of different pigments. Variation of coordinates for other features is partly due to the limitations presented by the colorimeter's aperture size, which made it impossible to isolate small areas without including undesired adjacent colors. Indeed, some colors could not be measured on a given map due to the

minuteness of the regions they occupied. Nonetheless, the colorimetric measurements capture the essential, optically-apparent palette presented by this group of maps. For colorimetric coordinates and additional remarks, see appendix III.4.

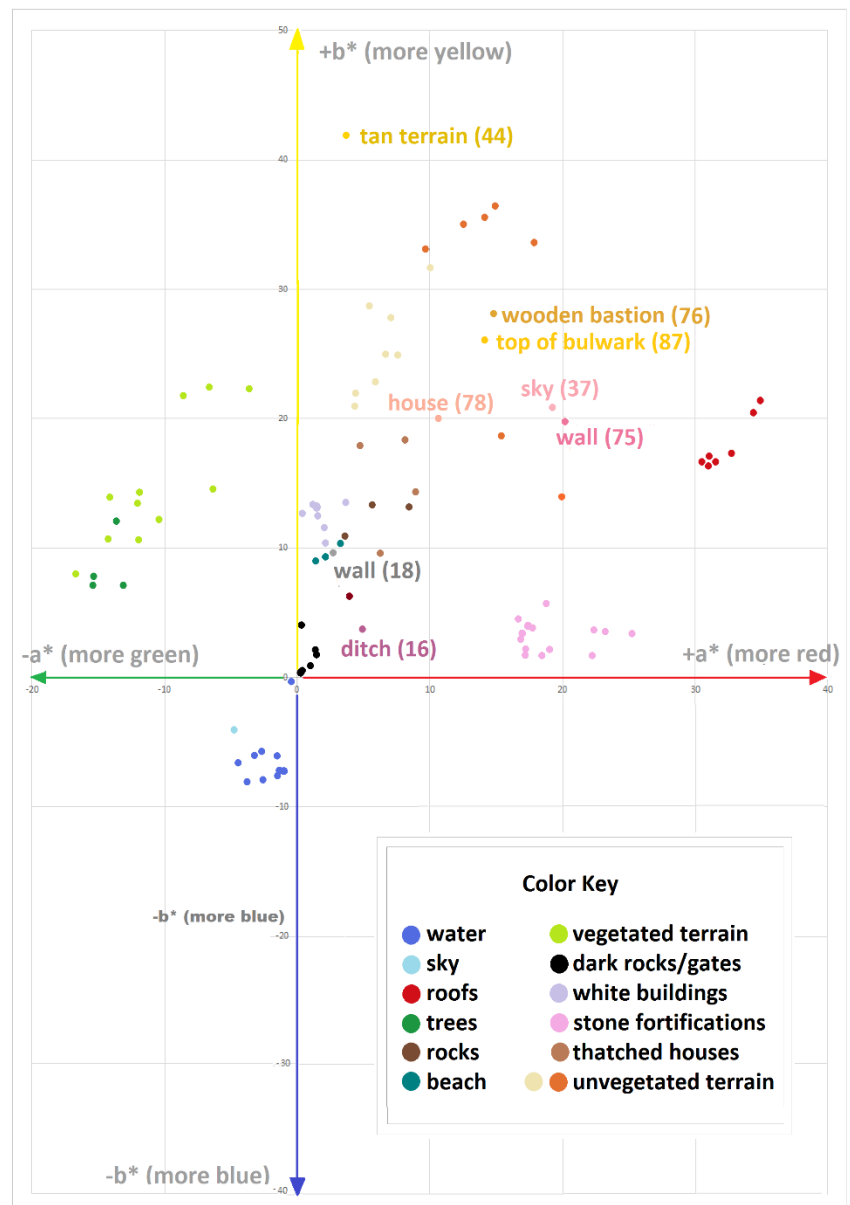
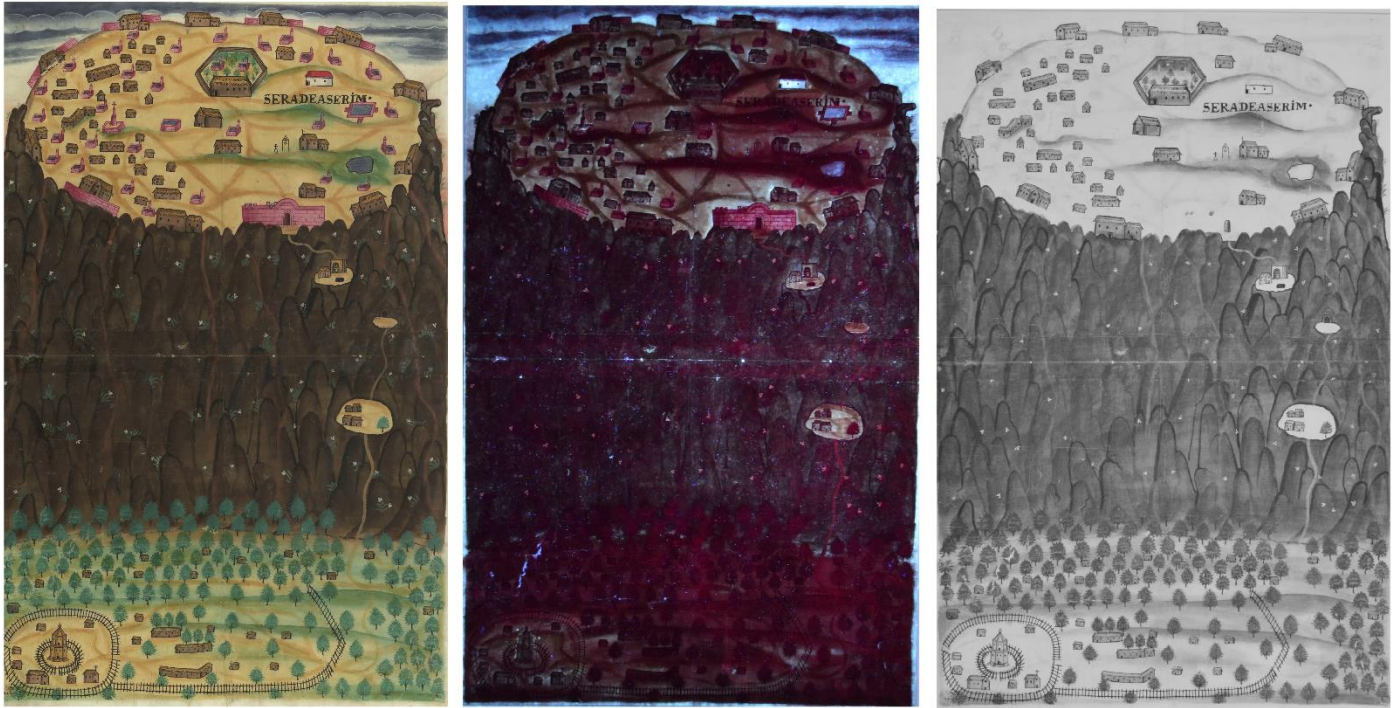


Figure 63: CIE  $a^*b^*$  colorimetric coordinates according to feature.

## 7.2: Technical photography



**Figure 64:** Map of 'Sera de Aserim' under normal illumination (left, copyright Biblioteca Pública de Évora); UV-IVF (middle); and NIR (right).

Technical photography did not indicate any differences in paints between the maps (i.e., the infrared transparency and ultraviolet-induced visible fluorescence of a red region on one map was the same as the that of the red of another map). The findings of technical photography are summarized in table 3, and expanded results are provided in Appendix III.3. No retouches were detected using these methods. While not conclusive, technical photography allowed cautious exclusions of some pigment hypotheses. Indian yellow, a color that is both visually similar to the yellow-tans of the maps and chronologically and regionally appropriate, was not suggested by the UVF-IV photographs, as it demonstrates a brilliant green to golden yellow fluorescence (Baer et al. 1986; Smith 2017).

The most curious feature of the paints used in the maps was a widespread reddish undertone detectable in several colors but most prominent in the light greens. It was not possible to identify in the literature any reference to such a behavior from a green pigment. Rather, the fluorescence appears to be connected with the opaque white pigment, which was evidently combined with many of the colors to improve opacity or change the color. The map of 'Sera de



**Figure 65:** Pink to tan ultraviolet-induced visible fluorescence of opaque white paint. (left) UVF-IV detail of the map of 'Damaõ'; (right) detail of map of 'Damaõ' under normal illumination.

**Table 3:** Summary of technical photography observations. Ratings of infrared transparency were made by visually identifying the most and least transparent regions, assigning them ranks of 1 (transparent) and 5 (opaque), and then scoring colors of intermediate infrared transparency on a scale of 1-5. Color changes observed under ultraviolet illumination are recorded descriptively.

<i>Colors found in two or more maps in the subset</i>				
Color	Color name	Regions	NIR imaging (1=transparent; 5=opaque)	UVF-IV imaging (color change)
	Medium blue	Water	2	Dark blue, sometimes with reddish undertones. At areas where paint is thin, bright electric blue.
	Light blue	Water	1	Light blue with pinkish undertones.
	Tan	"Roads"	1-2	Dull brown.
	Yellow-tan	Unvegetated terrain	1.5	Dull brown.
	Beige	Unvegetated terrain	1	Dull whitish-grey beige.
	Dark green	Trees	4-5	Very dark with reddish edges and undertones.
	Yellow-green	Vegetated terrain	3.5	Dark reddish color.
	Pale green	Vegetated terrain, some trees	3-3.5	Scarlet.
	Light pink	Stone fortifications	1-1.5	Slightly darker warmer pink.
	Dark pink	Stone fortifications	1.5-2	Darker pink.
	Black	Gates and outlines of houses	5	No change.
	Light brown	Thatched house walls	3-3.5	Darker, duller brown, sometimes with reddish undertones.
	Dark brown	Rocks	4-5	Darker with reddish undertones.
	Transparent white	Red-roofed house walls (unpainted)	1	Brilliant white.
	Opaque white	Opaque white "corrections", beaches	1	Dull orangeish pink to brilliant scarlet.
	Red	Roofs	1	Dull, dark red.
	Opaque gray	Cannons	3	Deep scarlet.
<i>Colors restricted to single maps in the subset</i>				
	Orange-pink (Mangalor)	Some fortifications	2	Dark pink.
	Pale warm pink (Mangalor)	House in Olala	1	Dull pinkish white.
	Warm pink wash (Sera de Aserim)	Sky	1	Darker pink, similar color change to the typical light pink and dark pink fortifications.
	Dark purple (Damaõ)	Moat	4	Dull blackish purple.
	Yellow-brown (Mangalor)	Tower	3.5	Very dark brown.
	Red-orange (Chaul)	Top of bastion	2	Magenta.
	Yellow-orange (Chaul)	Top of bastion	2	Slight darkening and dulling.
	Dark blue ( Damaõ )	Water	3.5	Dark blue.
	Blue wash (Sera de Aserim)	Sky	1.5	Cooler, darker blue (loss of yellow cast imparted by paper).
	Gray wash ( Damaõ )	Fortifications	2	Gray (slightly cooler in cast).

Aserim' is illustrative (figure 64). When the trees are painted on a light-colored backdrop, the green appears darker under the ultraviolet light source. However, when they are painted over dark areas (such as those overlapping the brown of the mountain), they show a vivid crimson color change. Adding white to the green paint would have been a reasonable strategy for increasing the hiding power of the paint, and this strategy is evident even under normal visible light in the slightly chalky, pallid appearance of the greens in these areas. Areas painted with opaque white (figure 65) also show an orange to bright pink color. Therefore, the most parsimonious explanation for the widespread reddish color is a mixing of other pigments with a particular white pigment, either as an opacifier or to modulate color.

Subsequent analyses demonstrated that the white pigment is lead-based (see Chapter 8). Lead white fluorescence is strongly depending on the binder in which it is mixed, and perhaps the binder or a pigment-binder interaction is the cause of the fluorescence (Contentino 2015). Another possibility is that the grains of calcium-rich substance found in the lead white regions by vp-SEM-EDS is siliceous chalk or kaolin, which may fluoresce red-violet (Eastman Kodak Company 1972, p. 26). It was not possible to find verification that the mixture of any of these whites with another color (green, blue) produces an intense red color change. This fluorescence pattern could not be conclusively explained by the conclusion of the thesis, but the question will be taken up again after preliminary characterization of the binder in Chapter 8.



## Chapter 8: Pigment and Binder Identification

Technical photography, colorimetry, and handheld digital microscopy did not indicate any difference in the paints used across the maps of the subset. FORS and h-XRF spectra were then recorded at the same spots used for colorimetry to provide complimentary, noninvasive information on the molecular and elemental characteristics of the pigments. These two techniques were first tasked with defining the number of pigments used in the maps; that is, with the identification of the core palette.

To make preliminary hypotheses about the pigments using the FORS data, the spectra acquired from maps were compared with mockups of historical pigments and mixtures in different binders prepared by Whitney Jacobs under the supervision of Dr. Catarina Miguel. Details on the mockups are provided in Appendix II.5.

The interpretation of the h-XRF spectra was complicated by the fact that the maps have been glued to Japanese tissue and are mounted in cardstock backings. It was not clear whether the elements detected were coming from the painted layer, or from any of several layers of material below (figure 66). That the incident beam penetrated through at least the uppermost paint layers became evident when analyzing a pale green tree painted on top of the mountain in the map of 'Sera de Aserim.' Mercury from the brown paint layer below was identified in the spectrum of this green zone. To

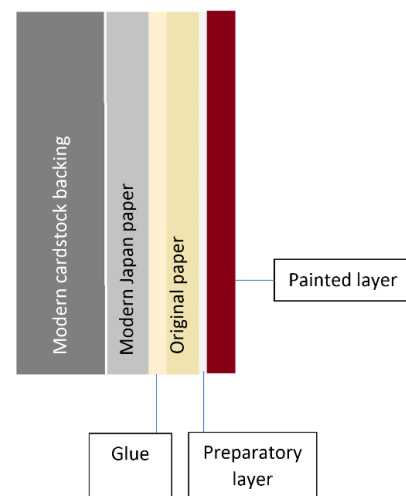


Figure 66: Stratigraphy of the maps.

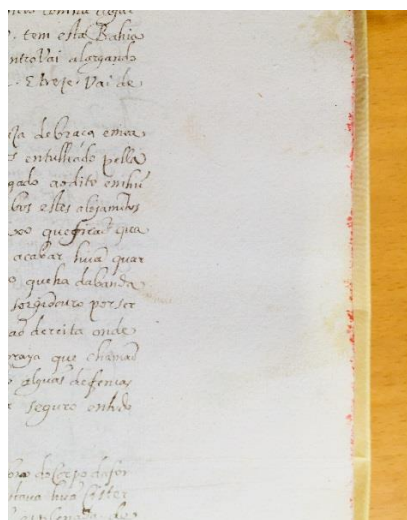


Figure 67: Edge painting on the text of the Évora codex.

minimize the contribution of underlying materials, the average normalized counts for each element in each of the papers analyzed was subtracted from the normalized counts of each respective element in the maps (see Appendix II.6 for more information). Nevertheless, it is important to note that due to variable thicknesses of the painted layers and the inability to strictly control the distance of the incident beam from the surface of the maps, the h-XRF results are most reliable for elements detected in large amounts.

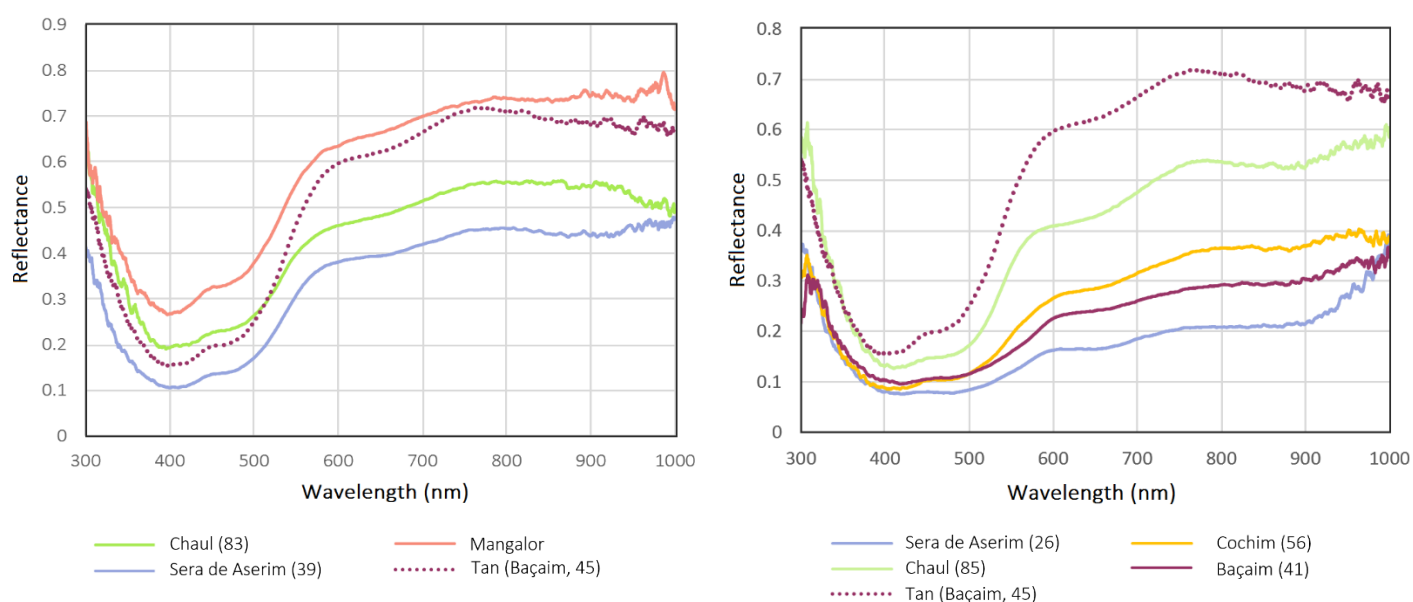
An interesting feature of the paper was revealed during the h-XRF analyses. On all the maps investigated, a reddish line ran along the edge of the pages, with small red dots sometimes found below. Despite the miniscule size of these dots, it was possible to take an h-XRF measurement. Besides the elements associated with the paper (i.e. preparatory layer, paper, and possibly Japanese paper), major amounts of mercury were detected. It is likely that when the maps were bound

together with Bocarro's text, the edges of the pages were painted in vermilion or cinnabar to give the codex a more attractive appearance. A similar red dotting and edge painting was noted in the text of the Évora codex (also housed in the Public Library of Évora) (figure 67).

## 8.1: Same pigments, different colors? Defining the core palette

Based on information acquired by observation of the paints with handheld digital microscopy, it appears that several “different” colors in the maps were combinations, overlays, or dilutions of two or more pigments. Our task in this section is to infer the way mixtures were used using FORS and h-XRF and seek further evidence that the pigments used between the maps were consistent. The identification of the pigments will follow in 8.2, synthesizing the data collected so far and using additional analytical methods to acquire robust evidence relating to both pigments used and their production method. The reliability of pigment identifications using only portable equipment (provided in tables 4 and 5) will be contrasted with the ultimate identifications. Additional h-XRF and FORS results are provided in Appendix III.5-6.

### 8.1.1: Beige, tan, and brown

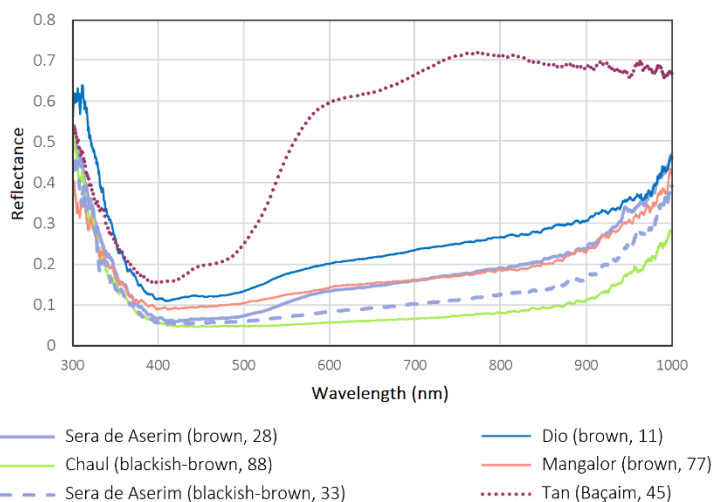


**Figure 68:** FORS spectra of representative beige regions compared with tan (left); representative light brown regions compared with tan (right). Note that the total reflectance for beige and tan regions should not be directly compared, because the exposure times for the two regions were different (see Appendix II.5). Numbers beside map names refer to measurement locations which are given in Appendix II.1.

Handheld XRF analysis of beige and tan regions exhibited the same major elements (iron and lead, with lesser amounts of manganese; see table 5). The differences between these zones is in the detected amounts of each element, not which elements are present. It can be posited, therefore, that a similar yellowish iron-based pigment is responsible for both colors, but it is diluted with water in an organic medium to paint beiges and applied relatively thickly (and with increased amount of a lead-based white) for the tan areas. The FORS spectra of the tan and beige regions support this interpretation. The spectral profiles of the two colors are similar, with the beige regions showing elevated reflectance overall, probably due to increased contribution from the underlying paper (figure 68, left).

The browns of thatched houses present reflectance spectra with bands, minima, and an inflection point of the steep slope at the same positions as the tan regions (figure 68, right). The elements detected by h-XRF included those seen in the tan regions (lead, iron, some manganese; see table 5). Additionally, in all the brown spots except for 21 (in the map of

‘Damađ’), mercury was present. The FORS spectral data in conjunction with the elemental analysis suggest that the browns used for the houses contain a mixture of an iron oxide pigment (probably yellow ochre) with some lead white and perhaps carbon black. We can also infer that other pigments (including a mercuric sulfide red) were added to modulate the color, but that the brown shades were flexibly mixed for each map. It should be mentioned that the absence of any mercuric sulfide red pigment in spot 21 affected the colorimetric results, resulting in the lowest  $a^*$  coordinate of all the light brown regions ( $a^* = +4.66$ ; compared with a mean  $a^*$  for all the brown house measurements of  $+7.22$ ). The brown houses had slightly elevated manganese counts respective to the tan regions, but the difference was too negligible to assume significant input of umbers or siennas.<sup>1</sup>



**Figure 69:** FORS spectra of medium and dark brown regions compared with representative tan region. Numbers beside map names refer to measurement locations which are given in Appendix II.1.

The browns of rocks were an even more heterogeneous group than those of the houses. Strikingly different approaches to the painting of rocks between maps (depending on the scale of the rocks, their location, and whether they were painted before or after surrounding map signs) have already been mentioned in Chapter 6. The FORS spectra of the brown rocks sometimes displayed the slight shoulder near 450 nm and inflection point at around 540 nm seen in the tans (spots 11 and 28); in other cases (33, 77, 88), these features were impossible to detect (figure 69). Particularly in the blackish-brown colors, the overall reflectance was too low to generate an edifying spectrum.

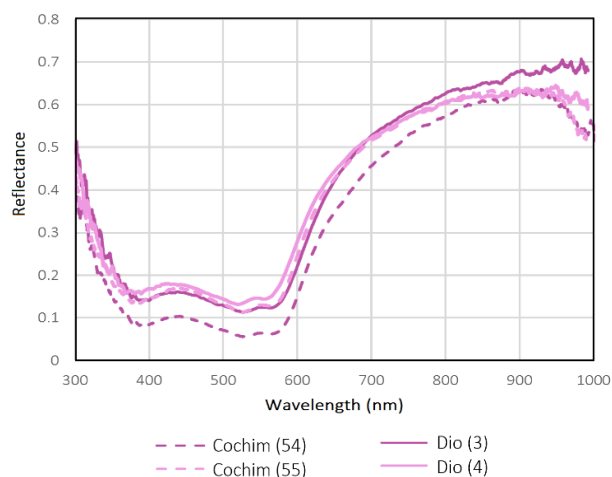
The same major elements noted in the tan, beige, and light brown regions (iron and lead) were found in all the brown rocks (table 5). However, the ratio of iron to lead in the brown regions of the rocks was far higher than in any of the previously listed colors. Manganese counts were also elevated in the brown rocks with respect to the tans, beiges, and light browns, but were recorded at levels far below lead and iron. A further difference was the detection of copper (in all brown rocks except spot 33) and mercury (in all brown rocks except 77).

Drawing conclusions from the elemental data discussed here is difficult; the experimental setup did not allow strict quantification, nor could we map elements extensively across the painted regions. For the moment, the following hypothesis is put forward: the browns of the rocks, like those of the houses, are a hodge-podge of pigments; a copper-based green, a mercuric sulfide red, an iron oxide, lead white, and perhaps an iron-based black and/or carbon-based black, mixed on an *ad hoc* basis until the desired shade was achieved

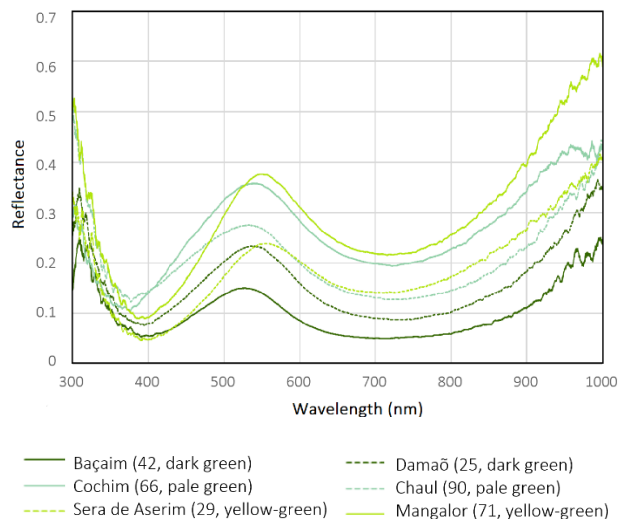
### 8.1.2: Light pink and dark pink

The analogous reflectance profiles of the light and dark pinks suggest the use of the same pink pigment (figure 70). The

<sup>1</sup> Umbers are brown earth pigments including iron oxides and approximately 5-20% manganese compounds. Siennas contain iron oxides and up to 10% manganese oxides (Eastaugh et al. 2004, pp. 339 and 377).



**Figures 70:** FORS spectra of representative light and dark pinks. Numbers beside map names refer to measurement locations which are given in Appendix II.1.



**Figure 71:** FORS spectra of representative greens. Numbers beside map names refer to measurement locations which are given in Appendix II.1.

major elements for the dark pink and light pink zones were identical: high quantities of lead, with minor amounts of tin and chromium (see table 5). The amount of lead does not differ significantly in the light and dark pink. Given the transparency of the dark pink and the likelihood that it is a lake pigment, it is probable that these regions were created by glazing saturated dark pink over already-painted light pink areas.

### 8.1.3: Light green, dark green, yellow-green

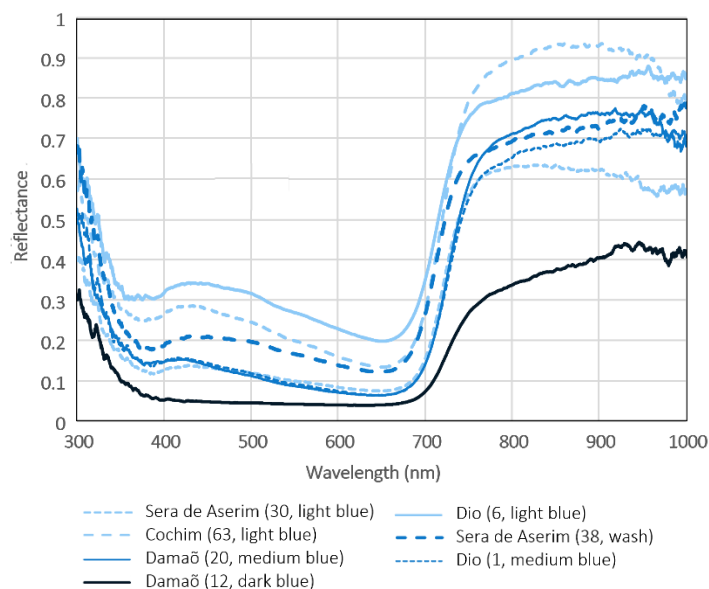
The FORS spectra for the greens (even within one color grouping of greens, such as the dark green of trees) exhibited some shifting of the reflectance maximum for the band between 400 and 700 nm but presented a similar profile overall (figure 71). Not surprisingly, the reflectance maxima for the yellow-green were recorded at higher wavelengths, i.e., towards yellower visible light (approximately 560-580 nm). The spectra for the pale greens and dark greens varied in reflectance intensity but displayed maxima at roughly the same wavelength.

The major elements for all the greens were the same: copper and lead, with lesser amounts of iron (table 5). The ratios of these elements may explain their variability in apparent color. Yellow-greens had the lowest average ratio of copper to iron counts, and dark greens the highest. The ratios of copper to lead also varied between the shades of green, with the highest ratio in the dark greens, and the lowest in the light greens. Based on the results so far, we can hypothesize that the range of green tints was obtained by mixing or layering three pigments: a copper-based green, a lead-based white, and an iron-based yellow.

### 8.1.4: Light blue, dark blue, medium blue

The FORS spectra of the medium and light blues shared a wide, asymmetric absorbance band from approximately 430 nm to 720 nm (figure 72). Within the blues, at least 4 preparations based on the same blue pigment can be conjectured as giving rise to the different shades observed. There is a blue pigment applied as a wash at spot 38 (figure 72); a blue pigment mixed with an opacifier or extender at spots 1 (figure 72), 13, 40, 51, 67, 82 (not included in figure 72; see Appendix III.5.6

for spectra); a blue pigment mixed with white at spots 6, 30, 63 (figure 72); and a blue pigment with minimum opacifier or mixed with black and applied over a medium blue (figure 72). The h-XRF analyses were compatible with these conclusions. In the case of the light blues, increased counts of lead probably denote color modulation by the addition of lead white. Between the medium and dark blue, the counts of all remaining elements were roughly comparable (table 5). It is likely that the dark blue and medium blue colors are produced by the same blue pigment and extender, but that the dark blue is mixed with or overpainted with a carbon-based black, which would not be detected by XRF.



**Figure 72:** FORS spectra of representative blues. Numbers beside map names refer to measurement locations which are given in Appendix II.1.

### 8.1.5: Occasional Colors

For colors seen on only one map but suspected of being mixtures, the same approach was taken: a comparison of their FORS spectra with the spectra from mockups and other colors from in maps, and appraisal of the elemental character of the pigments as discerned by handheld XRF. The process of deducing mixtures is laid out in greater detail in the table in Appendix III.7. Hypotheses regarding the pigments used are summarized in tables 4 and 5 below. It should be remembered that the goal of the h-XRF analyses was not determination of provenance, and that elemental variability at trace levels was neither a reliable indication of difference, nor of relevance to the present research. For a more detailed discussion of the data handling of the h-XRF results and the reasons for the caveat above, see Appendix II.6.

**Table 4:** Summary of occasional colors and their hypothesized constituents based on handheld digital microscopy, FORS, and h-XRF. See Appendix II.1 for locations of measurement spots. See Appendix III.7 for a more detailed discussion of the pigment hypotheses for selected occasional colors. Elements in bold text were detected in the highest quantities. Elements in parentheses were detected in low quantities.

Color	Spot number	FORS Assignment	Elements	Pigment hypothesis
Red-orange	86	Yellow ochre + ?	<b>Fe, Pb</b> (Hg, Mn, Sn)	Yellow ochre + HgS
Yellow-orange	87	Yellow ochre + ?	<b>Fe, Pb</b> , Hg (Al, Cr, Hg, Mn, Sn)	Yellow ochre + HgS
Orange-pink	75	Yellow ochre + ?	<b>Fe, Hg, Pb</b> (Cr, Cu, Mn, Sn)	Yellow ochre + HgS + pink lake pigment
Dark orange-pink	M.F.2	Cochineal lake + ?	<b>Fe, Hg, Pb</b> (Al, Cr, Cu, Mn, Sn)	Cochineal lake + yellow ochre + cinnabar
Purple-brown	16	<i>Spectrum not diagnostic</i>	<b>Fe, Pb</b> (Al, Cr, Mn, Si, Sn)	Cochineal lake + iron-rich black (iron gall ink or Mars black or carbon black + iron gall ink)
Warm pale pink	78	Yellow ochre + ?	<b>Fe, Pb</b> , Hg (Al, Cr, Mn, Sr, Ti)	Yellow ochre + HgS
Warm pink wash	37	HgS ?	<b>Hg, Pb</b> , Fe (Ba, Mn)	Yellow ochre + HgS
Olive green	Di.F.9	Yellow ochre+?	<b>Fe, Pb</b> (Al, Cr, Cu, Hg, Mn, Si, Ti, Zn)	Yellow ochre + copper-based green + HgS



**Table 5:** Summary of recurring colors and mixtures and possible pigments based on handheld digital microscopy, FORS, and h-XRF. Elements in parentheses were detected in low quantities. Elements with an asterisk (\*) were detected in only some of the measurement spots. When a detected element was clearly due to contribution of an adjacent color, it is not included in the table. The lead detected in almost every region is assumed to relate to lead white preparatory layer or admixture and is not included in the pigment hypothesis. See Appendices III.5 and III.6 for expanded FORS and h-XRF results. See Appendix II.1 for locations of measurement spots. Colors in gray are considered dilutions or mixtures of the colors in black. Elements in bold text were detected in the highest quantities.

Color	Spot numbers	FORS Assignment	Elements	Pigment hypothesis
Red	7, 24, 35, 48, 74, 93	Cinnabar or vermilion	<b>Hg, Pb</b> (Al*, Ca*, Cr*, Cu, Fe*, Sr, Zn)	HgS
Tan	8, 15, 36, 45, 49, 84	Yellow ochre	<b>Fe, Pb</b> (Al*, Mn, Cr*, Si*, Sn, Ti*, Zn)	Yellow ochre
Light brown	26, 41, 56, 85	Yellow ochre+?	<b>Fe, Pb, Hg*</b> (Al, Cr, Cu*, Mn, Si*, Sn*)	Yellow ochre + HgS + carbon black
Medium brown	11, 28, 77	Yellow ochre/spectra not diagnostic	<b>Fe, Pb, Cu</b> (Al, Cr, Hg*, K*, Mn, Si, Ti)	Iron oxide + copper-based green+ HgS + carbon black
Blackish-brown	33, 88	Spectrum not diagnostic	<b>Pb, Fe, Ca*</b> (Al, Cr, Cu*, Hg, K, Mn, Si, Ti, Zn)	Iron oxide + copper-based green + HgS + carbon black
Beige	9, 23, 39, 43, 52, 70, 83	Yellow ochre	<b>Fe, Pb</b> (Al*, Cr, Mn, Sn)	Yellow ochre (diluted)
Black	22, 64, 65	Spectra not diagnostic	<b>Pb, Fe, Ti*</b> (Al, Cr*, Cu, Hg*, K* Mn, Si, Zn*)	Iron-rich black (iron gall ink or Mars black or carbon black + iron gall ink) (for rocks at spots 64 and 65, possible overpainting or admixture of HgS)
Medium blue	1, 13, 40, 51, 67, 82	Indigo, Maya blue	<b>Fe, Ti</b> (Al, Cr, K, Ni*, P*, S*, Sr*, Pb, Zn)	Indigo or Maya blue+?
Light blue	6	Indigo, Maya blue	<b>Pb, Fe</b> (Cr, Ti, Mn, Al, Si, Zr)	Indigo or Maya blue + ?
Light blue	30	Indigo, Maya blue	<b>Pb, Fe, Cu</b> (K, Al, Cu, Cr, Mn, Si, Sr, Ti, Zr)	Indigo or Maya blue + ?
Light blue	67	Indigo, Maya blue	<b>Pb, Fe (Al, Cr, Cu, Mn, Si, Ti)</b>	Indigo or Maya blue + ?
Wash blue	38	Indigo, Maya blue	<b>Fe</b> (Al, Cu, K, Mn, Pb, S, Si, Sr, Ti, Zn)	Indigo or Maya blue + ?
Dark blue	12	Indigo	<b>Fe, Ti</b> (Al, Cr, K, Mn, P, S, Si, Zn)	Indigo + carbon black + ?
Dark pink	3, 32, 47, 54, 80, 92	Cochineal lake	<b>Pb</b> (Al*, Cr, Cu*, Fe*, Mn*, Sn)	Cochineal lake
Light pink	4, 20, 31, 46, 55, 73, 89	Cochineal lake	<b>Pb</b> (Al*, Cr, Cu*, Sn)	Cochineal lake
Dark green	5, 27, 42, 57, 91, Di.F.1, M.F.3	Malachite	<b>Cu, Pb</b> (Al*, Cr*, K*, Fe, Mn, Sn*, Ti*, Zn)	Malachite
Yellow green	29, 50, 61, 71	Malachite	<b>Cu, Pb</b> (Al*, Cr, Fe, Mn, Sn*, Zn*)	Yellow ochre + verdigris or malachite
Pale green	14, 25, 66, 72, 90	Malachite	<b>Cu, Pb, Fe</b> (Al*, Cr, Fe*, Mn, Sn*, Zn*)	Yellow ochre + verdigris or malachite
Pale green	Di.F.2, Di.F.3	Malachite	<b>Cu, Pb</b> (Al*, Cr, Fe, Hg, Mn, Sn)	Verdigris or malachite over remains of painted layer including HgS
Pale green	SA.X.1	No measurement	<b>Cu, Pb</b> (Cr, Hg, Mn, Sn, Ti, Zn,)	Verdigris or malachite over complex dark brown mixture including HgS
Opaque white	62, 69, 94, Da.F.1	Spectrum not diagnostic	<b>Pb, Fe, Sn, Zr</b> (Mn, Al, Cr)	Lead white

At the close of our investigations at the Évora Public Library, we can conservatively theorize the use of 7 pigments: red (either vermilion or cinnabar), black, white (probably lead white), yellowish-tan (probably yellow ochre), blue, green (copper-based), and dark pink (probably cochineal). These colors were mixed in various ways to produce a range of colors. With this overall framework in mind, we turn to each of the core colors to test and expand on the preliminary hypotheses.

From the subset of seven maps, four were selected to study in the laboratory ('Cochim,' 'Damaõ,' 'Dio,' and 'Mangalor') using Raman microscopy,  $\mu$ -FT-IR, VP-SEM-EDS, and LC-DAD-MS. As we have seen, the analyses up to this point had supported the conclusion that the same kind of pigments were used in each map. Thus, we can treat these four maps as a representative sample for the seven discussed so far, and cautiously extend any refinements to the materials characterizations to the rest of the subset.

## 8.2: The Core Palette in Detail

To discuss the core palette, we will move color by color. The contribution of each analytical technique to the pigment identification will be described and justified.

To recapitulate the work so far, using technical photography, colorimetry, handheld digital microscopy, FORS, and handheld XRF, we were able to determine a minimal possible number of pigments used in the maps. To varying degrees, these techniques also yielded hypotheses about the pigments used. In the laboratory, but still working *in situ* (that is, non-invasively), we then performed Raman microscopy on four of the maps. Finally, microsamples were taken

**Table 6:** Microsamples and analyses.

Sample	Region	Color	Analyses
Co.S.3	Letter "M"	Black	$\mu$ -FT-IR
Co.S.4	Outline of church	Black	$\mu$ -FT-IR ; VP-SEM-EDS
M.S.1	Gate	Black	VP-SEM-EDS
Co.S.1	Foam on rocks	White	$\mu$ -FT-IR
M.S.3	Foam on rocks	White	VP-SEM-EDS
Di.S.2	Beach	White	$\mu$ -FT-IR ; VP-SEM-EDS
Di.S.3	Water	Blue	$\mu$ -FT-IR
Da.S.2	Water	Blue	VP-SEM-EDS
Co.S.5	Pepper weight	Pink	LC-DAD-MS
M.S.2	Castle wall	Pink	LC-DAD-MS
Di.S.5	Fortification	Pink	$\mu$ -FT-IR ; VP-SEM-EDS
M.S.4a	Tree	Green	$\mu$ -FT-IR
M.S.4b	Tree	Altered green	$\mu$ -FT-IR
Co.S.2	Tree	Green	$\mu$ -FT-IR
Di.S.3	Terrain	Green	$\mu$ -FT-IR
Di.S.4	Terrain	Tan	$\mu$ -FT-IR
Da.S.3	Roof	Red	VP-SEM-EDS
Da.S.1	Paper	<i>Not applicable</i>	$\mu$ -FT-IR ; VP-SEM-EDS

from these four maps to resolve any remaining questions with the aid of  $\mu$ -FT-IR, VP-SEM-EDS, and LC-DAD-MS. The names, locations, and analyses performed on each of these samples are given in table 6. Further information on the sampling procedure can be consulted in Appendix II.8. Please see Appendix 3 for expanded results, organized by analytical technique; below, representative spectra will be reported.

### 8.2.1: Red (cinnabar)

**Technical photography:** Red areas appeared dark under an ultraviolet lamp and were semitransparent to infrared radiation. Such responses have been documented for vermilion and cinnabar (Cosentino 2015).

**FORS:** The reflectance spectra of the red regions measured in the maps display the same S-shaped profile noted in the mockups of cinnabar in gum Arabic (figure 73). This kind of band-to-band transition is a feature of semiconductors (Boselli 2010, p. 16; Cheilakou, Troullinos, & Kouï 2014), and can also be found in the spectra of pigments such as chrome red and cadmium sulfide (Pronti 2016, pp. 4-5; Nassau 1983, pp. 170-172). The inflection point for the reds from the maps is tightly centered at approximately 600 nm, making adulteration with minium ( $\text{Pb}_3\text{O}_4$ ) improbable, as minium's inflection point is at about 565 nm (Cucci et al. 2018). The cinnabar of the maps is likewise unlikely to be mixed with red ochre; in the mockup

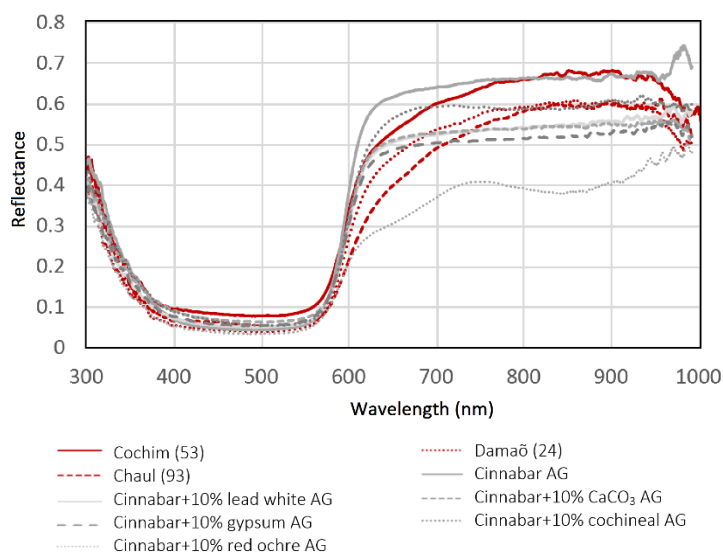
with only ten percent red ochre, characteristic broad absorption bands related to the ochre are already evident at around 660 nm and 850 nm (a shift from the usual 930 nm for the second band, perhaps owing to the HgS in the mixture) (Cheilakou, Troullinos, & Kouli 2014) (figure 73, light gray dotted line). These ochre-related bands are completely absent in the FORS spectra of the reds from the maps.

***h-XRF:*** The high counts of mercury gave further confirmation of vermilion or cinnabar (HgS). Sulfur could not be detected, because its  $K\alpha$  and  $K\beta$  lines were masked by the strong  $M\alpha$  and  $M\beta$  lines of the lead. The presence of lead in the red regions can be explained by mixture with minium or by a preparatory layer of lead white. Minium contribution, however, seems unlikely based on the FORS spectra.

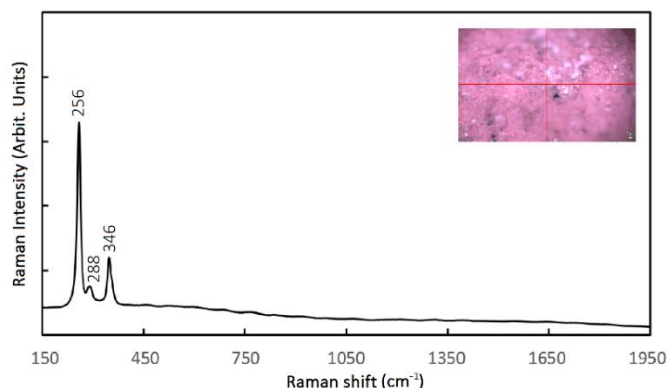
***Raman microscopy:*** The identification of a mercuric sulfide pigment was solidified by Raman microscopy (figure 74). The bands recorded in the red regions of the maps corresponded closely in location and relative intensity to the stretching vibrational bands for HgS in the literature (Scheuermann & Ritter 1969; Clark et al. 1997; C. Frausto-Reyes et al. 2009). The slight band shifting observed across the samples may be due to

the fact that changes in preparation of HgS and in orientation of its crystals with respect to the excitation source can affect the positions of spectral peaks (Frost, Martens, & Klopogge 2002) or could be related to the equipment. No grains of lead white were detected, so the lead discerned by the elemental analysis was probably due to a preparatory lead white wash underlying the red regions.

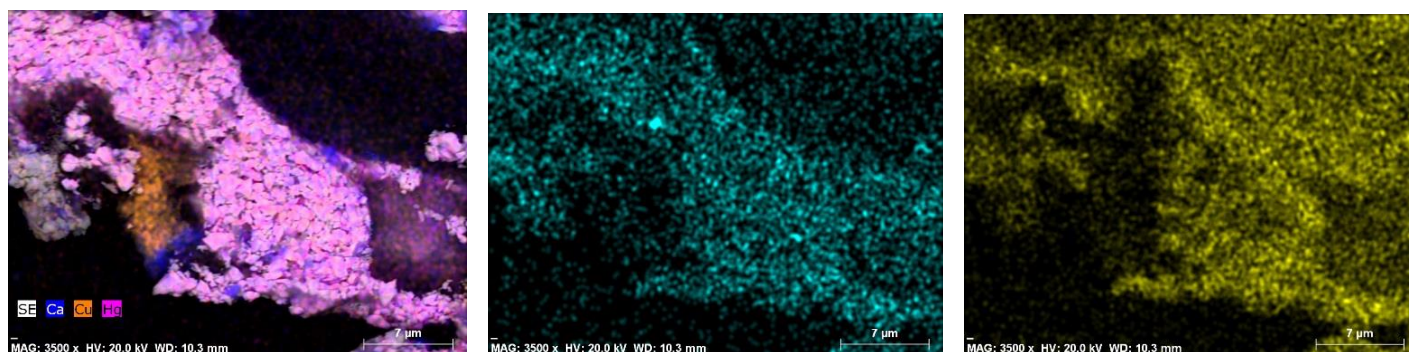
***VP-SEM-EDS:*** A mercuric sulfide red pigment can be obtained in at least two ways: by pulverizing the naturally-occurring mineral, or synthetically by a wet or dry process (Gettens, Feller, & Chase 1972). The pigment derived from the latter two processes is generally called vermilion, while a powdered and purified form of the mineral retains the mineral nomenclature. The source of a mercuric sulfide pigment can be tricky to pin down, but grain size and morphology have sometimes been employed to answer this question (*ibid.*) (table 7). Moreover, detection of minerals co-occurring with native cinnabar may validate the determination of the pigment's provenance. Native cinnabar is frequently associated with



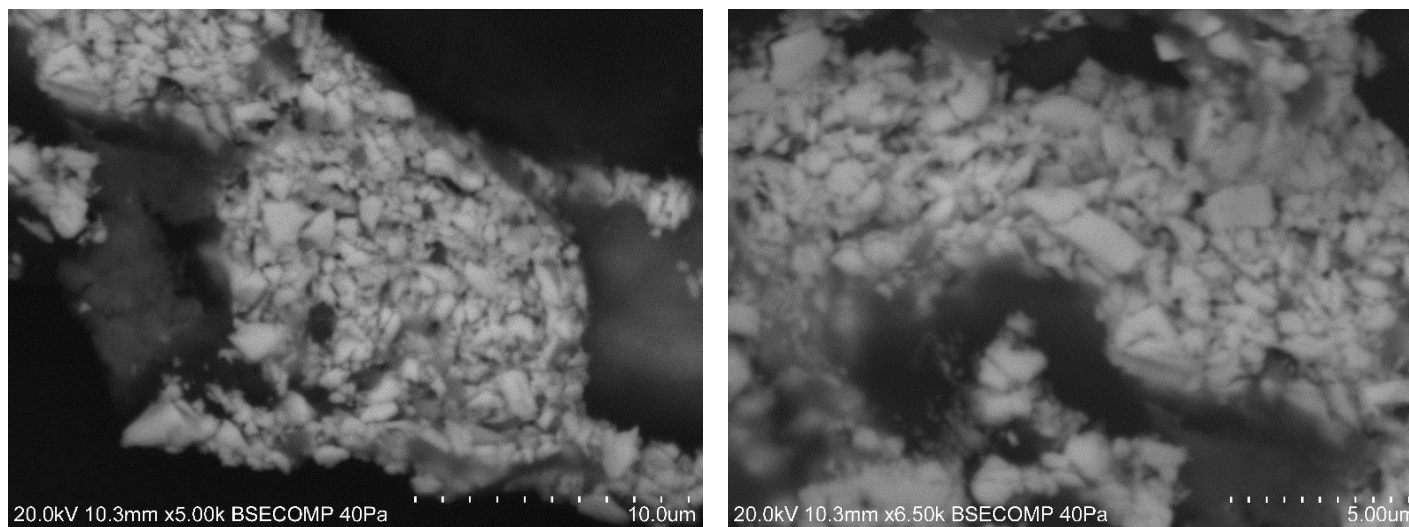
**Figure 73:** FORS spectra of representative red regions compared with mockups of cinnabar mixtures in gum Arabic (AG). Numbers beside map names refer to measurement locations which are given in Appendix II.1.



**Figure 74:** Representative Raman spectrum of a red roof (sample Di.R.7; see Appendix II.1 for location of sample on map).



**Figure 75:** EDS maps of the red microsample (Da.S.3; see Appendix II.1 for location of sample on map) showing calcium (blue), copper (orange) and mercury (pink) (left); iron (middle), and silicon (right).



**Figure 76:** SEM image of red microsample in BSE mode (Da.S.3; see Appendix II.1 for location of sample on map).

clays, calcite, pyrite, and quartz; thus, EDS detection of aluminum, silicon, calcium, and iron may signal the use of a non-synthetic pigment (Franquelo & Perez-Rodriguez 2016). EDS analysis of the microsample (Da.S.3) indicated that aluminum, silicon, and calcium impurities were present (figure 75) (see Appendix III.10.40-41).

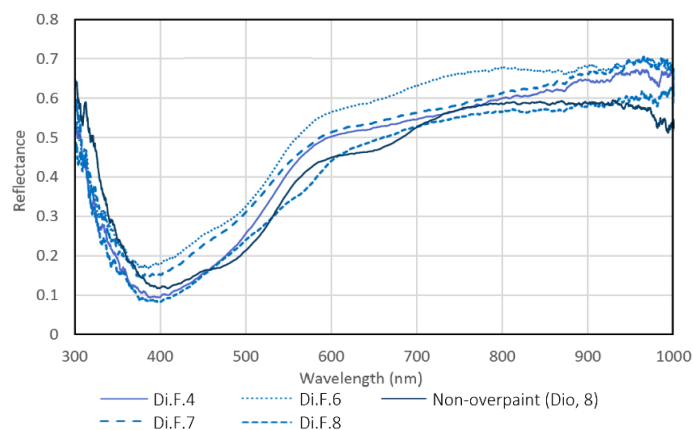
Turning to morphology, the heterogeneity of grain size and lack of sinterization in the red microsample are consistent with the exploitation of native cinnabar for the red pigment (figure 76). The silicon, calcium, and iron can therefore be interpreted as added confirmation of a non-synthetic pigment.

**Table 7:** Some morphological criteria for HgS pigment differentiation. Note that some of the differences in morphological description relate to the use of SEM by some authors and optical microscopy by others.

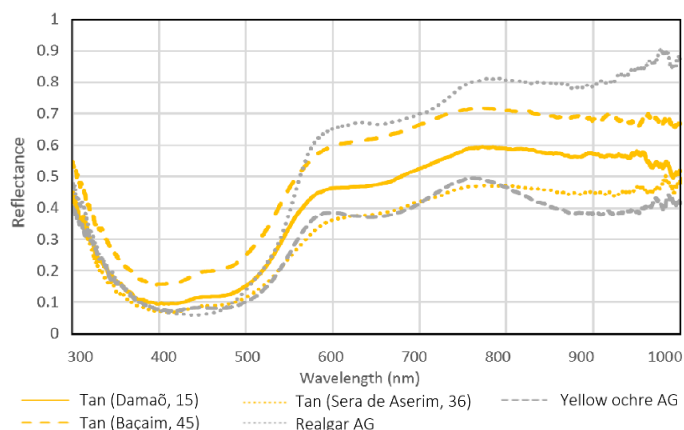
Pigment	Particle Morphology	Authors
<b>Vermilion (wet process)</b>	Well-shaped; hexahedral or agglomerated; particles roughly .2 µm to 1.6 µm	Miguel et al. 2014
	Fine, small particles and agglomerations	Gettens, Feller, & Chase 1972
	Fine particles (less than 1 µm)	Franquelo et al. 2016
<b>Vermilion (dry process)</b>	Rounder shape; wrinkling of surface; particles approx. .2 µm to 1.9 µm	Miguel et al. 2014
	Larger particles than wet process; large particles often having an elongated shape.	Gettens, Feller, & Chase 1972
<b>Cinnabar</b>	Particles with rounded edges; variable size, sometimes powdery	Gettens, Feller, & Chase 1972
	Thick, irregular particles; variable size	Franquelo et al. 2016



### 8.2.2: Tan (yellow ochre)



**Figure 77:** FORS spectra of overpainted tan regions compared with representative non-overpainted tan ('Dio'). Numbers beside map names refer to measurement locations which are given in Appendix II.1.



**Figure 78:** FORS spectra of selected tan regions compared with mockups of yellow ochre and realgar in gum Arabic (AG). Numbers beside map names refer to measurement locations which are given in Appendix II.1.

**Technical photography:** The tan regions were mostly transparent to infrared light. They appeared dull brown under UV illumination. Ultraviolet fluorescence in the visible region strongly influenced by the binder has been documented for ochre pigments (Cosentino 2015). An increased fluorescence in the beige washes was observed in the map of 'Dio,' especially in the areas of erasures and overpaints (see Appendix III.3.9). As the fluorescence followed the brushstrokes of the paint, it cannot be attributed to a varnish or coating, but must relate to the paints themselves. This raises the question: was the pigment used in these regions different, was it mixed with other pigments, or was it more liberally imbued with binder?

**FORS:** In response to the apparent difference in the beiges of the 'Dio' map, FORS analysis incorporated additional spots to investigate the tans and beiges of overpainted regions (Di.F.4, Di.F.6, Di.F.7, Di.F.8; see Appendix II.1 for location of these spots on the map). The FORS spectra of these tans differed from the typical profile of the tans of the maps (figure 77). A possible explanation would be uncovered during the handheld XRF analyses.

The "typical" tans of the maps produced similar spectra, albeit with variable intensities of reflectance (figure 78). The secondary minimum at approximately 660 nm supports the use of a yellow ochre in these regions (Elias et al. 2006). This minimum is weaker, however, than in the mockups of yellow ochre. Discrimination between ochres based on the inflection point of the sharp slope also lent some credibility to a hypothesis of yellow ochre. In the case of the "typical" tans on the maps, this inflection point is located at around 532 nm. This is close to the wavelength range for yellow ochre reported in the literature (from 535 to 565 nm) (*ibid.*). The pattern of minima and position of inflection point of the tans in the maps also resembled the reflectance profile for realgar (figure 78). Yellow ochre nonetheless remained a preferred theory, as the yellow ochre mockup and all the measured spots from the maps presented a weak reflectance band at about 435 nm, which was absent in the realgar spectrum.

**h-XRF:** The three most abundant elements recorded by handheld XRF were iron, lead, and manganese. These findings can be interpreted as the combination of lead white and an iron oxide pigment, probably predominantly goethite ( $\alpha$ -FeOOH) with some manganese oxides. Manganese oxides and hydroxides are present in variable proportions in umbers (5-20%) and

siennas (less than 10%) (Eastaugh et al. 2004) but can also be found in yellow ochre due to a substitution of manganese for iron in the source minerals (Gil et al. 2009).

Handheld XRF gave clues about the cause of the unusual FORS spectra and UVF-IV images for the overpaints on the Dio map. In these tan and beige regions, there was a reduction in average normalized counts of aluminum, iron, and manganese (compared with the other tans) and in two of the spots, mercury was detected. The mercury is likely to be the remains of the red roofs of the erased houses; its presence reinforces the theory that the deleted settlement had already been completed when the choice was made to remove it. The leftover cinnabar in these regions may have caused the anomalous FORS spectra. The reduction in the counts of elements associated with goethite could indicate a lower pigment-binder ratio in the paint used and may be the cause of the increased fluorescence in the UVF-IV photographs. No arsenic was detected in any of the spectra. The use of orpiment or realgar ( $\text{As}_2\text{S}_3$  and  $\alpha\text{-As}_4\text{S}_4$ ) was therefore rejected.

**Raman microscopy:** The only grains that scattered efficiently enough to overcome the background fluorescence were those of a reddish-brown color. The largest peak was reliably located between about  $404\text{ cm}^{-1}$  and  $412\text{ cm}^{-1}$ , with other peaks at approximately  $260\text{ cm}^{-1}$ ,  $315\text{ cm}^{-1}$ , and  $570\text{ cm}^{-1}$  (figure 79). Though some shifting of peaks was evident, the relative intensities and positions of the bands suggest goethite ( $\alpha\text{-FeOOH}$ ), which is a mineral found in yellow ochre (Froment, Tournié, & Colombari 2008; Edwards 2011). Raman microscopy permitted detection and identification of stray grains from other pigments in the tan regions as well. While not at such high densities as to be intentional color modulators, both carbon black grains and HgS grains were found (see appendix III.8.6 and III.8.12 for Raman spectra). These could signify the use of an improperly washed palette or mortar, or the employment of a single (not very well cleaned) brush to paint multiple areas.

**$\mu\text{-FT-IR}$ :** With goethite hypothesized as the principle coloring agent of the pigment, and lead white admixture established, the FT-IR analysis on a microsample from the map of 'Dio' (Di.S.4) added information about the constituents of the yellow pigment, allowing its conclusive identification as yellow ochre (figure 80). Ochres can form through

weathering of iron ores or as soils, with goethite-rich soils being more common in humid environments with moderate

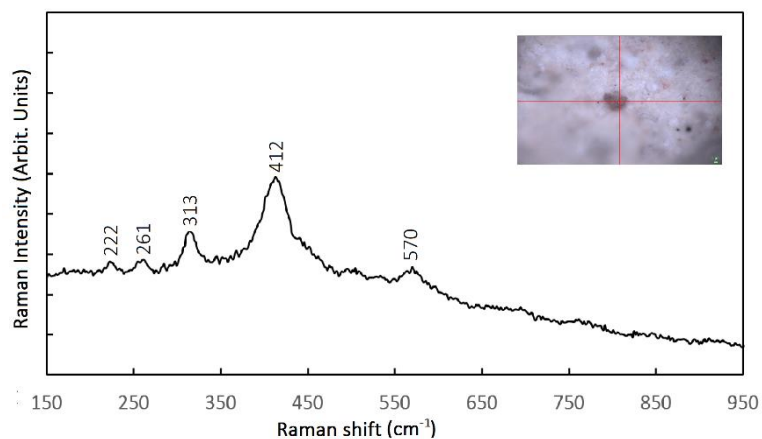


Fig. 79: Raman spectrum from a representative tan region (Di.S.4; *in situ*).

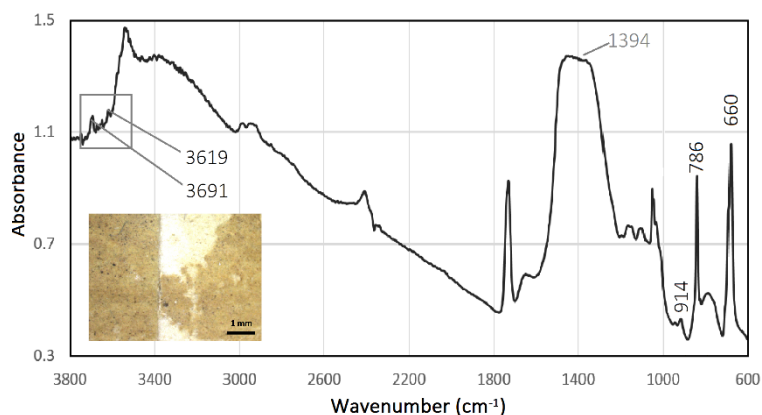


Figure 80: Infrared spectrum of tan region (Di.S.4; see Appendix II.1 for location of sample on map).

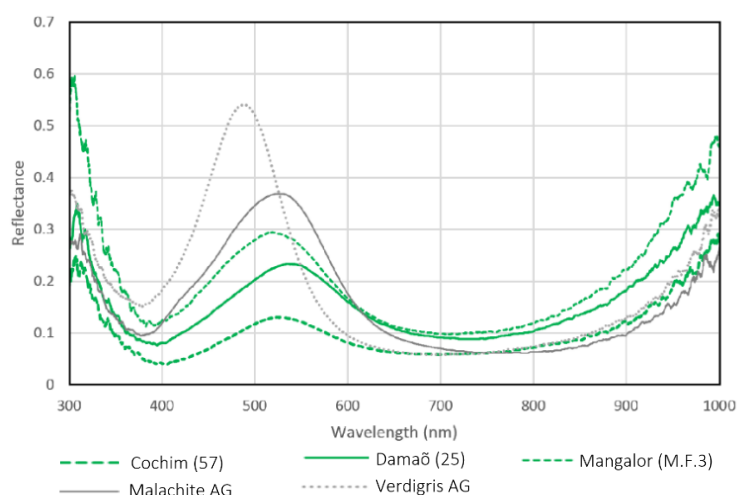
climates (Cornell & Schwartzmann 2003, p. 441). Thus, yellow ochre should be understood as a naturally-occurring mixture of minerals related to geological processes and exploited for artistic purposes, containing in variable quantities iron oxides and hydroxides, clays, feldspars, quartz, and carbonates (Eastaugh et al. 2004, p. 401). In the case of microsample Di.S.4, infrared absorbance bands related to kaolin ( $3691\text{ cm}^{-1}$ ,  $3619\text{ cm}^{-1}$ ,  $914\text{ cm}^{-1}$ ), other minerals/oxides included in ochres ( $786\text{ cm}^{-1}$ ,  $660\text{ cm}^{-1}$ ), and neutral lead carbonate ( $1394\text{ cm}^{-1}$ ) may be identified (Bikiaris et al. 2000; IRUG spectral database: IMP00080, IMP00488, IMP00268).

### 8.2.3: Green (copper proteinate)

*Technical photography:* Technical photography produced perplexing results for the green regions, as discussed in Chapter 7 (see Appendix III.3). We will return to this phenomenon in section 8.3 when describing binders. The green regions were moderately opaque to infrared light, a characteristic shared with verdigris, green earth, and malachite (Cosentino 2014b).

Apart from the tendency to fluoresce red when combined with the white pigment of the maps, the main color change for the green regions under ultraviolet light was a darkening.

*FORS:* The reflectance spectra from the dark green areas of the maps (figure 81) were most comparable with the mockup of malachite in gum Arabic, with reflectance maxima at 525-540 nm and a gradually rising slope from about 700-1000 nm.



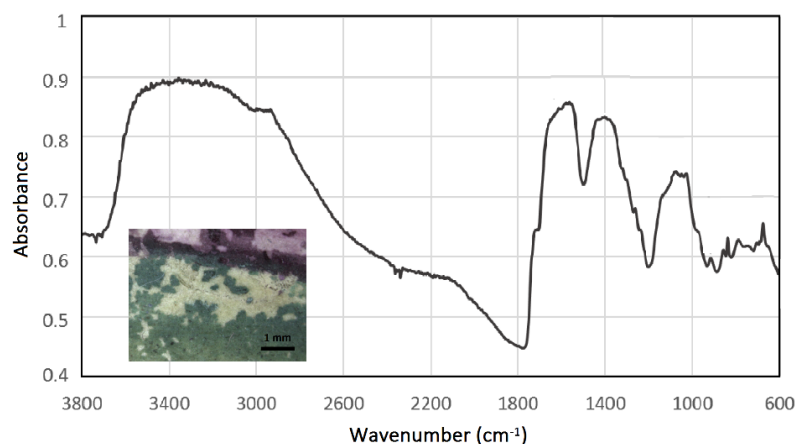
**Figure 81:** FORS spectra of representative green regions compared to mockups of verdigris and malachite in gum Arabic (AG). Numbers beside map names refer to measurement locations which are given in Appendix II.1.

*h-XRF:* Copper was the main element documented in the dark greens, along with lesser amounts of lead and

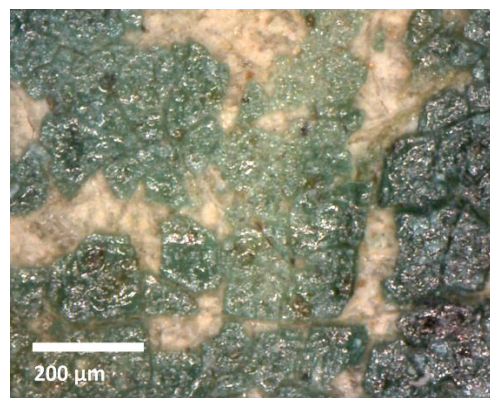
iron. The latter two elements can be understood as an attenuated contribution of the beige terrain wash over which the dark green regions are painted. Copper-based pigments include malachite ( $\text{Cu}_2\text{CO}_3(\text{OH})_2$ ), verdigris ( $\text{Cu}(\text{OH})_2 \cdot (\text{CH}_3\text{COO})_2 \cdot 5\text{H}_2\text{O}$ ), brochantite ( $\text{Cu}_4\text{SO}_4(\text{OH})_6$ ), Egyptian green ( $((\text{Ca}, \text{Cu}^{2+})_3(\text{SiO}_3)_3)$ ), and posnjakite ( $\text{Cu}_4(\text{SO}_4)(\text{OH})_6 \cdot (\text{H}_2\text{O})$ ). Interactions between verdigris and resins, oils, or proteinaceous binders may promote the formation of copper resinate, oleate, or proteinate, respectively. The absence of calcium and silicon in the examined regions excluded an assignment of Egyptian green. The presence or absence of sulfur was difficult to determine under the experimental conditions, so the use of posnjakite or brochantite would be evaluated by Raman microscopy and  $\mu$ -FT-IR.

*Raman microscopy:* The experimental setup did not allow acquisition of a legible spectrum for the green regions. This problem has been reported in the literature for Raman microscopy of verdigris and malachite using a 785-nm laser (Coccato et al. 2016; Caggiani, Cosentino, & Mangone 2016).

*$\mu$ -FT-IR:* The identity of the green pigments was finally elucidated by infrared spectroscopy (figure 82; for additional spectra,



**Figure 82:** Infrared spectrum of green microsample Di.S.3 (see Appendix II.1 for location of sample on map and Appendix III.9.1-4 for added infrared spectra of green microsamples.).



**Figure 83:** Digital microscopic image of a green region (spot 57, map of 'Cochim') showing glassy aspect and detachment without visible damage to paper support.

Appendix III.9.1-3). Malachite ( $\text{Cu}_2\text{CO}_3(\text{OH})_2$ ) had been the favored candidate based on the similarity of its FORS spectrum to the spectra of the dark greens of the maps. It has a well-defined infrared spectrum, with  $\text{CO}_3^{2-}$  stretching bands ( $1530\text{--}1350\text{ cm}^{-1}$ ), O-C-O bending bands ( $900\text{--}650\text{ cm}^{-1}$ ), OH bending bands ( $1100\text{--}1000\text{ cm}^{-1}$ ), and OH stretching bands ( $3700\text{--}3100\text{ cm}^{-1}$ ) (Derrick, Stulik, & Landry 1999, p. 199). Several of these bands were absent in the infrared spectra of the green microsamples from the maps.

The possibility of verdigris was consequently reevaluated. The verdigris infrared spectra in the literature demonstrate absorptions related to the asymmetric stretching of acetate at  $1635\text{ cm}^{-1}$ , symmetric stretching of acetate at  $1375\text{ cm}^{-1}$ , and OH stretching at  $3400\text{--}3100\text{ cm}^{-1}$  (*ibid.*). In all the green microsamples, bands near the expected positions for acetate absorptions were detected. However, the bands from the microsamples were broader than is usual for verdigris, and the anticipated ratio of asymmetric and symmetric band intensity was reversed.

These aspects of the infrared spectra are symptomatic of copper proteinate, a material resulting from the reaction of the acetate groups in verdigris with a proteinaceous binder. The appearance and behavior of copper proteinate greens is identical to the greens from the maps: glassy, prone to cracking, and showing a deep rich color (Scott et al. 2001). Infrared spectra of copper proteinate greens include bands from both verdigris and proteins but lack the specificity of each component that is observed in fresh mixtures. This has elicited speculation that copper proteinate, also known as “bottle green,” represents the end stage of a chemical interaction in which denatured collagen from a protein-based binder reacts with copper (II) ions in verdigris (*ibid.*). The existence of a chemically distinct new compound is reflected by the broad band combining the amide I, II, and acetate bands, and by the changes to the CH and NH stretching regions of the proteinaceous binder (Miguel et al. 2012). Copper proteinate’s propensity for cracking could be responsible for the misleading FORS spectra (see figure 83 for an example from the map of Cochim and Appendix III.2 for additional digital microscopic images of the dark green regions). It is logical that increased detachment and loss of the painted layer can affect the visible reflectance spectrum. With enough contribution of the parchment or paper support, a copper proteinate spectrum can begin to resemble that of malachite. Formation of copper proteinate may also explain why the paper support has not seen any of the damages typically associated with verdigris. It has been conjectured in the literature that the copper proteinate



complexation may be protective, as the support revealed when the paint detaches appears undegraded (Miguel 2012, p. 85).

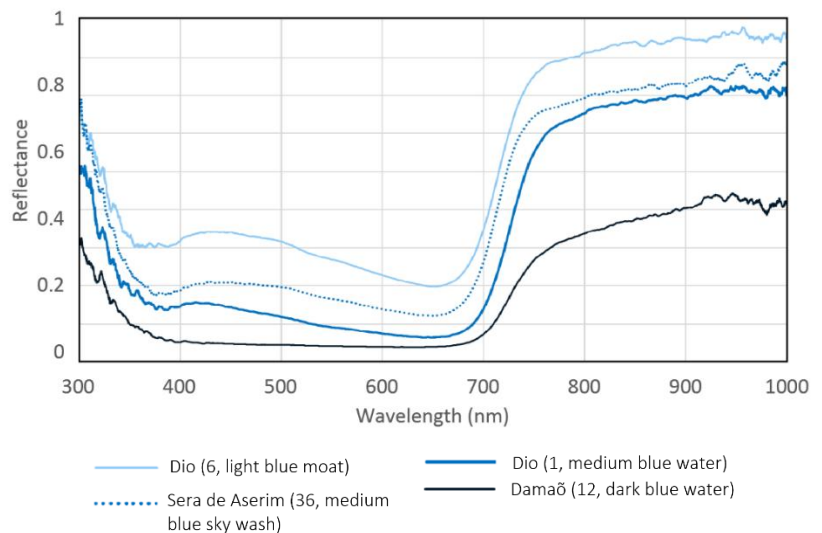
#### 8.2.4: Blue (indigo + ?)

*Technical photography:* Under ultraviolet illumination, the blue regions showed a dark blue to purple fluorescence. The degree to which reddish tones dominated seemed to depend on the amount of lead white added to the blue; in the map of 'Cochim,' this is clear when comparing the medium blue of the water to the light blue of the pond (see Appendix III.3.5). When applied as a wash, as in the sky of 'Sera de Aserim,' the fluorescence of the paint is combined with that of the paper, resulting in a dark, cool blue tone (Appendix III.3.17). The blue regions were nearly transparent to infrared radiation, leading early on to suspicion that the pigment was not ultramarine, Egyptian blue, blue bice, or azurite, which absorb infrared light and appear dark (Cosentino 2014b).

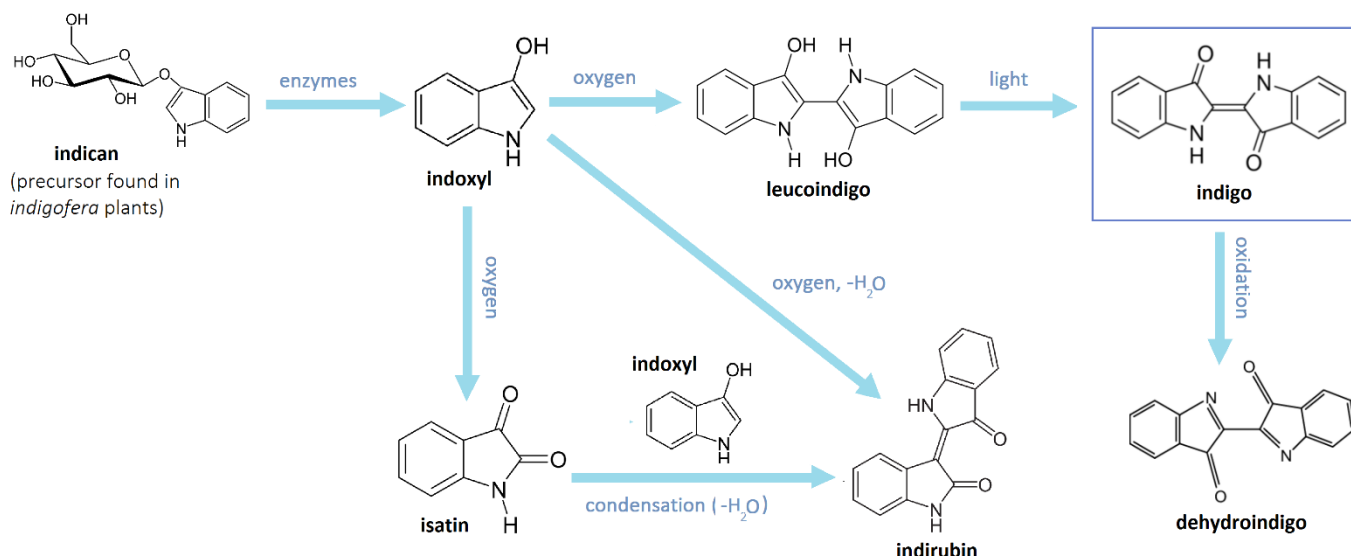
*FORS:* The FORS spectra of the blue regions (figure 84) presented a broad asymmetrical absorption band between approximately 410 nm and 665-680 nm (depending on the lightness of the blue, i.e., the amount of white pigment mixed in). The profiles of the spectra best correspond to the reflectance patterns of indigo-based pigments in the literature. Different authors have recorded rather variable spectra for indigo-based pigments. The spectra from the maps closely resemble that of Maya blue in gum Arabic prepared by Cosentino, with

its slight reflectance maximum at about 420 nm (Cosentino 2014a). Comparing with the spectra collected by other authors, the blues appear to be an intermediate between indigo and Maya blue (Leona et al. 2016) or to be a kind of Maya blue (Doménech et al. 2006). The reflectance pattern of Maya blue may result from an interplay between dehydroindigo (the oxidized version of the indigo molecule bonded to the clay matrix) and indigo (Doménech et al. 2006).

With a strong hypothesis of indigo already established, it is worth pausing here to consider the origins and chemistry of indigos. Indigo is the broad name for a group of blue dyes and pigments coming from several plant sources. All these plants contain a molecule called indican (figure 85, top left), and processing conditions during dye manufacture can give rise to variable quantities of indigotin, isatin, indirubin, and leucoindigo (Cardon 2014). Leucoindigo is colorless. Only on exposure to ultraviolet radiation (for example, in sunlight) can it convert to indigo (also called indigotin), which gives the famous blue color. Indirubin has a redder cast than indigo (indigotin). In typical indigo dye manufacture, the indigo is soaked



**Figure 84:** FORS spectra of representative blue regions. Numbers beside map names refer to measurement locations which are given in Appendix II.1.



**Figure 85:** Flowchart of indigo processing, including molecules relevant to discussion of Maya blue.  
Expanded and adapted from Doménech et al. (2006) and Cardon (2014).

in water, initiating a fermentation process that breaks the indican's glucoside bond and produces the indoxyl molecule (Clark et al. 1993). Agitation of the water introduces oxygen and promotes leucoindigo, isatin, and indirubin formation. Sunlight converts leucoindigo to indigo. After the dye has settled to the bottom of the soaking basins, it is removed, filtered, pressed into bricks, and dried (Schweppe 1997). If the indigo is heated with specific clays, another molecule called dehydroindigo may be formed. This molecule has been detected in Maya blue samples. Dehydroindigo formation in Maya blue is formally described as:



*Free energy change:* -50.4 kJ/mol (Tagle, Paschinger, & Infante 1990)

This reaction can become thermodynamically spontaneous with the addition of moderate heat and is compatible with the usual Maya blue synthesis method (Doménech et al. 2006). Thus, the presence of dehydroindigo may be a useful way of distinguishing between indigo-clay mixtures and versions of a true Maya blue pigment. This is particularly important given the fact that historical adulterants to indigo include clays (Church 1890, pp. 192-197).

The Maya blue pigment is frequently encountered as a brilliant sky- to turquoise-blue color, quite unlike the deep blues seen in the maps (Doménech et al. 2006). However, modern experimentation has demonstrated that its color can be manipulated by altering the ratio of clay (palygorskite or sepiolite) to indigo during the preparation, allowing for a variety of hues. The pigment is synthesized by heating together indigo and palygorskite or sepiolite for an extended period of time at a relatively low temperature (as little as 75 °C) (Van Olphen 1966; Kleber, Masshelein-Kleiner, & Thissen 1967). The rather straightforward procedure could presumably be stumbled upon accidentally if a pigment producer was fond of experimentation and had access to a suitable clay. Deposits of sepiolite and palygorskite can be found across the world,

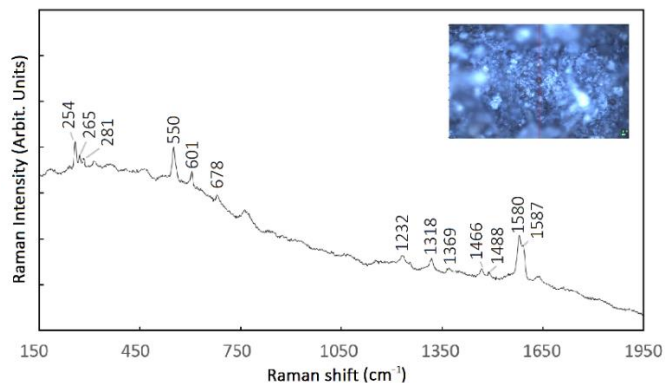
including important sources in the United States, China, Spain, India, Israel, and Senegal (Galan 1996; Murray & Zhou 2006; Verrecchia & Le Coustumer 1996). The similarity between the Maya blue FORS spectra and the FORS spectra of the blues of the maps may indicate aspects of indigo processing which must be examined.

Maya blue identification should not be made solely by color or the presence of indigo and an appropriate clay; arguably the most important aspect of the pigment is its durability (Fois, Gamba, & Tilocca 2003). The relationship between its constituent colorants and fibrous clays gives Maya blue impressive resistance to both microbial attack and chemical attack. The exact nature of the association is still subject to controversy (see Sánchez del Río et al. 2006 for an overview). Identification of the components of Maya blue (palygorskite or sepiolite and indigo) can be attempted using Raman spectroscopy, but the technique may not differentiate between a simple mixture of the two components and a true Maya blue (*ibid.*). Infrared spectroscopy may help elucidate the relationship between the clay and indigo; Leona et al. propose that the shifting and/or disappearance of indigo bands in samples of Maya blue can be sufficient for identification of the pigment (Leona et al. 2013). Other authors, however, found it difficult to detect the indigo bands at all because of indigo's low concentration in the pigment (Giustetto et al. 2005).

To sum up before moving on, the observed deviations from indigo reflectance spectra in the literature could be the result of a heating procedure involving indigo and clay. Another option is that the indigo was mixed with another blue pigment and the spectra presented in figure 83 represent a combination of their two reflectance profiles. Going forward, it will be crucial to clarify the non-indigo components of the paint.

**h-XRF:** The organic portion of the paint (i.e., indigo) would not have been registered by h-XRF. The elemental analysis is therefore indicative of extenders, added inorganic pigments, or the substrate. Handheld XRF spectrometry revealed higher quantities of aluminum in the medium blue regions than the pinks; a surprising result, given the predicted alum substrate of the pink lakes and the assumption that the blues consisted of indigo plus an extender like chalk or lead white. In fact, lead counts in the blue regions were lower than usual. The notion that the blues are a mixture of indigo and azurite ( $\text{Cu}_3(\text{CO}_3)_2(\text{OH})_2$ ) can be discarded, as copper was not recorded in large enough quantities. Whether ultramarine ( $\text{Na}_8\text{Al}_6\text{Si}_6\text{O}_{24}\text{S}_{2-4}$ ) was present could not be determined due to the detection limits of the handheld spectrometer.

**Raman microscopy:** Indigo is a large molecule with 84 vibrational modes (Schweppe 1997), giving rise to a Raman spectrum of greater complexity than any discussed so far in this thesis (figure 85). While previously the chief impediment to the acquisition of legible spectra was fluorescence from the organic binder, the possible contribution of a clay or another blue pigment must be evaluated in the case of the blues. When mixed with or precipitated onto a clay, the signals of some indigo bands may be obscured; in such instances, the region from about  $1630\text{ cm}^{-1}$  to  $250\text{ cm}^{-1}$  is the



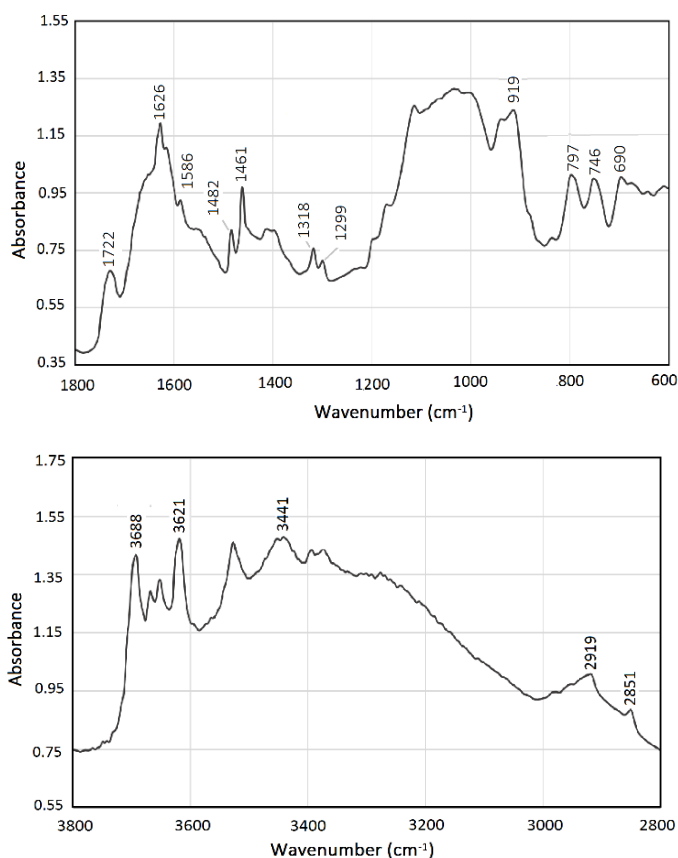
**Figure 86:** Raman spectrum of a blue region ('Dio,' spot 1; see Appendix II.1 for location of the measurement spot on the map).

most likely to reveal characteristic bands for indigo (Leona et al. 2013). The bands recorded in this region which are attributable to indigo are at  $1580\text{ cm}^{-1}$  (C=C and C=O stretching),  $1466\text{ cm}^{-1}$  (C-C stretching, C-O bending),  $1318\text{ cm}^{-1}$  (C-C stretching), and  $1232\text{ cm}^{-1}$  (C-H bending, C-N stretching) (interpretations based on Tatsch and Schrader, 1995). The presence of palygorskite may be indicated by the relative intensities of the bands at  $550\text{ cm}^{-1}$  and  $601\text{ cm}^{-1}$  (Sánchez del Río et al. 2006).

The position of the doublet at  $1580\text{ cm}^{-1}$  and  $1587\text{ cm}^{-1}$  has been examined for its potential insights into the complexation of indigo with palygorskite (*ibid.*). Due to the slight band shifting observed across the spectra and the uncertainty that palygorskite or sepiolite are present in the blue paint of the maps, it is not justified to go into more depth until more data is available. The alternative hypothesis that the blue is a combination of indigo and another blue pigment can be evaluated by the Raman analysis. Azurite admixture was ruled out by h-XRF. Ultramarine may now be considered. The pigment presents a strong band at  $583\text{ cm}^{-1}$ . This band was not observed in the Raman spectra of the blue regions of the maps.

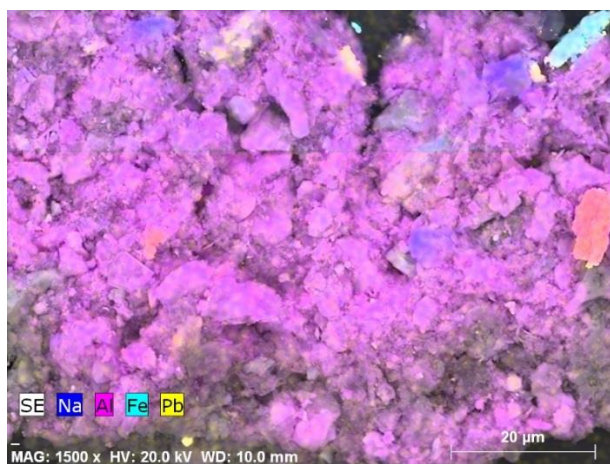
**$\mu$ -FT-IR:** The infrared spectra may be reflective of the simultaneous presence of indigo and at least two clays (figures 87-88). Kaolin is suggested by the characteristic strong OH stretching bands at  $3688\text{ cm}^{-1}$  and  $3621\text{ cm}^{-1}$  (Parker 1969). Sepiolite may be responsible for the bands at  $2929\text{ cm}^{-1}$  and  $2851\text{ cm}^{-1}$ , the shoulder towards higher wavenumbers on the band at  $1626\text{ cm}^{-1}$ , and the band at  $919\text{ cm}^{-1}$  (based on comparison of experimental spectra with spectra from the OPUS/Mentor version 6.5 software reference library). The presence of the clays has led to a broadening of some of the bands for indigo where it overlaps with the bands of clays. For example, the broad band at approximately  $1150\text{ cm}^{-1}$  to  $800\text{ cm}^{-1}$  can be interpreted as a combination of bands from indigo ( $1128\text{ cm}^{-1}$ ,  $1095\text{ cm}^{-1}$ ,  $1074\text{ cm}^{-1}$ ,  $1011\text{ cm}^{-1}$ ; Schweppe 1997) kaolin (asymmetric Si-O-Si stretching bands  $1100\text{--}1000\text{ cm}^{-1}$  and Si-O stretching bands  $910\text{--}830\text{ cm}^{-1}$ ; Derrick, Stulik, & Landry 1999) and sepiolite (OPUS/Mentor version 6.5 software reference library). It is difficult to extend interpretation any further, as the infrared spectroscopic study has been limited to one microsample whose size may have affected the quality of the spectra acquired.

**VP-SEM-EDS:** The elemental mapping afforded by SEM-EDS demonstrated that the blue microsample (Da.S.2) contains an

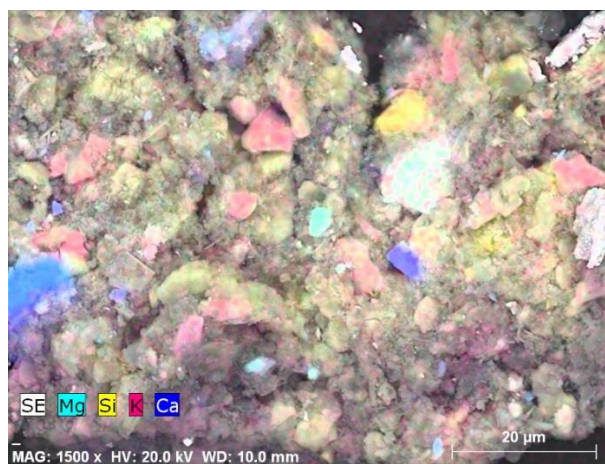


**Figures 87-88:** Infrared spectrum of a blue microsample (Di.S.3; see Appendix II.1 for location of sample on map) restricted to the  $1800\text{--}600\text{ cm}^{-1}$  absorption region (top), and restricted to the  $3800\text{--}2800\text{ cm}^{-1}$  absorption region (bottom).





**Figure 89:** Elemental map of blue microsample (Da.S.2; see Appendix II.1 for location of sample on map) showing sodium, aluminum, iron, and lead.



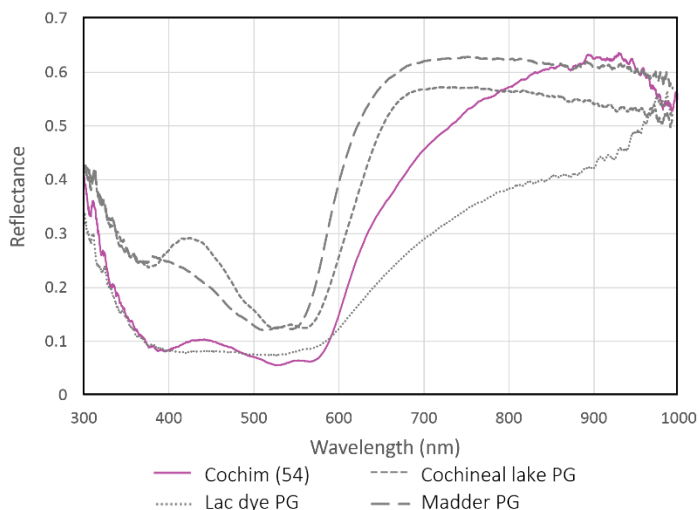
**Figure 90:** Elemental map of blue microsample (Da.S.2; see Appendix II.1 for location of sample on map) showing magnesium, silicon, potassium, and calcium.

array of aluminosilicates (figures 89-90; see also Appendix III.10.17-24). While identification of specific clays cannot be based on elemental composition alone, the EDS results seem compatible with the  $\mu$ -FT-IR indications for sepiolite ( $\text{Mg}_4\text{Si}_6\text{O}_{15}(\text{OH})_2 \cdot 6(\text{H}_2\text{O})$ ) and/or palygorskite ( $(\text{Mg},\text{Al})_2\text{Si}_4\text{O}_{10}(\text{OH}) \cdot 4(\text{H}_2\text{O})$ ) and kaolin ( $\text{Al}_2\text{H}_4\text{O}_9\text{Si}_2$ ). EDS confirmed the h-XRF observation that quantities of lead in the medium blue regions are suppressed; strange, since lead white is so liberally mixed with other colors in the maps. To use indigo as a pigment, artists generally acknowledged the need to add white; if not, the color was nearly black. The sudden switch to an aluminosilicate extender (or substrate) for the medium blues is significant. Not only does it represent a shift from the colorist's typical methods, but it is a deviation from the normal practices for lightening indigo to use as a paint. Both European sources like Cennini and Persian authors such as Qadi Ahmad propose grinding indigo with lead white to coax blue tones out of the inky dye (Minorsky 1959; Eastaugh, Walsch et al. 2004). The colorist of these maps does resort to lead white for the pale blue areas of water (as discussed above when disambiguating pigments from mixtures), but it is obvious that another substance is preferred as an extender for the rich medium blues. The data so far point to a mixture of clays, but the relative infrequency of magnesium-rich grains detected by EDS makes it unlikely that palygorskite or sepiolite are present in high enough quantities to produce a Maya-blue analogue. XRD has been undertaken to define the non-indigo components of the paint; additional results are forthcoming.

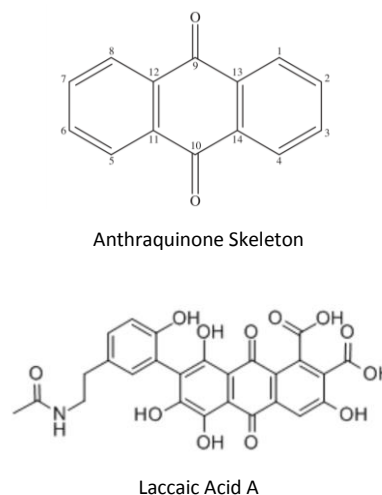
### 8.2.5: Pink (lac lake)

*Technical photography:* The slight fluorescence of the pink regions was compatible with the use of cochineal or kermes, as madder presents a fluorescence of a different hue, and lac does not fluoresce (Schweppe & Roosen-Runge 1986) (see Appendix III.3). The fluorescence of the pink regions on the map could be related to the lake pigment itself, or to the reddish fluorescence pattern correlated some mixtures including the lead white pigment. For this reason, technical photography was at best uninformative (and at worst misleading) in the identification of the pink lake pigment.

*FORS:* The spectra of the dark pink and light pink regions had a similar profile and were comparable to the cochineal and madder lake mockups (in the 300-600 nm region) and lac dye mockup (in the 600-1000 nm regions) (figure 91). These areas



**Figure 91:** FORS spectra of representative dark pink compared with mockups in parchment glue (PG). Number beside map name refers to measurement spot, indicated in Appendix II.1.



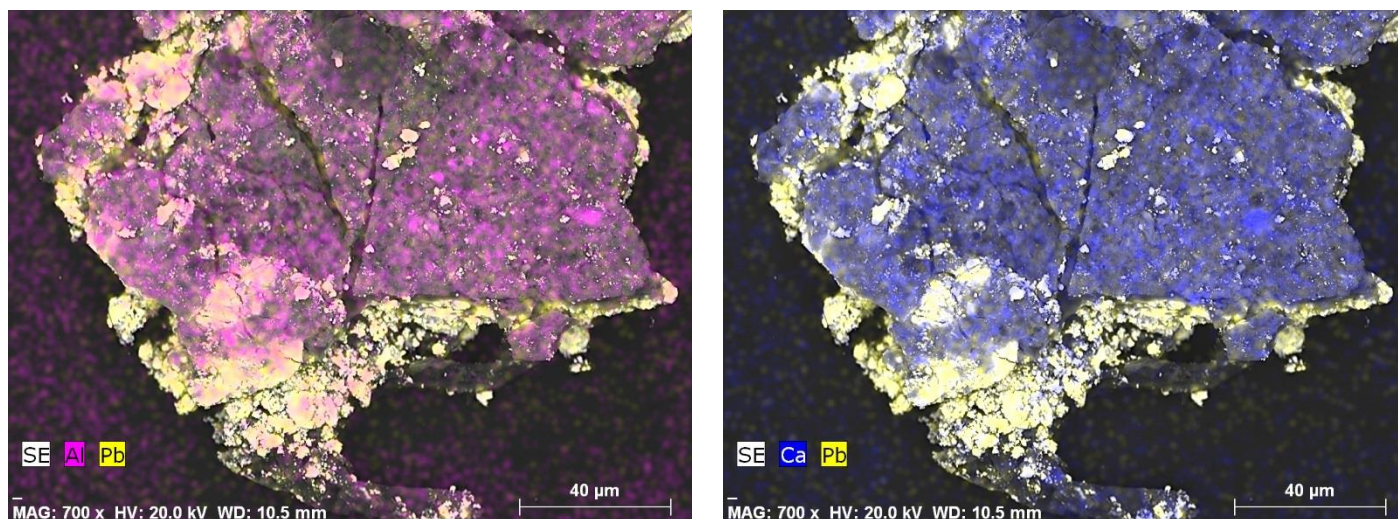
**Figure 92:** Anthraquinone and laccaic acid A.

shared a reflectance pattern with cochineal-dyed cottons fibers (Maynez-Rojas et al. 2017) and cochineal lake on paper (Schweppe & Roose-Runge 1986). Lac dye, cochineal, and kermes are derived from scale insects, and all contain chromophores based on the anthraquinone structure (see figure 92). Their absorbances in the visible range can be interpreted as  $n \rightarrow \pi^*$  transitions of the carbonyl (C=O) groups (Bisulca et al. 2008). As conclusive identification was only established by LC-MS, it is worth stressing here that FORS alone was inadequate for the lake source determination at the insect level. Moreover, although h-XRF and EDS analyses were suggestive of a lake pigment and an insect-based lake pigment (respectively), a discrimination between insect-based lakes would have been difficult to impossible with portable equipment and indeed, with some non-portable equipment.

**h-XRF:** The predominant element detected in the light and dark pink regions was lead. This is compatible with a tactic of lightening the dark pink paint by adding an opaque white pigment. Lake pigments include an organic component (here, laccaic acids, imperceptible by XRF) and an inorganic substrate (such as kaolin, aluminum hydroxide, and zinc oxide; Schweppe & Roosen-Runge 1986). Some elements from the substrate, if present in sufficient quantities, should be recorded in the h-XRF spectra. The limitations of the experimental setup impaired collection of much information about the inorganic portion of the lake pigment. Clues as to the formulation of the lake pigment remained scarce, and more investigation was required.

**Raman microscopy:** No useful Raman spectra were recorded for the pink regions, as the materials did not scatter light strongly enough to produce peaks exceeding the fluorescence of the binding media.

**VP-SEM-EDS:** The improved detection of lighter elements and spatial discrimination possible with SEM-EDS allowed a better understanding of the lake pigment substrate (figure 93). Lead continued to appear as a dominant element in the EDS spectra (see Appendix III.10.12-16) but elemental maps of lead distribution demonstrated that the lead was concentrated in the layer below the lake pigment, some of which was inadvertently collected during the microsampling. In the region of interest,



**Figure 93:** Elemental map of aluminum (pink) and lead (yellow) (left), and calcium (blue) and lead (yellow) (right) on pink microsample (Di.S.5; see Appendix II.1 for location of sample on map). The area rich in calcium and aluminum is the pink lake. The area high in lead is the underlying preparatory layer.

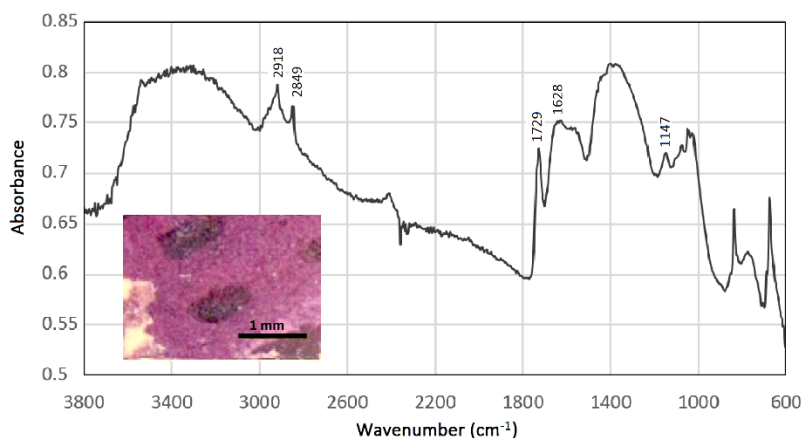
calcium and aluminum were observed, and aluminum, phosphorus, silicon, magnesium, copper, and sodium were also present in lesser but significant quantities. All these elements except aluminum have been detected in the bodies of scale insects used for red lake manufacture (Kirby et al. 2005). Their presence in the microsample could be from either the original sticklac mix or contamination during or after precipitation of the lake. The correlation of aluminum and calcium with the pink areas, and the relatively high quantity of the latter, may be related to a calcium-rich extender, a mixed alum and chalk substrate, or the process by which the lake was synthesized. The use of an extender is unlikely given the translucency of the dark pink lake pigment and a mixed substrate involving chalk will be considered using infrared spectroscopy. Historical recipes for the lake may reveal a synthesis-related source of calcium.

Lac lake synthesis involves extraction of the colorant from the insect exudate and precipitation onto an inorganic substrate (typically alum). The dyestuff can be obtained either directly (from sticklac, the exudate deposited by *Kerria lacca* on tree branches), or indirectly (by extraction from textiles colored with lac; see Clementi et al. 2008). Direct lac lake preparation around the turn of the 16<sup>th</sup> century is described in the Paduan manuscript *Ricette per Far Ogni Sorte di Colore*. The process entailed pulverization of the insect exudate (sticklac), mixture of the resulting powder in an alkaline solution, evaporation of the liquid over a fire, stirring (a silver spoon is recommended), and waiting a day or two. The resulting mass could be used as a pigment (Eastaugh, Walsch, Chaplin, & Siddall 2004, p. 214). A Judeo-Portuguese recipe attributed to the 13<sup>th</sup> century recommends soaking and heating sticklac in an alkaline mixture of purified urine filtered with lime and ashes. The colored mass could be strained from the liquid and used as paint (Melo 2016, pp. 163-170). Sadiqi Bek gives a Persian (and perhaps Mughal) recipe for the pigment, advising artists to boil the lac in a soda (alkaline) solution, possibly adding lime during the process (Purinton & Watters 1991). This last step of adding lime (CaO) could underlie the relatively high calcium content of the dark pink areas. While water alone can extract laccaic acids from sticklac, the use of alkaline solutions allowed the artist to draw out both the colorant and resin components of the exudate (Santos et al. 2015). Additionally, controlling the acidity of the solution could enable modification of the lake pigment's ultimate color. Laccaic

acid A is sensitive to pH, and with increased alkalinity the dye changes from a dark pink to a dark red (Melo 2016, p. 170) or from a dark red to a dark violet (Wongwad et al. 2012).

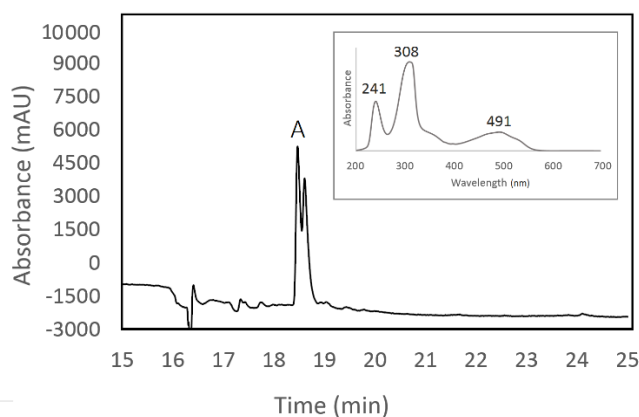
**$\mu$ -FT-IR:** The alum substrate inferred by EDS analysis can be detected in the infrared spectrum by the broad band in the OH stretching region ( $\sim 3400\text{ cm}^{-1}$ ) (Clementi et al. 2008) (figure 94). The absence of a band for chalk or gypsum is further evidence against the use of a mixed alum and chalk or alum and gypsum substrate. Rather, the results support the theory that the calcium detected by EDS relates to wood ash or lime involvement during the lake synthesis.

The identification of lac lake is sometimes based on detection of infrared absorption bands from shellac, which could be retained in the dye or added subsequently. The bands at  $2918\text{ cm}^{-1}$  and  $2849\text{ cm}^{-1}$  (C-H stretching) and  $1729\text{ cm}^{-1}$  (C=O stretching) may

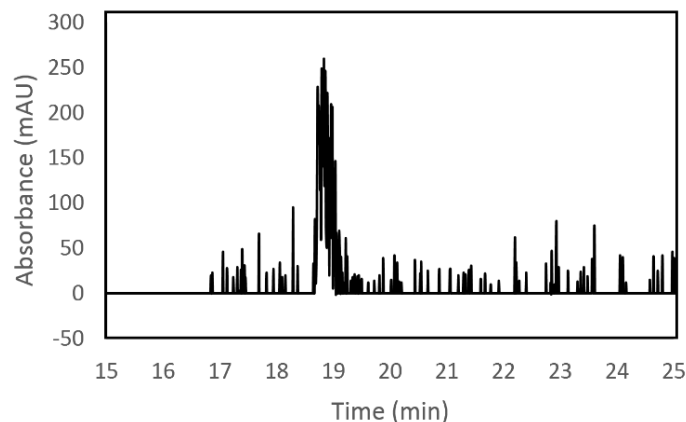


**Figure 94:** Infrared spectrum of a pink microsample (Di.S.5; see Appendix II.1 for location of sample on map).

be related to shellac (figure 94). Additionally, the region from  $1147\text{ cm}^{-1}$  to  $1000\text{ cm}^{-1}$  resembles the profile of the shellac C-O stretching bands (Sarkar & Kumar 2001; Clementi et al. 2008; Derrick, Stulik, & Landry 1999, p. 190). Clementi et al. report that in contrast with cochineal and kermes, lac lakes display a sulphate band at approximately  $1120\text{ cm}^{-1}$  (Clementi et al. 2008). This band may also be present in the spectrum from pink microsample at a slightly shifted position. The possible problems in attributing the C-H and C=O stretching bands to shellac will be addressed in the discussion of binders.



**Figure 95:** PDA chromatogram recorded at 500 nm with inset UV-Vis spectrum of major peak from pink microsample (Co.S.5 and M.S.2; locations of microsamples on maps are given in Appendix II.1).  $R_t = 18.47\text{ min}$ .



**Figure 96:** MS chromatogram in single ion monitoring mode at  $m/z$  536 of pink microsample combining samples Co.S.5 and M.S.2. Locations of microsamples on maps are given in Appendix II.1.

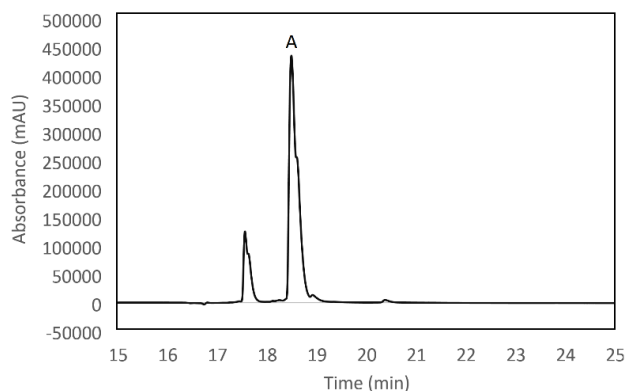
**LC-DAD-MS:** LC-MS provided robust identification of the insect source of the lake. Discrimination of cochineal, kermes, and lac hinges on detection of their respective chromophores. Cochineal's color is an emergent property of the carminic acid (with some kermesic and flavokermesic acid) in the bodies of *Dactylopius coccus*, *Porphyrophora polonica*, and *P. hamelii*



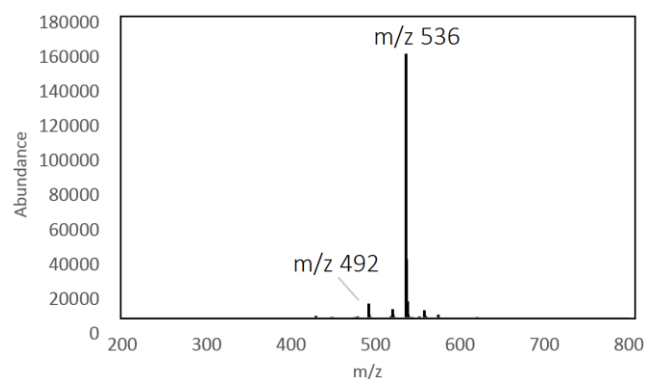
insects. Kermes, coming from the *Kermes vermilio* insect, gets its color from kermesic (with some flavokermesic) acid. Finally, lac is produced by *Kerria lacca* insects, and its main chromophores are laccaic acids (Cardon 2014, pp. 695-696; Schweppe & Roosen-Runge 1986).

The extracted dyestuff of the pink microsample was injected into the LC-DAD-MS with the mass spectrometer set to single ion monitoring mode to increase the system's sensitivity to ions of interest. The ions selected were those produced from laccaic acid A ( $m/z$  536), carminic acid ( $m/z$  491), and kermesic acid ( $m/z$  329) (Santos et al. 2015; Lech & Jarosz 2011). The only ion that produced a strong peak was the ion with an  $m/z$  ratio 536. The UV spectrum (inset in figure 94) confirmed that the material being detected was a red dye. Taking together the retention time, absorbance maxima of the UV spectrum, and  $m/z$  ratio of the most abundant ion, it suddenly appeared that the lake pigment was not cochineal or kermes, but lac.

To solidify the findings, a lac dye standard was injected using the same experimental conditions but with the MS running in single reaction mode (figures 97-98). A similar PDA chromatogram was produced. In order to verify that the major peak (point A, figures 95 and 97) in the PDA chromatograms of the pink sample and lac dye standard corresponded to laccaic acid A, single reaction monitoring (SRM) mode was chosen for mass spectrometry to confirm a fragmentation pattern documented for this acid, in which a parent ion of a mass to charge ( $m/z$ ) ratio 536 produces a daughter ion with an  $m/z$  ratio of 492 (Petroviciu, Albu, & Medvedovici 2010). Precisely such a pattern was observed in the lac dye reference standard for the peak at A (figure 97).



**Figure 97:** PDA chromatogram recorded at 500 nm of lac dye standard, showing major peak (A) at  $R_t = 18.51$  min.



**Figure 98:** MS chromatogram in SRM mode corresponding to peak A in figure 96 of lac dye standard showing fragmentation of the parent ion with a  $m/z$  ratio 536 into a daughter ion with  $m/z$  ratio 492.

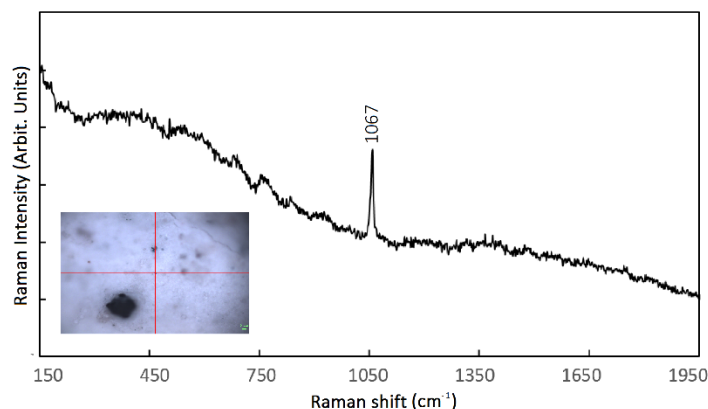
### 8.2.6: White (basic and neutral lead carbonates)

*Technical photography:* NIR photography was not diagnostic of a specific white pigment. The fluorescence pattern observed in the UVF-IV images will be discussed in section 8.3.

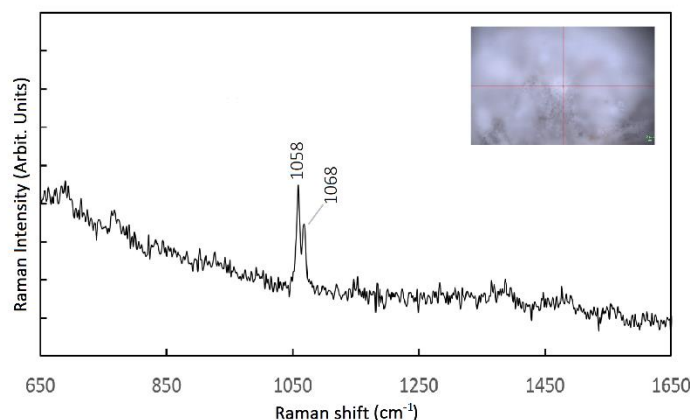
*FORS:* Reflectance spectra of the white regions did not aid in the pigment's identification.

*h-XRF:* Lead dominated the handheld XRF spectra from the opaque white regions.

*Raman microscopy:* The Raman spectra of the accessible opaque white regions showed bands at around  $1068\text{ cm}^{-1}$ , a slight



**Figure 99:** Raman spectrum of white region (Di.R.6; see Appendix II.1 for location of measurement spot on map).



**Figure 100:** Raman spectrum of white region, with doublet (Da.R.6; see Appendix II.1 for location of measurement spot on map).

shift towards higher wavenumbers from the lead white spectra reported in the literature (figures 99-100). The modest band shifting can be attributed to the equipment used and does not reflect on the character of the paint. The singlet recorded in most of the spectra is compatible with neutral lead carbonate ( $\text{PbCO}_3$ , the synthetic analogue of the mineral cerussite). In a few cases, a doublet with reduced intensity and one peak shifted to lower wavenumbers was observed, corresponding to basic lead carbonate ( $2\text{Pb}_3(\text{CO}_3)_2(\text{OH})_2$ , the synthetic analogue of the mineral hydrocerussite) (Brooker et al. 1983).

This finding is contrary to the traditionally assumed composition of a synthetic lead white pigment, which is mainly basic lead carbonate and possesses only minor amounts of neutral lead carbonate (Gettens et al. 1993). A key determinant of the final ratio seems to pertain to the use of manure as the carbon dioxide source for lead white synthesis. Lead white can be made in several ways. According to the “Dutch process” created in the late 1500s, sheets of lead were placed in jars containing vinegar. The jars were then sealed with manure. The vinegar vapor caused the lead to transform into lead acetate, and the heat and carbon dioxide emitted by the manure promoted the formation of basic and neutral lead carbonates. When lead white is synthesized with an inorganic flux of carbon dioxide, only neutral lead carbonate was produced (Sanchez-Navas et al. 2013). When the lead white was sealed without a heat or carbon dioxide source, only lead acetate was formed (Pires et al. 2010). In terms of historical explanations, an excess of neutral lead carbonate may be indicative of post-synthesis treatments in acidic conditions (such as soaking in vinegar) that aimed to remove impurities in the paint (Gonzalez et al. 2015). Alternatively, neutral lead carbonate can sometimes be formed *in situ*. The chemical reactions describing the two processes are given below.

Formation of neutral lead carbonate by post-synthesis acid treatment

$$2\text{Pb}_3(\text{CO}_3)_2(\text{OH})_2 + 2 \text{CH}_3\text{COOH} \rightarrow \text{PbCO}_3 + 2\text{H}_2\text{O} + \text{Pb}(\text{CH}_3\text{COO})_2$$

Formation of neutral lead carbonate *in situ* by atmospheric action

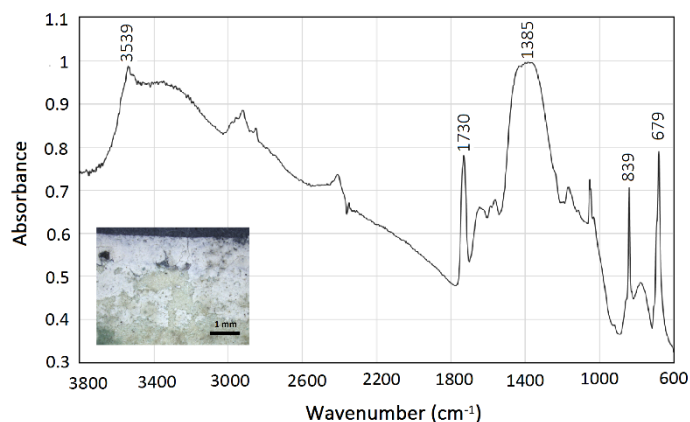
$$2\text{Pb}_3(\text{CO}_3)_2(\text{OH})_2 + \text{CO}_2 \rightarrow 3\text{PbCO}_3 + \text{H}_2\text{O}$$

(Gonzalez et al. 2015)

Gonzalez et al. were able to raise the neutral lead carbonate content of the pigment by washing and grinding it with vinegar (*ibid.*). They reported *in situ* transformation by atmospheric action on powdered samples of basic lead carbonate, but not

on basic lead carbonate dispersed in linseed oil. It is unclear whether the permeability of the binder in the maps is adequate to allow *in situ* neutral lead carbonate formation. At the present, the ratio of the two crystallites cannot be strictly established. Future research should attempt to specify the neutral to basic lead carbonate ratio in maps and explore the susceptibility of lead white to *in situ* conversion when prepared with binders other than linseed oil.

**$\mu$ -FT-IR:** The infrared spectrum of a white microsample (Di.S.2) confirmed the presence of both basic and neutral lead carbonates in the maps. The OH stretching band at 3539  $\text{cm}^{-1}$  (figure 101) is typical for basic lead carbonates. Both basic and neutral lead carbonates have a strong  $\text{CO}_3^{2-}$  stretching band at about 1415  $\text{cm}^{-1}$  and bending band at about 680  $\text{cm}^{-1}$ . A weak band is also anticipated at around 1730  $\text{cm}^{-1}$  (Brooker et al. 1983), which in the Di.S.2 spectrum may have been amplified by the binder (see section 8.3). Neutral lead

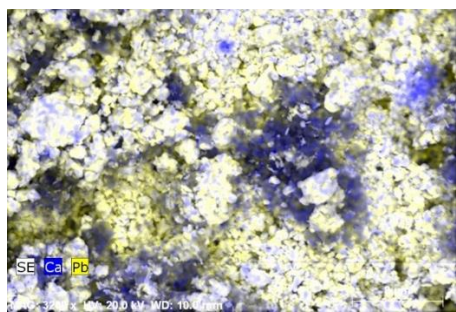


**Figure 101:** Infrared spectrum of a white microsample (Di.S.2; see Appendix II.1 for location on map).

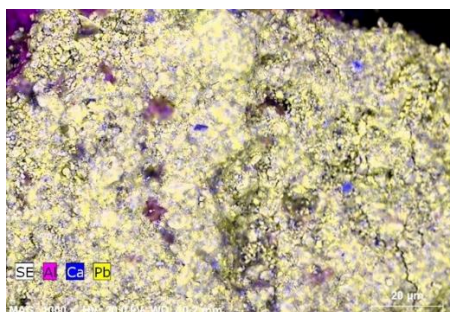
carbonate has a sharp stretching band at about 678  $\text{cm}^{-1}$  (Brooker 1983; Siidra 2018), which in basic lead carbonate is positioned at approximately 682  $\text{cm}^{-1}$ . In the infrared spectrum of the microsample, we can see a strong band at 678  $\text{cm}^{-1}$  with a shoulder at around 682  $\text{cm}^{-1}$ , which would seem to suggest bands from both forms of lead carbonate combined into one peak. Finally, the strong band at 839  $\text{cm}^{-1}$  has been observed in samples of mineral cerussite (Siidra 2018), but not in mineral hydrocerussite (Brooker 1983; Siidra 2018). By extension, we can expect that the intense band at 839  $\text{cm}^{-1}$  is caused by significant quantities of synthetic cerussite, i.e. neutral lead carbonate, in the microsample.

**VP-SEM-EDS:** With EDS, it was possible to distinguish elements that h-XRF did not discern. One of these was calcium, which appeared in small clusters (see figures 97-98). This may be due to mixture of chalk with the lead white to increase its opacity, a practice which has been documented in the historical literature (Gettens et al. 1993). Calcium's relative scarcity and the absence of bands related to chalk or gypsum in the infrared spectrum cast doubt on this proposition. More investigation is needed to understand this element's presence in the lead white pigment.

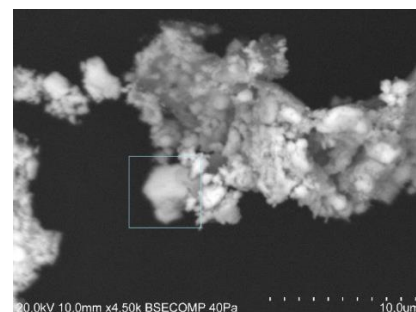
Using the scanning electron microscope, a cursory glimpse at the particle morphology was also undertaken. Having detected both neutral and basic lead carbonates, we attempted to locate grains of either lead carbonate on the basis of crystal structure (as described in Sanchez-Navas et al. 2013). The authors found that by following the "Dutch" method, the precipitates showed low crystallinity with a combination of hydrocerussite and cerussite particles. Basic lead carbonate has been reported to appear as very fine particles with prismatic morphology (Eastaugh & Walsch 2004, p. 302). Neutral lead carbonate should display smaller particles with euhedral to subeuhedral hexagonal plates (*ibid.* p.299). The particles viewed by SEM were found to be heterogenous and poorly shaped, with an overall aspect similar to the synthetic lead white described by Sánchez-Navas et al. (Sánchez-Navas et al. 2013). A possible occurrence of neutral lead carbonate has been



**Figure 102:** EDS map elemental distribution on a white microsample showing lead (yellow) with calcium (blue) (Di.S.2; see Appendix II.1 for location of sample on map).



**Figure 103:** EDS map of elemental distribution on white microsample showing lead (yellow), calcium (blue) and aluminum (from the blue paint below) (M.S.3; see Appendix II.1 for location of sample on map).



**Figure 104:** BSE image of white microsample with possible neutral lead carbonate crystal (Di.S.2; see Appendix II.1 for location of sample on map).

tentatively identified in figure 104; however, the limitations of the experimental parameters made detailed characterization and firm conclusions regarding particle morphology impossible.

#### 8.2.7: Black (bone or ivory black, with possible addition of iron gall ink or vine black)

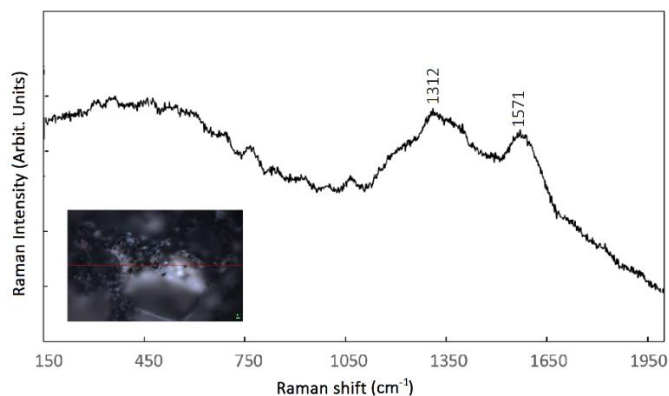
*Technical photography:* Technical photography was not useful for identification of the black pigment (Cosentino 2014b).

*FORS:* FORS could not be exploited for pigment characterization in the black regions, as black pigments do not demonstrate distinctive reflectance spectra (Boselli 2010, p. 17).

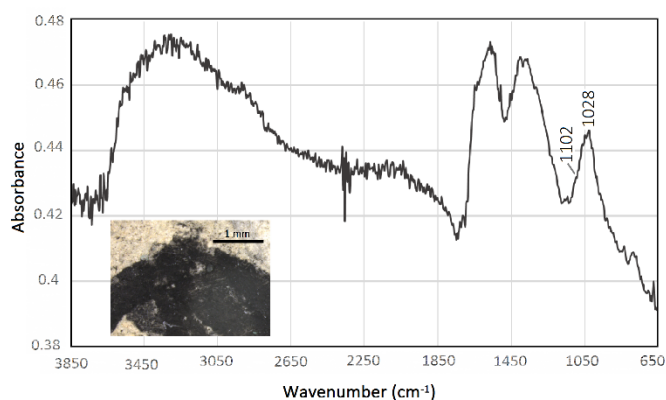
*h-XRF:* Due to the small size of the black regions, they could not be easily analyzed using h-XRF. The first indications as to their source came from handheld XRF analyses aiming to characterize any surface treatment on the “unpainted” white regions. It was noted that the more the black outline encroached on the white analysis zone, the higher the counts of iron that were recorded, suggesting the use of iron gall ink. It has been noted that detection of iron alone is not adequate for definitive identification of this pigment, but that the concomitant presence of copper and zinc can improve confidence in the assignment, as they indicate the use of vitriols along with iron sulfate (Aceto & Calà, 2017). These elements were also present in the spots in question (see Appendix III.6).

*Raman microscopy:* The black regions accessible to analysis showed a typical carbon black profile, with a wide doublet at approximately  $1312\text{ cm}^{-1}$  and  $1571\text{ cm}^{-1}$ , which correspond respectively to the  $\text{sp}^3$  and  $\text{sp}^2$  C-C bonds of graphite (Miguel 2012, p. 90) (figure 105). Carbon black pigments can be produced by burning either plant or animal materials, and the relative intensity of the above bands can be indicative of their source. Across the accessible black regions on the maps, the band at about  $1312\text{ cm}^{-1}$  (C-C  $\text{sp}^3$ ) presented greater intensity than the band around  $1570\text{ cm}^{-1}$  (C-C  $\text{sp}^2$ ). This pattern is consistent with an animal source for the black, such as incinerated bones or ivory (Marucci et al. 2018). The other signature of a bone or ivory black is a small band at approximately  $960\text{ cm}^{-1}$ , which has been attributed to the symmetric stretching of  $\text{PO}_3^{2-}$  ions from residual calcium phosphate (van der Weerd et al. 2004). Due to the fluorescence of the organic binder, it was impossible to detect this band, and further investigation was undertaken for definitive identification.



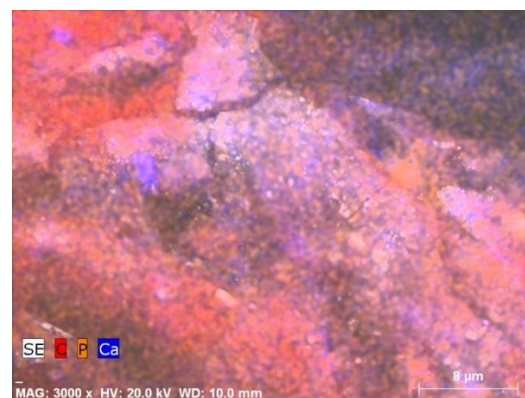


**Figure 105:** Raman spectrum of black region (Co.S.3, *in situ*; see Appendix II.1 for location of measurement on map).

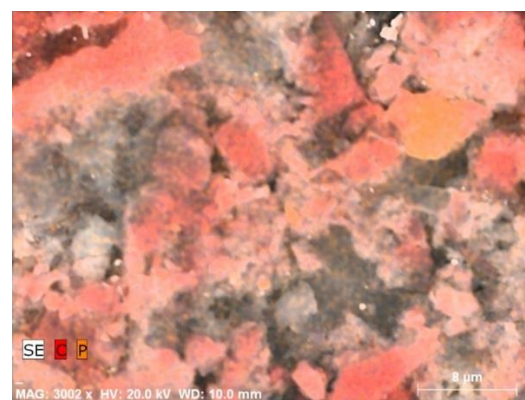


**Figure 106:** Infrared spectrum of microsample from black region (Co.S.3; see Appendix II.1 for location of sample on map).

*μ-FT-IR:* As the ink in the black regions formed very thin layers, extraction of microsamples was challenging and the samples taken were the smallest of any color. This adversely affected the quality of the infrared spectra (see especially the infrared spectrum of microsample Co.S.4 in Appendix III.9.7). Nonetheless, some features of the pigments could be deduced (figure 106). The iron registered by h-XRF spectrometry suggested that iron gall ink could have been added to the carbon black identified by Raman spectroscopy. The infrared spectrum of iron gall ink can be broken down into absorptions arising from tannic acid, and those from the iron sulphate. Iron sulphate's strongest band is at about 1050  $\text{cm}^{-1}$ , whereas tannic acid absorbs at multiple wavenumbers but most intensely at about 1200  $\text{cm}^{-1}$ . These bands were not evident in the spectra of either of the black microsamples. In the higher-quality spectrum (Co.S.3), a band at 1028  $\text{cm}^{-1}$  with a slight shoulder at about 1100  $\text{cm}^{-1}$  was identified. These absorptions can be attributed to two stretching vibration modes of the phosphate ion  $(\text{PO}_4)^{3-}$  from low-crystallinity apatite (Daveri, Malagodi, & Vagnini 2018; Tomasini, Siracusano, & Maier 2012) and lend added support to the hypothesis that the black is derived from animal bones.



**Figure 107:** EDS map of elemental distribution of black microsample (M.S.1) showing carbon (red), phosphorus (orange), and calcium (blue).



**Figure 108:** EDS map of elemental distribution of black microsample (Co.S.4) showing carbon (red) and phosphorus (orange).

*VP-SEM-EDS:* EDS finalized the hypothesis introduced in the previous analyses regarding the source carbon black in the ink. Calcium and phosphorus were both detected in relatively high quantities which provided a last piece evidence for the use of bone black (figures 107-108; Appendix III.10.25-34).

It is still unclear whether the iron detected in these samples is related to the minor contribution of iron gall ink to the black pigment or has another explanation. Elemental mapping showed that iron was correlated with silicon and

magnesium and strontium in microsample Co.S.4 (for a representative EDS spectrum from such a region, see Appendix III.10.28). In microsample M.S.1, strontium and silicon were closely correlated, but iron did not appear to be strongly correlated to any other element. Iron, magnesium, strontium, and silicon were all detected in samples of vine black by Tomasini et al. The infrared spectra for these samples showed their strongest absorbances at 999 cm<sup>-1</sup> (for Zecchi brand vine black) and 1066 cm<sup>-1</sup> (for Kremer brand vine black) (Tomasini, Siracusano, & Maier 2012). At low intensities, these bands are not incompatible with the spectra observed for the black samples from the maps. It is possible that during the incineration of bones or ivory, some amount of charred vegetal fuel became incorporated into the black coke pigment.

### 8.3: Binder

The quality of the FT-IR spectra was adversely affected by the small size of the microsamples, meaning that it was not possible to conclusively establish the binding media used in the maps, and whether different binders were used on different pigments. This will be an excellent direction for future research, as the binder may dictate the artistic approach (i.e., the painting methods used).

The binders employed in the maps could be animal-based, plant-based, or a combination (see table 8). Animal-based binders include egg (either whole egg, yolk, or egg white) and animal glue. Dry egg yolk is primarily composed of lipids and protein (about 63% and 33%, respectively, Powrie and Nakai 1986), while dry egg white is mainly protein (Casoli, Berzioli, & Cremonesi 2013). The lipids in fresh egg yolks are 62% triglyceride, 33% phospholipid, and <5% cholesterol (Anton 2017). Animal glues are made by denaturing the water-insoluble collagen naturally found in the hooves and skins of animals to form water-soluble gelatin. This can be achieved by boiling (Schellmann 2007). Although animal glue also has proteins and lipids, its lipid content is lower and presents infrared absorbances of lesser intensity and at slightly different positions than egg yolk (Dooley et al. 2013). The plant-based gum most suitable for watercolor painting is gum

Table 8: Overview of expected infrared absorption bands (from Derrick, Stulik, & Landry 1999; Smith 2017)	
Binders/ additives	Characteristic absorption bands (wavenumbers of bands)
Egg	N-H stretching (3400-3200 cm <sup>-1</sup> ) C-H stretching (3100-2800 cm <sup>-1</sup> ) C=O stretching (amide I, 1750-1600 cm <sup>-1</sup> ) C=O stretching (carboxylic acids and esters, ~1715 cm <sup>-1</sup> ) C-N-H bending (amide II, 1565-1500 cm <sup>-1</sup> ) C-H bending (amide III, ~1450 cm <sup>-1</sup> )
Hide glue	N-H stretching (3400-3200 cm <sup>-1</sup> ) C-H stretching (3100-2800 cm <sup>-1</sup> ) C=O stretching (1660-1600 cm <sup>-1</sup> ) C-N-H stretching (1565-1500 cm <sup>-1</sup> ) C-H bending (1480-1300 cm <sup>-1</sup> )
Gum Arabic	O-H stretching band (3600-3200 cm <sup>-1</sup> ) C-H stretching bands (3000-2800 cm <sup>-1</sup> ) O-H bending band (1650 cm <sup>-1</sup> ) C-H bending band (1480-1300 cm <sup>-1</sup> ) C-O stretching band (1300-900 cm <sup>-1</sup> )
Shellac	O-H stretching band (3600-3200 cm <sup>-1</sup> ) C-H stretching bands (3100-2800 cm <sup>-1</sup> ) C=O stretching bands (1740-1640 cm <sup>-1</sup> ) C-C stretching band (1650-1600 cm <sup>-1</sup> ) C-H bending bands (1480-1300 cm <sup>-1</sup> ) C-O stretching bands (1300-900 cm <sup>-1</sup> )

Arabic. It is soluble in water and prepared from the exudate of acacia trees (notably *Acacia senegal*) (Derrick, Stulik, & Landry 1999, p. 179). Gum Arabic is a complex polysaccharide whose precise chemical composition is determined by numerous factors, including the species and growing conditions of the plant of origin and the processing and purification protocol to which the gum is subjected (Williams & Phillips 2009). Although plant gums do contain amino acids (*ibid.*), their most prominent infrared absorption bands are related to the polysaccharide portion (Derrick, Stulik, & Landry 1999, p. 179).

The black (Co.S.3, Co.S.4), white (Co.S.1), blue (Di.S.3), pink (D.S.5), and tan (Di.S.4) microsamples presented C-H

stretching bands at about  $2920\text{ cm}^{-1}$  and  $2850\text{ cm}^{-1}$ , as well as a C=O ester stretching band approximately  $1725\text{ cm}^{-1}$ , a profile showed with the infrared spectrum of egg yolk (see Appendix III.9 for all infrared spectra). The band at approximately  $1725\text{ cm}^{-1}$  may be an oxidized triglyceride, indicating aged egg yolk. Further indication of an egg yolk binder can be seen in the infrared spectrum of the lead white microsample (Co.S.1). Addition of lead white to egg yolk has been reported to result in a splitting of the amide II band due to changes in hydrogen bonding. This alteration persists even as the paint film ages (Meilunas et al. 1990). A similar feature is observed in the aforementioned white microsample, although at  $1580\text{ cm}^{-1}$  and  $1562\text{ cm}^{-1}$ , rather than at  $1542\text{ cm}^{-1}$  and  $1515\text{ cm}^{-1}$  as reported by Meilunas et al.

Alternatively, the bands at approximately  $2920\text{ cm}^{-1}$ ,  $2850\text{ cm}^{-1}$ , and  $1725\text{ cm}^{-1}$  could signal the addition of shellac to the paints (Derrick, Stulik, & Landry 1999; p. 190). Complicating matters, it is difficult to rule out the presence of plant gums. Examining the IRUG spectrum for gum Arabic, we find that its most pronounced bands are centered at  $\sim 3450\text{ cm}^{-1}$  (wide),  $\sim 2918\text{ cm}^{-1}$ ,  $1614\text{ cm}^{-1}$ ,  $1421\text{ cm}^{-1}$ , and  $1040\text{ cm}^{-1}$  (IRUG filename: ICB00001). Some of these bands are consistent with the profile observed in the microsamples.

Reactions between verdigris and a proteinate binder have been described in the identification of the green pigment. Pigment-binder interactions may likewise underlie the fluorescence observed by UVF-IV photography. The infrared spectra of the white, blue, pink, tan, and green microsamples all showed signs of proteinate binders. The green paints mixed heavily with lead white, the blues, and the whites showed a pink to red color change under ultraviolet illumination. The fluorescence of the pink lakes may be a related phenomenon, since lac lake fluorescence has not been documented. It may be that an interaction between the lead white and binder in specific paint formulations contributes to the reddish visible fluorescence these regions.

It is also possible that more than one kind of binder was used in the execution of the maps, creating regions of color-correlated fluorescence. This seems less probable, since the tan paints do not demonstrate a color change under ultraviolet illuminations but seem to contain the same binder. On the other hand, the extent to which binder fluorescence affects the appearance of the final paint under ultraviolet illumination is pigment-dependent. Ultraviolet-induced fluorescence of lead white, for instance, is highly affected by the binder. Attempts to observe the same brilliant fluorescence in analogous conditions with mockups of lead white in various binders were unsuccessful. However, the mockups are only four years old (compared to the nearly 400 years the maps have reached) and did not include mixtures of lead white with the pigments of interest from the maps. A study of the binders of the maps in greater detail will enable the creation of comparable reproductions in order to fully comprehend the cause of this fluorescence.

## 8.4: Materials in Context

The palette described shows connections to European as well as Mughal and non-Mughal Indian painting traditions. We will now consider the pigments used and the ways they are used to attempt to understand the colorist of the maps better as an artist.

The exploitation of cinnabar as a red pigment is documented in European paintings (Gettens, Feller, & Chase 1993) as well as in 17<sup>th</sup> century Mughal and Rajput manuscripts (Ravindran 2010). Its presence in the maps is hardly region-specific,



**Figure 109:** Cinnabar from the Almadén District, Spain.  
Source: <http://www.mindat.org/photo-238896.html>

but its handling is suggestive. Cinnabar in the maps is reserved for small areas where it can be painted thickly. It is used only once as a wash, and then in a very limited region (spot 37, on the map of ‘Sera de Aserim’). The application of lac lake over cinnabar (to make details on the roofs) is also a traditional approach (Gettens, Feller, & Chase 1993). It is curious that cinnabar was used in the maps, considering vermilion’s alleged proliferation by the fourteenth century (*ibid.*). Unfortunately, the literature documenting artists’ shift from cinnabar to vermilion is not yet extensive enough to account for this choice. It bears mention that in the early 1500s Duarte Barbosa links vermilion to Chaul, saying that: “There is also a great

consumption in [Chaul] of quicksilver and vermilion for the interior, and for the kingdom of Guzarat [Gujarat], which copper, quicksilver, and vermilion is brought to this place by the Malabar merchants, who get it from the factories of the king of Portugal; and they get more of it by way of Mekkah [Mecca], which comes there from Diu” (from Barbosa’s *Description of the Coasts of East Africa and Malabar*, 1866 translation by H.E.J. Stanley; quoted in da Cunha 1876, p. 33). Whether Barbosa means vermilion in the modern sense is not certain. See figure 109 for an image of native cinnabar.

Indigo-based blues have been seen in Jain artworks, Mughal-period Indian manuscripts, and European art from the 17<sup>th</sup> century and earlier (Lee, Thompson, & Daniels 1997; Bhowmik 1967; Fischer 2011; Schweppe 1997). The indigo of the maps was likely cultivated in or adjacent to the *Estado*: Tomé Pires says that indigo was grown in Malaca (Pires 1944, p. 43), and both Tavernier and Pyrard link it to Cambay and Surat (Tavernier 1889/1676, p. 50; Pyrard 1887/1611, p. 359). However well-situated, the Portuguese may have needed to go through middlemen to get their indigo. They could have purchased it from the Gujarati merchants trading in “anil” who frequented major port cities like Goa (Linschoten 1885/1596, p. 252). Their probable inability to acquire indigo directly from its growers may have been matter of territorial jurisdiction: the north Indian regions of production were under Mughal control, and inland cultivation fell beyond the coastal footholds of the Portuguese (Nadri 2016, p. 97). Bocarro remarks on this topic, saying “The principal reason why [the Mughal king], or better to say tyrant, holds these lands, especially those in the kingdom of Cambay, is for those three herbs of *anfião* [opium], indigo, and cotton [...] which are better than any mines of gold or silver [...]” (Bocarro 1992, p. 79, author’s translation). Prior to intensified growing and export from Brazil, much of the indigo consumed in Europe was imported from Iran and India, manufactured from any of several species in the *Indigofera* genus (Balfour-Paul 1999). Balfour-Paul has outlined the ways that indigo was prepared for either local use or long-distance trade in 15<sup>th</sup>-18<sup>th</sup> century India (*ibid.*). Some signs of such processes may remain in the indigo paint of the maps. When the non-indigo components of the paint have been more fully characterized, a new level of interpretation will be possible.

By the 17<sup>th</sup> century, efforts to suppress indigo imports and save the European woad industries had been abandoned



(Schweppe 1997). The Portuguese in India were in an excellent position to capture indigo traffic to Europe. Although competition and the vicissitudes of Indo-Portuguese relations would gradually reduce the Portuguese share of the indigo sold to Europe (Nadri 2016, p. 99), in the year 1630 it still amounted to over ten percent of the export value from the *Estado* (Disney 1978, pp. 113-114). While crucial to Portuguese profits abroad, it is not entirely clear whether indigo would have been considered a luxury material for a map produced in India. See figure 110 for a botanical illustration of the *Indigofera* plant.

Verdigris was used in Indian watercolor paintings as well as European works (Bhowmik 1970; Lee, Thompson, & Daniels 1997; Kühn 1993). To our knowledge, copper proteinate has not been observed in non-European artworks. Its formation, however, is not incompatible with historical Indian paint preparations. Although plant gums are assumed to have been the primary binder used in Mughal miniatures and Rajput paintings (Wheeler 1997; Bhowmik 1967; Reiche et al. 2005; Fischer 2011), Qadi Ahmad's early 17<sup>th</sup>-century treatise on painting mentions egg yolk as a binder as well (Minorsky 1959, p. 198), fish glue is reported as an adhesive for gilding on Mughal artworks (Bhowmik 1967), and

hide glue's use as a binder in Indian painting has been referenced, although the source of this information is unclear (Jariwala 2010). It seems likely that both European and Indian practices could have caused copper proteinate to develop.

Lead white is pervasive in both European and Mughal painting of the time period under study (Gettens, Kühn, & Chase 1993; Ravindran 2010). Sadiqi Bek, a Persian painter writing in the beginning of the 17<sup>th</sup> century, mentions washing the pigment in vinegar after synthesis. Considering the connections between Persian and Mughal (and some Rajput) painting traditions, this advice that may also have been used in Indian lead white manufacture (Dickson & Welch 1981). It is possible that such a treatment was applied to the lead white of the maps, as previously discussed. However, the use of neutral to basic lead carbonate ratios to infer post-synthesis treatment demands more experimental support, and post-synthesis treatments in specific painting cultures have not been conclusively established by this marker. More study is also required to assess the ratio of the two lead carbonates in the white pigment of the maps.

The maps' extensive deployment of lead white as an opacifier and color-modulator merits note. In copying and adapting (respectively) the Évora codex maps, Maris Carneiro (MS 1639 Carneiro) and Teixeira Albernaz I (MS c.1635 Teixeira Albernaz) readily exploit the wash technique (figure 111). In contrast, the Resende maps in the Évora codex are practically gouache (a technique in which pigments, opacifiers, and binders are combined to form a water-soluble opaque



**Figure 110:** Botanical illustration of *Indigofera* plant. From *Plantae selectae quarum imagines ad exemplaria naturalia Londini, in hortis curiosorum nutrita* by Ehret & Trew. Source: <https://www.biodiversitylibrary.org/pageimage/677979>





**Figure 111:** Details from maps of ‘Dio.’ (Left) MS c.1635 Teixeira Albernaz; (middle) MS 1639 Carneiro; (right) Évora codex.

paint). This technique in the Évora codex maps is obviously different from 17<sup>th</sup> century European watercolor. It is less clear whether it is also distinct from the Mughal miniature method. The latter approach is frequently termed “opaque watercolor.” Its connection with gouache is debated among scholars, with some using the terms interchangeably (see Welch et al. 1987, p. 17; Lee, Thompson, & Daniels 1997) and others insisting that Mughal “opaque watercolors” are built up in layers of extremely pure pigments and are therefore not properly termed gouache (Fischer 2011).

Lac has been used in a variety of contexts, including 12<sup>th</sup>-century Buddhist manuscripts from India; Mughal and Rajput paintings of the 16<sup>th</sup> and 17<sup>th</sup> centuries; English, French, and Italian oil paintings; and Portuguese medieval illuminations (Jariwala 2010; Kirby, Spring, & Higgitt 2005; Melo et al. 2011). It is referenced in both European and Persian treatises (Barkeshli 2013; Castro, Miranda, & Melo 2016). One 13<sup>th</sup> century Persian treatise describes a pink created identically to the pinks on the maps: by mixing lead white and lac (Barkeshli 2013). Bocarro mentions lac as a commodity coming from the Mughal kingdoms and Cambodia (Bocarro 1992, pp. 79 and 257), and traded between Cochim and Bengal (*ibid.* p. 206). He refers to it by the name “lacre de formiga” apparently due to the belief that it was manufactured by ants in a manner analogous to the wax and honey production of bees (Bluteau 1713, p. 175) (see figure 112 for an illustration of the *Kerria lacca* life cycle). A dictionary the early eighteenth century defines “lacre de formiga” as

“A sort of wax, or gum, which is made in India and especially in Pegù...[which is] pulled from the tree and is of a color close to red, mixed with other ingredients, from which you can easily take the dye. In his relation of a voyage [...] P. Man. Godinho says that there is much lac in the States of the Mogor [Mughal]” (Bluteau 1716, p. 14, author’s translation).

The usage of lac across painting cultures of the 17<sup>th</sup> century is hard to determine because of the frequent invasiveness of the analyses required to identify scale insect lakes (Isacco & Darrah 1993). By the time the maps were made, Mexican cochineal was heavily exported to Europe by Spanish colonists (Marichal 2014). The demand for and use of cochineal relative to kermes and brazilwood in European dyeing has been investigated (Serrano, Hallett, & Bommel 2011) but the extent to which trends in textile dyeing are connected to trends in lake pigment production is less obvious. Moreover, when and whether Mexican cochineal would have penetrated Goan markets is uncertain. In the absence of definitive

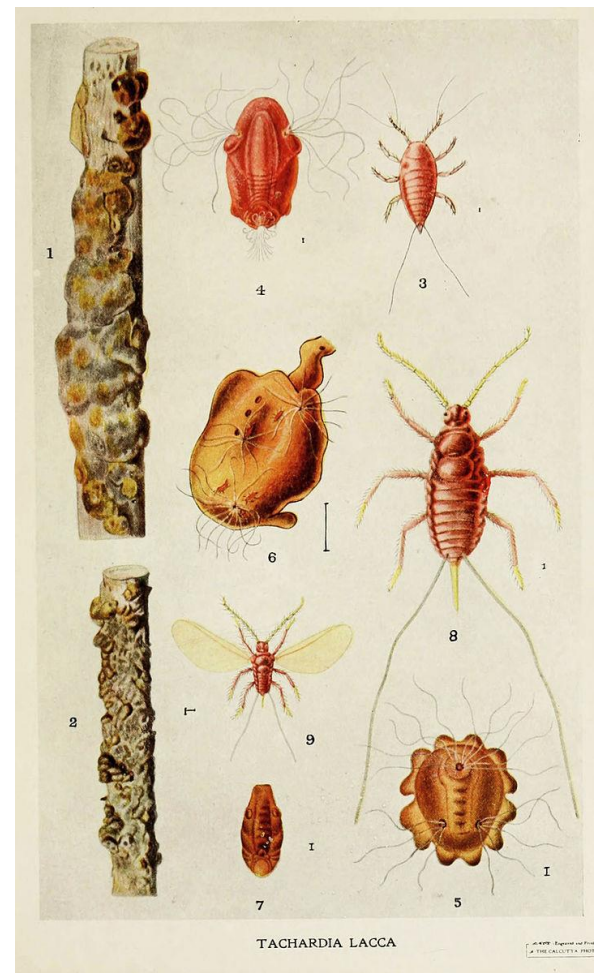
characterization, some authors have assumed that when serviceable local options are available, novelty luxury goods are passed over. On this reasoning, for example, some scholars have assumed that the red lakes in Persian manuscripts are either madder or kermes (Tanevska et al. 2014). A study of the dyes used in Safavid and Mughal textiles seems to support this thesis, with the authors finding that the Indian textiles were most often colored with lac, which could be sourced locally (Shibayama et al. 2015).

Based on its color and translucency, it seems probable that the same lac lake formed the underdrawing on the maps. The use of lac for this purpose has not, to our knowledge, been reported in Western manuscript/cartographic practices, which typically made use of cheaper and duller-colored materials, such as carbon-based inks and iron gall ink (Turner et al 2018). It may have a place in the Persian (and by extension, Mughal) tradition; one study of Persian illuminations found the use of twelve different colors for underdrawings, among them red and purple (Purinton and Watters 1991).

To sum up, many questions remain about the lac in the maps. Is its presence a sign that cochineal was not widely available in Goa at the time, or too costly for the mapmaker? Or does it represent the cleaving of a local artist to a familiar material? Or finally, was it chosen specifically due to the slightly shiny surface it can impart if prepared so that shellac remains in the paint?

Regardless of the implications of its use, the handling of the paint may be significant. The use of lac as a glaze exploits one of its most desirable properties: its translucency. This approach is undertaken in small areas, such as the details on the red roofs of houses and to draw the outlines of bricks on fortifications. The predominant use of the lake is mixed heavily with white, however. By doing so, the artist is essentially rejecting the transparency of watercolors, and again turns towards the miniaturist's method.

Ochre use can tell us little about the maps, as the color has been used since prehistory across the world (Cornell & Schwertmann 2003, pp. 509-510). Perhaps the only notable aspect of its use in the maps is that it demonstrates a sensible conservatism on the part of the artist. Rather than use a more flamboyant, exotic, or expensive color for the terrain, the colorist chose to paint the humble ochre, which quite effectively gets the job done and provides a gentle counterpoint to the rich, bright colors elsewhere in the maps. The ochres are also notable for being the one pigment applied in something akin to a wash (for the beige terrain).



**Figure 112:** 1909 illustration of *Kerria lacca* life cycle. From *Indian Insect Life: a Manual of the Insects of the Plains* by Maxwell-Lefroy. Source: <https://www.flickr.com/photos/biodivlibrary/6280048728/in/set-72157627975114672>

Bone black and ivory black (carbon cokes) have been identified in European art dating to well before the 17<sup>th</sup> century (Eastaugh, Walsch, Chaplin & Siddall 2004, p. 84). At the present, its use or non-use in Rajput and Mughal miniature schools is unclear. No mention of bone black preparation is made in the Sadiqi Bek and Qadi Ahmad treatises. Although carbon black is frequently referenced as a pigment in Mughal and Rajput paintings (Johnson 1972, p. 141; Fischer 2011, p. 793; Ravindran et al. 2011), the source of the black is frequently unexplored. Ohri has reported that in some regions of India, burned ivory was used for black pigments (Ohri 2001, p. 30). The source of the blacks on the maps (bone versus ivory) is likely impossible to determine. Added analytical information on the carbon blacks used by non-European artists in 17<sup>th</sup> century India would allow a better contextualization and possible identification of the artist's background.

Until the binder can be fully characterized, its interpretation will be delayed.

Overall, the maps demonstrate a good comprehension of the properties of painting materials, which suggests the involvement of a professional artist. The hands-on role artists prior to the 19<sup>th</sup> century played in the preparation of their materials makes it even more unlikely that a hobbyist executed the coloring (Stulik 2000). These factors support the hypothesis that Resende did not color the maps himself. The pigments of the maps are myriad: from ancient and unassuming colors like earths and bone blacks, to magical, almost alchemical colors like lead white and verdigris. They also include colors that could have been sourced locally, such as lac and indigo. The pigments used in the maps are not characteristic of a specific painting tradition but underline the tremendous value of color to multiple cultures, and the lengths to which artists will go to secure the perfect hue.

## Final Remarks and Future Research

The thesis has sought to describe several aspects of the maps. From an iconographic perspective, we have seen that while a relatively “standard” set of map signs were employed, local contexts and political concerns led to struggles to codify cultures. Where the dichotomy of housing type and distribution can appear to be a straightforward proclamation of Portuguese superiority, closer examination reveals a more complicated situation. The maps are ambiguous in their function as an advertisement of territorial dominance; perhaps so much so that the editing of the map of ‘Dio’ was necessitated. We have demonstrated that the maps walk a fine line between iconographic standardization and the desire to record peculiarities of specific cities. All of these features are evident at the level of design and are connected to choices made by the draughtsman (presumably Resende).

On this foundation of research, future iconographic study should explore the ways cultural coexistence versus segregation is demonstrated cartographically in the Portuguese *Estado da Índia*. Another topic of interest is the development of map signs for non-Christian religious buildings. Archival research may provide clearer picture of Resende’s life, character, and the role he played in creating the maps. Comparative research will also be helpful in identifying additional cartographic models for the maps of the Évora codex.

We have seen that at the coloring level, the maps veer away from many markers of European watercolor for the period, even when compared to related cartographic works. The discontinuity of underdrawing style and coloring style observed for the trees is particularly suggestive of a division of labor between a draughtsman and colorist. The consistent sequence in which the coloring of map features is executed may indicate a strictly-controlled workshop setting for the painting, or the involvement of only one painter. The maps share some aspects of their palette, paint application, and approach with Mughal and Rajput traditions, although the pigments used are not culturally specific.

The thesis has focused on the maps of several key fortresses of India, and the most obvious step forward will be expansion of the research to other maps from the Évora codex. A study contrasting the materials and methods of the Évora codex maps with those from related codices (such as the ones referenced in figure 2) would also be revealing. Other topics for materials studies have already been mentioned over the course of the thesis but can be recapitulated briefly. First, clarification of the nature of the binder(s) is an essential next step. This information can assist in interpreting the way the paint is applied and may shed light on the colorist’s background. Moreover, binder-pigment interactions could underlie the unusual ultraviolet fluorescence patterns observed through technical photography, and without understanding of the binder, it will be difficult to model and explain this phenomenon. Secondly, work is in progress to characterize the non-indigo components of the blue pigment, which can provide information on the intended use of the blue (for long-distance export versus local use) and potentially give hints at the quality and cost of the pigment. Future research into additives in indigo-based paints will be essential for the creation of spectral databases of greater utility to researchers, using mixtures that reflect actual production techniques.



Another topic of considerable interest is the use of different red lakes during the 16<sup>th</sup>-17<sup>th</sup> centuries in art produced in India. While the rise of Mexican cochineal in European dyeing during this period is well-known, whether and when Mexican cochineal penetrated Mughal, Rajput, and Goan markets is not clear. This pigment's use in India would provide an unambiguous indicator of European impact on the materials used by local artists (another being paper, which is better documented). However, this process cannot currently be reconstructed due to the lack of insect-level red lake identification across the painting traditions active in 16<sup>th</sup>-17<sup>th</sup> century India. A major question to be explored is whether/at what speed trends in painting lakes followed the zeitgeist of dyeing materials. That is, as a new dyestuff came into vogue, did painters rapidly adopt its lake into their palettes, or stick with what they knew?

This preliminary study of the Évora codex maps has been the first to investigate the artistic materials used and to explore its design and context in depth. More broadly, the work has endeavored to demonstrate the richer interpretation of maps that can be achieved with an interdisciplinary approach.

## BIBLIOGRAPHY: PRIMARY SOURCES

- Bocarro, A. (1992). *O Livro das Plantas de Todas as Fortalezas, Cidades, e Povoações da Índia Oriental*. (I. Cid, Ed.) Lisbon: Imprensa Nacional-Casa da Moeda.
- Carre, B. (1947). *The Travels of the Abbé Carre in India and the Near East. 1672-1674. Vol. 1*. (M.E.F. Fawcett, Trans. & C. Fawcett, Ed.). London: Robert Maclehose and Co. Ltd.
- Knox, R. (1681). *An Historical Relation of the Island Ceylon in the East-Indies*. London: Richard Chiswell.
- Linschoten, J.H. van (1885). *The Voyage of John Huyghen van Linschoten to the East Indies. Vol. 1. From the Old English Translation of 1598*. (A.C. Burnell, Ed.). London: Whiting and Co. (Original work published 1596).
- Noronha, M.L. de (1937). *Diário do 3º Conde de Linhares, Vice-Rei da Índia*. Lisbon: Biblioteca Nacional.
- Pires, T. (1944). *The Suma Oriental of Tomé Pires (an account of the East, from the Red Sea to Japan, written in Malacca and India in 1512-1515) and the Book of Francisco Rodrigues (rutter of a voyage in the Red Sea, nautical rules, almanack and maps, written and drawn in the East before 1515), Vol. 1*. (A. Cortesão, Trans.). London: Robert Maclehose and Co. Ltd.
- Polo, M. (1993). *The Travels of Marco Polo. Vol. 2*. (H. Yule, Trans. & H. Cordier, Ed.). Mineola: Dover Publications. (Original work published c. 1300).
- Pyrard, F. (1887). *The Voyage of François Pyrard of Laval to the East Indies, the Maldives, the Moluccas and Brazil. Vol. 1*. (A. Gray, Trans.). London: Whiting and Co. (Original work published 1611).
- Queyroz, F. de (1930). *The Temporal and Spiritual Conquest of Ceylon*. (S.G. Perera, Trans. & P.E. Pieris, Ed.) Colombo: Government Printer.
- Tavernier, J.B. (1889). *Travels in India by Jean Baptiste Tavernier, Baron of Aubonne. Vol. I*. (V. Ball, Trans.). London: McMillan & Co. (Original work published 1676).
- Thevenot, M. de & Careri, J.F.G. (1949). *Indian Travels of Thevenot and Careri (being the third part of the travels of M. de Thevenot into the Levant and the third part of a voyage round the world by Dr. John Francis Gemelli Careri)*. (S. Sen., Ed.). New Delhi: National Archives of India. (Original work published 1656).

## BIBLIOGRAPHY: BOOKS AND STUDIES

- Aceto, M. & Calà, E. (2017). Analytical evidences of the use of iron-gall ink as a pigment on miniature paintings. *Spectrochimica Acta Part A*, 187, 1-8.
- Ainsworth, M.W. (1989). Northern Renaissance drawings and underdrawings: a proposed method of study. *Master Drawings*, 27(1), 5-38.
- Alegria, M.F., Daveau, S., Garcia, J.C., & Relaño, F. (2007). Portuguese cartography in the Renaissance. In Woodward, D. (Ed.), *The History of Cartography, Vol. 3. Cartography in the European Renaissance. Part I*. Chicago: University of Chicago Press.

- Anton, M. (2007). Composition and structure of hen egg yolk. In Huopalahti, R., López-Fandiño, R., Anton, M., & Schade, R. (Eds.), *Bioactive Egg Compounds*, Berlin: Springer.
- Archer, M. (1972). *Company Drawings in the India Office Library*. London: Her Majesty's Stationery Office.
- Archer, M. (1992). *Company Paintings: Indian Paintings of the British Period*. London: Victoria and Albert Museum.
- Arnold, T. (2001). *Renaissance at War*. London: Cassell & Co.
- Astengo, C. (2007). The Renaissance chart tradition in the Mediterranean. In Woodward, D. (Ed.), *The History of Cartography, Vol. 3. Cartography in the European Renaissance. Part I*. Chicago: University of Chicago Press.
- Axelrod, P. & Fuerch, M.A. (1996). The flight of the deities: Hindu resistance in Portuguese Goa. *Modern Asian Studies*, 30(2), 387-421.
- Baer, N.S., Joel, A., Feller, R.L., & Indictor, N. (1986). Indian Yellow. In Feller, R.L. (Ed.), *Artists' Pigments. A Handbook of Their History and Characteristics, Volume 1*. Washington: National Gallery of Art Publishing Office.
- Bai, D., Messinger, D.W., & Howell, D. (2017). Hyperspectral analysis of cultural heritage artifacts: pigment material diversity in the Gough map of Britain. *Optical Engineering*, 56(8),
- Baker, D. (1991). Arab papermaking. *The Paper Conservator*, 15(1), 28-35.
- Balfour-Paul, J. (1999). Indigo in South and South-east Asia. *Textile History*, 30(1), 98-112.
- Barendse, R.J. (2002). *The Arabian Seas: the Indian Ocean World of the Seventeenth Century*. New York: Routledge.
- Barkeshli, M. (2013). Paint palette used by Iranian masters based on Persian medieval recipes. *Restaurator*, 34(2), 101-133.
- Barnes, B.F. (1939). A spectrophotometric study of artists' pigments. *Technical Studies in the Field of the Fine Arts*, 7, 120-130.
- Beach, M.C. (1975). The context of Rajput painting. *Ars Orientalis*, 10, 11-17.
- Beach, M.C. (2008). *The New Cambridge History of India, I:3. Mughal and Rajput Painting*. Cambridge: Cambridge University Press.
- Beazley, K. (1991). Mineral fillers in paper. *The Paper Conservator*, 15, 17-27.
- Bhowmik, S.K. (1970). A note on the use and deterioration of verdigris in Indian watercolor painting. *Studies in Conservation*, 15(2), 154-156.
- Bikiaris, D., Sister Daniila, Sotiropoulou, S., Katsimbiri, O., Pavlidou, E., Moutsatou, A.P., & Chrysoulakis, Y. (2000). Ochre-differentiation through micro-Raman and micro-FTIR spectroscopies: application on wall paintings at Meteora and Mount Athos, Greece. *Spectrochimica Acta Part A*, 56, 3-18.
- Bisulca, C., Picolillo, M., Bacci, M., & Kunzelman, D. (2008). UV-Vis-NIR reflectance spectroscopy of red lakes in paintings. *Papers from the 9<sup>th</sup> International Conference on NDT of Art*.
- Bloom, J.M. (2001). *Paper before Print: The History and Impact of Paper in the Islamic World*. New Haven: Yale University Press.

- Bloom, J.M. (2017). Papermaking: The Historical Diffusion of an Ancient Technique. In Jöns, H., Meusburger, P., & Hefferman, M. (Eds.), *Mobilities of Knowledge* (51-66). Springer Open.
- Bluteau, D.R. (1713). *Vocabulario Portuguez e Latino, Autorizado com Exemplos dos Melhores Escritores Portuguezes, e Latinos, e Offerecido a El-Rey de Portugal D. Joaõ V.* Coimbra.
- Bluteau, D.R. (1716). *Vocabulario Portuguez e Latino, Autorizado com Exemplos dos Melhores Escritores Portuguezes, e Latinos, e Offerecido a El-Rey de Portugal D. Joam V.* Lisbon.
- Boselli, L. (2010). *Non-invasive spectroscopic study of 19<sup>th</sup> century artists' materials* (Doctoral dissertation). University of Ferrara, Italy.
- Boxer, C.R. (1960). The *carreira da India*, 1650-1750. *The Mariner's Mirror*, 46(1), 35-54.
- Boxer, C.R. (1973). *The Portuguese Seaborne Empire, 1415-1825*. London: Pelican Books.
- Brooker, M.H., Sunder, S., Taylor, P., & Lopata, V.J. (1983). Infrared and Raman spectra and X-ray diffraction studies of solid lead (II) carbonates. *Canadian Journal of Chemistry*, 61, 494-502.
- Caggiani, M.C., Cosentino, A., & Mangone, A. (2016). Pigments Checker version 3.0, a handy set for conservation scientists: a free online Raman spectra database. *Microchemical Journal*, 129, 123-132.
- Cardon D. (2014). *Le monde des teintures naturelles*. Belin Sciences.
- Casoli, A., Berzioli, M., & Cremonesi, P. (2012). The chemistry of egg binding medium and its interactions with organic solvents and water. *Smithsonian Contributions to Museum Conservation*, 3, 39-44.
- Castro, R. (2016). *The book of Birds in Portuguese scriptoria: preservation and access* (Doctoral dissertation). Universidade Nova de Lisboa, Portugal.
- Castro, R., Miranda, A., & Melo, M.J. (2016). Interpreting lac dye in medieval written sources: new knowledge from the reconstruction of recipes relating to illuminations in Portuguese manuscripts. In Eyb-Green, S., Townsend, J., Pilz, K., Kroustallis, S., & Leeuwen, I. van (Eds.), *Sources in Art Technology: Back to Basics*. London: Archetype Publications.
- Cavaleri, T., Giovagnoli, A., & Nervo, M. (2013). Pigments and mixtures identification by visible reflectance spectroscopy. *Procedia Chemistry*, 8, 45-54.
- Centeno, S., Guzman, M.I., Yamazakikleps, A., & della Védova, C.O. (2004). Characterization by FTIR of the effect of lead white on some properties of proteinaceous binding media. *Journal of the American Institute of Conservation*, 43(2), 139-150.
- Cheilakou, E., Troullinos, M., & Kouli M. (2014). Identification of pigments on Byzantine 33 wall paintings from Crete (14th century AD) using non-invasive Fiber Optics Diffuse Reflectance Spectroscopy (FORS). *Journal of Archaeological Science*, 41, 541-55.
- Church, A.H. (1890). *The Chemistry of Paints and Pigments*. London: Seeley & Co. Ltd.
- Cid, I. (1992). *O Livro das Plantas de Todas as Fortalezas, Cidades, e Povoações da Índia Oriental. Vol. I: Estudo e Índices*. Lisbon: Imprensa Nacional-Casa da Moeda.
- Clark, R.J.H. (2003). Raman microscopy in the identification of pigments on manuscripts and other works of art. *In Scientific*

- Examination of Art. Modern Techniques in Conservation and Analysis*. Washington: The National Academies Press.
- Clark, R.J.H., Cooksey, C.J., Daniels, M.A.M., & Withnall, R. (1993). Indigo, woad, and Tyrian purple: important vat dyes from antiquity to the present. *Endeavor*, 17(4), 191-199.
- Clark, R.J.H., Gibbs, P.J., Seddon, K.R., Brovenko, N.M., & Petrosyan, Y.A. (1997). Non-destructive *in situ* identification of cinnabar on ancient Chinese manuscripts. *Journal of Raman Spectroscopy*, 28, 91-94.
- Clementi, C., Doherty, B., Gentili, P.L., Miliani, C., Romani, A., Brunetti, B.G., & Sgamellotti, A. (2008). Vibrational and electronic properties of painting lakes. *Applied Physics A*, 92, 25-33.
- Clements, J.C. (1991). The Indo-Portuguese creoles: languages in transition. *Hispania*, 74(3), 637-646.
- Clements, J.C. (2015). Portuguese settlement of the Chaul/Korlai area and the formation of Korlai creole Portuguese. *Journal of Language Contact*, 8, 13-35.
- Coccato, A., Bersani, D., Coudray, A., Sanyova, J., Moens, L., & Vandenabeele, P. (2016). Raman Spectroscopy of green minerals and reaction products with an application in cultural heritage research. *Journal of Raman Spectroscopy*, 57(12), 1429-1443.
- Cohn, M.B. (1977). *Gouache and Wash: A Study of the Development of the Materials of Watercolor*. Cambridge: William Hays Fogg Art Museum.
- Collingham, L. (2006). *Curry. A Tale of Cooks and Conquerors*. Oxford: Oxford University Press.
- Collings, T. & Milner, D. (1984). The nature and identification of cotton paper-making fibers in paper. *The Paper Conservator*, 8, 59-71.
- Cormack, L.B. (2007). Maps as educational tools in the Renaissance. In Woodward, D. (Ed.), *The History of Cartography, Vol. 3. Cartography in the European Renaissance. Part I*. Chicago: University of Chicago Press.
- Cornell, R.M. & Schwertmann, U. (2003). *The Iron Oxides: Structure, Properties, Reactions, Occurrences, and Uses (2<sup>nd</sup> Edition)*. New York: Wiley VCH.
- Cortese, A., & Teixeira da Mota, A. (1960a). *Portugaliae Monumenta Cartographica. Vol. 4*. Lisbon: Imprensa Nacional Casa de Moeda.
- Cortese, A., & Teixeira da Mota, A. (1960b). *Portugaliae Monumenta Cartographica. Vol. 5*. Lisbon: Imprensa Nacional Casa de Moeda.
- Cosentino, A. (2014a). FORS spectral database of historical pigments in different binders. *E-Conservation Journal*, 2, 54-65.
- Cosentino, A. (2014b). Identification of pigments by multispectral imaging; a flowchart method. *Heritage Science*, 2(8), 1-12.
- Cosentino, A. (2015). Effects of different binders on technical photography and infrared reflectography of 54 historical pigments. *International Journal of Conservation Science*, 6(3), 287-298.
- Cosgrove, D. (1985). Prospect, perspective, and the evolution of the landscape idea. *Transactions of the Institute of British Geographers*, 10(1), 45-62.
- Craddock, P.T. (2009). *Scientific Investigation of Copies, Fakes, and Forgeries*. Burlington: Elsevier Butterworth-Heinemann.



- Cucci, C., Bracci, S., Casini, A., Innocenti, S., Picollo, M., Stefani, L., Rao, I.G., & Scudieri, M. (2018). The illuminated manuscript *Corale* 43 and its attribution to Beato Angelico: Non-invasive analysis by FORS, XRF and hyperspectral imaging techniques. *Microchemical Journal*, 138, 45-57.
- Cunha, G.J. da (1876). *Notes on the History and Antiquities of Chaul and Bassein*. Bombay: Thacker, Vining & Co.
- Dąbrowski, J., & Simmons, J.S.G. (2003). Permanence of early European hand-made papers. *Fibres & Textiles in Eastern Europe*, 11(1), 8-13.
- Daveri, A., Malagodi, M., & Vagnini, M. (2018). The bone black pigment identification by noninvasive, in situ infrared reflection spectroscopy. *Journal of Analytical Methods in Chemistry*, 2018.
- Degano, I., Ribechini, E., Modugno, F., & Colombini, M.P. (2009). Analytical methods for the characterization of organic dyes in artworks and in historical textiles. *Applied Spectroscopy Reviews*, 44(5), 363-410.
- Delano-Smith, C. (2007). Signs on printed topographical maps, ca. 1470-ca. 1640. In Woodward, D. (Ed.), *The History of Cartography, Vol. 3. Cartography in the European Renaissance. Part I*. Chicago: University of Chicago Press.
- Delano-Smith, C. & Kain, R.J.P. (2009) Cartography, History of. In Kitchin, R. & Thrift, N. (Eds.), *International Encyclopedia of Human Geography, vol. 1*, pp. 428-440. Oxford: Elsevier.
- Derrick, M.R., Stulik, D., & Landry, J.M. (1999). *Infrared Spectroscopy in Conservation Science*. Los Angeles: The Getty Conservation Institute.
- Dickson, M.B. & Welch, S.C. (1981). Appendix 1: The Canons of Painting by Sadiqi Bek. In Firdausī, Dickson, M.B., & Welch, S.C. *The Houghton Shahnameh, Volume 1*. Cambridge: Harvard University Press.
- Dimand, M.S. (1944). The Emperor Jahangir, connoisseur of paintings. *The Metropolitan Museum of Art Bulletin*, 2(6), 196-200.
- Dimand, M.S. (1953). Mughal painting under Akbar the Great. *Metropolitan Museum of Art Bulletin*, 30(2), 46-51.
- Disney, A.R. (1978). *Twilight of the Pepper Empire: Portuguese trade in Southwest Asia in the Early 17<sup>th</sup> Century*. Cambridge: Harvard University Press.
- Disney, A.R. (1996). Portuguese Goa and the Great Indian Famine of 1630-1631. In Kulakarnī, A.R., Nayeem, M.A., & de Souza, T.R. (Ed.s), *Mediaeval Deccan History: Commemoration Volume in Honour of P.M. Joshi*. Bombay: Popular Prakashan Pvt. Ltd.
- Doménech, A., Doménech-Carbó, M.T., & Vázquez de Agredos Pascual, M.L. (2006). Dehydroindigo: a new piece into the Maya blue puzzle from the voltammetry of microparticles approach. *Journal of Physical Chemistry B*, 110, 6027-6039.
- Dooley, K.A., Lomax, S., Zeibel, J.G., Ricciardi, P., Hoenigswald, A., Loew, M., & Delaney, J.K. (2013). Mapping of egg yolk and animal skin glue paint binders in Early Renaissance paintings using near infrared reflectance imaging spectroscopy. *Analyst*, 138(17), 4828-48.
- Duran, A., Perez-Rodriguez, J.L., Espejo, T., Franquelo, M.L., Castaing, J., & Walter, P. (2009). Characterization of illuminated manuscripts by laboratory-made portable XRD and micro-XRD systems.
- Eastaugh, N., Walsch, V., Chaplin, T., & Siddall, R. (2004). *Pigment Compendium: A Dictionary of Historical Pigments*.

Burlington: Elsevier Butterworth-Heinemann.

Eastaugh, N. & Walsh, V. (2004). *The Pigment Compendium: Optical Microscopy of Historical Pigments*. Burlington: Elsevier Butterworth-Heinemann.

Eastman Kodak Company (1972). *Ultraviolet and Fluorescence Photography*. Rochester: Eastman Kodak Company.

Eaton, N. (2006). Nostalgia for the exotic: creating an Imperial art in London, 1750-1793. *Eighteenth-Century Studies*, 39(2), 227-250.

Edwards, H.G.M. (2011). Analytical Raman spectroscopic discrimination between yellow pigments of the Renaissance. *Spectrochimica Acta Part A*, 80, 14-20.

Elias, M., Chartier, C., Prévot, G., Garay, H., & Vignaud, C. (2006). The colour of ochres explained by their composition. *Materials Science and Engineering B*, 127, 70-80.

Elkins, J. (1994). *Poetics of Perspective*. Ithaca, N.Y.: Cornell University Press.

Espejo, T., Duran, A., Lopez-Montes, A., & Blanc, R. (2010). Microscopic and spectroscopic techniques for the study of paper supports and textile used in the binding of hispano-arabic manuscripts from Al-Andalus: A transition model in the 15<sup>th</sup> century. *Journal of Cultural Heritage*, 11, 50-58.

Fernandes, J. (2008). Indo-Portuguese art and the space of the Islamicate. *Parnas*, 7, 41–50.

Fischer, E. (2011). The Technique of Indian Painters: A short note. In Beach, M.C., Fischer, E., & Goswamy, B.N., *Masters of Indian Painting, Volume 2*. New Delhi: Niyogi Books.

Flores, J. (2015). *Nas Margens do Hindustão: o estado da Índia e a expansão mongol ca. 1570-1640*. Coimbra: Imprensa da Universidade de Coimbra.

Fois, E., Gamba, A., & Tilocca, A. (2003). On the unusual stability of Maya blue paint: molecular dynamics simulations. *Microporous and Mesoporous Materials*, 57, 263-272.

Franquelo, M.L. & Perez-Rodriguez, J.L. (2016). A new approach to the determination of the synthetic or natural origin of red pigments through spectroscopic analysis. *Spectrochimica Acta A*, 166, 103-111.

Frausto-Reyes, C., Ortiz-Morales, M., Bujdud-Pérez, J.M., Magaña-Cota, G.E., & Mejía-Falcón, R. (2009). Raman spectroscopy for the identification of pigments and color measurement in Dugès watercolors. *Spectrochimica Acta Part A*, 74, 1275-1279.

Froment, F., Tournié, A., & Colomban, P. (2008). Raman identification of natural red to yellow pigments: ochre and iron-containing ores. *Journal of Raman Spectroscopy*, 39, 560-568.

Frost, R.L., Martens, W.N., & Klopogge, J.T. (2002). Raman spectroscopic study of cinnabar (HgS), realgar (As<sub>4</sub>S<sub>3</sub>) and orpiment (As<sub>2</sub>S<sub>3</sub>) at 298 and 77K. *Neues Jahrbuch für Mineralogie*, 12, 469-480.

Frost, R.L., Klopogge, J.T., & Williams, P. (2003). Raman spectroscopy of lead sulphate-carbonate minerals: implications for hydrogen bonding. *Neues Jahrbuch für Mineralogie*, 12, 529-542.

Galan, E. (1996). Properties and applications of palygorskite-sepiolite clays. *Clay Minerals*, 31, 443-453.

Garside, P. & Wyeth, P. (2003). Identification of cellulosic fibers by FTIR spectroscopy. *Studies in Conservation*, 48, 269-275.

- Gaspar, J.A. & Leitão, H. (2018). Luis Teixeira, c. 1585: The earliest known chart with isogonic lines. *Imago Mundi*, 70, 221-228.
- Gettens, R.J., Feller, R.L., & Chase, W.T. (1993). Vermilion and Cinnabar. In Roy, A. (Ed.), *Artists' Pigments. A Handbook of Their History and Characteristics, Volume 2*. Washington: National Gallery of Art Publishing Office.
- Gettens, R.J., Kühn, H., & Chase, W.T. (1993). Lead White. In Roy, A. (Ed.), *Artists' Pigments. A Handbook of Their History and Characteristics, Vol. 2*. Washington: National Gallery of Art Publishing Office.
- Gil, M., Green, R., Carvalho, M.L., Seruya, A., Queralt, I., Candeias, A.E., & Mirão, J. (2009). Rediscovering the palette of Alentejo earth pigments: provenance establishment and characterization by LA-ICP-MS and spectra-colorimetric analysis. *Applied Physics A*, 96, 997-1007.
- Giustetto, R., Llabrés i Xamena, F.X., Ricchiardi, G., Bordiga, S., Damin, A., Gobetto, R., & Chierotti, M.R. (2005). Maya blue: a computation and spectroscopic study. *Journal of Physical Chemistry*, 109, 19360-19368.
- Gonzalez, V., Calligaro, T., Wallez, G., Eveno, M., Toussaint, K., & Menu, M. (2015). Composition and microstructure of the lead white pigment in Masters paintings using HR Synchrotron XRD. *Microchemical Journal*, 125, 43-49.
- Gonzalez, V., Gourier, D., Calligaro, T., Toussaint, K., Wallez, G., & Menu, M. (2017). Revealing the origin and history of lead-white pigments by their photoluminescence properties. *Analytical Chemistry*, 89(5), 2909-2918.
- Grünwedel, A. (1901). Revised and enlarged by Burgess, J., trans. Gibson, A. *Buddhist Art in India*. London: Bernard Quaritch.
- Guineau, B. & Vichard, V. (1987). *Committee for Conservation: 8<sup>th</sup> Triennial Meeting, Sydney, Australia, 6-September, 1987*. Preprints, vol. 2. Marina del Rey: The Getty Conservation Institute.
- Hale, J. (2007). Warfare and cartography, ca. 1450 to ca. 1640. In Woodward, D. (Ed.), *The History of Cartography, vol. 3: Cartography in the European Renaissance*. Chicago: The University of Chicago Press.
- Harley, J.B. (1988a). Maps, knowledge, and power. In Cosgrove, D. & Daniels, S. (Eds.), *The Iconography of Landscapes: Essays on the Symbolic Representation, Design, and Use of Past Environments*. Cambridge: Cambridge University Press.
- Harley, J.B. (1988b). Silences and secrecy: the hidden agenda of cartography in Early Modern Europe. *Imago Mundi*, 40, 57-76.
- Howard, I.P. & Allison, R.S. (2011). Drawing with divergent perspective, ancient and modern. *Perception*, 40, 1017-1033.
- Hunter, D. (1978). *Papermaking. The History and Technique of an Ancient Craft*. New York: Dover Publications, Inc.
- Irwin, G. (1962). Malacca Fort. *Journal of Southeast Asian History*, 3(2), 19-44.
- Jacobs, W. (2016). *The fingerprinting of the materials used in Portuguese illuminated manuscripts: origin, production and specificities of the 16<sup>th</sup> century Antiphonary paints from the Biblioteca Pública de Évora* (Master thesis). Univeristy of Évora, Portugal.
- Jane, J.-L., Kasemsuwan, T., Leas, S., Zobel, H., & Robyt, J.F. (1994). Anthology of starch granule morphology by scanning electron microscopy. *Starch – Stärke*, 46(4), 121-129.

- Jariwala, K. (2010). The Materials and Techniques of Indian Painting. In Crill, R. & Jariwala, K. (Eds.), *The Indian Portrait, 1560-1860*. Ahmedabad: Mapin Publishing Pvt. Ltd.
- Jayasuriya, S. de S. (2008). *The Portuguese in the East. A Cultural History of a Maritime Trading Empire*. London: I.B. Tauris & Co. Ltd.
- Johnson, B.B. (1972). The technique of Indian miniature painting. In Pal, P. (Ed.), *Aspects of Indian Art: Papers Presented in a Symposium at the Los Angeles County Museum of Art*. Leiden: E.J. Brill.
- Kagan, R.L. & Schmidt, B. (2007). Maps and the Early Modern state: official cartography. In Woodward, D. (Ed.), *The History of Cartography, Vol. 3. Cartography in the European Renaissance. Part I*. Chicago: University of Chicago Press.
- Kirby, J., Spring, M., & Higgit, C. (2005). The technology of lake pigment manufacture: study of the dyestuff substrate. *National Gallery Technical Bulletin*, 26, 71-87.
- Kleber, R., Massshelein-Kleiner, L., & Thissen, J. (1967). Étude et identification du "Bleu Maya." *Studies in Conservation*, 12, 41-56.
- Kogou, S., Neate, S., Coveney, C., Miles, A., Boocock, D., Burgio, L., Cheung, C.S., & Liang, H. (2016). The origins of the Selden map of China: scientific analysis of the painting materials and techniques using a holistic approach. *Heritage Science*, 4(28), 1-24.
- Kossak, S. (1997). *Indian Court Painting: 16<sup>th</sup>-19<sup>th</sup> Century*. New York: The Metropolitan Museum of Art.
- Kühn, H. (1993). Verdigris and Copper Resinate. In Roy, A. (Ed.), *Artists' Pigments. A Handbook of Their History and Characteristics, Volume 2*. Washington: National Gallery of Art Publishing Office.
- Lech, K. & Jarosz, M. (2011). Novel methodology for the extraction and identification of natural dyestuffs in historical textiles by HPLC-UV-Vis-ESI MS. Case study: chasubles from the Wawel Cathedral collection. *Analytical and Bioanalytical Chemistry*, 399(9), 3241-3251.
- Lee, L.R., Thompson, A., & Daniels, V.D. (1997). Princes of the house of Timur: conservation and examination of an early Mughal painting. *Studies in Conservation*, 42(4), 231-240.
- Leona, M. (2009). Microanalysis of organic pigments and glazes in polychrome works of art by surface-enhanced resonance Raman scattering. *Proceedings of the National Academy of Sciences of the United States of America*, 106(35), 14757-14762.
- Leona, M., Casadio, F., Bacci, M., & Picollo, M. (2013). Identification of the pre-Columbian pigment Maya blue on works of art by noninvasive UV-Vis and Raman spectroscopic techniques. *Journal of the American Institute for Conservation*, 43(1), 39-54.
- Lewin, M. & Pearce, E.M. (Eds.) (1998). *Handbook of Fiber Chemistry (2<sup>nd</sup> Edition)*. New York: Marcel Dekker, Inc.
- Lewincamp, S. & McNaught-Reynolds, A. (2010). Pigment analysis and treatment of four Dutch East India Company vellum charts. *Contributions to the 2010 AICCM Book, Paper and Photographic Materials Symposium*, 34-39.
- Lliveras-Tenorio, A., Mazurek, J., Restivo, A., Colombini, M.P., & Bonaduce, I. (2012). The development of a new analytical model for the identification of saccharine binders in paint samples. *PloS ONE*, 7(11), 1-17.
- Losty, J.P. (2012). Identifying the artist of the Codex Casanatense 1889. *Anais de Historia de Alem-Mar*, 13, 13-40.

- Loureiro, R.M. (2008). Historical notes on the Portuguese fortress of Malacca (1511-1641). *Revista de Cultura*, 27, 78-96.
- Luengo, P. (2017). Architectural hybridity in Iberian Southeast Asia, 1580-1640. *Itinerario*, 41(2), 353-374.
- Lynn, J.A. (1991) The *trace italienne* and the growth of armies: the French case. *The Journal of Military History*, 55(3), 297-330.
- Machado, D.R. (1752). *Bibliotheca Lusitana. Historica, Critica, e Cronologica. Vol. 3*. Lisbon: Office of Ignacio Rodrigues.
- Manso, M. & Carvalho, M.L. (2009). Application of spectroscopy techniques for the study of paper documents: a survey. *Spectrochimica Acta Part B*, 64, 482-490.
- Manso, M., Carvalho, M.L., Queralto, I., Vicini, S., & Princi, E. (2011). Investigation of the composition of historical and modern Italian papers by energy dispersive x-ray fluorescence (EDXRF), x-ray diffraction (XRD), and scanning electron microscopy energy dispersive spectrometry (SEM-EDS). *Applied Spectroscopy*, 65(1), 52-59.
- Marichal, C. (2014). Mexican cochineal and European demand for a luxury dye, 1550-1850. In Aram, B. & Yun-Casalilla, B. (Eds.), *Global Goods and the Spanish Empire, 1492-1824*. London: Palgrave Macmillan UK.
- Martens, W., Frost, R.L., Klopogge, J.T., & Williams, P.A. (2003). Raman spectroscopic study of basic copper sulphates-implications for copper corrosion and 'bronze disease.' *Journal of Raman Spectroscopy*, 34, 145-151.
- Marucci, G., Beeby, A., Parker, A.W., & Nicholson, C.E. (2018). Raman spectroscopic library of medieval pigments collected with five different wavelengths for investigation of illuminated manuscripts. *Analytical Methods*, 10, 1219-1236.
- Mattoso, J. (Dir.) (2010). *Património de Origem Portuguesa no Mundo-Ásia, Oceania. Arquitectura e Urbanismo*. Lisbon: Calouste Gulbenkian Foundation.
- Maxwell, W.G. (1911). Barretto de Resende's Account of Malacca. *Journal of the Straits Branch of the Royal Asiatic Society*, 60, 1-24.
- Maybury, I.J., Howell, D., Terras, M., & Viles, H. (2018). Comparing the effectiveness of hyperspectral imaging and Raman spectroscopy: a case study on Armenian manuscripts. *Heritage Science*, 6(42), 1-15.
- Maynez-Rojas, M.A., Casanova-González, E.C., & Ruvalcaba-Sil, J.L. (2017). Identification of natural red and purple dyes on textiles by Fiber-optics Reflectance Spectroscopy. *Spectrochimica Acta Part A*, 178, 239-250.
- Meilunas, R.J., Bentsen, J.G., & Steinberg, A. (1990). Analysis of aged paint binders by FTIR spectroscopy. *Studies in Conservation*, 35(1), 33-51.
- Melo, M.J. (2009) History of natural dyes in the ancient Mediterranean world. In Bechtold, T. & Mussak, R. (Eds.), *Handbook of Natural Colorants*. West Sussex: John Wiley & Sons Ltd.
- Melo, M., Miranda, A., Miguel, C., Lemos, A., Claro, A., Castro, R., Muralha, S., Lopes, J.A., & Gonçalves, A.P. (2011). The colour of medieval Portuguese illumination: an interdisciplinary approach. *Revista de História da Arte N.º Especial*, 146-169.
- Melo, M.J., Nabais, P., Guimarães, M., Araújo, R., Castro, R., Oliveira, M.C., & Whitworth, I. (2016). Organic dyes in illuminated manuscripts: a unique cultural and historic record. *Philosophical Transactions. Series A, Mathematical, Physical, and Engineering Sciences*, 12
- Miguel, C. (2012). Le vert et le rouge: *a study on the materials, techniques and meaning of the green and red colours in*



*medieval Portuguese illuminations* (Doctoral dissertation). Universidade Nova de Lisboa, Portugal.

- Miguel, C., Pinto, J.V., Clarke, M., & Melo, M.J. (2014) The *alchemy* of red mercury sulfide: the production of vermilion for medieval art. *Dyes and Pigments*, 102, 210-217.
- Minorsky, V. (1959). Minorsky, trans. Calligraphers and Painters: A Treatise by Qadi Ahmand, Son of Mir-munshi (C. A.H. 1015/A.D. 1606). *Freer Gallery of Art Occasional Papers*, 3(2).
- Mortensen, A. (2006). Carotenoids and other pigments as natural colorants. *Pure Applied Chemistry*, 78(8), 1477-1491.
- Moti, C. (1919). *Jain Miniature Paintings from Western India*. Ahmedabad: Sarabhai Manilal Nawab.
- Mounier, A., Le Bourdon, G., Aupetit, G., Belin, C., Servant, L., Lazare, S., Lefrais, Y., & Daniel, F. (2014). Hyperspectral imaging, spectrofluorimetry, FORS and XRF for the non-invasive study of medieval miniatures materials. *Heritage Science*, 2(24), 1-12.
- Mundy, B. (1996). *The Mapping of New Spain. Indigenous Cartography and the Maps of the Relaciones Geograficas*. Chicago: The University of Chicago Press.
- Murray, H.H. & Zhou, H. (2006). Palygorskite and Sepiolite (Hormites). In Kogel, J.E., Trivedi, N.C., Barker, J.M., & Krukowski, S.T. (Eds.), *Industrial Minerals & Rocks: Commodities, Markets, and Uses*. Littleton: Society for Mining, Metallurgy, and Exploration, Inc.
- Nadri, G.A. (2016). *The Political Economy of Indigo in India, 1580-1930*. Boston: Brill.
- Naravane, M.S. (1998). *The Maritime and Coastal Forts of India*. New Delhi: APH Publishing Corporation.
- Nassau, K. (1983). *The Physics and Chemistry of Color: The Fifteen Causes of Color*. New York: John Wiley & Sons.
- Newitt, M. (2005). *A History of Portuguese Overseas Expansion, 1400-1668*. New York: Routledge.
- Nöller, R. (2015). Cinnabar reviewed: characterization of the red pigment and its reactions. *Studies in Conservation*, 60(2), 79-87.
- Nunes, M., Revlas, C., Figueira, F., Campelo, J., Candeias, A., Caldeira, A., & Ferreira, T. (2015). Analytical and microbiological characterization of paper samples exhibiting foxing stains. *Microscopy and Microanalysis*, 21, 63-77.
- Ohri, V.C. (2001). *The Technique of Pahari Painting: An Inquiry into Materials, Methods and History (based upon observation and field-work)*. New Delhi: Aryan Books International.
- Ovarlaz, S., Chaze, A-M., Giulieri, F., & Delamare, F. (2006). Indigo chemisorption in sepiolite. Application to Maya blue formation. *Comptes Rendus Chemie*, 9, 1243-1248.
- Parker, T.W. (1969). A classification of kaolinities by infrared spectroscopy. *Clay Minerals*, 8, 135-141.
- Patel, B.K. & Seetharaman, K. (2006). Effect of heating rate on starch granule morphology and size. *Carbohydrate Polymers*, 65(3), 381-385.
- Pearson, M.N. (1987). *The New Cambridge History of India, vol. 1, part 1: The Portuguese in India*. Cambridge: The Cambridge University Press.
- Pearson, M.N. (1998). *Port Cities and Intruders: The Swahili Coast, India, and Portugal in the Early Modern Era*. Baltimore:

the Johns Hopkins University Press.

- Petroviciu, I., Albu, F., & Medvedovici, A. (2010). LC/MS and LC/MS/MS based protocol for identification of dyes in historic textiles. *Microchemical Journal*, 95, 247-254.
- Phipps, E. (2010). *Cochineal Red. The Art History of a Color*. New Haven: Yale University Press.
- Pires, J., Gonçalves, P., Carvalho, A., Mendoça, M., & Cruz, A.J. (2010). Theory vs. practice: synthesis of white lead following ancient recipes. 185-200.
- Powrie, W.D. & Nakai, S. (1986). The chemistry of eggs and egg products. In *Egg Science and Technology (3<sup>rd</sup> Edition)*, Stadelman, W.J. & Cotterill, O.J. (Eds.) Westport: Avi Publishing Co.
- Pronti, L. (2016). *Multispectral imaging of paintings. Potentialities and limitations of the technique in relation with the chemical and optical properties of pictorial materials* (Doctoral dissertation). Sapienza University of Rome & the University of Avignon.
- Purinton, N., & Watters, M. (1991). A study of the materials used by Medieval Persian painters. *Journal of the American Institute for Conservation*, 30(2), 125-144.
- Raczynski, A. le C. de. (1847). *Dictionnaire Historico-Artistique du Portugal*. Paris: Jules Renouard & Co.
- Rahman, M.M.M. & Sayed-Esfahani, M.H. (1979). Scanning electron microscope study of flax fibres. *Indian Journal of Textile Research*, 4, 149-152.
- Ramaswami, N.S. (1979). *Indian Monuments*. New Delhi: Abhinav Publications.
- Ramaseshan, S. (1989). The history of paper in India up to 1948. *Indian Journal of History of Science*, 24(2), 103-121.
- Ravindran, T.R., Arora, A.K., Subba Rao, R.V., & Raj, B. (2011). Raman spectroscopic study of medieval Indian art of the 17<sup>th</sup> century. *Journal of Raman Spectroscopy*, 42(4), 803-807.
- Rees, R. (1980). Historical links between cartography and art. *Geographical Review*, 70(1), 60-78.
- Rei, C. (2011). *Turning Points in Leadership : Shipping Technology in the Portuguese and Dutch Merchant Empires*. Vanderbilt University Department of Economics Working Papers, no. 1123. Vanderbilt University Department of Economics.
- Reiche, I., Britzke, R., Bukalis, G., Reinholz, U., Weise, H.-P., & Gadebusch, R.D. (2005). An external PIXE study: Mughal painting pigments. *X-Ray Spectrometry*, 34, 42-45.
- Ricciardi, P., Delaney, J.K., Facini, M., Zeibel, J.G., Picollo, M., Lomax, S., & Loew, M. (2012). Near infrared reflectance imaging spectroscopy to map paint binders in situ on illuminated manuscripts. *Angewandte Chemie*, 124, 5705-5708.
- Sánchez del Rio, M., Picquart, M., Haro-Poniatowski, E., van Elslande, E., & Uc, V.H. (2006). On the Raman spectrum of Maya blue. *Journal of Raman Spectroscopy*, 37(10), 1046-1053.
- Sánchez-Navas, A., López-Cruz, O., Velilla, N., & Vidal, I. (2013). Crystal growth of lead carbonates: influence of the medium and relationship between structure and habit. *Journal of Crystal Growth*, 376, 1-10.
- Sanderson, K. (2007). Making it stick: paste on paper. *The Book and Paper Group Annual*, 26, 155-159.

- Santos, J.R. dos & Mendiratta, S.L. (2011). Goa, Damão e Diu aos Olhos de Resende: Análise Comparativa das Vistas Representadas. *Oriente*, 20, 51-62.
- Santos, R., Hallett, J., Oliveira, M.C., Sousa, M.M., Sarraguça, J., Simmonds, M.S.J., & Nesbitt, M. (2015). HPLC-DAD-MS analysis of colorant and resinous components of lac-dye: A comparison between *Kerria* and *Paratrichardina* genera. *Dyes and Pigments*, 118, 129-136.
- Scammell, G.V. (1982). England, Portugal, and the Estado da Índia c. 1500-1635. *Modern Asian Studies*, 16(2), 177-192.
- Schellman, N. (2007). Animal glues: a review of their key properties relevant to conservation. *Studies in Conservation*, 52, 55-66.
- Scheuermann, W. & Ritter, G.J. (1969). Raman spectra of cinnabar (HgS), realgar (As<sub>4</sub>S<sub>4</sub>) and orpiment (As<sub>2</sub>S<sub>3</sub>). *Z. Naturforsch.*, 24 a, 408-411.
- Schweppe, H. & Roosen-Runge, H. (1986). Carmine. In Feller, R.L. (Ed.), *Artists' Pigments. A Handbook of Their History and Characteristics, Volume 1*. Washington: National Gallery of Art Publishing Office.
- Schweppe, H. (1997). Indigo and Woad. In Fitzhugh, E.W. (Ed.), *Artists' Pigments. A Handbook of Their History and Characteristics, Volume 3*. Washington: National Gallery of Art Publishing Office.
- Scott, D.A., Narayan, K., Schilling, M.R., Turner, N., Taniguchi, Y., & Khanjian, H. (2001). Technical examination of a fifteenth-century German illuminated manuscript on paper: a case study in the identification of materials. *Studies in Conservation*, 46(2), 93-108.
- Serrano, A., Hallett, J., & Bommel, M.R. (2011). The Red Road of the Iberian Expansion: cochineal and the global dye trade. ARCHLAB Transnational Access BM/C2RMF/NGL, CHARISMA ARCHLAB User's Reports.
- Shibayama, N., Wypyski, M., & Gagliardi-Mangilli, E. (2015). Analysis of natural dyes and metal threads used in 16<sup>th</sup>-18<sup>th</sup> century Persian/Safavid and Indian/Mughal velvets by HPLC-PDA and SEM-EDS to investigate the system to differentiate velvets of these two cultures. *Heritage Science*, 3(12), 1-20.
- Shokoohy, M. and Shokoohy, N. (2003). The Portuguese fort at Diu. *South Asian Studies*, 19(1), 169-203.
- Shokoohy, M. and Shokoohy, N. (2010). The island of Diu, its architecture and historic remains. *South Asian Studies*, 70(2), 161-192.
- Silva, R.R.K. de (1988). *Illustrations and Views of Dutch Ceylon 1602-1796. A comprehensive work of pictorial reference with selected eye-witness accounts*. London: Serendib Publications.
- Silveira, L. (1957). *Ensaio de iconografia das cidades portuguesas do ultramar, vol. 1*. Lisbon: Ministerio do Ultramar.
- Sinopoli, C.M. (2000). From the lion throne: political and social dynamics of the Vijayanagara empire. *Journal of the Economic and Social History of the Orient*, 43(3), 364-398.
- Sivaratnam, C. (1964). *An outline of the cultural history and principles of Hinduism*. Colombo: Stangard Printers.
- Smith, G.D. & Clark R.J.H. (2001). Raman microscopy in art history and conservation science. *Studies in Conservation*, 46(2), 91-106.
- Smith, G.D. (2017). Cow urine, Indian yellow, and art forgeries: an update. *Forensic Science International*, 276, 30-34.

- Sohoni, P. (2013). Medieval Chaul under the Nizam Shahs. An archaeological and historical investigation. In Parodi, L.A. (Ed.), *The Visual World of Muslim India*, London: I.B. Tauris & Co. Ltd.
- Soudavar, A. (1999). Between the Safavids and the Mughals: art and artists in transition. *Journal of Persian Studies*, 37, 49-66.
- Stulik, D.C. (2000). Paint. In Taft, W.S. Jr. & Mayer, J.W. (Eds.), *The Science of Paintings*. New York: Springer-Verlag.
- Subrahmanyam, S. (1984). The Portuguese, the port of Basrur, and the rice trade, 1600-50. *The Indian Economic and Social History Review*, 21(4), 433-462.
- Subrahmanyam, S. (2012). *The Portuguese Empire in Asia, 1500-1700: A Political and Economic History*. West Sussex: Wiley-Blackwell.
- Tagle, A.; Paschinger, H., & Infante, G. (1990). Maya blue: its presene in Cuban colonial wall paintings. *Studies in Conservation*, 35, 156-159.
- Tanevska, V., Nastova, I., Minčeva-Šukarova, B., Grupče, O., Ozcatat, M., Kavčić, M., & Jakovlevska-Spirovska, Z. (2014). Spectroscopic analysis of pigments and inks in manuscripts: II. Islamic illuminated manuscripts (16<sup>th</sup>-18<sup>th</sup> century). *Vibrational Spectroscopy*, 73, 127-137.
- Tatsch, E. & Schrader, B. (1995). Near-Infrared Fourier transform Raman spectroscopy of Indigoids. *Journal of Raman Spectroscopy*, 26, 467-473.
- Tomasini, E., Siracusano, G., & Maier, M.S. (2012). Spectroscopic, morphological and chemical characterization of historic pigments based on carbon. Paths for the identification of an artistic pigment. *Microchemical Journal*, 102, 28-37.
- Turner, N.K., Schmidt Patterson, C., MacLennan, D.K., Trentelman, K. (2018). Visualizing underdrawings in medieval manuscript illuminations with macro-X-ray fluorescence scanning. *X-Ray Spectrometry, Special Issue (in press)*.
- Valadas, S., Freire, R., Cardoso, A., Mirão, J., Vandenabeele, P., Caetano, J.O., & Candeias, A. New insight on the underdrawing of 16<sup>th</sup> Flemish-Portuguese easel paintings by combined surface analysis and microanalytical techniques. *Micron*, 85, 15-25.
- Van Olphen, H. (1966). Maya blue: a clay-organic pigment? *Science*, 154(3749), 645-646.
- Van der Weerd, J., Smith, G.D., Firth, S., & Clark, R.J.H. (2004). Identification of black pigments on prehistoric Southwest American potsherds by infrared and Raman spectroscopy. *Journal of Archaeological Science*, 31(10), 1429-1437.
- Van der Werf, I.D., Calvano, C.D., Germinario, G., Cataldi, T.R.I., & Sabbatini, L. (2017). Chemical characterization of medieval illuminated parchment scrolls. *Microchemical Journal*, 134, 146-153.
- Verrecchia, E.P. & Le Coustumer, M-N. (1996). Occurrence and genesis of palygorskite and associated clay minerals in a Pleistocene calcrete complex, Sde Boqer, Negev Desert, Isreal. *Clay Minerals*, 31, 183-202.
- Vitorino, T., Casini, A., Cucci, C., Melo, M.J., Picollo, M., & Stefani, L. (2015). Non-invasive identification of traditional red lake pigments in fourteenth to sixteenth centuries paintings through the use of hyperspectral imaging techniques. *Applied Physics A*, 121(3), 891-910.
- Ward, W.R. (ed.) (2008). *The Grove Encyclopedia of Materials and Techniques in Art*. Oxford: Oxford University Press.
- Welch, S.C. (1985). *India: Art and Culture, 1300-1900*. New York: Metropolitan Museum of Art.

- Welch, S.C., Schimmel, A., Swietochowski, M.L., & Wheeler, M.T. (1987). *The Emperors' Album: Images of Mughal India*. New York: The Metropolitan Museum of Art.
- Welu, J.A. (1987). The sources and development of cartographic ornamentation in the Netherlands. In Woodward, D. (Ed.), *Art and Cartography: Six Historical Essays*. Chicago: University of Chicago Press.
- Wheatley, P. (1954). A curious feature on early maps of Malaya. *Imago Mundi*, 11, 67-72.
- Wheeler, M. (1997). Conservation and mounting of leaves from the Akbarnama. *Victoria & Albert Museum Conservation Journal*, 24, 14-18.
- Williams, P.A. & Phillips, G.O. (2009). Gum arabic. In Phillips, G.O. & Williams, P.A. (Eds.), *Handbook of Hydrocolloids (2<sup>nd</sup> Edition)*. Cambridge: Woodhead Publishing Limited.
- Winters, R., Hume, J.P., & Leenstra, M. (2017). A famine in Surat in 1631 and Dodos on Mauritius: a long lost manuscript rediscovered. *Archives of Natural History*, 44(1), 134-150.
- Wolters, M. (2012). Drawing → underdrawing → painting: compositional evolution in the working process of Joachim Beuckelaer. *Journal of Historians of Netherlandish Art*, 4(2).
- Wongwad, E., Jimtaisong, A., Saewan, N. & Krisadaphong, P. (2012). Preparation of lake pigment from Thai lac dye. *IPCBE*, 34, 73-78.
- Woodward, D. (2007). Cartography and the Renaissance: Continuity and Change. In Woodward, D. (Ed.), *The History of Cartography, Vol. 3. Cartography in the European Renaissance. Part I*. Chicago: University of Chicago Press.
- Wouters, J. (1985). High performance liquid chromatography of anthraquinones: analysis of plant and insect extracts and dyed textiles. *Studies in Conservation*, 30(3), 119-128.
- Wouters, J., Grzywacz, C.M., & Claro, A.A. (2011). Comparative investigation of hydrolysis methods to analyze natural organic dyes by HPLC-PDA. *Studies in Conservation*, 56, 231-249.
- Županov, I.G. (2005). *Missionary Tropics: the Catholic frontier in India (16<sup>th</sup>-17<sup>th</sup> centuries)*. Ann Arbor: University of Michigan Press. 216-218.



## APPENDIX I: TOPONYMS AND REPRODUCTIONS OF BPE MAPS

### I.1: TOPONYMS AND MODERN NAMES OF REGIONS DEPICTED IN THE MAPS

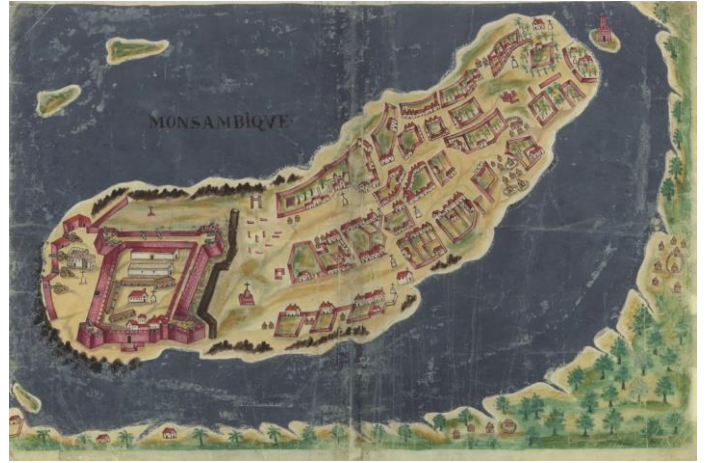
	Country or Region	Name in Map	Portuguese Name	Modern Name
1	Mozambique	Sofala	Sofala	Beira
2	Mozambique	Monsambique	Moçambique	Mozambique (Fort of Saint Sebastian)
3	Kenya	Mombaca	Mombaça	Mombasa (Fort Jesus)
4	Oman	Coriate	Curiate, Cidabo	Qurayat
5	Oman	Mascate	Mascate	Muscat
6	Oman	Matara	Matará	Mutrah
7	Oman	Sibo	Sibo	As Sib
8	Oman	Borca	Borca	Birka
9	Oman	Soar	Soar	Sohar
10	United Arab Emirates	Corfacam	Corfação	Khawr Fakkân
11	United Arab Emirates	Qvelba	Quelbá	Kalba
12	United Arab Emirates	Libedia	Libédia	al-Bidyah
13	Oman	Mada	Madá	Madhah
14	United Arab Emirates	Doba, Dvbo, Mocombi	Dobá, Dubo, Mocombi	Diba al Hisn, Dubo, Mocombi
15	North India	Dio	Diu	Diu
16	North India	Damaõ, Forte Sam Irm <sup>o</sup>	Damão, São Jerónimo	Daman
17	North India	Samgês, Danv	São Gens, Danu	Sanjan, Dahanu
18	North India	Chichana, Tarapor	Tarapor	Tarapur
19	North India	Maim, Sirgam	Maim, Sirgão	Shirgaon, Mahim-Kelve
20	Goa	Manora, Agaçaim	Manorá and Agaçaim	Agaçaim
21	North India	Sera de Aserim	Serra de Asserim	Asherigad
22	North India	Baçaim	Baçaim	Vasai Fort
23	North India	Tana	Tana	Thane
24	North India	Mombaim, Ilha de Carania	Mombaim, Ilha de Carania	Mumbai, Karanja
25	North India	Moro de Chavl	Morro de Chaul	Korlai Fort
26	North India	Chavl	Chaul	Chaul (Revdanda Fort)

27	Goa	Agoada, Bardes, Divar, and Choraõ	Aguada, Bardês, Divar, and Chorão	Aguada, Bardez, Divar, Chorão
28	Goa	Mormvgaõ, Rachol, Salsete	Mormugão, Rachol, and Salcete	Mormugão, Rachol, Salcete
29	Meridional India	Cambolim	Cambolim	Coondapoor
30	Meridional India	Barcalor	Barcelor	Basrur
31	Meridional India	Mangalor	Mangalor	Mangaluru
32	Meridional India	Cananor	Cananor	Kannur
33	Meridional India	Cranganor	Cranganor	Kodungallor (fortress now called Kottappuram Fort)
34	Meridional India	Cochim	Cochim	Kochi
35	Meridional India	Covlam	Coulão	Kollan
36	Sri Lanka	Manar	Manar	Mannar
37	Sri Lanka	Negvmba	Negumbo	Negombo
38	Sri Lanka	Calitvre	Calituré	Kalutara
39	Sri Lanka	Gvale	Gale	Galle
40	Sri Lanka	Bahia de Tanavare	Baía de Tanavare	<i>Not found</i>
41	Sri Lanka	Bahia de Beligaõ em Seilaõ	Baía de Beligão	Weligama
42	Sri Lanka	Batecalov	Batecalou	Batticaloa
43	Sri Lanka	Triqvilimale	Triquinimale	Trincomalee
44	Sri Lanka	Iafanapatam	Jafanapatão	Jaffna Patnam
45	Meridional India	San Tome	São Tomé de Meliapor	Mylapore
46	Malaysia	Malaca	Malaca	Malacca
47	China	Macao	Macau	Macao
48	Indonesia	Solor	Solor	Solor

## I.2: MAPS OF THE ÉVORA CODEX



(1) Sofala



(2) Monsambique



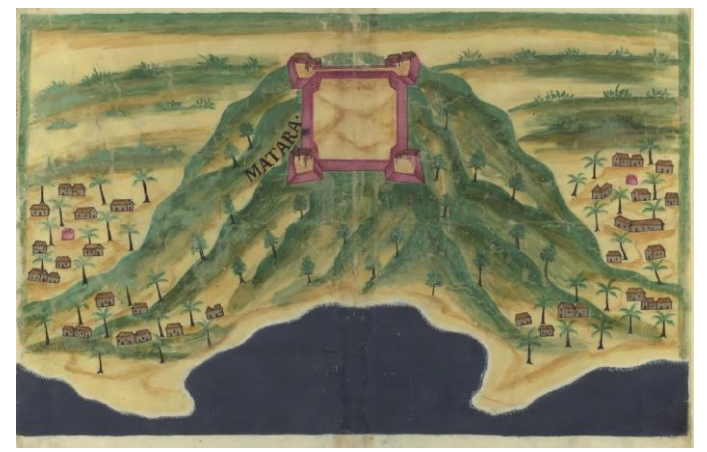
(3) Mombaça



(4) Coriate

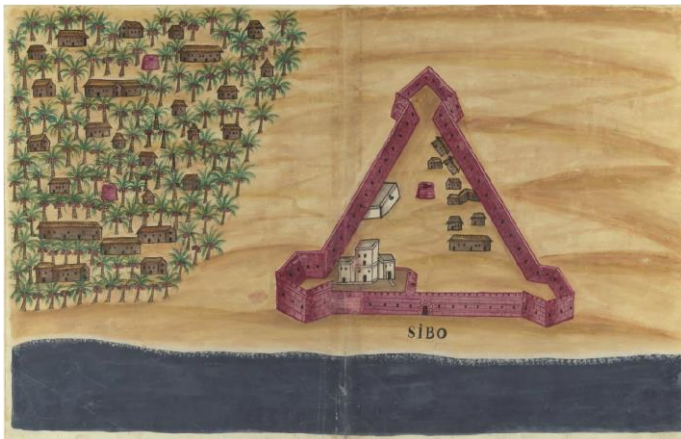


(5) Mascate



(6) Matara





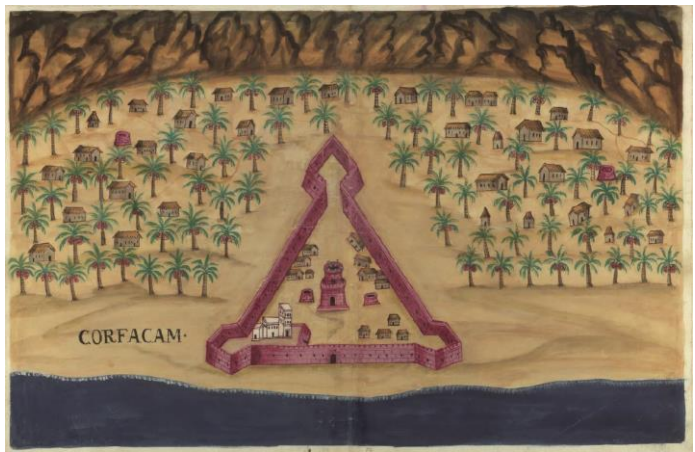
(7) Sibo



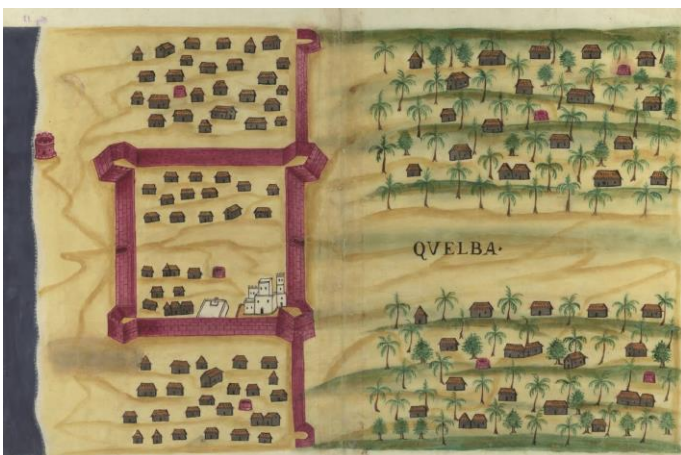
(8) Borca



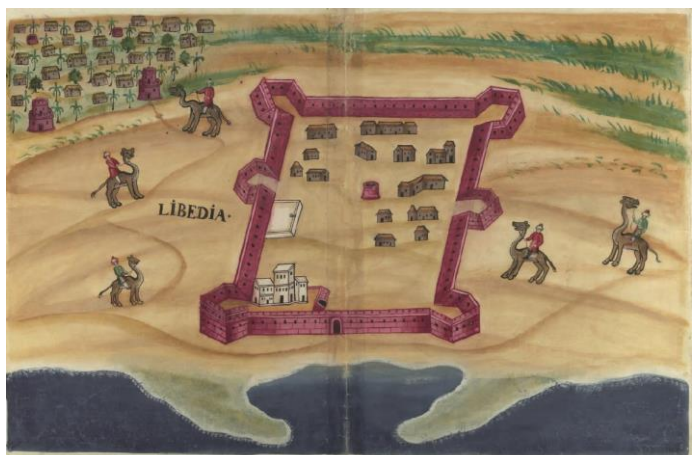
(9) Soar



(10) Corfacam

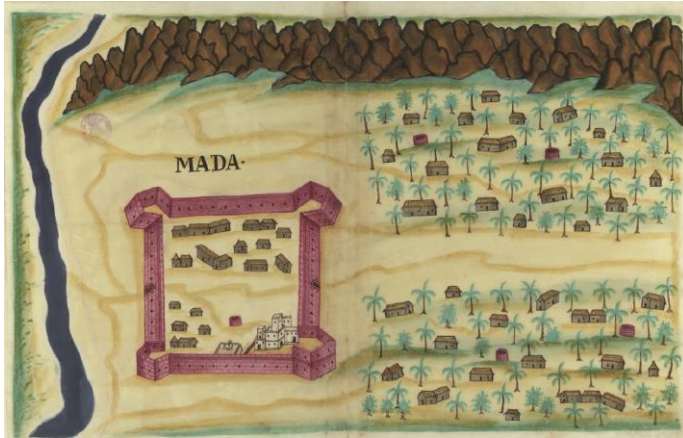


(11) Quelba



(12) Libedia





(13) Mada



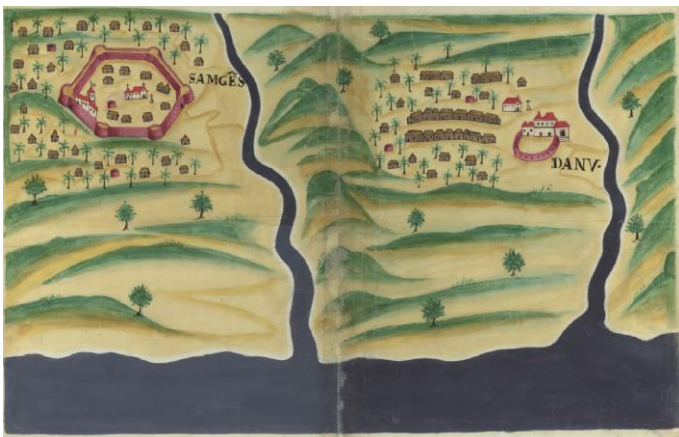
(14) Dubo, Doba, and Mocombi



(15) Dio



(16) Damao



(17) Samges and Danu

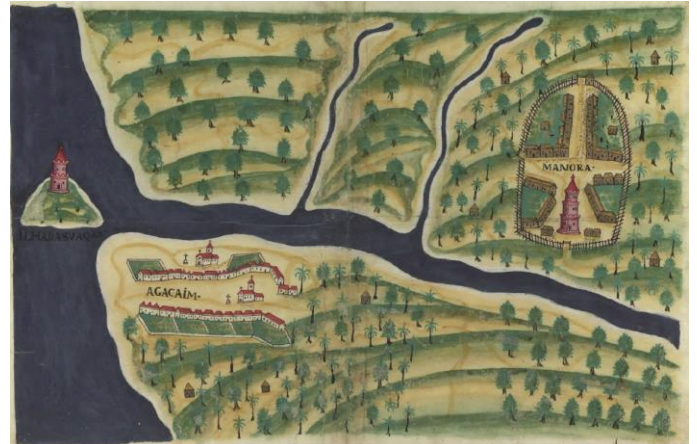


(18) Tarapor and Chichana





(19) Sirgam and Maim



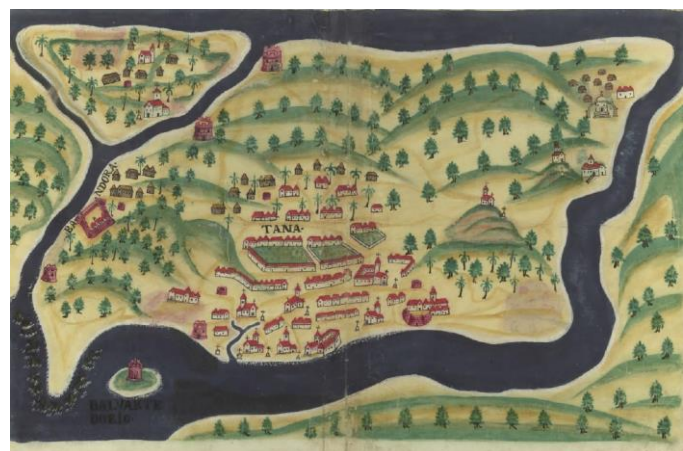
(20) Agaçaim, Manora, and Ilha das Vaças



(21) Sera de Aserim



(22) Baçaim



(23) Tana and Bandora



(24) Mombaim and Ilha de Carania





(25) Moro de Chaul



(26) Chaul



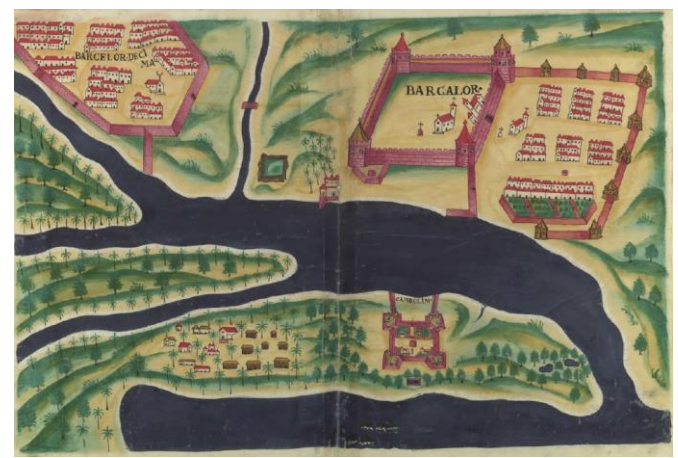
(27) Agoada, Bardes, Divar, and Choraõ



(28) Mormgaõ, Rachol, and Salsete



(29) Cambolim

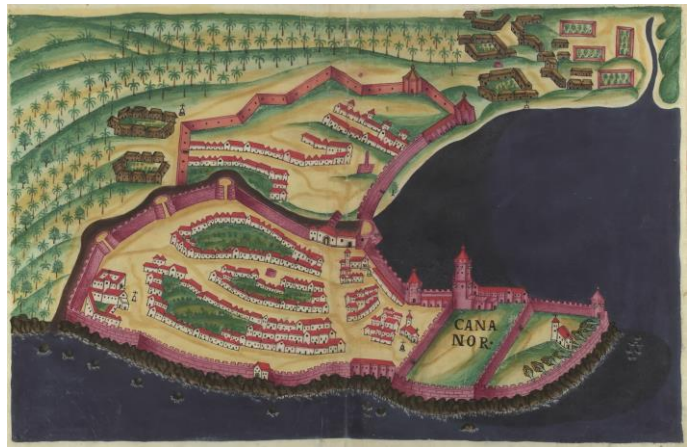


(30) Barçalor and Barçalor de Cima

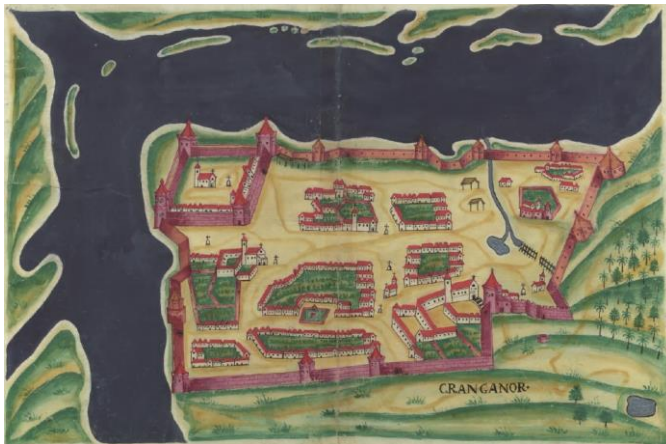




(31) Mangalor, Banguel, and Olala



(32) Cananor



(33) Cranganor



(34) Cochim



(35) Coulam

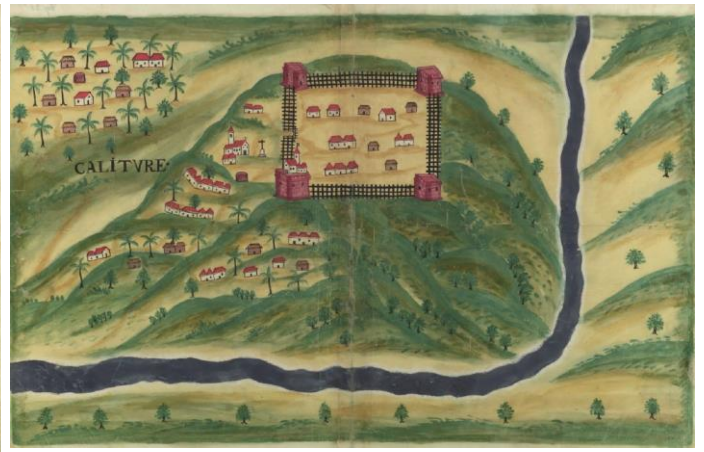


(36) Manar





(37) Negumbo



(38) Calitvre



(39) Guale



(40) Bahia de Tanavare



(41) Bahia de Beligaõ em Seilaõ



(42) Batecalou

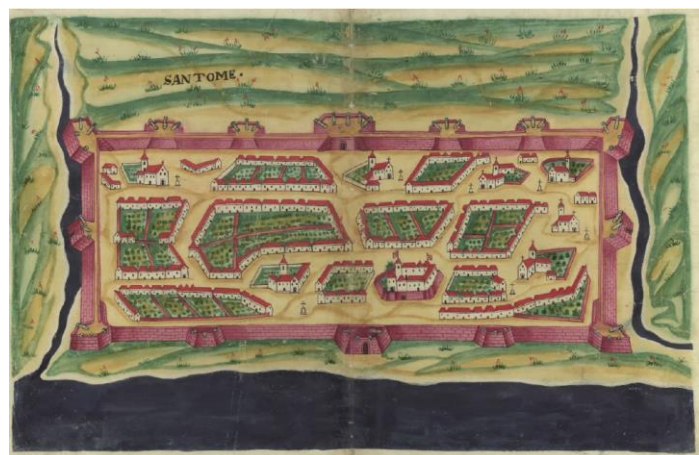




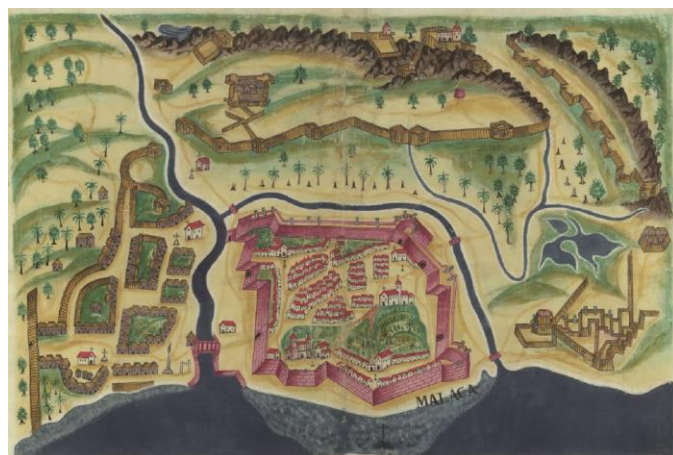
(43) Triquilimala



(44) Jafanapatam



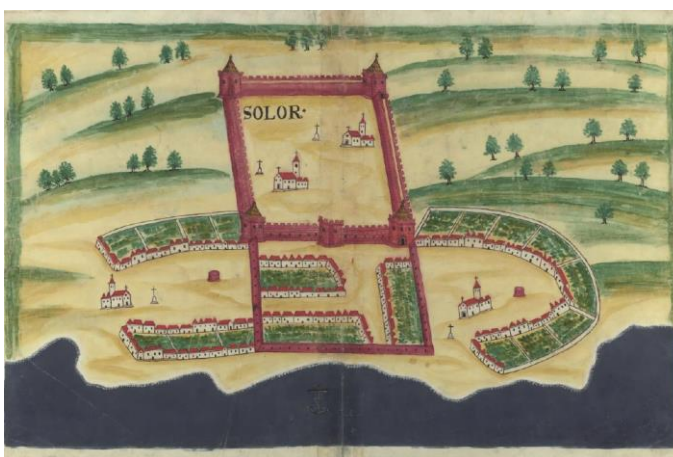
(45) San Tome



(46) Malacca



(47) Macao



(48) Solor



## APPENDIX II: MATERIALS AND METHODS

II.1: Identification and naming of measurement spots

II.2: Technical photography (UVF-IV, NIR)

II.3: Handheld digital microscopy

II.4: Colorimetry

II.5: FORS and reference mockups

II.6: h-XRF spectrometry

II.7: Raman microscopy

II.8: Microsampling

II.9:  $\mu$ -FT-IR

II.10: VP-SEM-EDS

II.11: LC-DAD-MS

### II.1 IDENTIFICATION AND NAMING OF MEASUREMENT SPOTS

While technical photography and examination on the light box allowed collection of information across the entire map, the remaining instrumental techniques were restricted to smaller regions. To specify the areas of analysis, a numbering system was established while performing colorimetry. During FORS and XRF analyses, supplemental spots were added to clarify questions raised by the previous analyses. These are identified by the prefix F or X (respectively), then an abbreviated map name, and then a number. Thus, for example, a spot added during the FORS analysis to the map of Dio would be referred to in the body of the text as Di.F.1. Because of the limitations posed by the geometry of the Raman microscope, it was not possible to access some of these regions previously studied by colorimetry, FORS, or XRF. Substitute spots used in the Raman investigation are identified by the abbreviated map name, the prefix R, and a number. FORS and XRF analyses on the unpainted paper margins of the maps are simply noted as verso or recto, with a reference to the map name. The locations of these analyses are indicated on the maps below without annotation. Lastly, locations of sampling are marked and numbered, with the prefix S. When an analysis was performed *in situ* on a region that was subsequently selected for microsampling, this parameter is noted in the presented spectrum.

II.1.1: Baçaim (Ba.)



II.1.2: Chaul (Ch.)





II.1.3: Cochim (Co.)



II.1.4: Damaõ (Da.)





Il.1.5: Dio (Di.)



Il.1.6: Mangalor (M.)





II.1.7: Sera de Aserim (SA.)



## II.2: TECHNICAL PHOTOGRAPHY

Technical photography was undertaken on the maps of 'Baçaim,' Chaul, 'Cochim,' 'Damaõ,' 'Dio,' 'Mangalor,' 'Moro de Chaul,' 'Salsete,' and 'Sera de Aserim.' The results are presented as the photographs themselves (Chapter 7 and in Appendix III.3) and as a summary of observations (Chapter 7). Visible light photography was not undertaken, as the maps have already been digitalized by the Évora Public Library (<http://purl.pt/27184>). Infrared transparency was scored by visually determining the maximal and minimal transparency found in the maps and assigning ranks for those between them. While these rankings are subjective, they offer a rough description of the overall results. Synopsis of the color changes observed in UVF-IV is descriptive, with the intention of capturing the full range of alteration.

UVF-IV: A Nikon D3100 14.2MPx digital single reflex (DSLR) camera with a 10.0-55.0mm f/3.5-5.6 lens was used in conjunction with a Hoya 77 filter (<http://www.microglobe.co.uk/hoya-77mm-uv-ir-cut-screw-in-glass-filter-p-9991.html>). The camera was modified to acquire full-spectrum images. Images were acquired in RAW mode with an exposure time of ten seconds to improve fluorescence detection. The ultraviolet radiation source was 2 Labino® MPXL UV PS135 lamps (35W PS135 UV Midlight 230V) with built-in filters for 310 nm-400 nm (peak at 365 nm). To ensure the safety of the maps during the investigation, the lamps were held at a distance of 3 meters from the painted surface at an approximately 45 degree angle, and the maps were only illuminated for the time required to acquire the image.

NIR: A Nikon D3100 14.2MPx digital single reflex (DSLR) camera with a 10.0-55.0mm f/3.5-5.6 lens modified to acquire full-spectrum images was used in combination with an X-Nite 780 filter (77 mm diameter, 2.3 mm thickness) with a 780 nm cutoff at 50% and an 850 nm passband of > 99%.

### II.3: HANDHELD DIGITAL MICROSCOPY

Two Dino-Lite handheld digital microscopes with DinoCapture 2.0 software were used to acquire a total of 1381 magnified images from the maps of 'Baçaim,' Chaul, 'Cochim,' 'Damaõ,' 'Dio,' 'Mangalor,' and 'Sera de Aserim.' A Dino-Lite Premier AM7013MZT4 (with magnification of 430x-435x) was used to observe the texture and behavior of the paints, as well as to explore areas in which mixtures and overlays were suspected to be present. A Dino-Lite Premier AM413-FVW (with magnification of 20x-200x) was used to document the extent of underdrawing in the maps, as well as to elucidate the sequence in which the various aspects of the maps were colored. Microscopic images may be found in Chapter 6, as well as in Appendix III.2 and as supportive data in the table of complex mixtures in Appendix III.7.

### II.4: COLORIMETRY

Non-invasive measurement of the chromatic palette was taken *in situ* of a total of 108 points on the maps of 'Baçaim,' Chaul, 'Cochim,' 'Damaõ,' 'Dio,' 'Mangalor,' and 'Sera de Aserim.' The colorimetric data was acquired after calibration with black and white standards, and the SCE (matte) setting was used. Three measurements of each point were taken to ensure representativeness of color. The data was recorded using the DataColor CheckPlusII (Lawrenceville, NJ), using an aperture size UXAV (2.5mm). The colorimetric measurements were taken in the CIE  $L^*a^*b^*$  chromatic space as defined by the International Commission on Illumination, and the results reflect readings of three parameters: lightness ( $L$ , 0-100), position on the red-green axis ( $a$ ; the higher the value, the more red the color is), and position on the yellow-blue axis ( $b$ ; the higher the value, the more yellow the color is). Colorimetric data is presented as a scatterplot of  $a^*$  and  $b^*$  coordinates in chapter 7 and in full in Appendix III.4.

### II.5: FORS & MOCKUPS FOR COMPARISON OF SPECTRAL PROFILES

Fiber optic reflectance spectroscopy was performed *in situ* on 82 points in the maps 'Baçaim,' Chaul, 'Cochim,' 'Damaõ,' 'Dio,' 'Mangalor,' and 'Sera de Aserim.' The analyses were performed with the aid of an Lr1-T v.2 compact spectrometer (ASEQ instruments) with a 50  $\mu$ m slit. The instrument has a spectral range of 300-1000 nm and a spectral resolution of less than 1 nm. The spectra were recorded on ASEQ CheckTR software. Each spot was measured three times to ensure consistency of results, and representative spectra are reported in Chapter 8 and Appendix III.5. Calibration prior to measurements was made using Whatman filter paper. To avoid oversaturation (i.e., reflectance exceeding 100%), particularly in the near-infrared region, exposure times were varied based on color. For blues, an exposure time of 200 milliseconds was used; for pale yellows, beiges, and whites, 130 milliseconds; and for all remaining colors, 150 milliseconds.

To facilitate identification of pigments in the maps, the FORS spectra were compared with the spectra of mockups of pigments and mixtures (taken on the same equipment, with the same parameters). The mockups were created by Whitney Jacobs for an Erasmus Mundus Master in Archaeological Materials Science thesis under the supervision of Dr. Catarina Miguel in 2016. The pigments and binder were purchased from Kremer Pigments. The gum Arabic binder was prepared in a 10% solution (by weight) in water. The parchment support was acquired from the Musée de Parchemin in Rouen, France. The ratio of pigment to binder for the mockups was 1:4 (by weight).

FORS spectra can be found in Chapter 8 and in Appendix III.5.

## II.6: h-XRF

A Bruker tracer III-SD handheld X-ray fluorescence spectrometer was used to record elemental information for paints on the maps of 'Baçaim,' Chaul, 'Cochim,' 'Damaõ,' 'Dio,' 'Mangalor,' and 'Sera de Aserim.' The device is equipped with a 10 mm<sup>2</sup> Xflash<sup>®</sup> SDD, an Rh target (maximum voltage 40 kV), and a Peltier-cooled detector (typical resolution: 145 eV at 100,000 cps). Analyses were performed at 40 kV and 12.5 µA without the use of a filter, with an acquisition time of 90 seconds. The spectrometer was positioned on a tripod at approximately 2 mm from the painted surface to make a total of 129 measurements. The spectra were collected with S1PXRF software and interpreted using ARTAX software. XRF results can be found in Chapter 8 and Appendix III.6.

### *Data processing and interpretation of results*

The counts for each element were first normalized against the rhodium K-lines. Considering the thinness of the paint layers, the likelihood of contribution from the three layers of paper behind them was high. Spectra from each of the individual papers (original paper support, Japanese paper, modern cardboard backing) were recorded to attempt to understand the nature and extent of this contribution. The counts of each element present in the original paper support were averaged across the maps, and then subtracted from the counts for the corresponding element detected in the painted spots.

An alternative approach would have been to subtract the counts from the paper from the counts for a spot painted on that paper; for example, subtracting the counts of aluminum detected on the 'Mangalor' map recto sheet from the counts of aluminum detected in a red that was painted on the 'Mangalor' map recto sheet. However, considering the relatively homogeneous nature of the elements detected in the papers, and the possibility that the thickness of the surface coating or glue below (and therefore, elemental counts) varied randomly across space, it was determined that an average would better capture this contribution overall. This subtraction procedure risks excluding elements that are truly present in the pigment; it tends to yield incomplete data but with fewer "false positives". Thus, the absence or presence of a minor element in a given color from one map to the other is not treated necessarily as compelling evidence of a true difference in the pigments.

Another important factor in the XRF results relates to spot size. As the h-XRF measurements were taken without making direct contact with the maps, the area of analysis sometimes extended beyond the color region of interest, causing a

contribution of adjacent pigments. The uncertainties remaining after the handheld XRF analyses were addressed by the use of additional analytical techniques including Raman microscopy,  $\mu$ -FT-IR, and VP-SEM-EDS.

## II.7: RAMAN MICROSCOPY

Raman microscopy was performed both *in situ* and on microsamples of the maps of 'Cochim,' 'Dio,' 'Damaõ,' and 'Mangalor.' An Xplora (HORIBA) Raman spectrometer with a 28 mW diode laser (operating at 785 nm) and Olympus microscope was used. The laser was focused by an Olympus 50x lens and 10% of the laser power was applied to the painted surface. An exposure time of 5 seconds with 5 accumulations was used. The spectra were acquired for the region of 100-2000  $\text{cm}^{-1}$ . Raman spectra can be found in Chapter 8 and in Appendix III.8.

## II.8: MICROSAMPLING

Microsamples of pigments and paper were removed from the maps of 'Cochim,' 'Dio,' 'Damaõ,' and 'Mangalor' from regions at which paint loss had already occurred, or in the case of the paper, from the edge of the page. The microsamples from 'Cochim,' 'Dio,' and 'Mangalor' were extracted by Dr. Catarina Miguel. The microsamples from 'Damaõ' were extracted after extensive observation and training by Sima Krtalic. The samples were removed with microchisels from Ted Pella micro tools with the aid of a LEICA M205C stereomicroscope (magnification range 7.8-160x) complemented by a Leica DFC295 camera and an external fiber optic light source. The regions from which samples were extracted are noted in light green in AP II.1.

## II.9: $\mu$ -FT-IR

Infrared spectra were acquired in transmission mode from microsamples of the maps of 'Cochim,' 'Dio,' 'Damaõ,' and 'Mangalor.' A Hyperion 3000 (Bruker) infrared spectrometer with a single point MCT detector, liquid nitrogen cooling system, and 15x objective lens was used. The microsamples were pressed and mounted in S.T. Japan diamond anvil compression cells to enable analysis. The spectral range of the analyses was 4000-650  $\text{cm}^{-1}$ , with a resolution of approximately 4  $\text{cm}^{-1}$ . The quality of the spectra was found to be adversely affected by the very small size of the microsamples. The spectra were analyzed using OPUS/Mentor software (version 6.5). Background spectra were taken prior to each analysis to minimize the influence of ambient atmospheric water vapor and carbon dioxide on the measurements. Infrared spectra are presented in Chapter 8 and in Appendix III.9.

## II.10: VP-SEM-EDS

VP-SEM-EDS analyses were performed on microsamples from the maps of 'Cochim,' 'Dio,' 'Damaõ,' and 'Mangalor.' A variable pressure scanning electron microscope (HITACHI 3700N) paired with an energy dispersive X-ray spectrometer (Bruker Xflash 5010 SDD EDS) was used. The uncoated samples were analyzed at an atmospheric pressure of 40 Pa. The paper microsample was examined with an acceleration voltage of 15-20 kV, and the paint microsamples with a voltage of 20 kV. SEM images were acquired in backscattering mode. The resolution of the EDS spectra at the Mn  $K\alpha$  line is 123 eV.



The EDS spectra were analyzed using Esprit 1.9 software (Bruker). SEM images can be found in chapters 5 and 8, and EDS spectra can be consulted in Appendix III.10.

## II.11: LC-DAD-MS

Dark pink microsamples Co.S.5 and M.S.2 were combined for analysis by high performance liquid chromatography with an autosampler coupled to photodiode array (DAD) and mass spectrometry detectors (MS). An LCQ Fleet Thermo Finnigan mass spectrometer with an electrospray ionization source and ion trap mass was used. The analytical column used was a reversed phase Zorbax E Zorbax Eclipse XDB C<sub>18</sub> (Narrow-Bore, particle size 3.5  $\mu\text{m}$ , 150 mm  $\times$  2.1 mm). The analysis was kindly performed by Ana Manhita of Hercules Laboratory.

The extraction procedure followed the methodology proposed by Wouters et al. (Wouters et al. 2011). Sample extraction was performed over four hours with 200  $\mu\text{L}$  of hydrochloric acid solution, lyophilized, and then re-dissolved in 50  $\mu\text{L}$  of methanol mixed with water (1:1 v/v). The supernatant was collected following centrifuging and injected into the LC-DAD-MS system. A lac dye standard from Kremer Pigments was injected into the system for comparison after being dissolved in ultrapure water and filtered through a .45  $\mu\text{m}$  PTFE syringe filter.

MS analysis was performed with a capillary temperature of 300 degrees C, a source voltage of 5.0 kV, a source current of 100.0  $\mu\text{A}$ , and a capillary voltage of -17.0 V. Negative ion mode was used. Analytes from the pink microsample were detected in SIM mode with m/z 329, 491, and 536 selected. For the lac dye standard, SRM mode was selected (m/z 536  $\rightarrow$  492, 30.0% normalized collision energy). The column temperature was set to 30 degrees C and tray temperature 24 degrees C. Chromatographic separation was performed with a mobile phase at a flow rate of 0.2 mL min<sup>-1</sup>. The mobile phase consisted of 0.1% (v/v) formic acid solution (A) and acetonitrile (B) using the following elution program: linear gradient from 0 to 63% of solvent B (0–14 min) and from 63 to 90% of solvent B (14–25 min); isocratic with 90% of solvent B (25–30 min). 20  $\mu\text{L}$  of sample was injected. The DAD detector was programmed to scan from 200 to 800 nm.

## APPENDIX III: EXPANDED RESULTS, ORGANIZED BY INSTRUMENTAL TECHNIQUE

III.1: Images of maps illuminated from below (using the lightbox)

III.2: Handheld digital microscopic documentation of paint textures

III.3: Technical photography (by map; visible light photographs copyright Biblioteca Pública de Évora)

III.4: Colorimetric coordinates in CIE-LAB color space (organized by color)

III.5: FORS spectra

III.6: h-XRF elemental data presented for elements of interest in arbitrary units following the data treatment described in Appendix II.6.

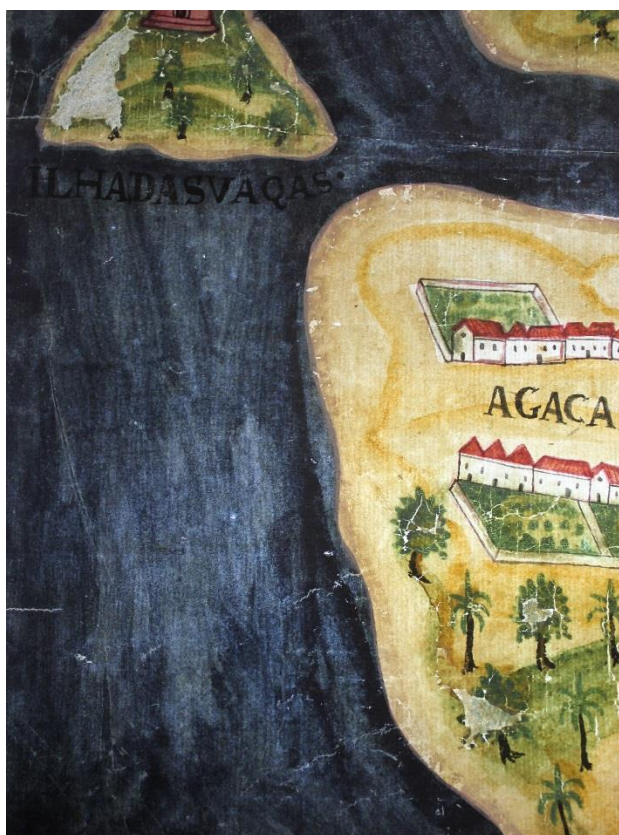
III.7: Inference of mixtures

III.8:  $\mu$ -Raman spectra (organized by color)

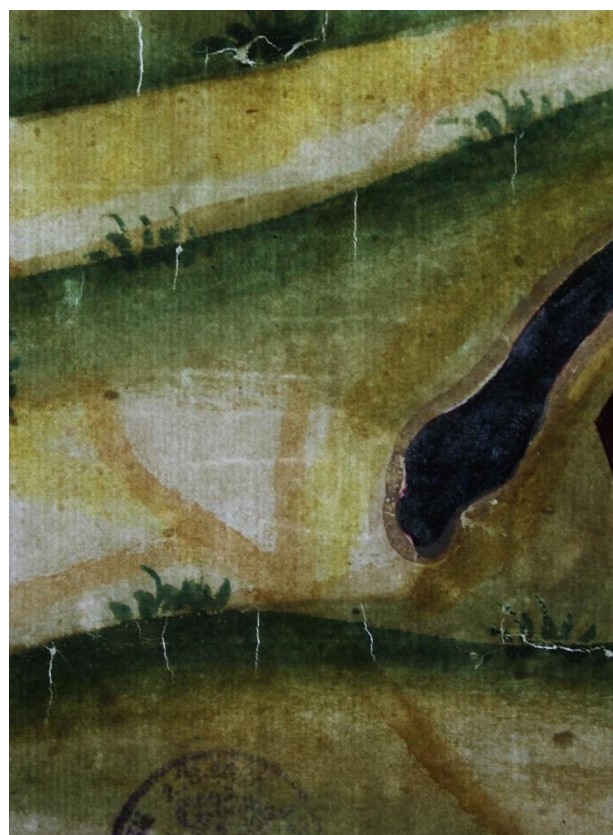
III.9:  $\mu$ -FT-IR spectra

III.10: EDS spectra

### III.1: SUPPLEMENTAL PHOTOGRAPHS OF MAPS ILLUMINATED FROM BELOW USING THE LIGHTBOX



Map of 'Agaçaim' and 'Manora'

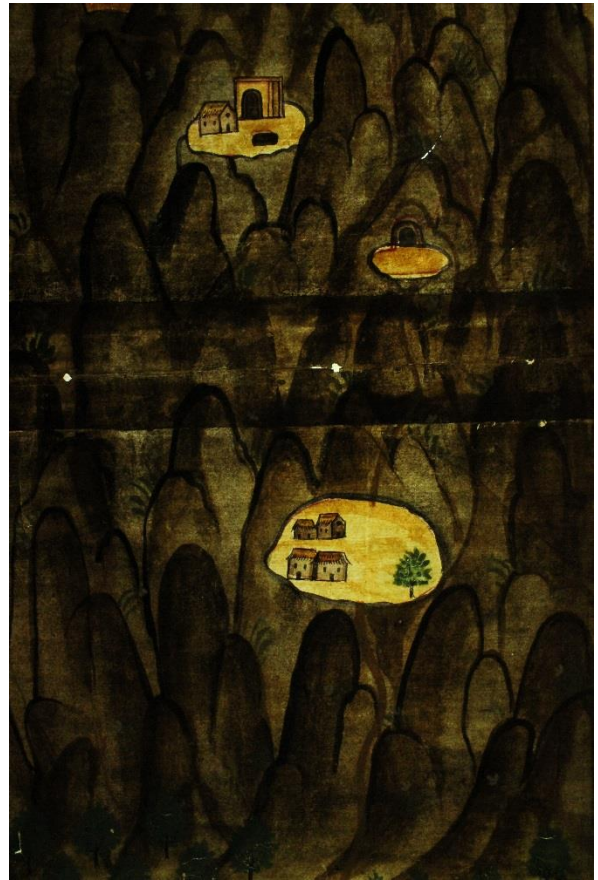


Map of 'Baçaim' (showing faint watermark in the center of the image).





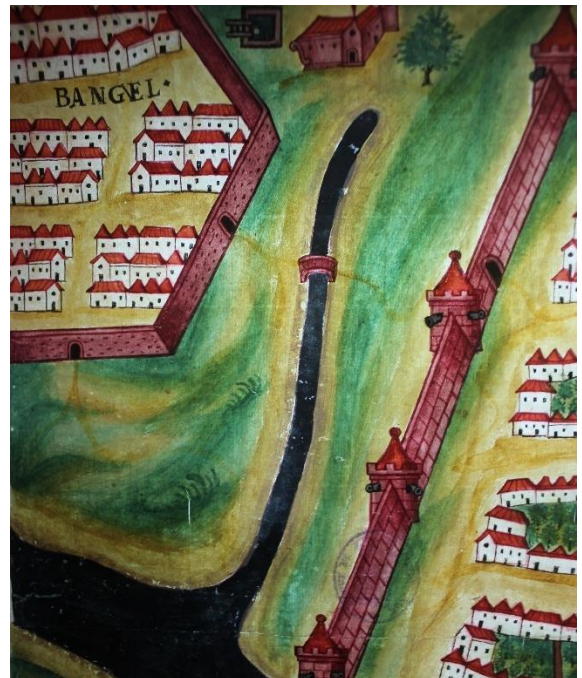
Map of 'Sera de Aserim'



Map of 'Sera de Aserim'



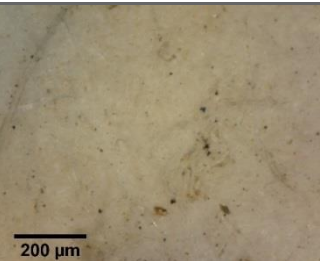
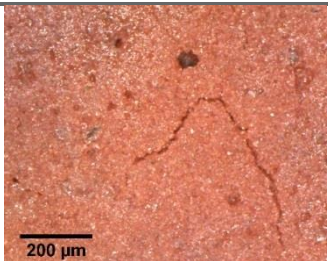
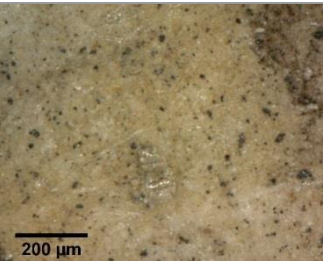
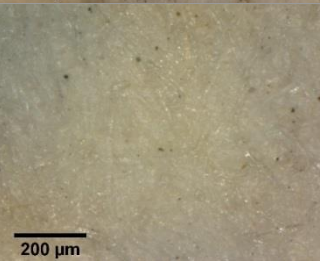
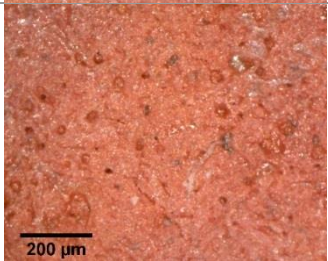
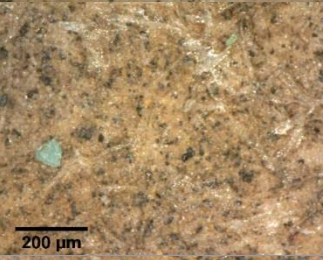
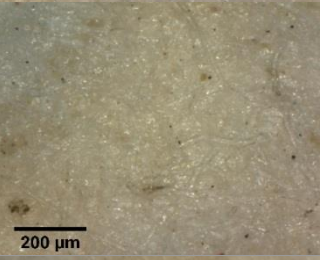
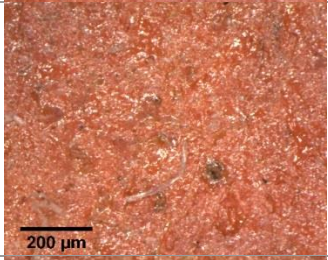
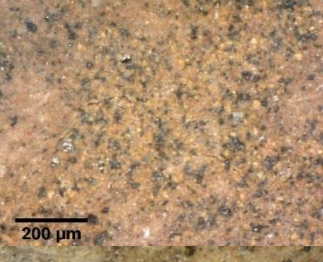
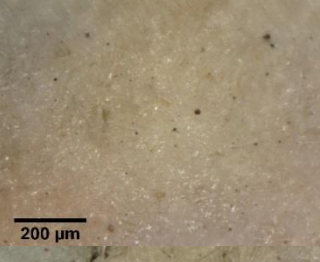
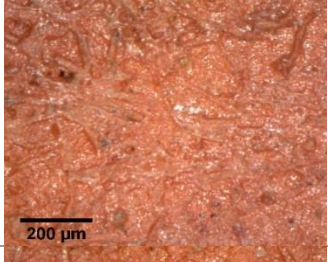


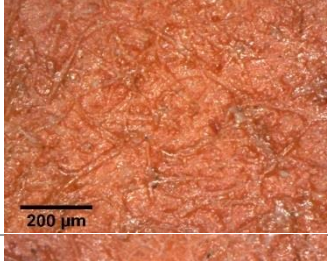
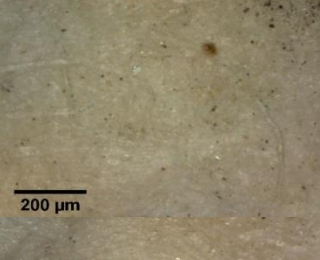
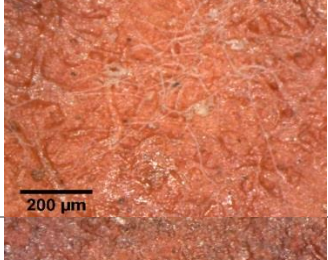
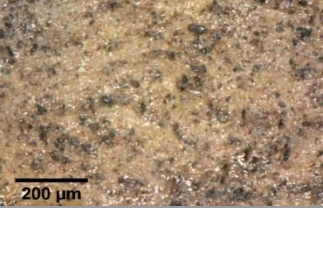
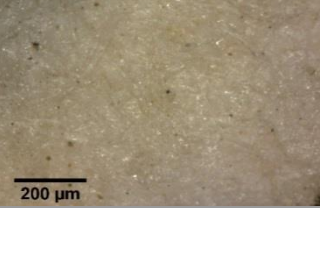
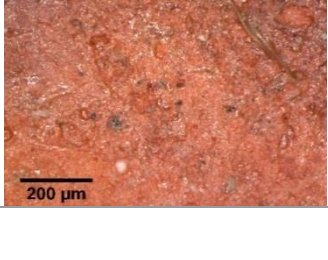
Map of 'Dio



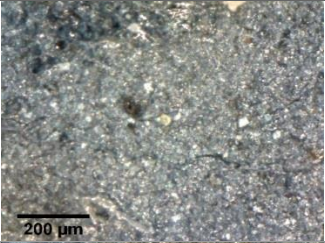
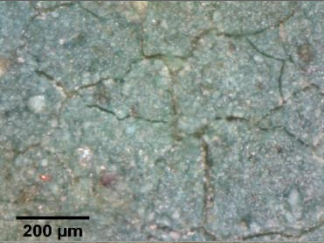
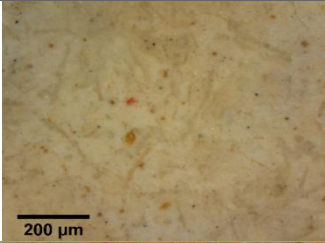
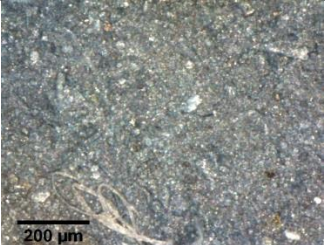
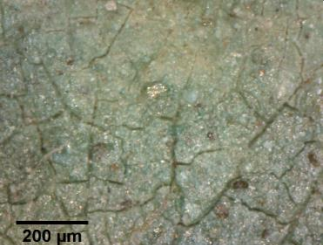

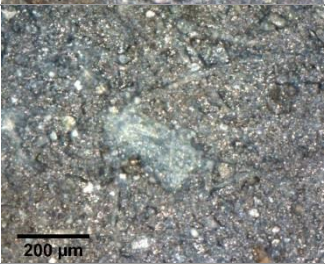
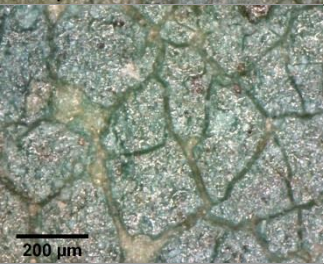
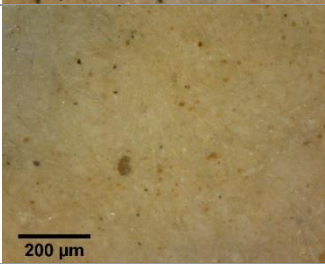
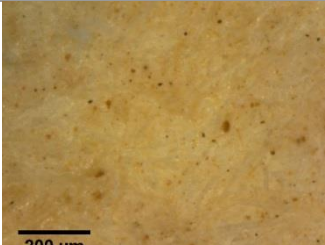
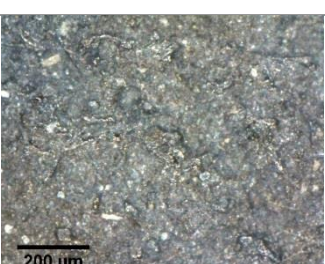
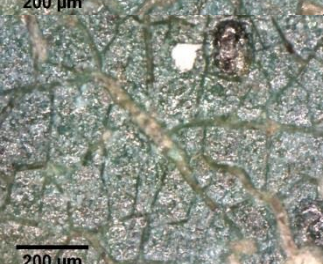


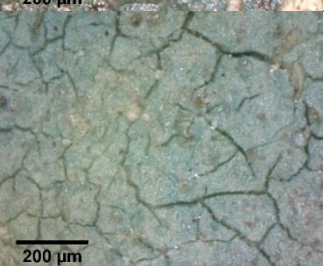
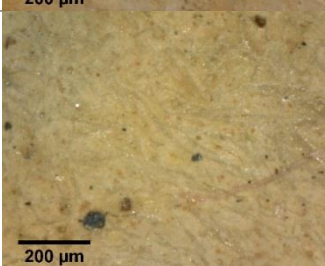



Map of 'Mangalor'



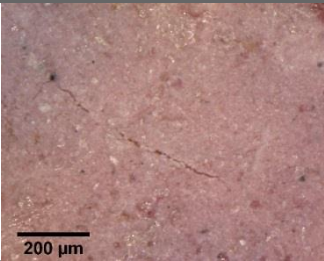
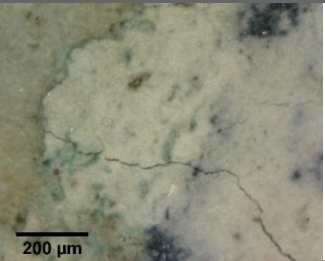
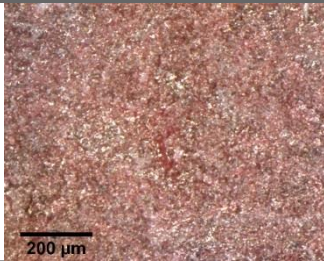
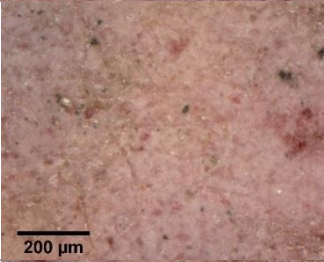
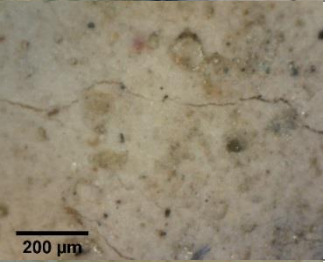
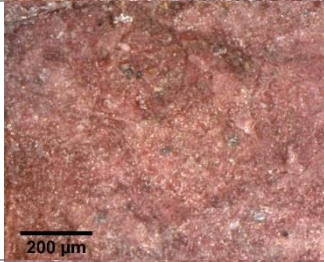
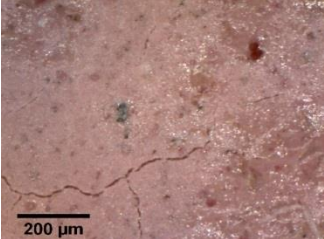


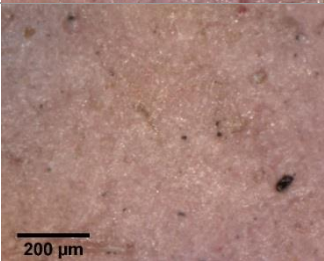

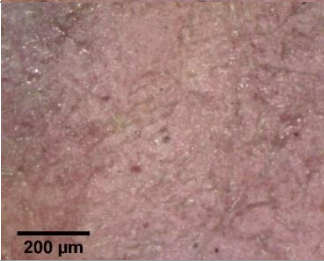
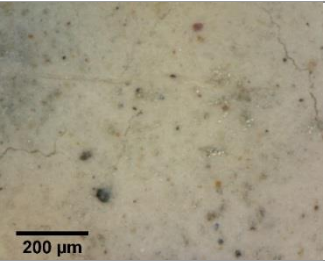
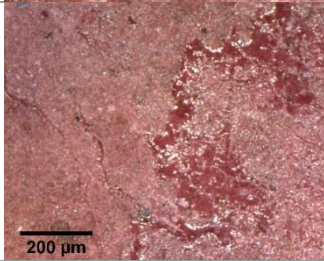
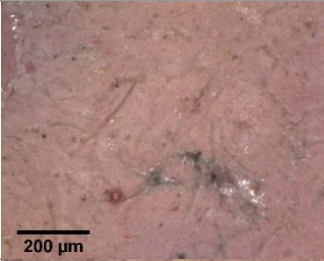
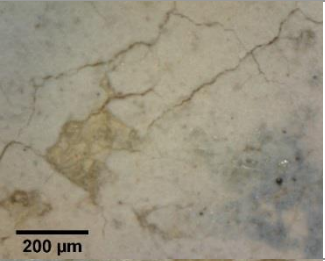
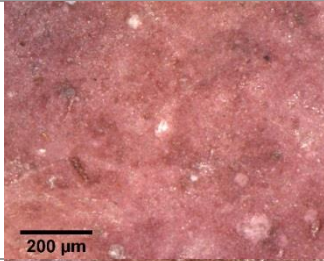
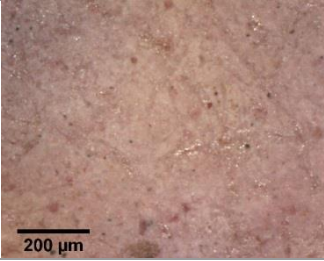
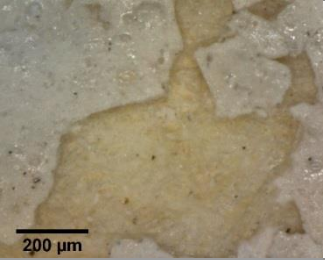

### III.2: DIGITAL MICROSCOPIC IMAGES OF PAINT TEXTURES

Map name	Brown walls	White walls	Red Roof
Dio	Not applicable.		
Damaõ			
Baçaim			
Sera de Aserim			
Cochim			
Mangalor	Not applicable.		
Chaul			



Map name	Medium blue water	Dark green trees	Beige terrain
Dio			
Damaõ			
Baçaim			
Sera de Aserim	Not applicable.		
Cochim			
Mangalor			
Chaul			

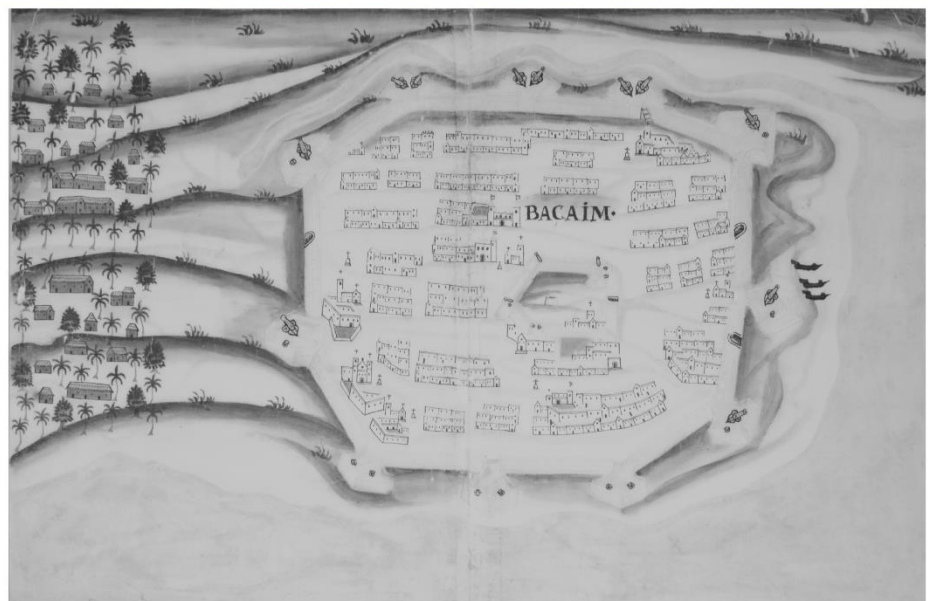


Map name	Light pink buildings		Dull white beach		Dark pink buildings
Dio					
Damaõ					
Baçaim					
Sera de Aserim			Not applicable.		
Cochim					
Mangalor					
Chaul					



### III.3: TECHNICAL PHOTOGRAPHY

III.3.1-2: 'Baçaim'





III.3.3-4: Chaul



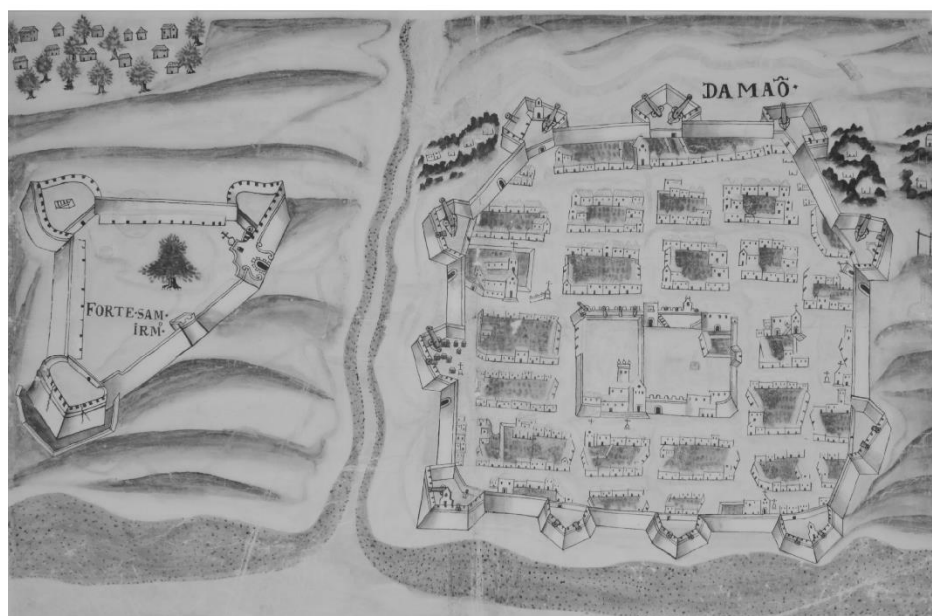
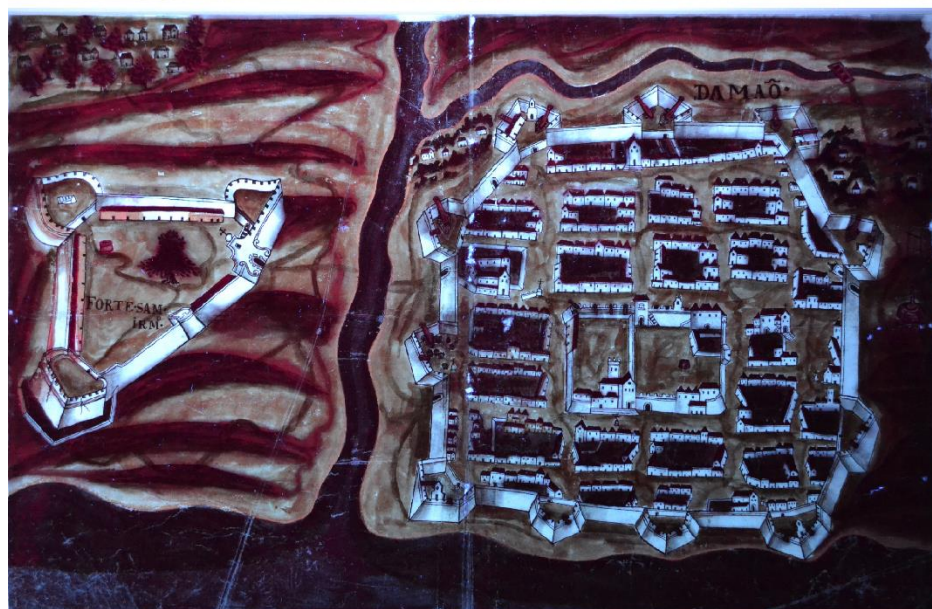


III.3.5-6: 'Cochim'



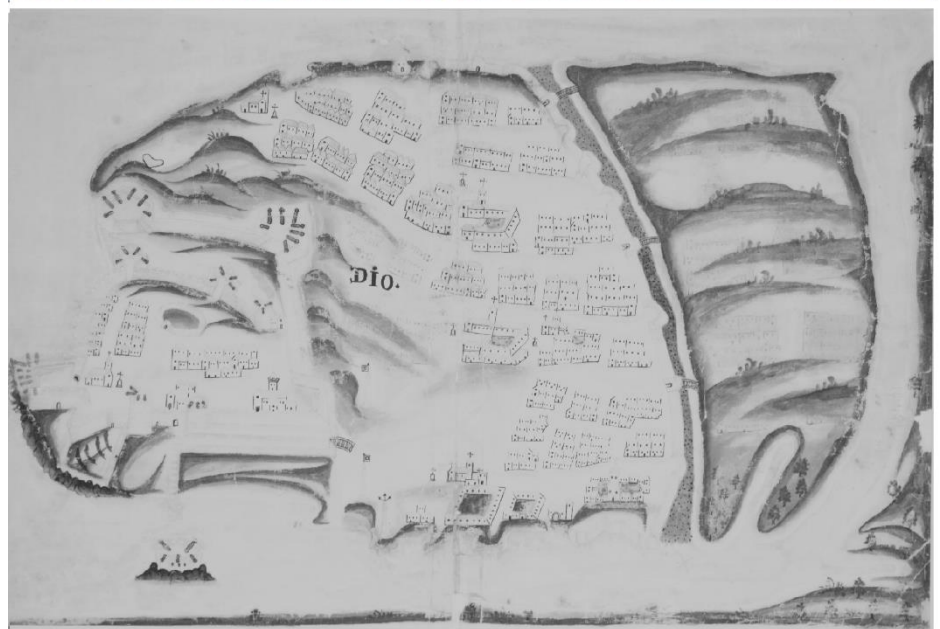


III.3.7-8: 'Damaõ'



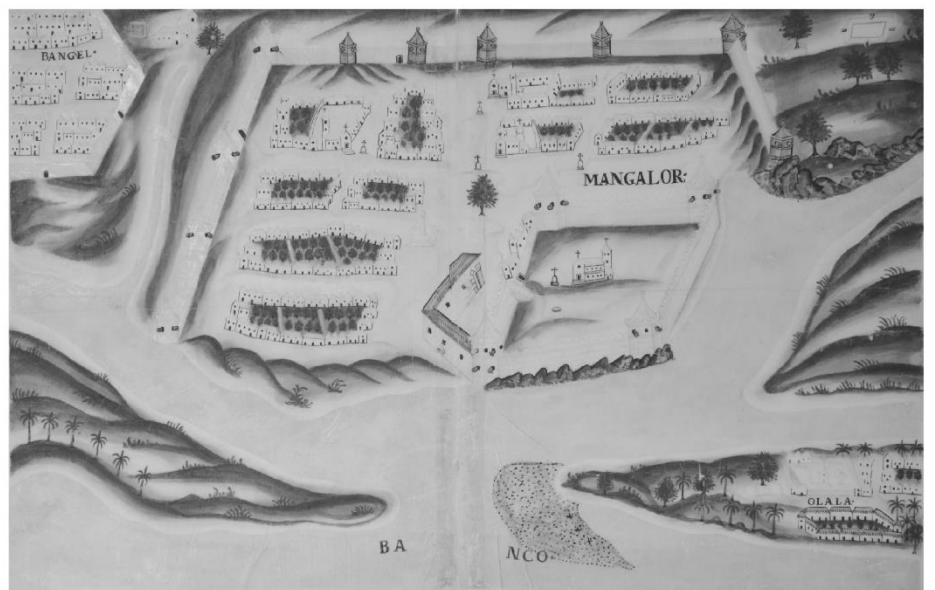


III.3.9-10: 'Dio'



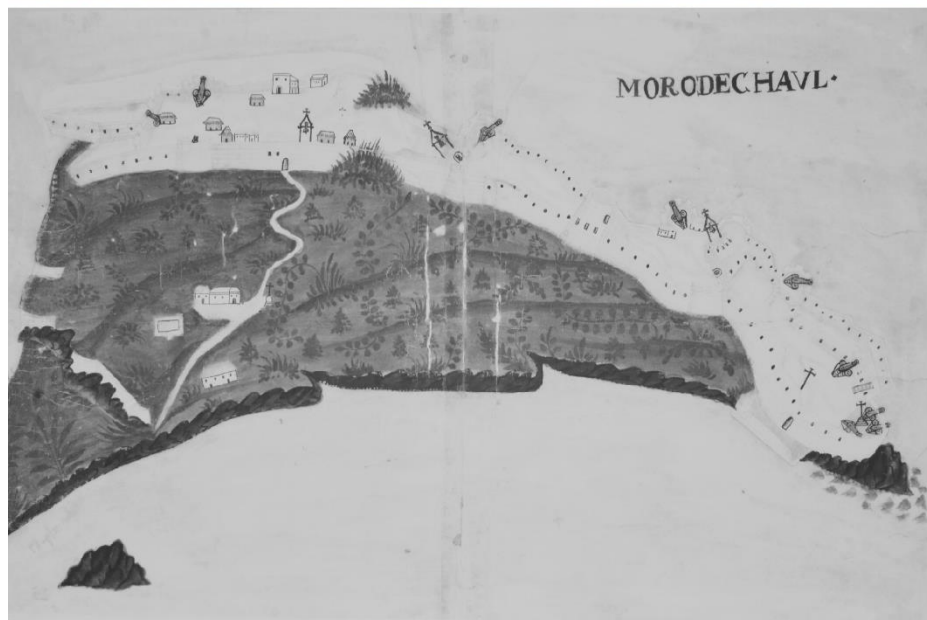
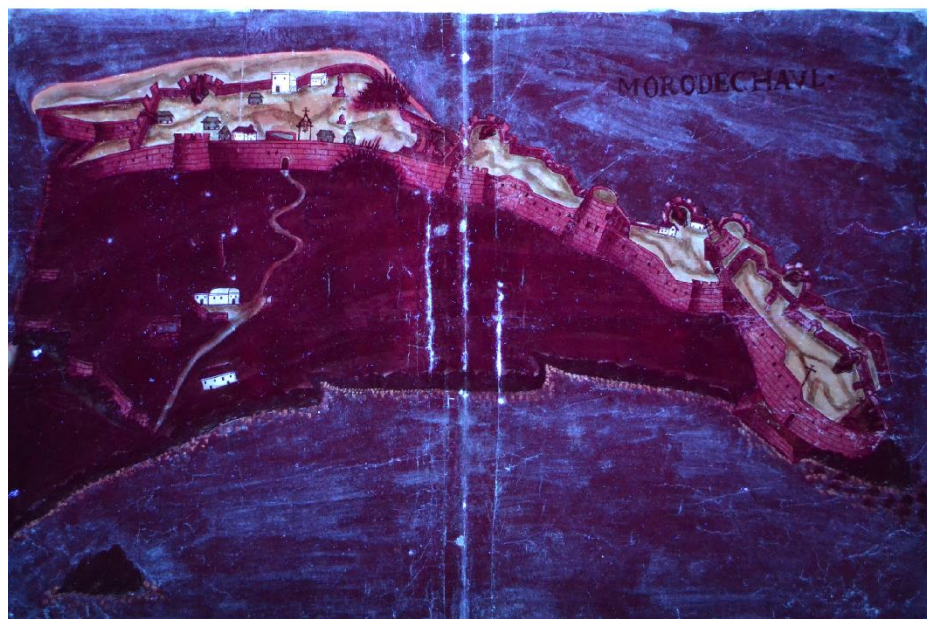


III.3.11-12: 'Mangalor'





III.3.13-14: 'Moro de Chaul'



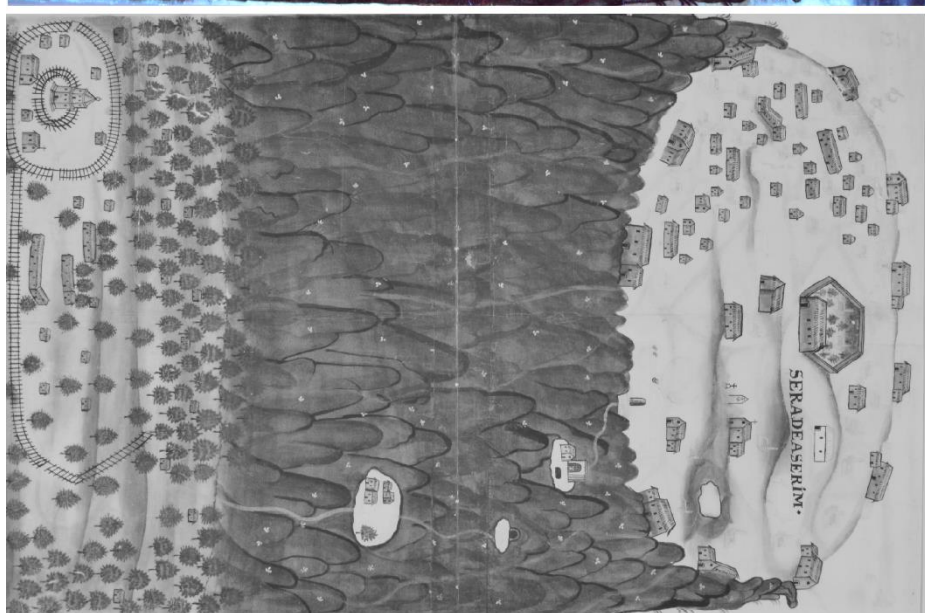


III.3.15-16: 'Salsete'





III.3.17-18: 'Sera de Aserim'



### III.4: COLORIMETRIC COORDINATES IN CIE-LAB COLOR SPACE

Color		Spot	Map Name	Region	CIE L	CIE a	CIE b	CIE C	CIE h
Green	Dark	5	Dio	Terrain	53.49	-14.2	13.91	19.88	135.58
Green	Dark	27	Sera de Aserim	Tree	43.96	-15.42	7.91	17.33	152.85
Green	Dark	42	Baçaim	Tree	40.08	-15.42	7.21	17.02	154.93
Green	Dark	57	Cochim	Tree	37.73	-13.13	7.07	14.91	151.71
Green	Dark	68	Mangalor	Terrain	52.74	-16.69	7.93	18.48	154.58
Green	Dark	91	Chaul	Terrain	45.83	-14.3	10.79	17.92	142.96
Green	Whitish	14	Damaõ	Terrain	54.47	-10.48	12.39	16.22	130.22
Green	Whitish	25	Damaõ	Tree	49.35	-13.64	12.1	18.23	138.4
Green	Whitish	66	Cochim	Terrain	60.78	-11.97	13.44	18	131.68
Green	Whitish	72	Mangalor	Terrain	63.61	-6.43	14.66	16.01	113.69
Green	Whitish	90	Chaul	Terrain	54.54	-11.97	10.8	16.13	137.94
Green	Yellowish	29	Sera de Aserim	Terrain	53.46	-8.71	21.79	23.47	111.79
Green	Yellowish	50	Baçaim	Terrain	53.2	-11.87	14.45	18.7	129.41
Green	Yellowish	61	Cochim	Terrain	58.3	-3.58	22.37	22.66	99.1
Green	Yellowish	71	Mangalor	Terrain	63.51	-6.68	22.45	23.42	106.56
Pink	Light	4	Dio	Fortification	53.68	17.15	2.15	17.29	7.14
Pink	Light	20	Damaõ	Well	48.77	17.49	3.92	17.92	12.64
Pink	Light	31	Sera de Aserim	Fortification	57.31	17.27	4.02	17.73	13.09
Pink	Light	46	Baçaim	Fortification	54.9	18.37	1.68	18.45	5.22
Pink	Light	55	Cochim	Fortification	49.69	18.96	2.21	19.09	6.64
Pink	Light	73	Mangalor	Fortification	58.58	17.13	1.74	17.21	5.8
Pink	Light	89	Chaul	Fortification	54.55	16.68	4.55	17.29	15.25
Pink	Dark	3	Dio	Fortification	35.87	16.75	3.2	17.05	10.8
Pink	Dark	19	Damaõ	Pillory	43.04	16.89	3.52	17.25	11.77
Pink	Dark	47	Baçaim	Fortification	33.91	22.28	3.83	22.61	9.77
Pink	Dark	54	Cochim	Fortification	36.57	22.15	1.73	22.21	4.46
Pink	Dark	80	Mangalor	Fortification	37.89	25.07	3.43	25.3	7.8
Pink	Dark	92	Chaul	Fortification	31.52	18.74	5.76	19.6	17.07
Pink	Orangeish	75	Mangalor	Fortification	52.71	20.1	19.97	28.33	44.8
Pink	Warm pale	78	Mangalor	House in Olala	62.2	10.64	20.11	22.75	62.12
Pink	Warm (wash)	37	Sera de Aserim	Sky	59.51	19.08	20.95	28.34	47.67
Blue	Medium	1	Dio	Water	34.78	7.1	-7.1	7.38	254.4
Blue	Medium	2	Dio	Water	37.94	-2.66	-7.82	8.26	251.23
Blue	Medium	13	Damaõ	Water	33.18	-1.47	-7.14	7.29	258.35
Blue	Medium	40	Baçaim	Water	31.84	-1.58	-5.97	6.18	255.15
Blue	Medium	51	Cochim	Water	31.32	-1.61	-7.44	7.61	257.78
Blue	Medium	67	Mangalor	Water	31.4	-1.05	-7.19	7.27	261.7
Blue	Medium	82	Chaul	Water	35.6	-2.71	-5.71	6.32	244.65
Blue	Medium (wash)	38	Sera de Aserim	Sky	42.38	-4.85	-4.01	6.3	219.57
Blue	Dark	12	Damaõ	Water	26.47	-0.51	-0.09	0.52	190.2
Blue	Light	6	Dio	Moat	46.85	-4.46	-6.49	7.87	235.51
Blue	Light	30	Sera de Aserim	Pond	42.38	-4.85	-4.01	6.3	219.57
Blue	Light	63	Cochim	Pond	41.73	-3.81	-7.98	8.84	244.45
Red	Medium	7	Dio	Roof	40.5	32.76	17.36	37.07	27.92
Red	Medium	24	Damaõ	Roof	38.46	31.48	16.77	35.67	28.05
Red	Medium	35	Sera de Aserim	Roof	40.83	34.41	20.5	40.05	30.79
Red	Medium	48	Baçaim	Roof	39.9	30.83	16.51	34.97	28.17
Red	Medium	53	Cochim	Roof	43.31	30.48	16.69	34.75	28.71
Red	Medium	74	Mangalor	Roof	39.9	30.83	16.51	34.97	28.17
Red	Medium	93	Chaul	Roof	41.83	34.83	21.44	40.91	31.62
Red	Orangeish	86	Chaul	Bastion	44.41	19.79	14.07	24.28	35.42
Beige	Medium	9	Dio	Terrain	71.44	4.25	21.08	21.51	78.59
Beige	Medium	23	Damaõ	Terrain	68.88	7	27.89	28.76	75.92
Beige	Medium	39	Sera de Aserim	Terrain	64.74	9.99	31.77	33.3	72.55
Beige	Medium	43	Baçaim	Terrain	72.67	4.34	22.03	22.45	78.86
Beige	Medium	52	Cochim	Terrain	68.38	6.53	25.05	25.89	75.4
Beige	Medium	58	Cochim	Terrain	69.22	5.79	22.83	23.55	75.77
Beige	Medium	70	Mangalor	Terrain	66.79	5.32	28.76	29.25	79.52
Beige	Medium	83	Chaul	Terrain	66.15	7.56	25.05	26.17	73.2
Tan	Medium	8	Dio	Terrain	59.16	9.74	33.17	34.57	73.63



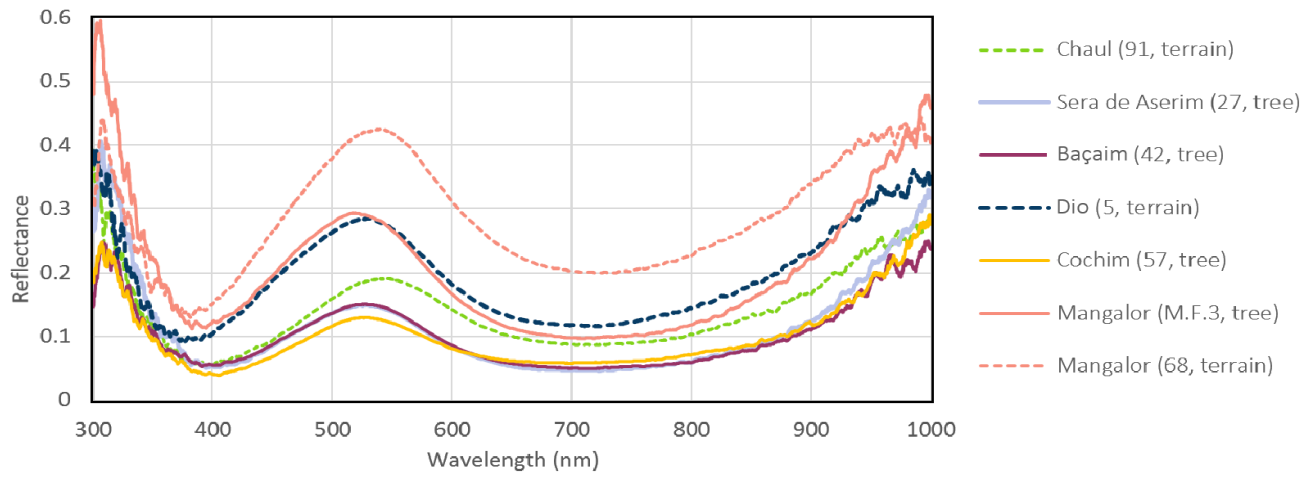
### III.4: COLORIMETRIC COORDINATES (cont.)

Color	Spot	Map	Region	CIE L	CIE a	CIE b	CIE C	CIE h	Color
<b>Tan</b>	Medium	15	Damaõ	Terrain	56.33	14.88	36.51	39.43	67.82
<b>Tan</b>	Medium	36	Sera de Aserim	Terrain	52.78	17.83	33.65	38.09	62.08
<b>Tan</b>	Medium	45	Baçaim	Terrain	61.89	14.06	35.61	38.28	68.46
<b>Tan</b>	Medium	59	Cochim	Terrain	60.65	12.58	35.06	37.25	70.26
<b>Tan</b>	Dull yellowish	76	Mangalor	Tower	48.74	14.8	28.2	31.85	62.31
<b>Tan</b>	Reddish	84	Chaul	Terrain	51.72	15.35	18.8	24.27	50.77
<b>Tan</b>	Orangeish	87	Chaul	Bastion	55	14.08	26.12	29.67	61.67
<b>Tan</b>	Bright yellowish	44	Baçaim	Terrain	66.62	3.6	42.01	42.17	85.11
<b>Brown</b>	Light	21	Damaõ	House	55.15	4.66	18	18.6	75.49
<b>Brown</b>	Light	26	Sera de Aserim	House	39.93	8.39	13.22	15.66	57.6
<b>Brown</b>	Light	41	Baçaim	House	41.09	8.8	14.41	16.89	58.58
<b>Brown</b>	Light	56	Cochim	House	47.04	8.08	18.38	20.08	66.28
<b>Brown</b>	Light	85	Chaul	House	46.35	6.17	9.67	11.47	57.45
<b>Brown</b>	Medium	11	Dio	Rock	38.38	3.48	11.06	11.59	72.54
<b>Brown</b>	Medium	28	Sera de Aserim	Rock	30.83	3.94	6.36	7.49	58.22
<b>Brown</b>	Medium	77	Mangalor	Rock	41.03	5.57	13.46	14.56	67.53
<b>Brown</b>	Blackish	33	Sera de Aserim	Rock	25.34	0.24	0.61	0.65	68.65
<b>Brown</b>	Blackish	64	Cochim	Rock	30.61	0.23	4.17	4.17	86.87
<b>Brown</b>	Blackish	65	Cochim	Rock	29.26	1.32	1.85	2.27	54.43
<b>Brown</b>	Blackish	88	Chaul	Rock	27.78	1.27	2.22	2.55	60.26
<b>Black</b>	Dark	22	Damaõ	Gate	28.2	0.9	0.97	1.32	47.21
<b>Black</b>	Dark	81	Mangalor	Gate	28.18	0.34	0.7	0.78	64.05
<b>Gray</b>	Medium	18	Damaõ	Fortification	52.64	2.56	9.82	10.15	75.4
<b>White</b>	Bright	10	Dio	House	74.16	1.31	13.2	13.27	84.32
<b>White</b>	Bright	17	Damaõ	Fortification	73.11	1.4	13.12	13.19	83.92
<b>White</b>	Bright	34	Sera de Aserim	House	73.45	1.17	13.4	13.46	85.01
<b>White</b>	Bright	49	Baçaim	House	74	2.11	10.38	10.59	78.51
<b>White</b>	Bright	60	Cochim	<i>Camara</i>	71.95	0.31	12.7	12.7	88.59
<b>White</b>	Bright	79	Mangalor	Church	75.07	1.48	12.62	12.7	83.32
<b>White</b>	Bright	95	Chaul	House	68.07	3.62	13.55	14.03	75.03
<b>White</b>	Dull	62	Cochim	Beach	69.95	2.01	9.33	9.55	77.83
<b>Purple</b>	Brownish	16	Damaõ	Ditch	28.17	4.86	3.8	6.17	38.04

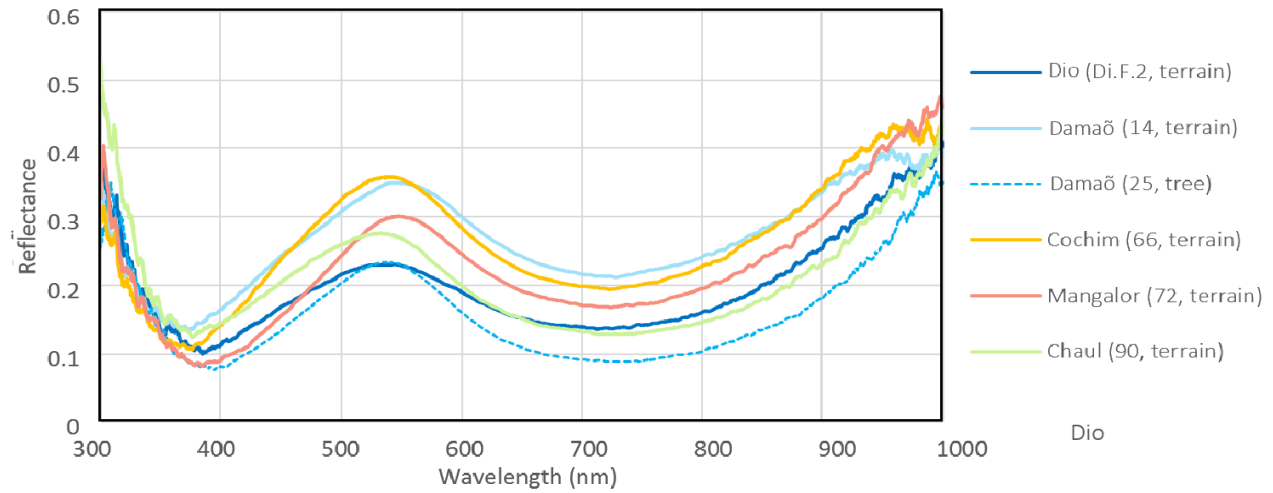
### III.5: FORS SPECTRA

#### Repeated Colors

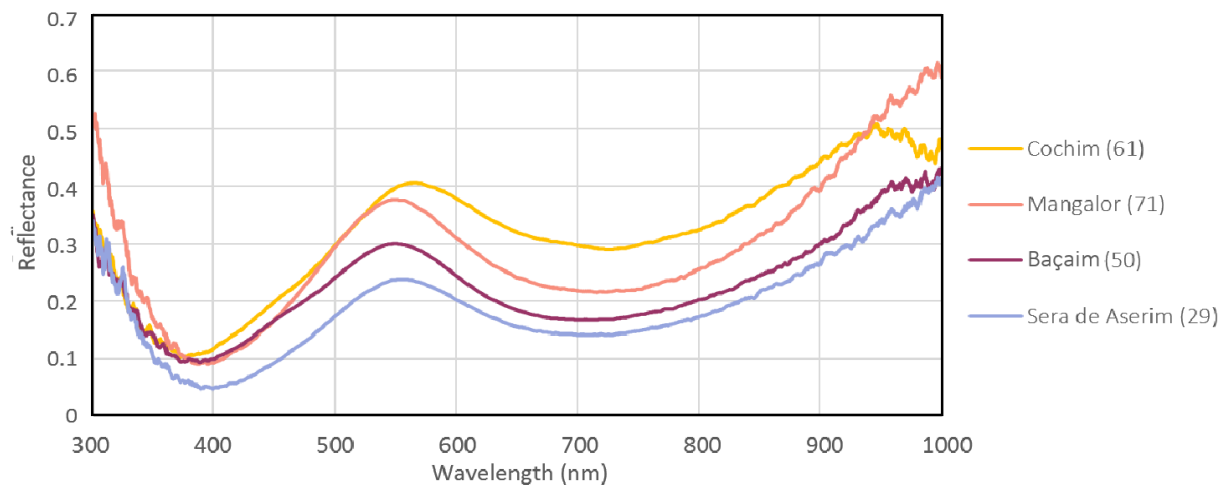
III.5.1: Dark green trees and terrain



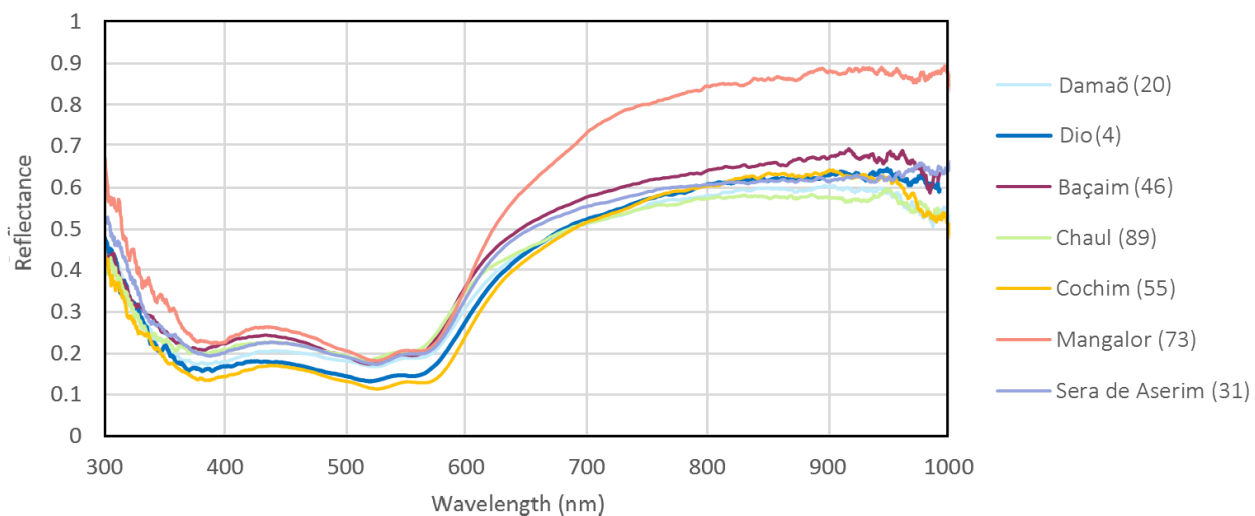
III.5.2: Whitish-green trees and terrain



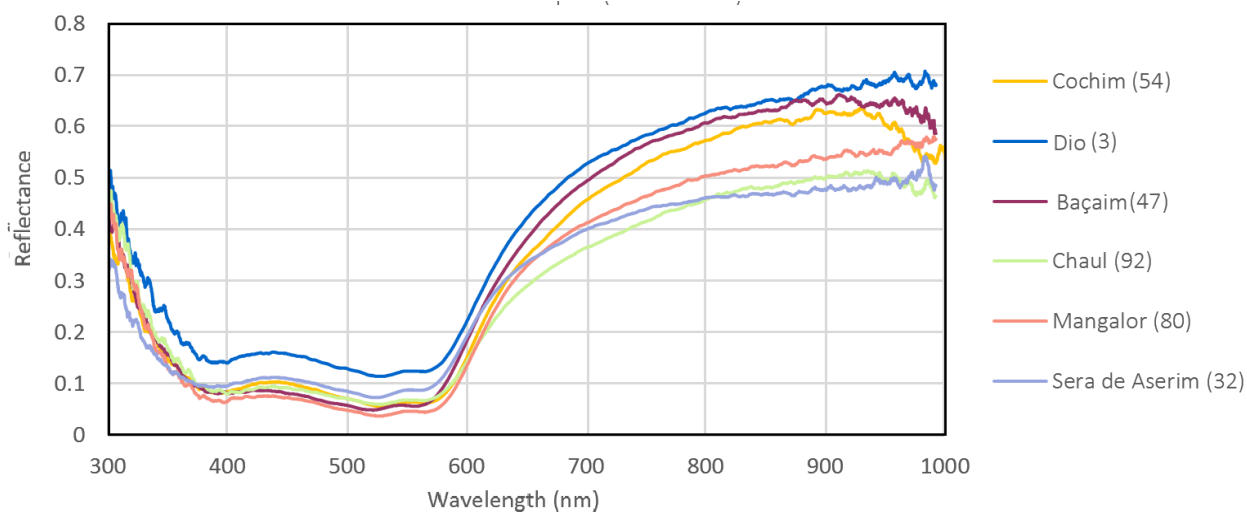
III.5.3: Yellowish-green trees and terrain



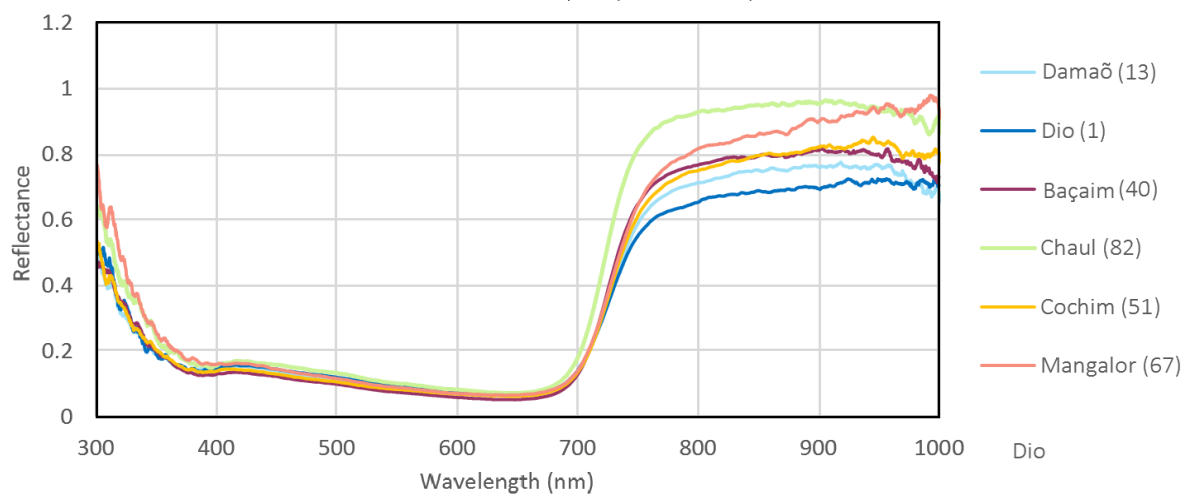
III.5.4: Light pink (fortifications)



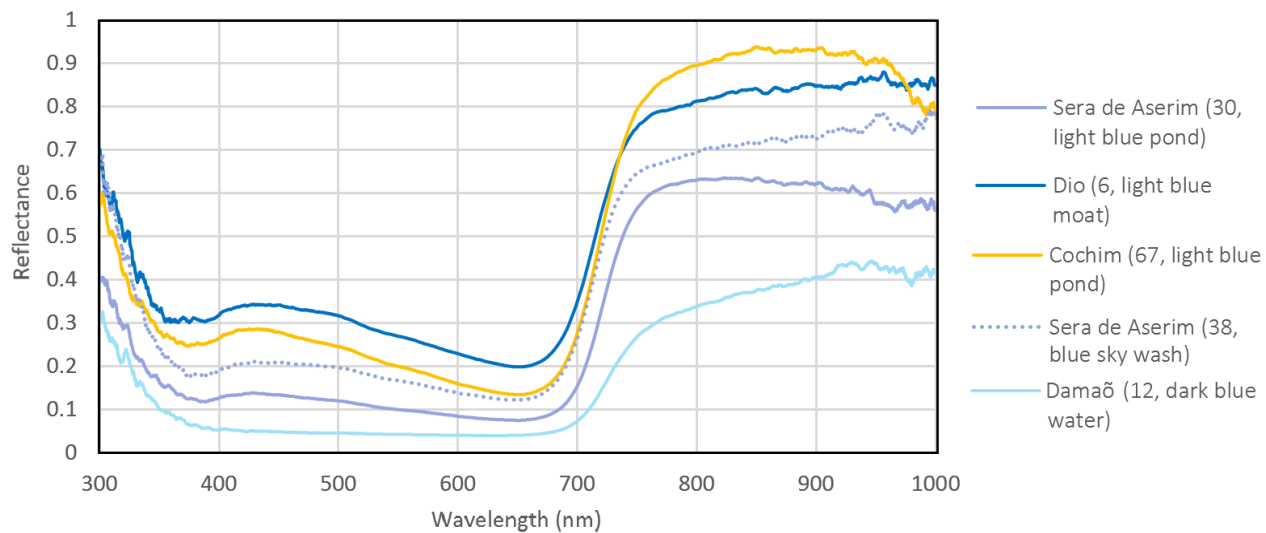
III.5.6: Dark pink (fortifications)



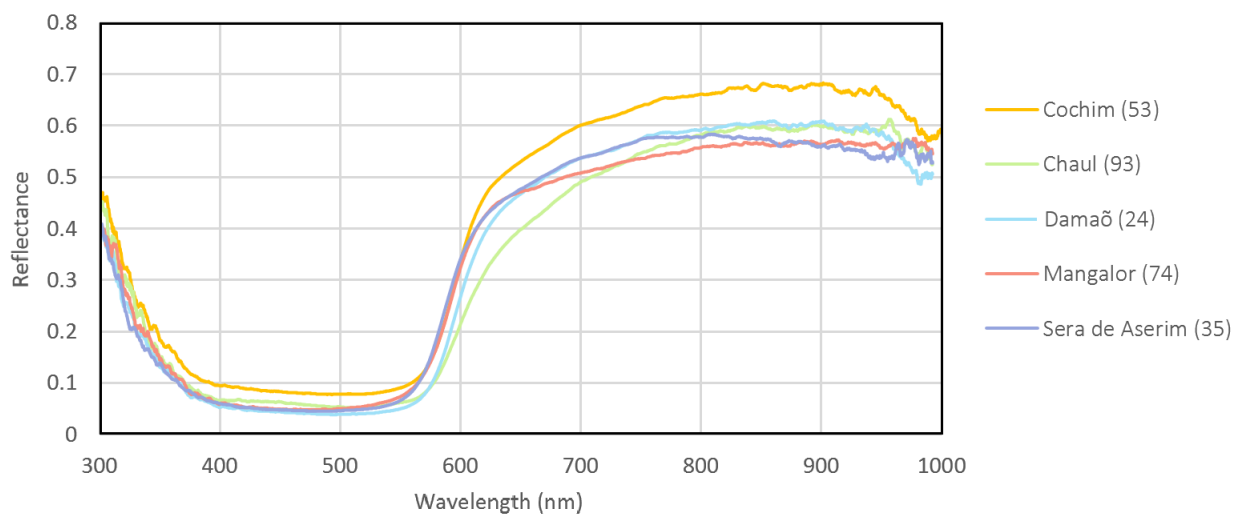
III.5.6: Medium blue (water)



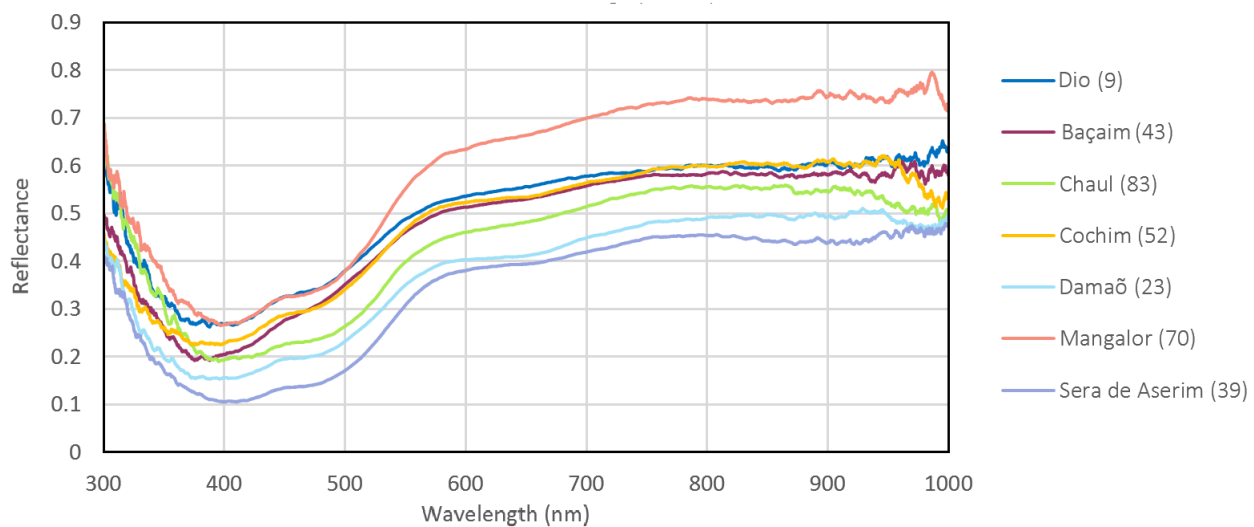
III.5.7: Light, dark and wash blue



III.5.8: Red (roofs)

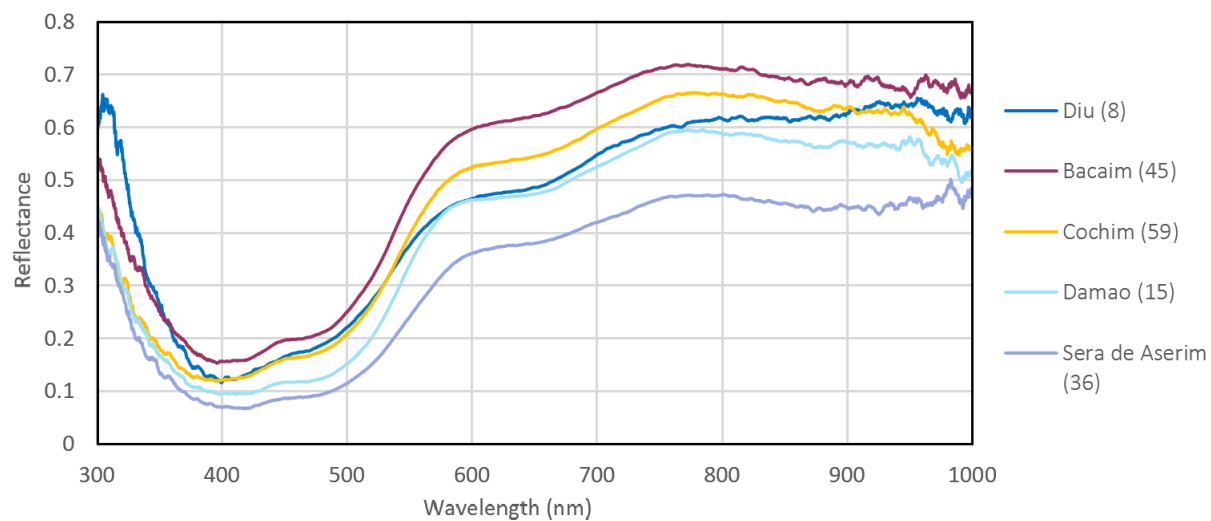


III.5.9: Beige (terrain)

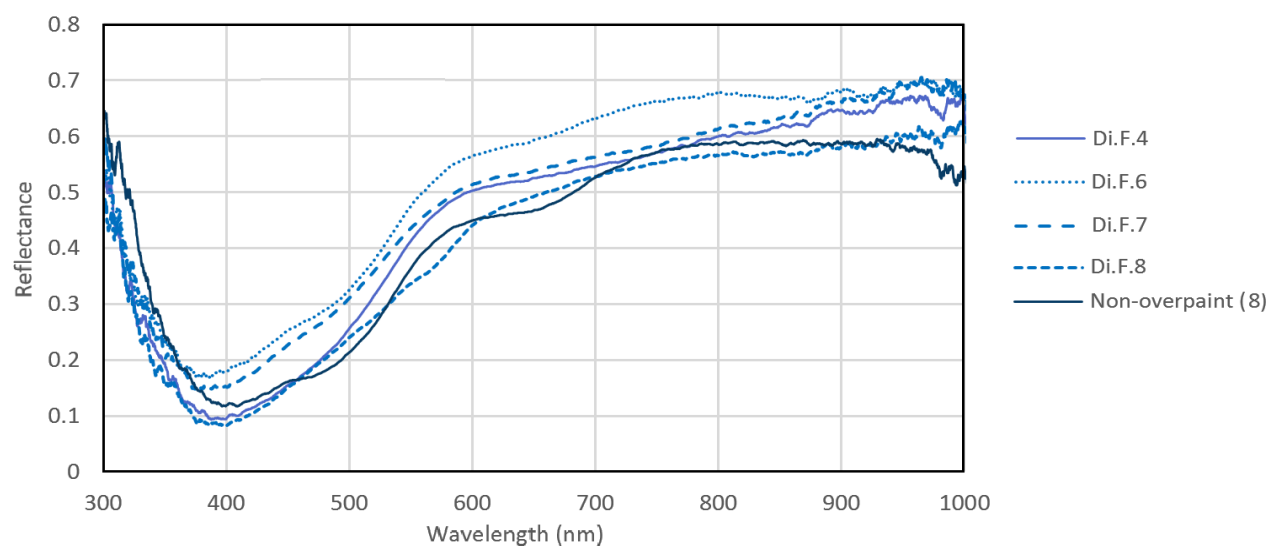




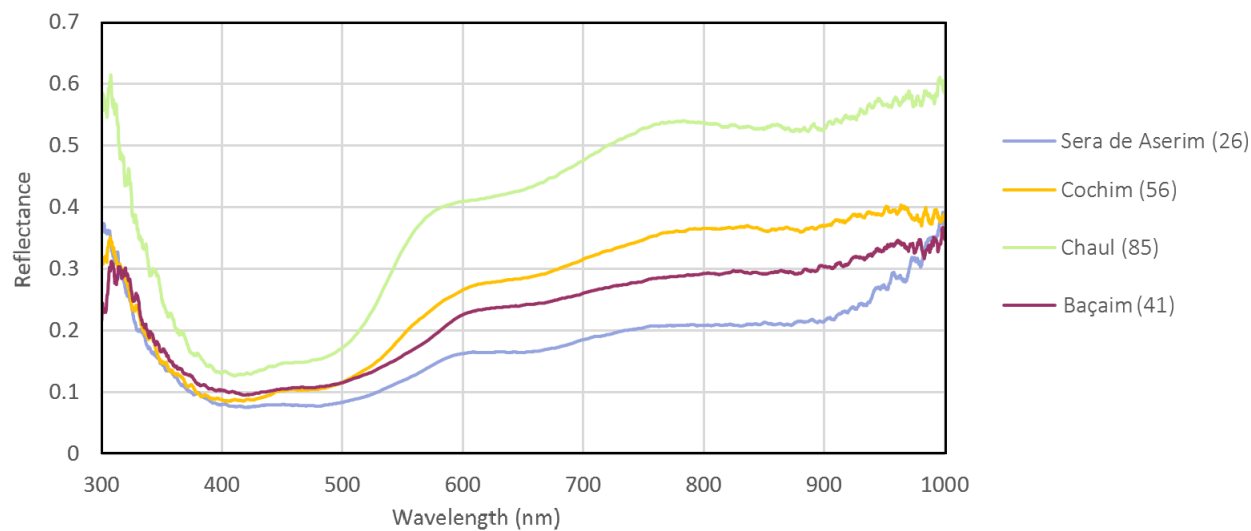
III.5.10: Tan (terrain)



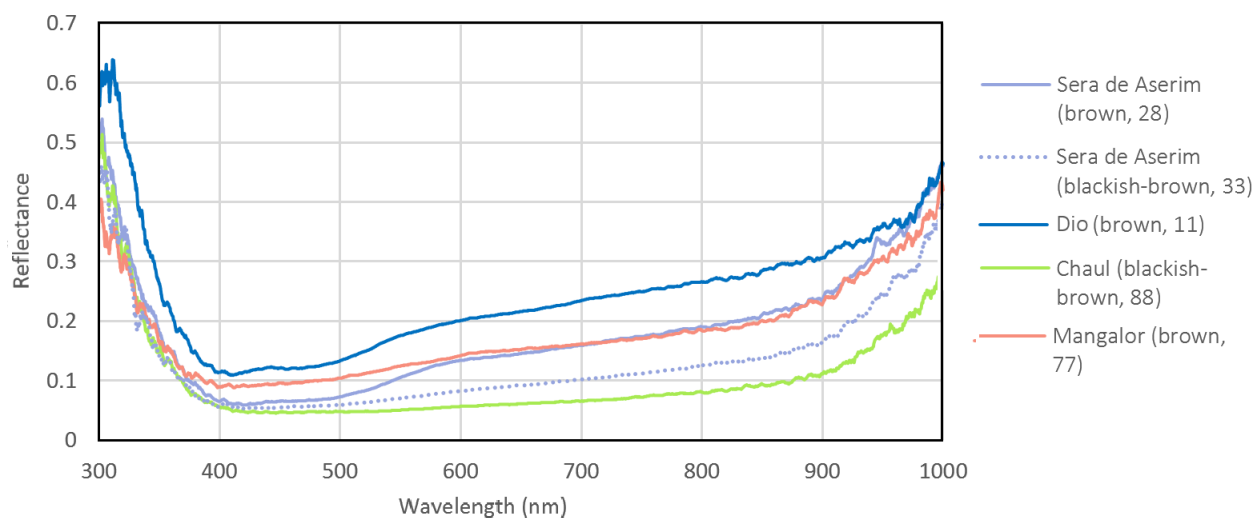
III.5.11: Tan (overpaints, Dio)



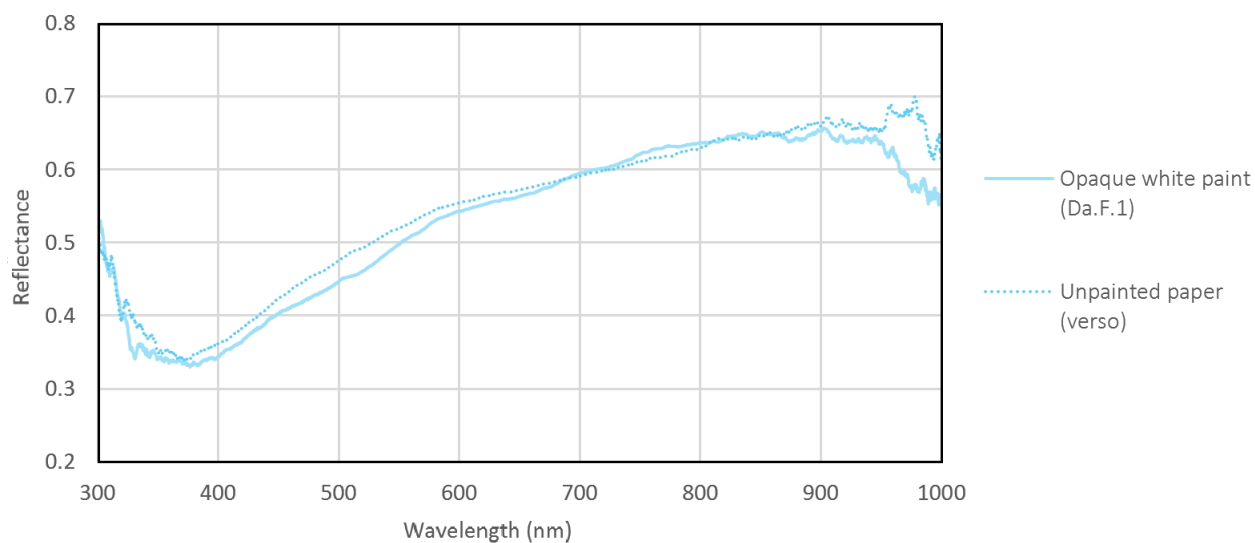
III.5.12: Light brown (houses)



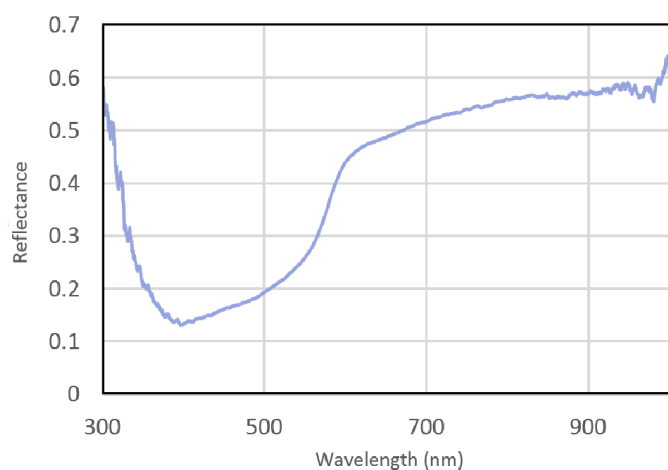
III.5.13: Medium to blackish-brown (rocks)



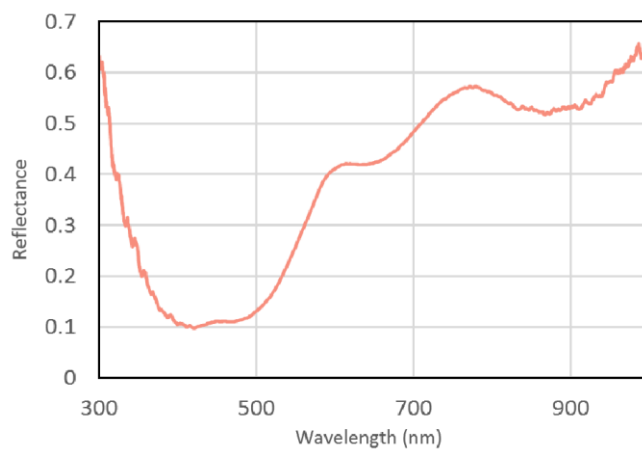
III.5.14: White paper and paint (Damaão)



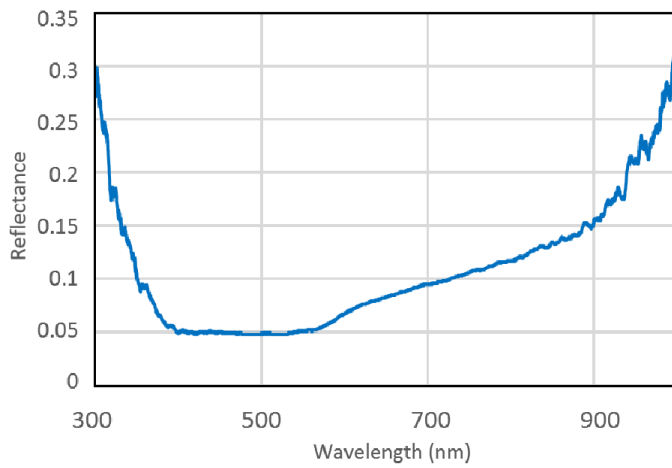
### Occasional colors



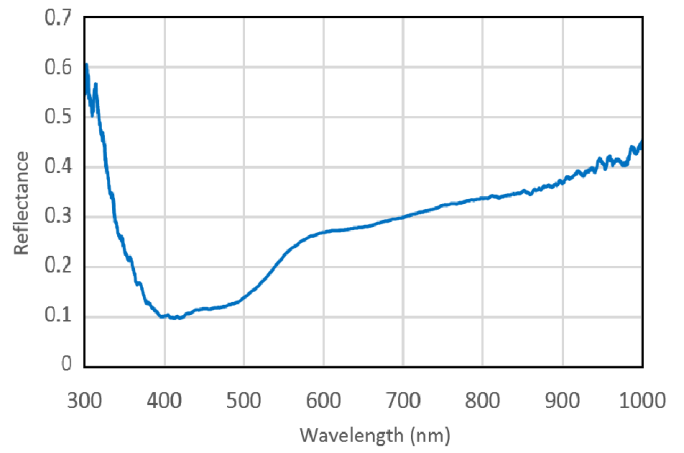
III.5.15: 37 (warm pink sky wash, Sera de Aserim)



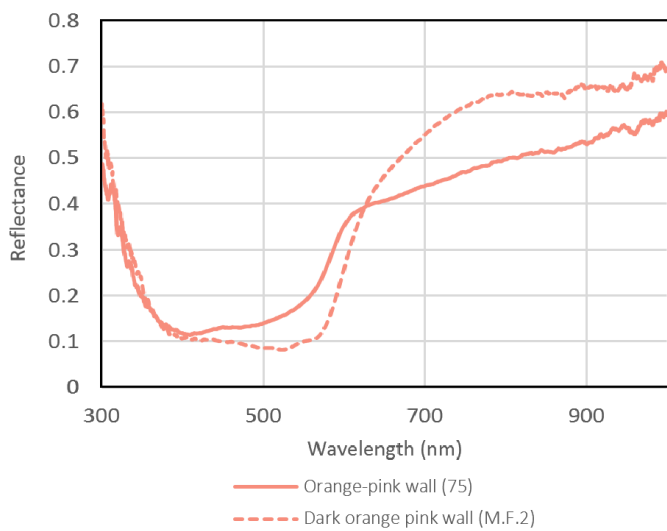
III.5.16: 78 (warm pale pink, Mangalor)



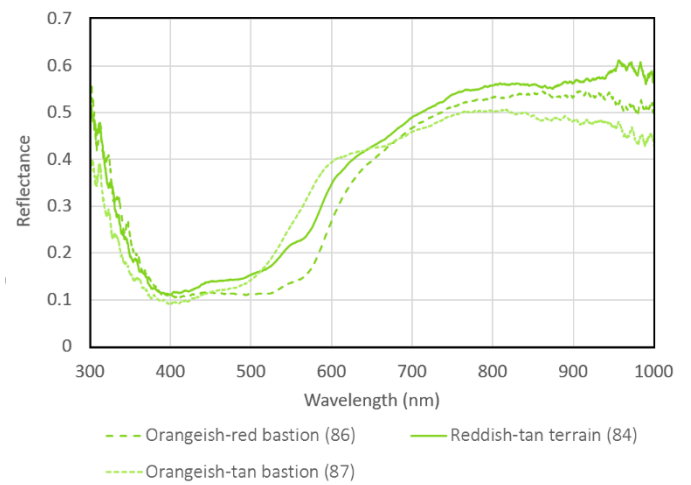
III.5.17: 16 (purple-brown ditch, Dio)



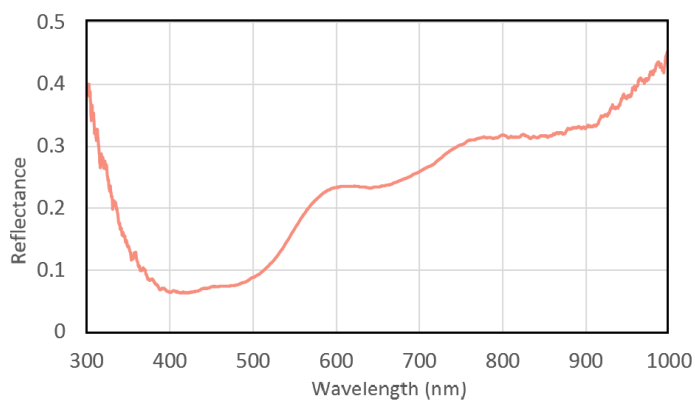
III.5.18: Di.F.9 (olive to brown "bull ring")



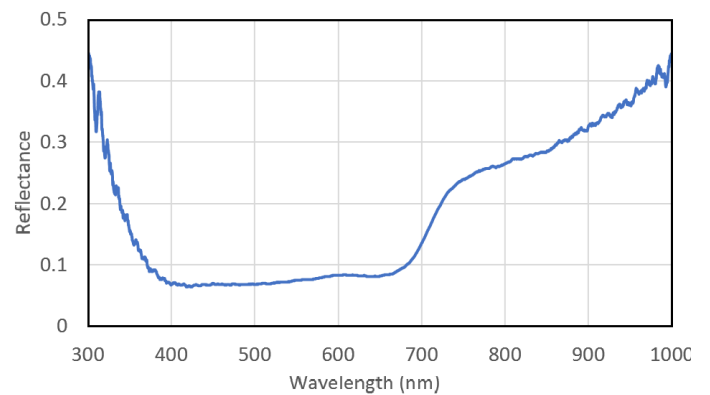
III.5.19



III.5.20



III.5.21: 76 (dull yellowish-tan tower, Mangalar)



III.5.22: 5 (stippled inlet, Dio)

Color	Spot	Al	Ca	Cr	Cu	Fe	Hg	Hg	K	Mn	Ni	P	Pb	Pb	S	Si	Sn	Sn	Sr	Ti	Zn
		K12	K12	K12	K12	K12	11	M1	K12	K12	K12	K12	K12	11	K12	K12	K12	11	K12	K12	K12
Paper Support	V. B.	23	10277	25	796	2260	0	0	69	249	6595	24	504	0	85	90	18	0	503	548	58
	R. B.	21	12846	17	899	2587	0	0	113	294	7039	24	609	0	127	99	21	0	439	589	91
	V. Ch.	33	10646	71	994	2592	0	0	108	285	6974	23	650	0	87	61	8	0	428	289	99
	R. Ch.	16	11370	50	1240	2530	0	0	195	275	6880	30	663	0	176	40	5	0	375	253	141
	V. C.	17	12978	45	1312	2664	0	0	25	299	6948	23	1203	0	167	116	16	0	459	552	119
	R. C.	15	11511	14	4938	2329	0	0	149	246	6351	18	1132	0	169	85	10	0	445	507	131
	V. Di.	20	13120	47	1224	2340	0	0	99	226	6191	27	1797	0	256	99	15	0	420	247	90
	R. Di.	18	11502	30	926	2330	0	0	206	242	6026	23	1456	0	218	112	25	0	364	240	121
	V. Da.	27	13090	64	966	2684	0	0	104	280	6921	23	725	0	158	88	19	0	434	344	140
	R. Da.	18	12238	53	919	2597	0	0	145	226	6828	49	607	0	205	108	21	0	317	306	123
	V. M.	21	14842	68	919	2505	0	0	67	259	7038	25	492	0	143	92	2	0	426	556	103
	R. M.	16	13529	44	877	2469	0	0	27	264	6784	29	567	0	146	68	25	0	442	551	93
	T. SA.	15	11358	28	1063	2353	0	0	176	247	6097	19	526	0	133	90	10	0	410	460	81
	B. SA.	10	12486	0	1019	2215	0	0	95	245	5642	29	620	0	122	93	7	0	381	497	86
	5	4	0	0	218819	1353	0	0	0	85	0	0	42667	1025	0	0	125	0	0	0	30
Dark green	27	12	0	2	263001	1884	0	0	0	161	0	0	15462	1094	0	0	0	0	0	0	295
	42	2	0	0	189119	492	0	0	0	97	0	0	40607	2105	0	0	0	0	0	0	228
	57	4	0	0	111544	772	0	0	0	82	0	0	115975	3509	0	0	35	0	0	0	169
	68	5	0	0	234566	259	0	0	0	61	0	0	39514	1680	0	0	0	0	0	0	186
	91	0	0	7	276785	2936	0	0	36	31	0	0	56262	1382	0	0	0	0	0	353	395
	Di.F.1	0	0	16	123529	1065	0	0	0	39	0	0	117531	3192	0	0	96	0	0	0	18
	M.F.3	0	0	47	1909	10250	1201	103	497	413	0	0	17533	752	0	0	0	0	0	0	246
	14	4	0	51	70861	4214	0	0	0	77	0	0	113637	5106	0	0	105	0	0	0	0
	25	0	0	0	173980	0	0	0	0	27	0	0	57289	2789	0	0	13	0	0	0	187
	66	1	0	14	45824	571	0	0	0	113	0	0	73453	5641	0	0	0	0	0	0	0
Whitish green	72	0	0	9	33357	220	0	0	0	145	0	0	56605	6676	0	0	0	0	0	0	0
	90	6	0	0	147920	1046	0	0	206	156	0	15	17783	1503	0	0	0	0	0	0	218
	Di.F.2	7	0	51	49893	855	3471	203	0	75	0	0	141061	3631	0	0	167	0	0	0	0
	Di.F.3	0	0	23	35771	1673	753	273	0	66	0	0	147843	5305	0	0	204	0	0	0	0
	SA.X.1	0	0	30	228494	28555	357	0	0	54	0	0	49433	2372	0	0	28	0	0	113	207
	29	6	0	27	86372	654	0	0	0	57	0	0	44921	3917	0	0	0	0	0	0	44
Yellow-green	50	5	0	30	98895	3089	0	0	0	76	0	0	81106	3845	0	0	46	0	0	0	31
	61	21	0	7	64582	1527	0	0	0	95	0	0	74241	4191	0	0	0	0	0	0	17
	71	0	0	13	54981	149	0	0	0	162	0	0	63587	7233	0	0	16	0	0	0	0
	4	0	0	71	0	0	0	0	0	0	0	0	146844	5944	0	0	168	0	0	0	0
Light pink	20	7	0	118	0	0	0	0	0	0	0	0	121180	7662	0	0	116	0	0	0	0
	31	0	0	60	0	0	0	0	0	0	0	0	125808	7425	0	0	130	0	0	0	0
	46	0	0	104	0	0	0	0	0	0	0	0	151216	6025	0	0	192	0	0	0	0
	55	9	0	116	375	0	0	0	0	0	0	0	114794	4385	0	0	69	0	0	0	0
	73	0	0	75	124	0	0	0	0	0	0	0	112866	7316	0	0	74	0	0	0	0
	89	0	0	56	0	0	0	0	0	0	0	0	117892	7315	0	0	93	0	0	0	0



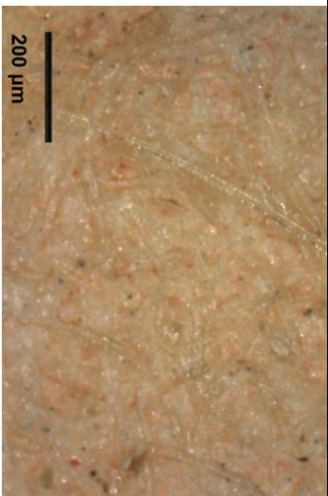
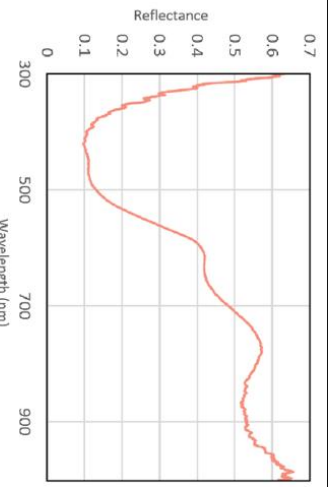
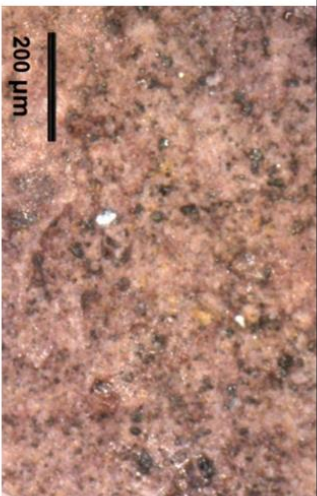
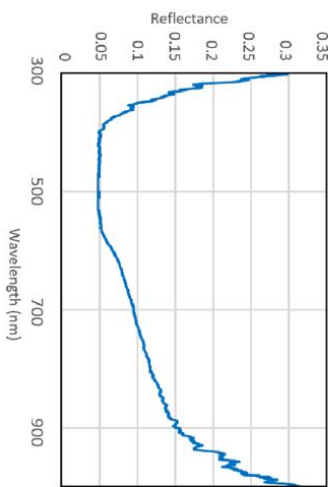
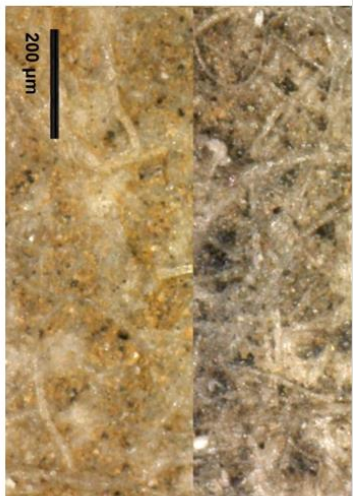
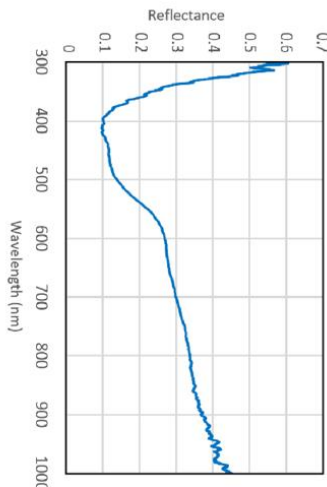
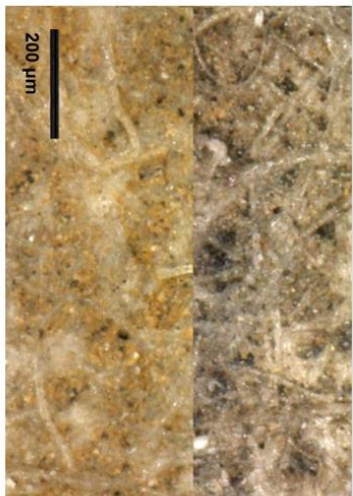
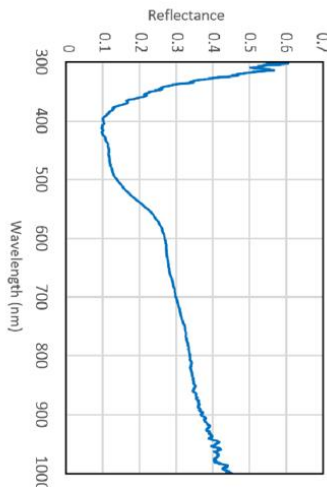
III.6: h-XRF (cont.)

Color	Spot	Al	Ca	Cr	Cu	Fe	Hg	Hg	K	Mn	Ni	P	Pb	Pb	S	Si	Sn	Sn	Sr	Ti	Zn
		K12	K12	K12	K12	K12	l1	M1	K12	K12	K12	K12	K12	l1	K12	K12	K12	l1	K12	K12	K12
Dark pink	3	0	0	61	0	0	0	0	0	0	0	0	138832	6315	0	0	145	0	0	0	0
	32	0	0	69	0	0	0	0	0	0	0	0	122128	7663	0	0	139	0	0	0	0
	47	2	0	65	0	0	0	0	0	0	0	0	151387	6605	0	0	219	0	0	0	0
	54	0	0	31	101	0	0	0	0	0	0	0	143042	8260	0	0	210	0	0	0	0
	80	15	0	49	55	0	0	0	0	0	0	0	101504	7538	0	0	68	0	0	0	0
	92	0	0	47	771	1570	0	0	0	144	0	0	95229	5922	0	0	37	0	0	0	0
	37	0	0	0	0	1427	6610	492	0	162	0	0	13500	814	0	0	0	0	0	0	0
	75	0	0	26	301	7214	10894	665	0	79	0	0	85763	4323	0	0	37	0	0	0	0
Misc. pink	78	18	0	1	2075	12355	3513	305	0	199	0	0	18315	1263	0	0	0	0	5	69	0
	M.F.2	10	0	23	737	7940	11571	813	0	90	0	0	89904	5626	0	0	49	0	0	0	0
Medium blue	1	442	0	108	0	5076	0	0	725	209	0	0	1459	0	64	1344	0	0	0	2962	4
	13	456	0	133	0	11475	0	0	1060	270	0	2	414	0	0	1506	0	0	30	3971	8
	40	314	0	92	0	6496	0	0	776	270	0	0	142	0	0	1012	0	0	72	2734	23
	51	327	0	123	0	9598	0	0	868	298	158	4	733	0	9	1159	0	0	90	3556	5
	67	551	0	217	0	7884	0	0	824	254	0	2	1252	0	41	1546	0	0	75	4904	75
	82	364	0	77	0	3661	0	0	525	203	0	3	416	0	3	1141	0	0	56	1917	56
	38	95	0	0	357	1857	0	0	168	241	0	0	319	0	16	307	0	0	26	453	22
	6	45	0	48	0	403	0	0	332	135	0	0	80243	5231	141	1196	0	0	0	329	0
Misc. blue	12	343	0	90	0	7930	0	0	758	332	0	22	552	0	0	0	0	0	0	2391	4
	30	138	0	60	931	2021	0	0	233	228	0	0	11936	1339	0	438	0	0	13	952	0
	63	104	0	105	353	3037	0	0	0	137	0	0	94238	5183	0	368	0	0	169	1098	0
	7	0	0	23	0	0	63564	2107	0	49	0	0	61593	1815	0	0	0	0	0	0	0
	24	0	0	86	0	8	85894	4226	0	48	0	0	15897	17	0	0	0	0	435	0	109
	35	1	0	93	447	0	64121	5034	0	37	0	0	6819	0	0	0	0	0	431	0	81
	48	0	0	90	0	0	78887	3444	0	51	0	0	10898	135	0	0	0	0	433	0	123
	74	0	0	88	160	0	59894	4918	0	51	0	0	24945	217	0	0	0	0	331	0	56
Red	93	2	0	47	0	0	57130	2923	0	98	0	0	52559	1975	0	0	0	0	273	0	0
	B.	0	411	0	0	0	1272	15	0	234	574	4	0	0	129	0	0	0	0	280	0
Red dots	S. de A.	0	931	35	0	0	1428	0	0	211	0	0	0	0	40	0	0	0	0	229	0
	Ch.	5	0	65	0	10	620	0	0	263	1403	0	0	0	15	0	0	0	0	0	0
	9	1	0	40	0	1109	0	0	0	93	0	0	86015	5584	0	0	37	0	0	0	0
	23	10	0	62	0	5229	0	0	0	70	0	0	67909	5906	0	0	19	0	0	0	0
	39	12	0	31	36	8370	0	0	0	114	0	0	83029	7679	0	0	43	0	0	0	0
	43	0	0	10	0	225	0	0	0	85	0	0	87849	6526	0	0	47	0	0	0	0
	52	6	0	60	1077	5123	0	0	0	149	0	0	97054	6485	0	0	49	0	0	0	0
	70	10	0	38	736	3180	0	0	0	114	0	0	104014	7811	0	0	68	0	0	0	0
Beige	83	0	0	18	0	4899	0	0	0	160	0	0	73188	6228	0	0	23	0	0	0	0

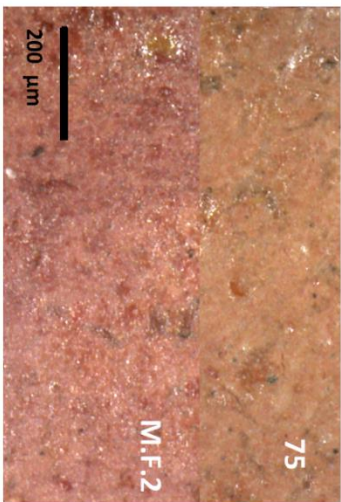
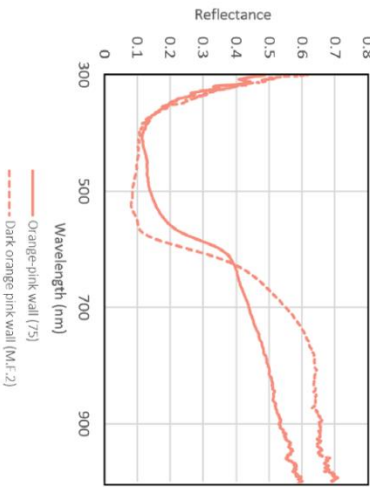
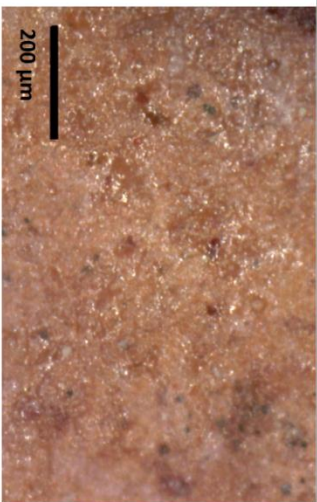
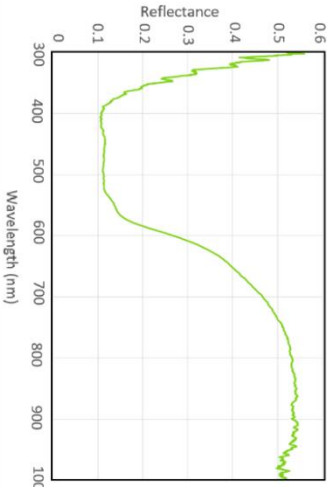
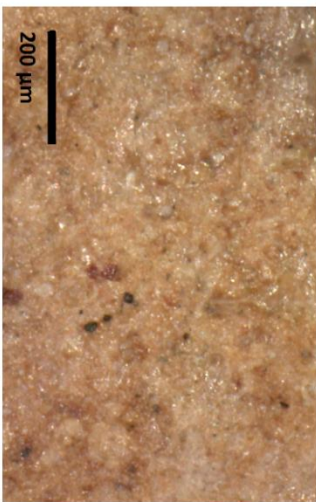
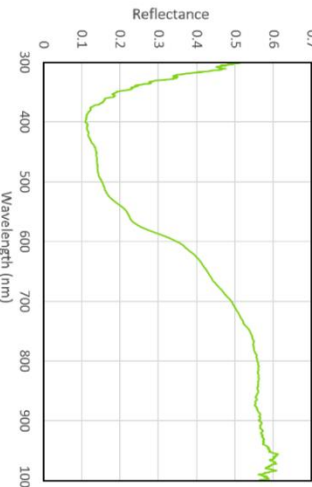
### III.6: h-XRF (cont.)

Color	Spot	Al	Ca	Cr	Cu	Fe	Hg	Hg	K	Mn	Ni	P	Pb	Pb	S	Si	Sn	Sn	Sr	Ti	Zn
		K12	K12	K12	K12	K12	I1	M1	K12	K12	K12	K12	K12	I1	K12	K12	K12	I1	K12	K12	K12
	8	8	0	58	0	7021	0	0	0	59	0	0	135612	6441	0	0	146	0	0	0	73
	15	26	0	82	0	32215	0	0	0	87	0	0	73759	5221	0	115	0	0	0	63	5
	36	11	0	43	247	26457	1527	248	0	53	0	0	87444	2830	0	18	0	0	0	84	0
	45	34	0	0	1121	25875	0	0	0	119	0	0	55788	3339	0	56	0	0	0	58	0
	59	13	0	3	0	17637	0	0	0	74	0	0	82340	3919	0	0	0	0	0	31	0
	Da.F.2	15	0	85	0	6820	0	0	0	44	0	0	83562	5462	0	0	0	0	0	0	0
	Da.F.3	14	0	61	0	11831	0	0	0	130	0	0	80129	6999	0	23	0	0	0	0	0
	Di.F.4	0	0	62	0	0	329	258	0	80	0	0	146572	4429	0	0	0	1	0	0	0
	Di.F.6	0	0	47	0	5342	0	0	0	95	0	0	127614	7484	0	0	0	0	0	0	0
	Di.F.7	0	0	32	16818	1761	418	280	0	58	0	0	129740	5124	0	0	0	0	0	0	0
	M.F.1	49	0	32	0	17107	0	0	0	96	0	0	79303	5919	0	15	4	0	0	0	0
	44	8	0	0	0	5476	0	0	0	96	0	0	42949	3255	0	0	14	0	0	0	0
	70	10	0	38	736	3180	0	0	0	114	0	0	104014	7811	0	0	68	0	0	0	0
	76	107	0	158	2306	157172	698	26	40	305	0	0	6348	171	0	409	0	0	0	1052	43
	84	12	0	24	0	11382	0	0	0	139	0	0	87256	5875	0	161	43	0	0	0	0
	87	20	0	20	0	15771	2712	398	0	213	0	0	87986	3647	0	0	44	0	0	0	0
	21	15	0	44	239	25919	0	0	0	129	0	0	43454	3728	0	171	0	0	0	166	0
	26	9	0	70	0	28569	8996	465	0	28	0	0	101438	3739	0	0	54	0	0	49	0
	56	64	0	52	1655	62655	2017	282	0	210	0	0	31132	2286	0	190	0	0	0	377	0
	85	56	0	24	0	37887	2546	350	0	351	0	0	88898	3787	0	113	31	0	0	239	0
	41	15	0	72	0	42409	8081	520	0	154	0	0	38329	1582	0	0	0	0	0	190	0
	77	38	0	9	16197	43466	0	0	0	215	0	0	34744	2758	0	156	0	0	0	308	0
	28	91	0	192	263	113436	982	82	428	268	0	0	1675	58	0	529	0	0	0	1834	0
	33	6	2866	40	0	33354	573	115	439	364	0	0	2473	86	0	97	0	0	0	304	0
	11	58	0	110	379	83054	497	93	105	227	0	0	16895	932	0	207	0	0	0	397	62
	64	255	0	105	334	22185	116	116	829	330	0	0	13448	742	0	1169	0	0	0	3199	5
	88	71	0	47	1909	10250	1201	103	497	413	0	0	17533	752	0	866	0	0	0	1714	13
	22	13	0	0	208	1480	0	0	0	204	0	0	15235	2249	0	81	0	0	0	0	0
	10	11	0	14	0	0	0	0	0	179	0	0	26626	497	1784	0	0	0	0	0	0
	17	13	578	0	0	0	0	0	0	203	0	0	1055	0	132	37	0	0	0	0	0
	34	1	0	0	253	0	438	1	0	209	0	0	5018	17	306	1	0	0	0	30	0
	49	3	0	0	0	0	4705	46	0	208	437	0	500	0	135	0	0	0	0	34	0
	60	8	0	5	981	0	0	0	0	208	437	0	500	0	297	0	0	0	0	13	0
	79	1	2000	0	0	0	490	0	0	266	149	0	167	0	51	0	0	0	0	20	0
	95	11	0	20	271	735	334	0	287	228	3	39	1909	0	345	3	0	0	0	0	16
	Da.F.1	0	0	69	0	2588	0	0	0	72	0	0	137869	7415	0	0	202	0	0	0	0
	86	0	0	0	0	2458	1630	408	0	163	0	0	94275	5162	0	0	39	0	0	0	0
	Di.F.5	111	0	25	0	23964	6871	342	146	219	0	0	31173	1447	0	463	0	0	0	910	0
	Di.F.9	22	0	47	116	45767	384	0	0	233	0	0	14457	1585	0	142	0	0	0	139	72
	16	16	0	95	0	8173	0	0	0	74	0	0	112089	6033	0	42	88	0	0	0	0
	SA.X.2	27	0	103	1847	45909	12174	1000	0	160	0	0	25342	1711	0	89	0	0	0	359	0

### III.7: MIXTURE INFERENCE OF SELECTED OCCASIONAL COLORS

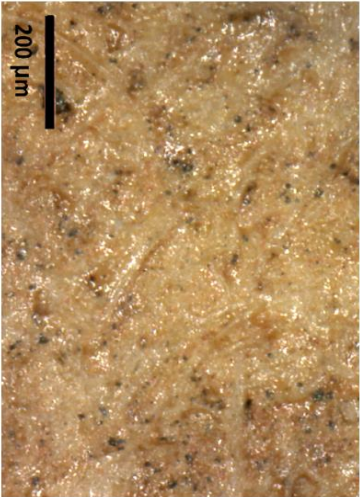
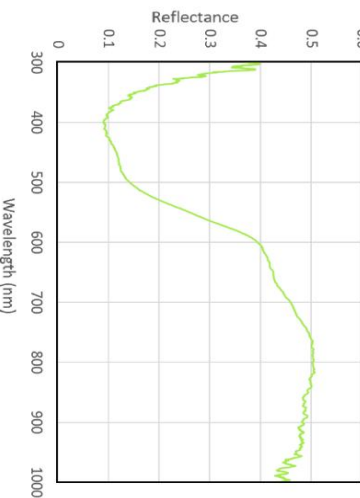

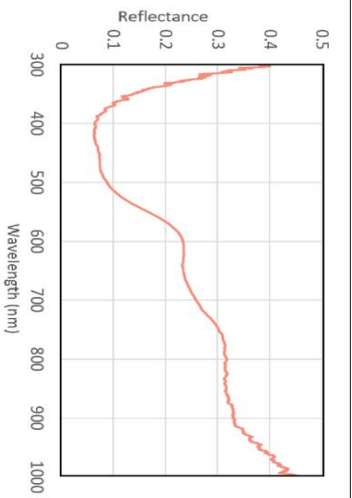
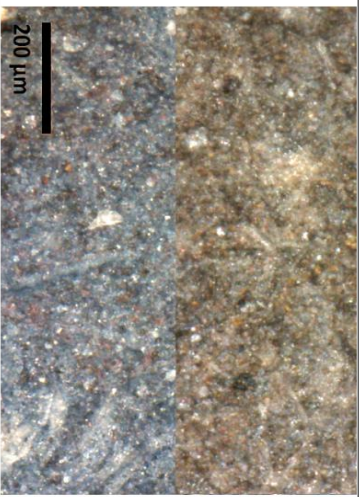
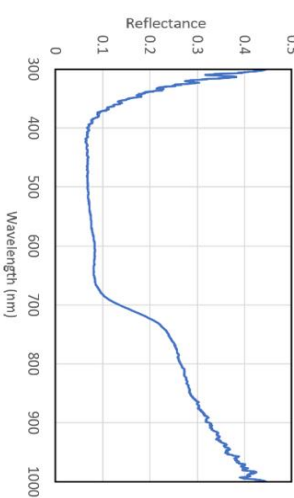
Color	Digital microscopy	FORS	XRF	Conclusions
Warm pale pink (78)			<b>Pb, Fe, Hg (Al, Sr, Ti)</b>	Lead white Yellow ochre Cinnabar
Purple-brown ditch (16)			<b>Pb, Fe (Al, Sn, Si, Mn, Cr)</b>	Lead white Carbon black Yellow ochre Cochineal lake
Olive-green to brown (Di.F.9)	<p>Black pigment + yellow ochre + lake pigment (pink)</p> 	<p><i>Spectrum not diagnostic</i></p> 	Lead white + iron oxide + lake pigment <b>Pb, Fe (Hg, Cu, Cr, Al, Mn, Si, Ti, Zn)</b>	Lead white Carbon black Yellow ochre
	<p>Black pigment + yellow ochre + HgS</p> 	<p>Yellow ochre</p> 	Lead white + iron oxides + HgS + copper-based green	With minor amounts of cinnabar and copper-based green

### III.7: MIXTURE INFERENCE OF SELECTED OCCASIONAL COLORS (cont.)

Color	Digital microscopy	FORS	XRF	Conclusions
Orange-pink walls (75, M.F.2)			<p>(75) <b>Pb, Fe, Hg</b> (Cr, Cu, Mn, Sn)</p> <p>(M.F.2) <b>Pb, Fe, Hg</b> (Al, Cr, Cu, Mn, Sn)</p>	<p>Lead white Yellow ochre Cinnabar Cochineal lake</p>
Orangeish-red bastion (86)			<p>Lead white + iron oxide + HgS + lake pigment</p> <p><b>Pb, Fe, Hg</b> (Mn, Sn)</p>	<p>Lead white Yellow ochre Cinnabar Cochineal lake</p>
Reddish-tan terrain (84)			<p>Lead white + HgS + iron oxide + lake pigment</p> <p><b>Pb, Fe</b> (Al, Cr, Mn, Si, Sn)</p>	<p>Lead white Yellow ochre Cochineal lake</p> <p><i>With very minor amounts of cinnabar and carbon black</i></p>

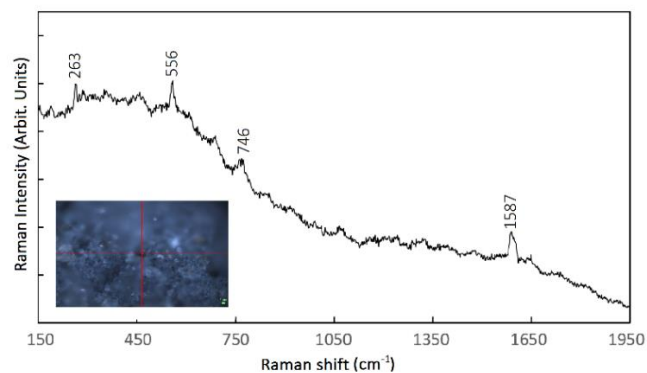


### III.7: MIXTURE INFERENCE FOR SELECTED OCCASIONAL COLORS (cont.)

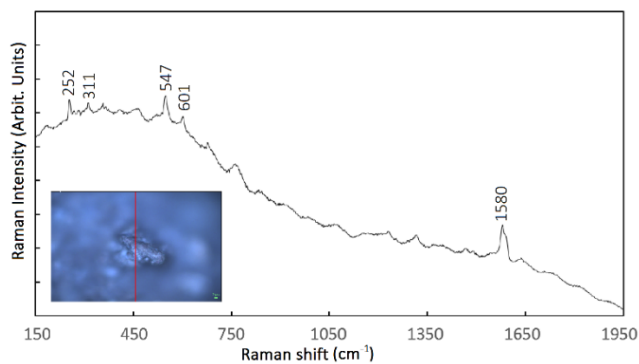
Color	Digital microscopy	FORS	XRF	Conclusions
Orangeish-tan bastion (87)			Pb, Fe, Hg (Al, Cr, Mn, Sn)	Lead white Yellow ochre Cinnabar  <i>With minor amounts of cochineal lake pigment</i>
Dull yellowish-tan tower (76)	Yellow ochre + black pigment	Yellow ochre	Lead white + iron oxides + HgS	Yellow ochre Lead white Carbon black  <i>With minor amounts of cinnabar</i>
			Fe, Pb (Al, Cr, Cu, Hg, K, Mn, Ti, Si, Zn)	
Stippled inlet (Di.F.5)	Yellow ochre + black pigment	Yellow ochre	Iron oxide + lead white + HgS	Indigo Yellow ochre Lead white Cinnabar  <i>With stippling and admixture of carbon black, and minor contribution of the cochineal lake</i>
	Indigo + black pigment + pink lake pigment + yellow ochre	Indigo + yellow ochre	Pb, Fe, Hg (Al, Cr, K, Mn, Si, Ti)	
			Lead white + iron oxides + HgS + lake pigments (pink and blue)	

## III.8: $\mu$ -RAMAN SPECTRA (BY COLOR)

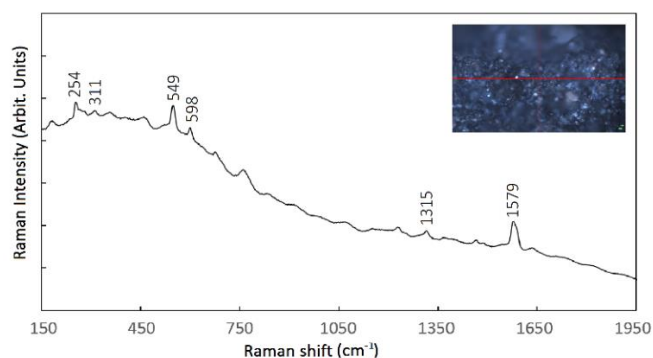
### Blue regions



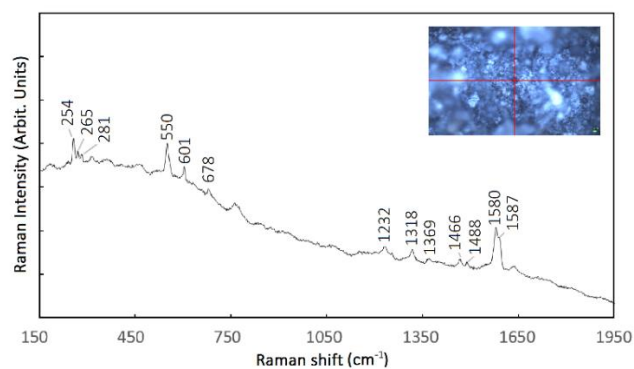
III.8.1: 63 (light blue, Cochim)



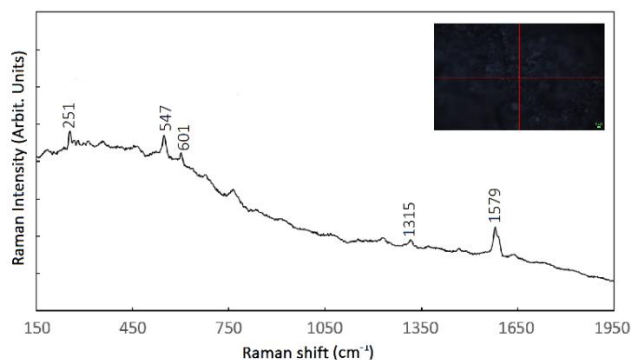
III.8.2: Co.R.6 (medium blue)



III.8.3: Da.R.2

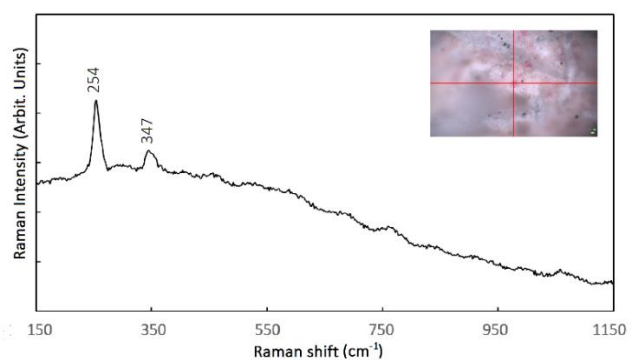


III.8.4: 1 (Dio)

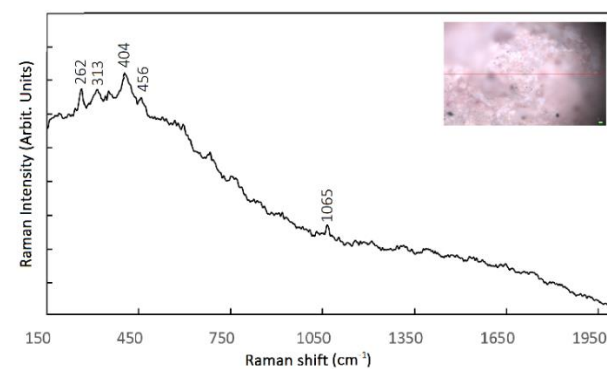


III.8.5: M.R.5

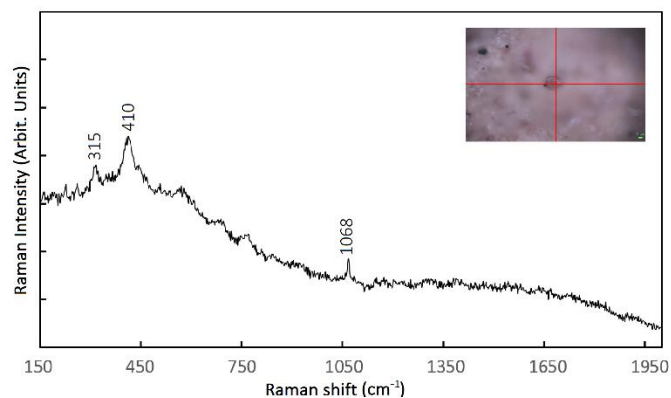
### Tan Regions



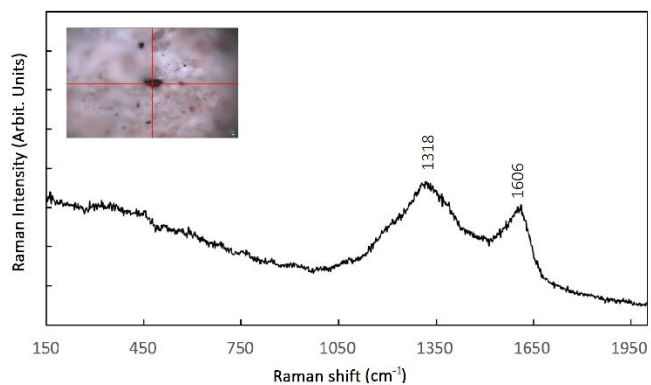
III.8.6: Co.R.4



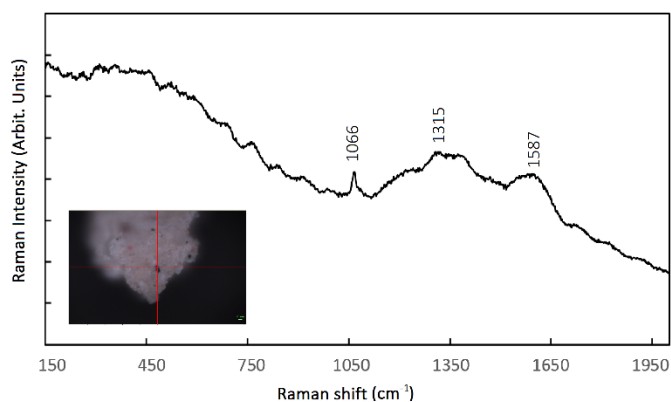
III.8.7: 15 (Damaõ)



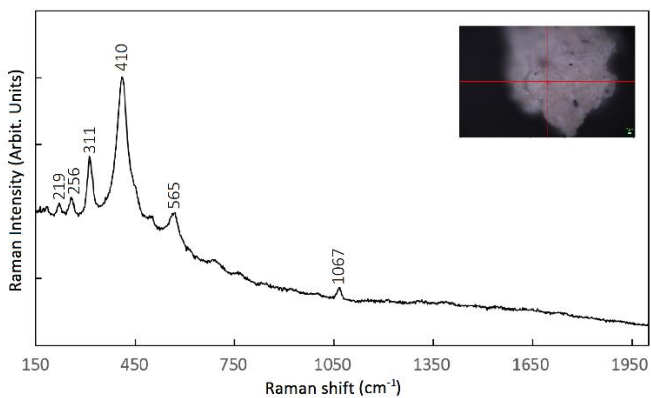
III.8.8: Da.F.3



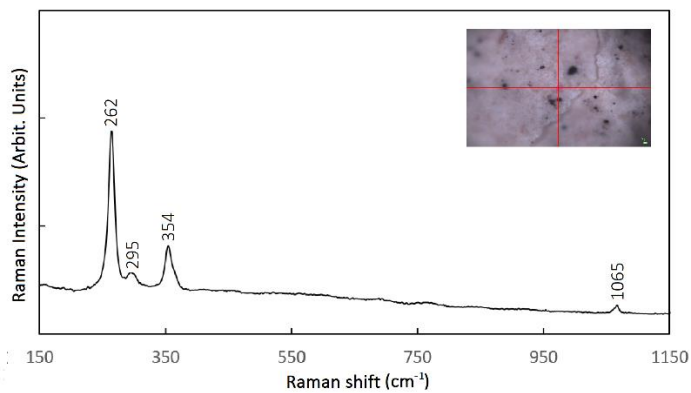
III.8.9: Da.F.3



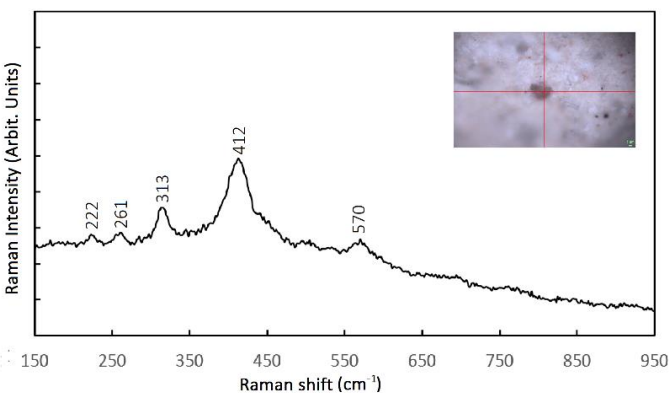
III.8.10: Di.S.4 (sample)



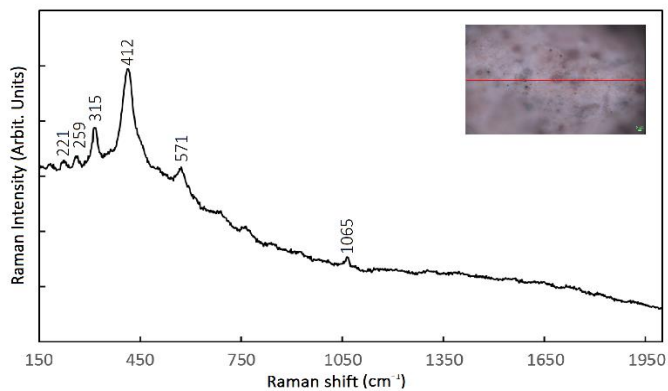
III.8.5.11: Di.S.4 (sample)



III.8.12: Di.S.4 (*in situ*)

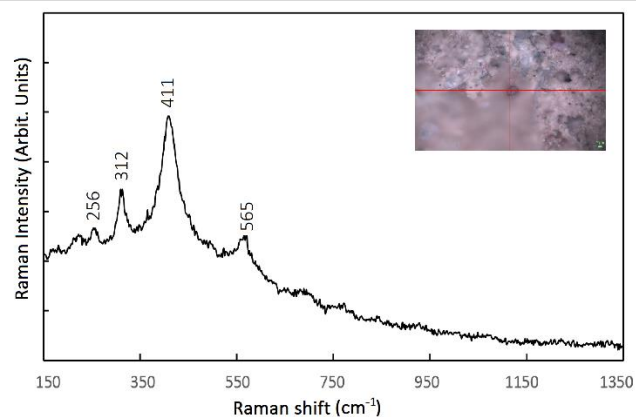


III.8.13: Di.S.4 (*in situ*)

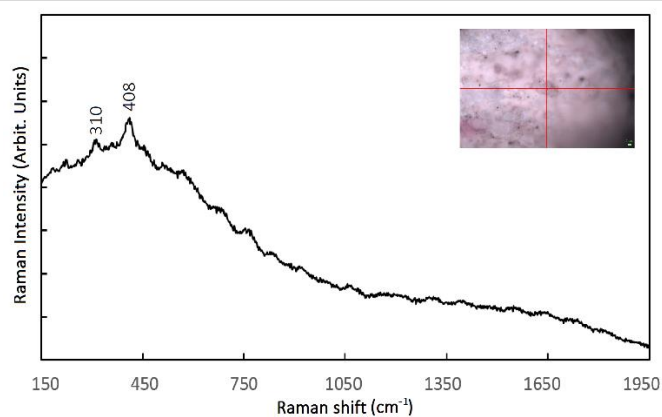


III.8.14: M.R.4

## Brown and brownish-tan regions

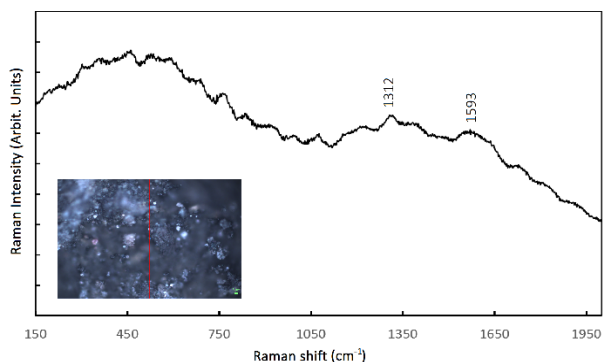


III.8.15: Co.R.5

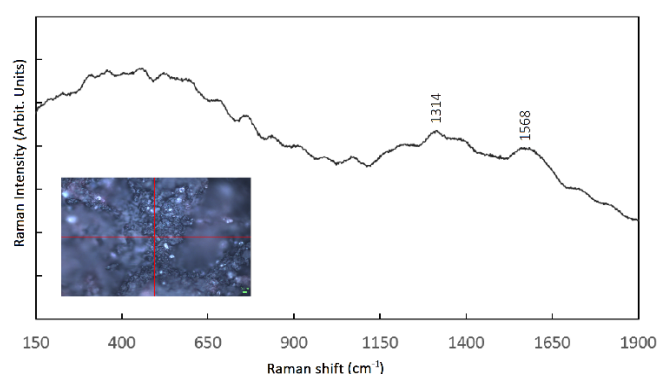


III.8.16: Da.R.1

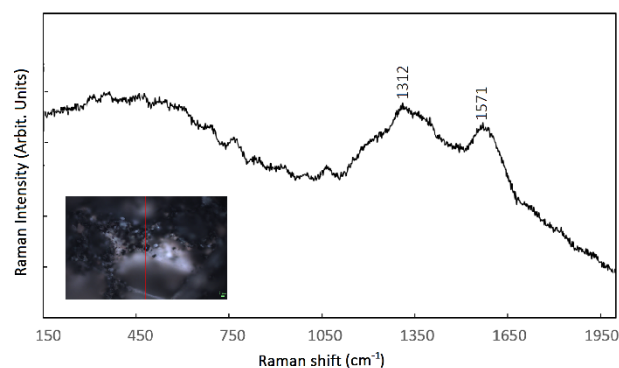
## Black regions



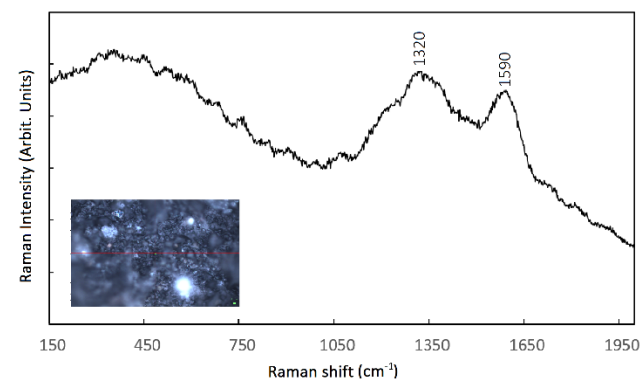
III.8.17: 64 (Cochim)



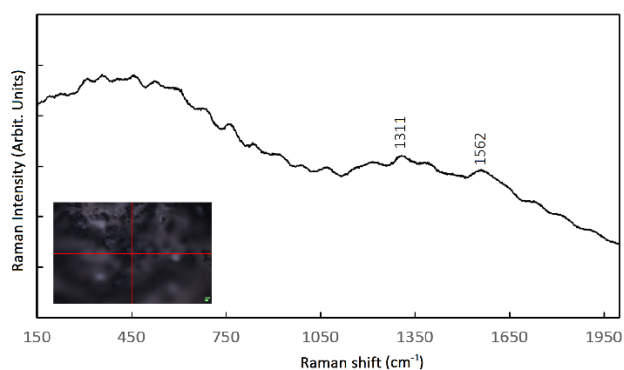
III.8.18: Co.R.2



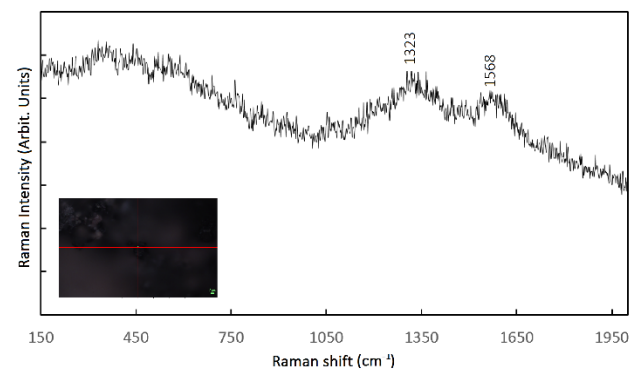
III.8.19: Co.S.3 (*in situ*)



III.8.20: Da.R.4

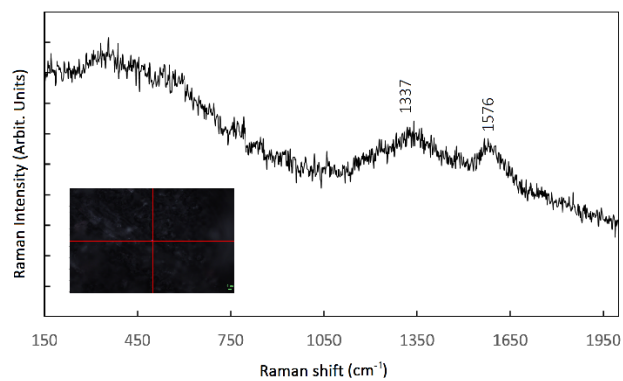


III.8.21: Di.R.8



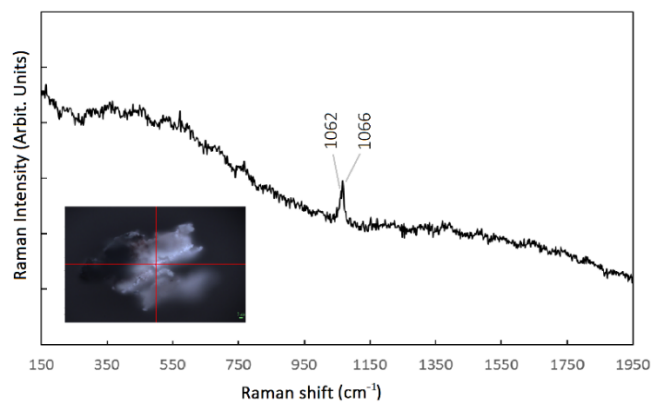
III.8.22: 77 (Mangalor)



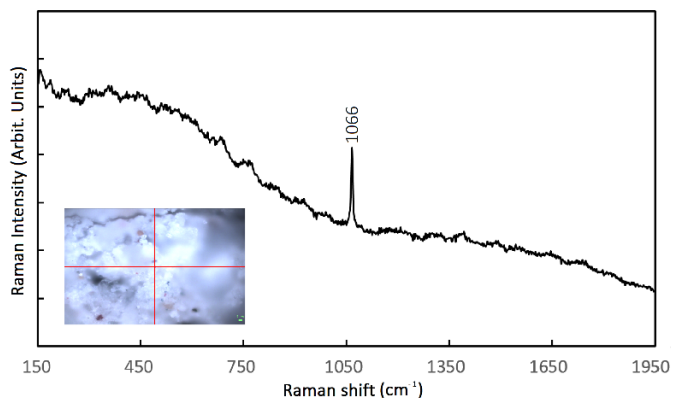


III.8.23: M.R.1

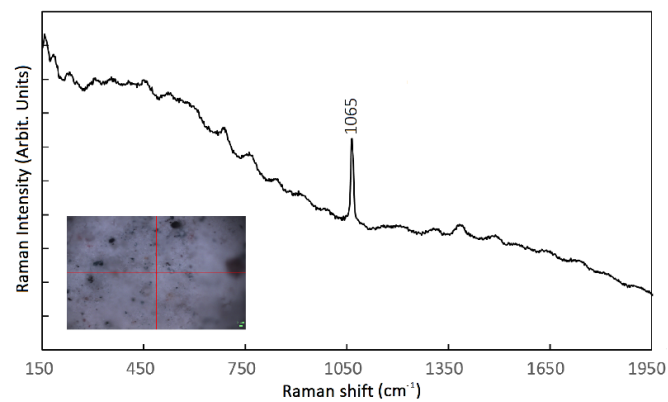
## White Regions



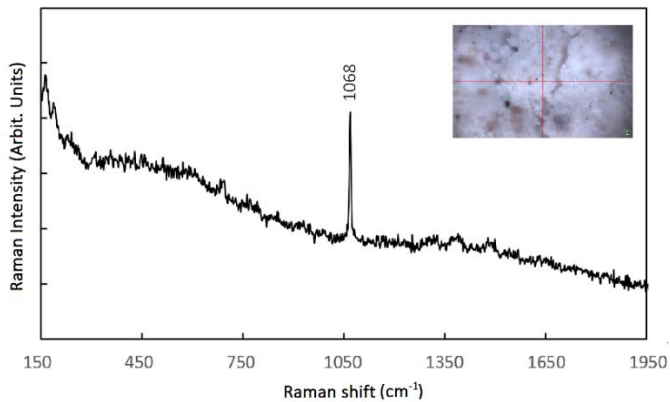
III.8.24: Co.S.1 (sample)



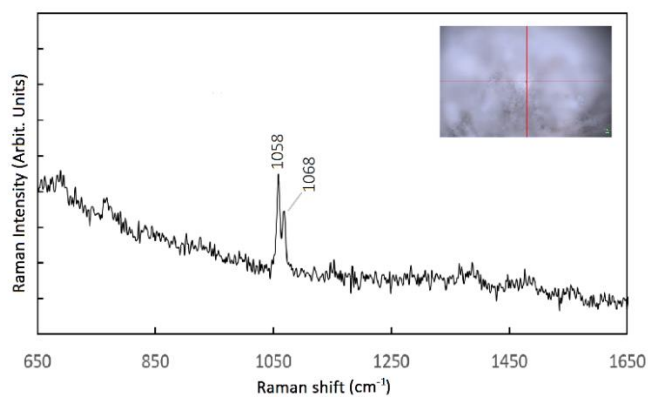
III.8.25: Co.R.1



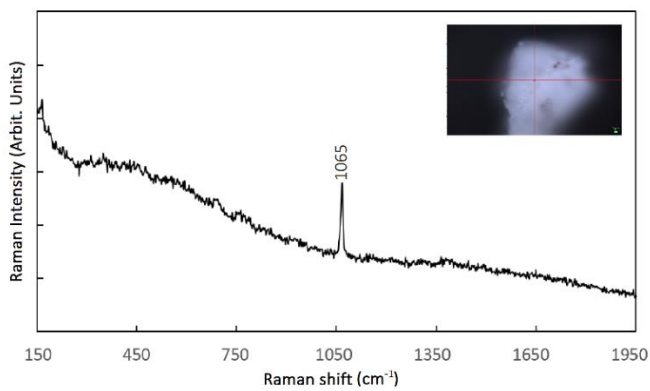
III.8.26: Da.R.3



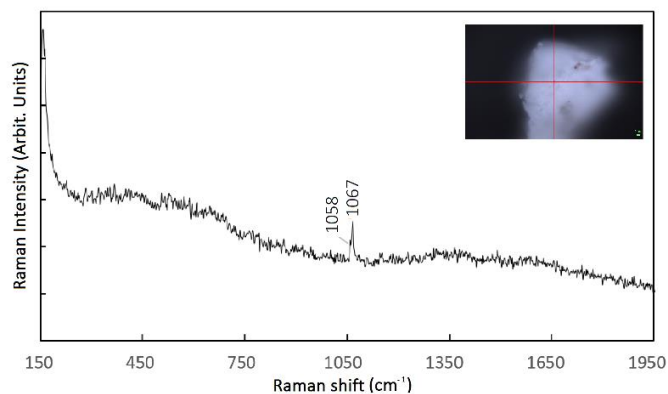
III.8.27: Da.R.6



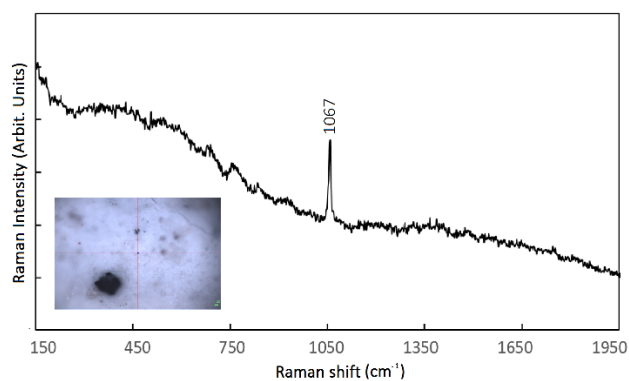
III.8.28: Da.R.6



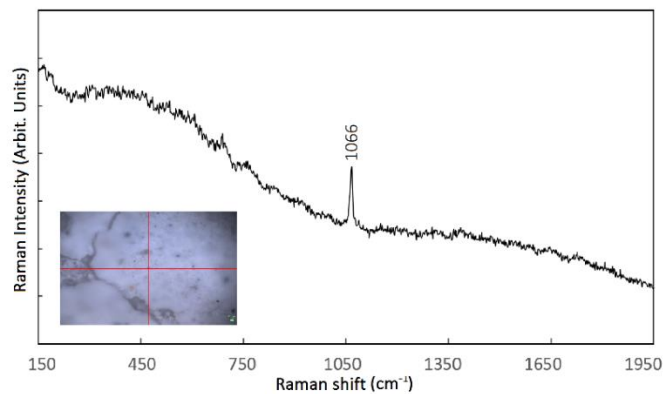
III.8.29: Di.S.2



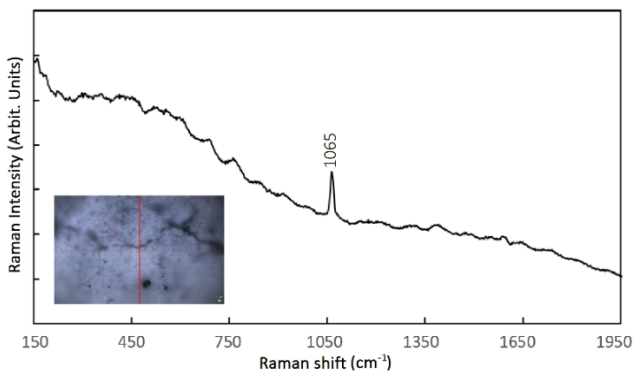
III.8.30: Di.S.2



III.8.31: Di.R.6

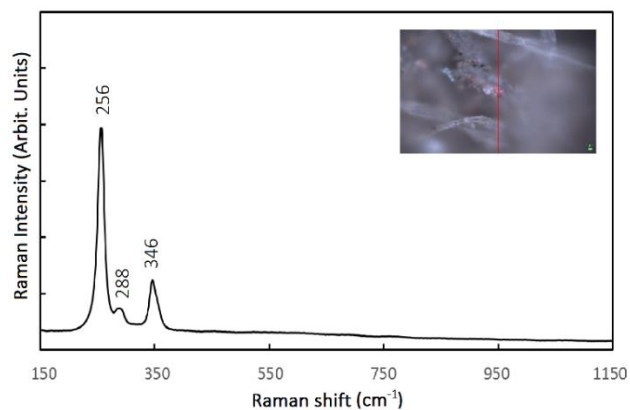


III.8.32: 69 (Mangalor)

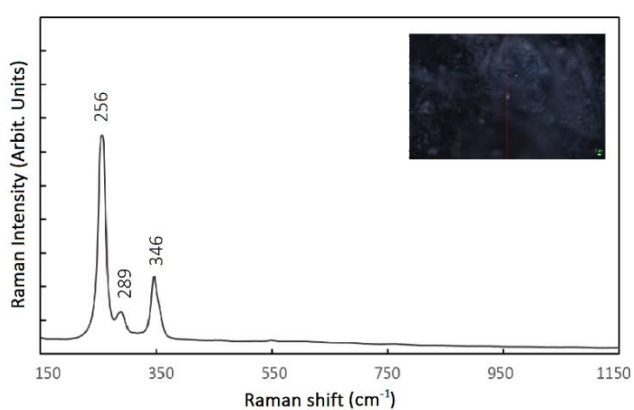


III.8.33: M.R.6

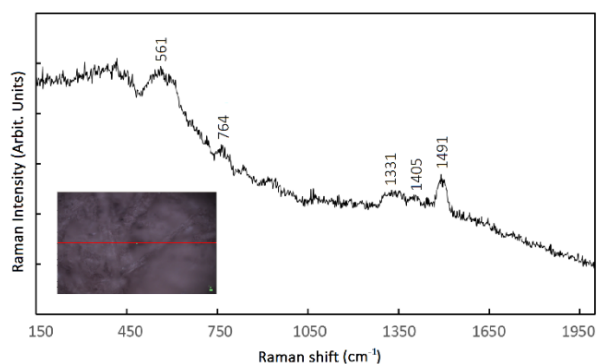
### Regions of Occasional Colors



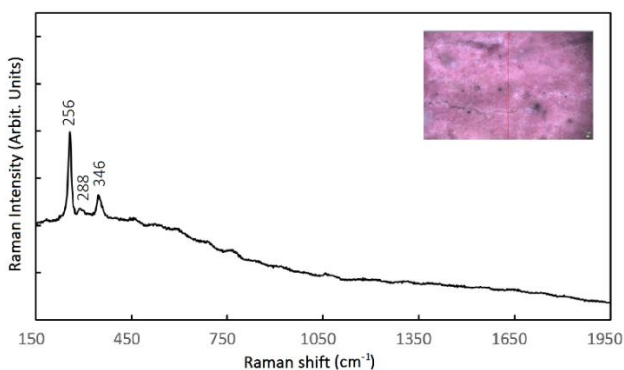
III.8.34: Di.F.9 (olive to brown "bull pen")



III.8.35: Di.R.4 (rocks in overpainted bastion)

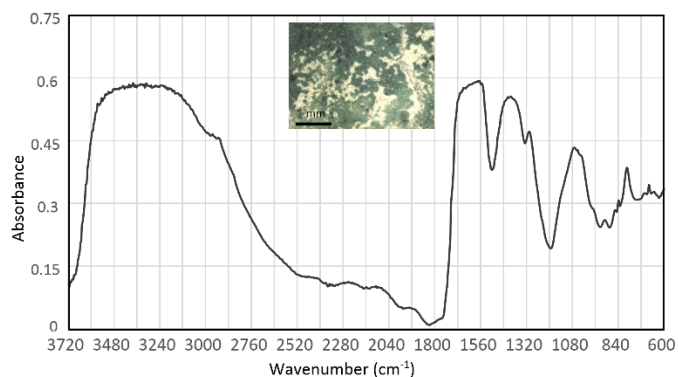


III.8.36: Di.R.9 (ink number on the bottom of the page)

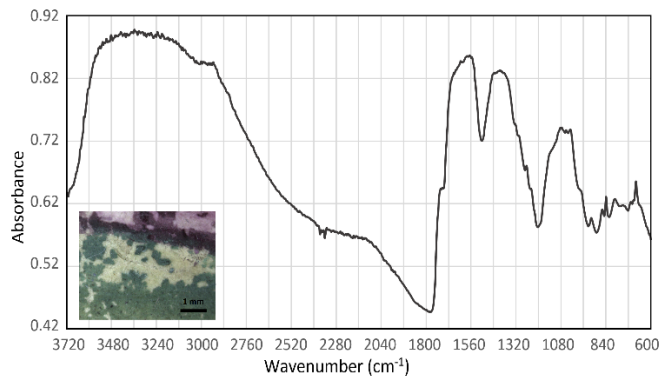


III.8.37: M.F.2 (orange-pink walls)

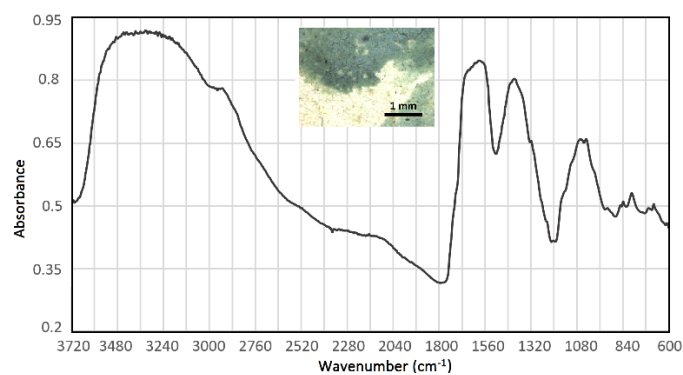
### III.9: $\mu$ -FT-IR SPECTRA (BY COLOR)



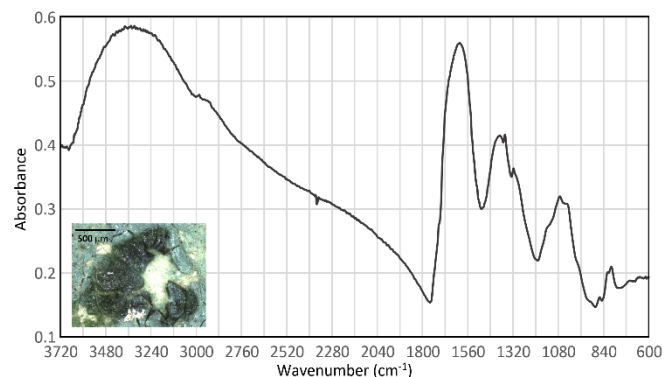
III.9.1: Co.S.2 (green)



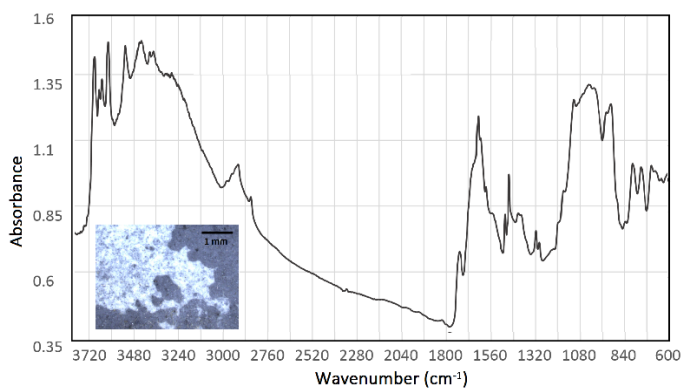
III.9.2: Di.S.3 (green)



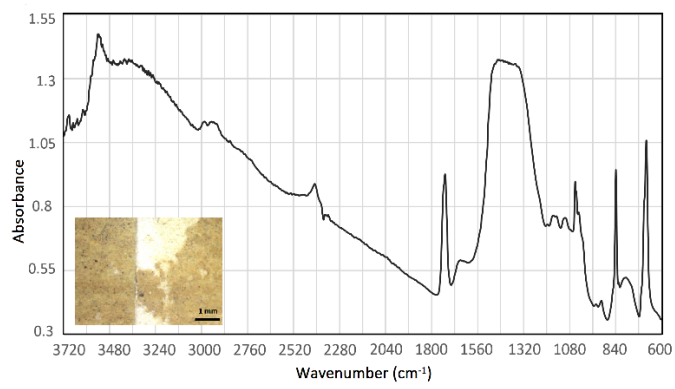
III.9.3: M.S.4a (green)



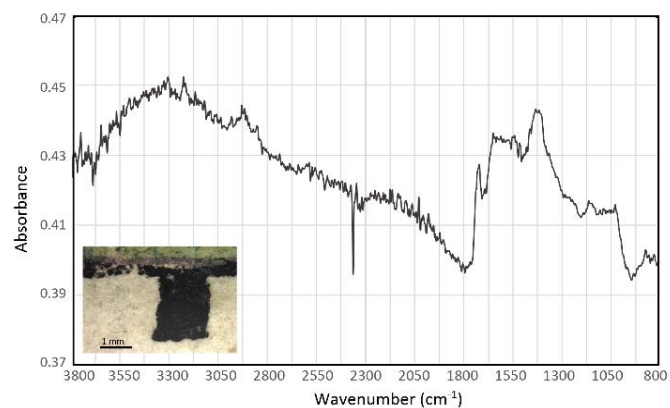
III.9.4: M.S.4b (altered green)



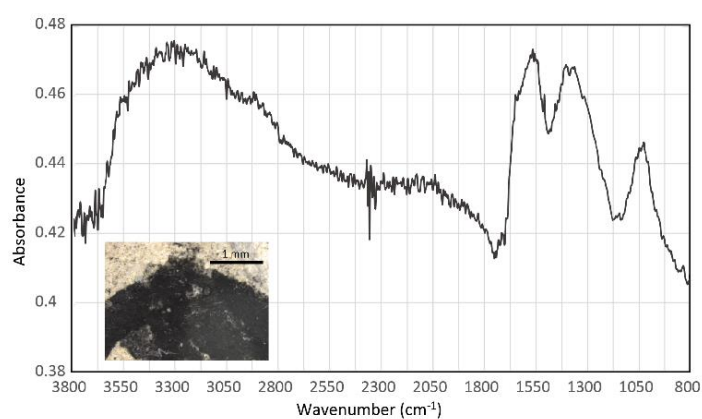
III.9.5: Di.S.1 (blue)



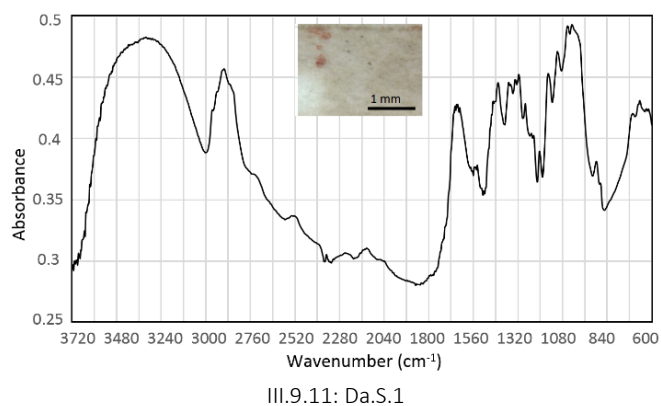
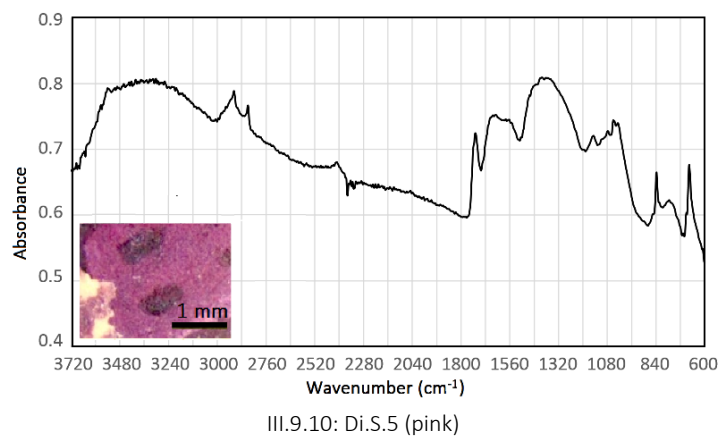
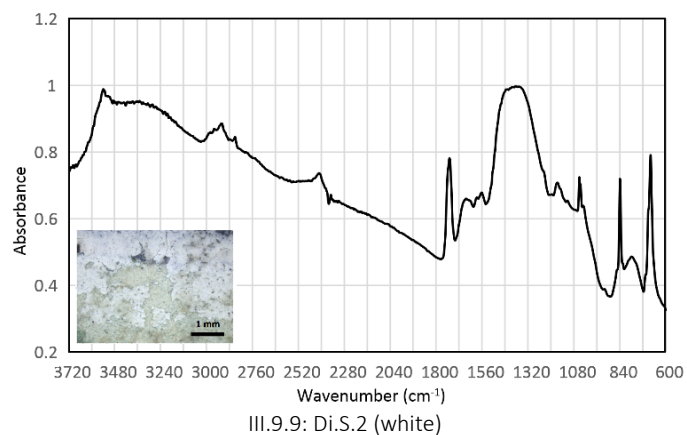
III.9.6: Di.S.4 (tan)



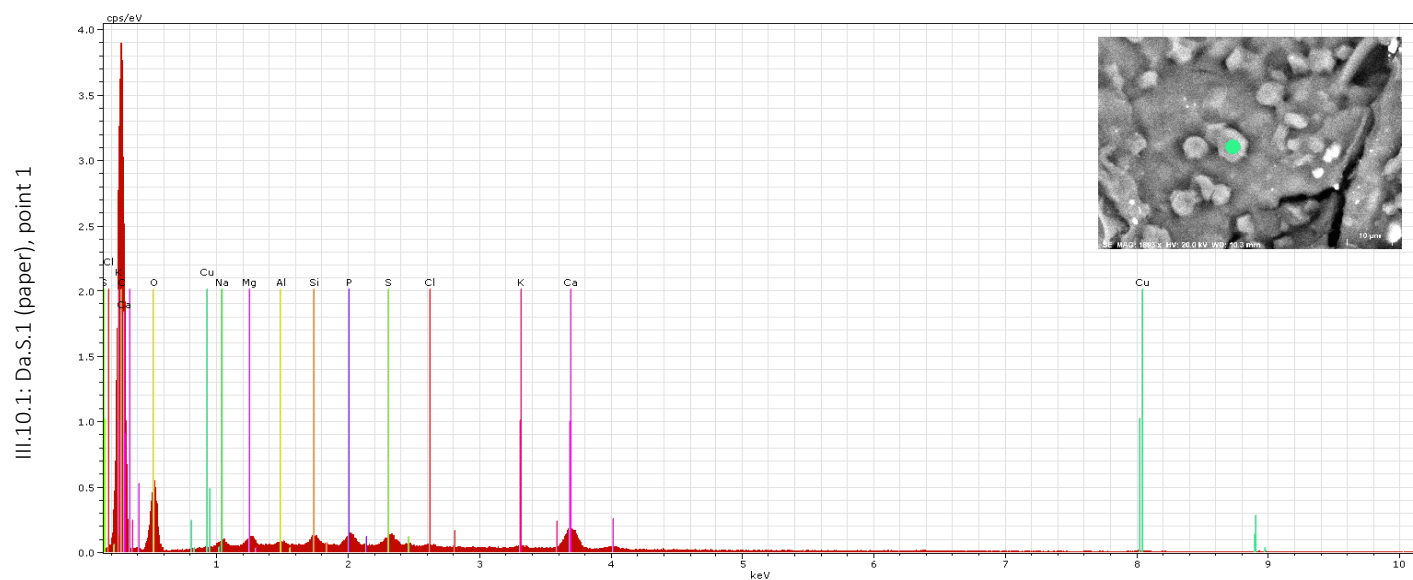
III.9.7: Co.S.4 (black)



III.9.8: Co.S.3 (black)

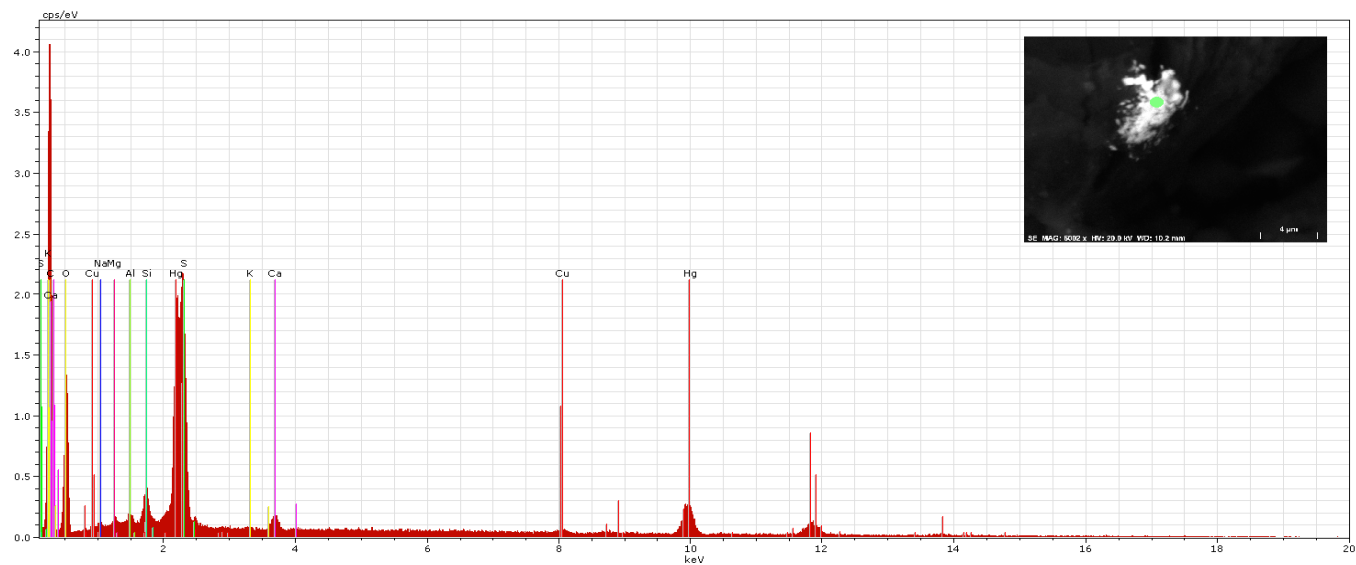


### III.10: EDS SPECTRA (BY COLOR)

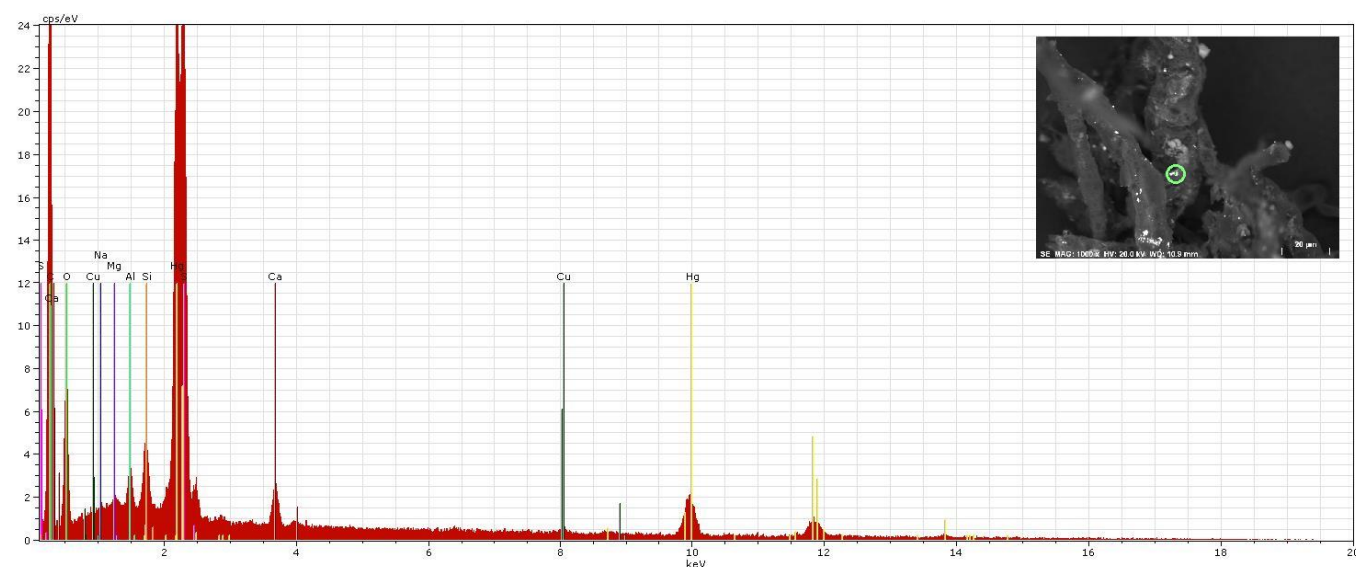




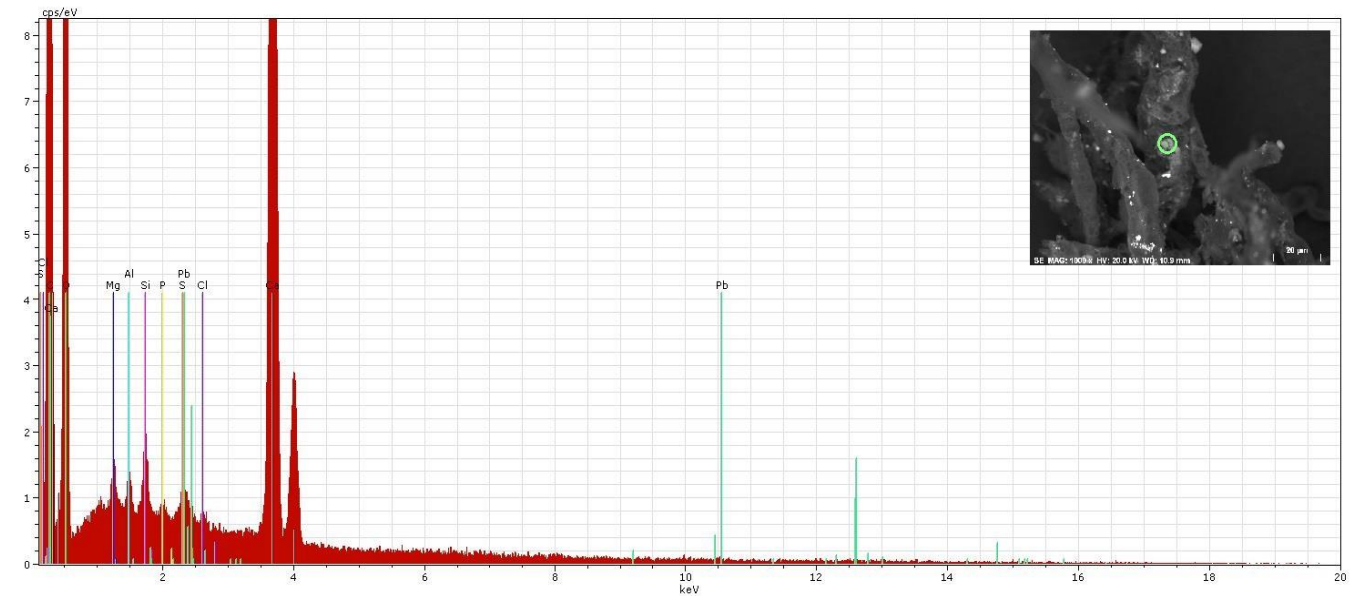
III.10.2: Da.S.1 (paper), point 2



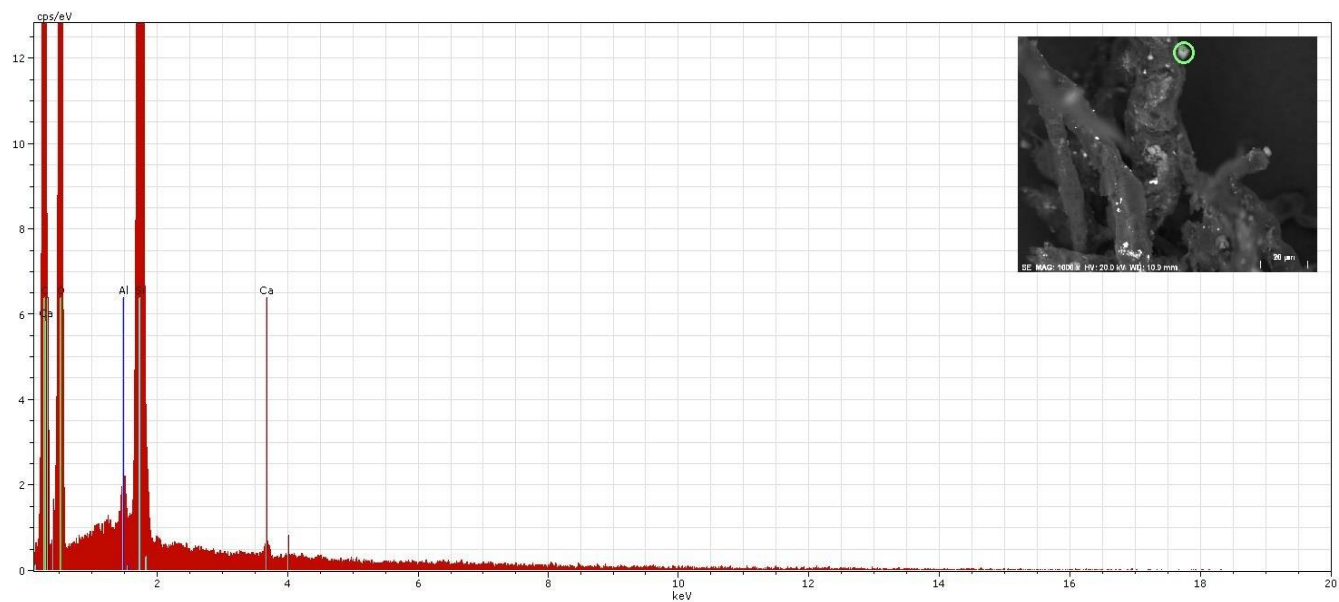
III.10.3: Da.S.1 (paper), point 3



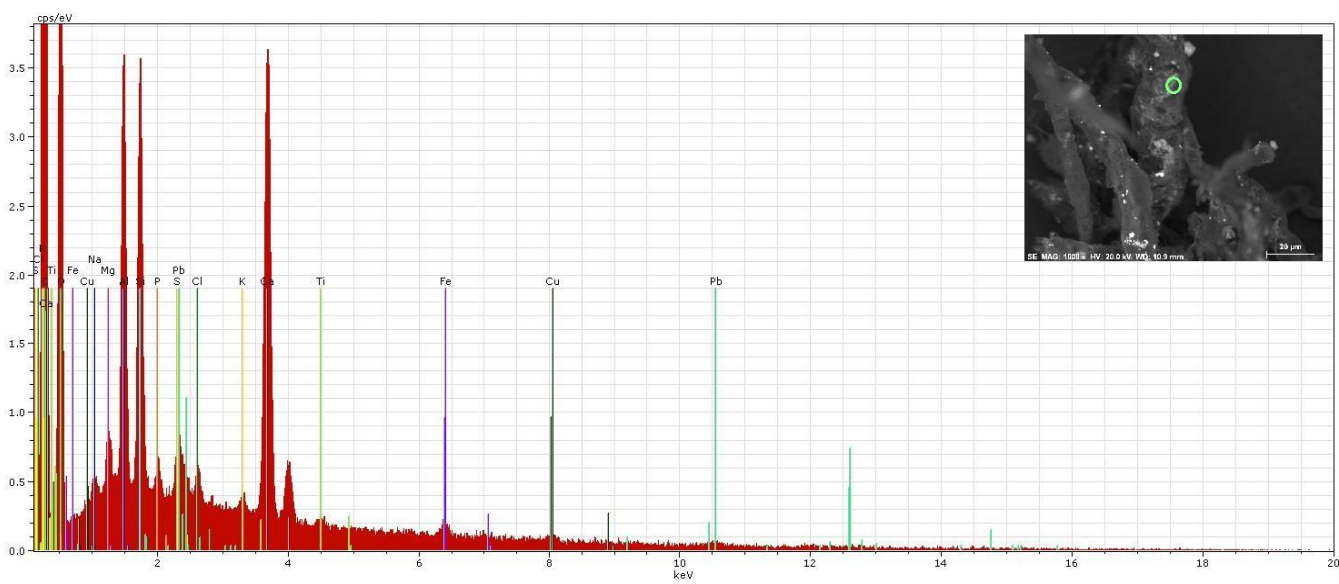
III.10.4: Da.S.1 (paper), point 4



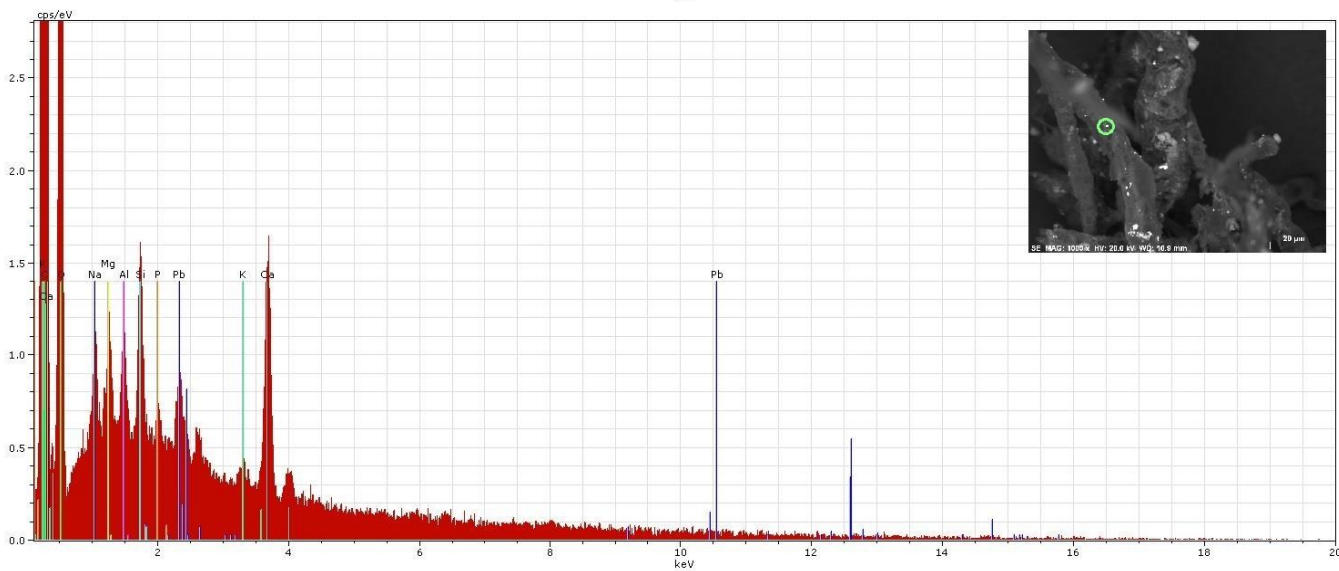
III.10.5: Da.S.1 (paper), point 5



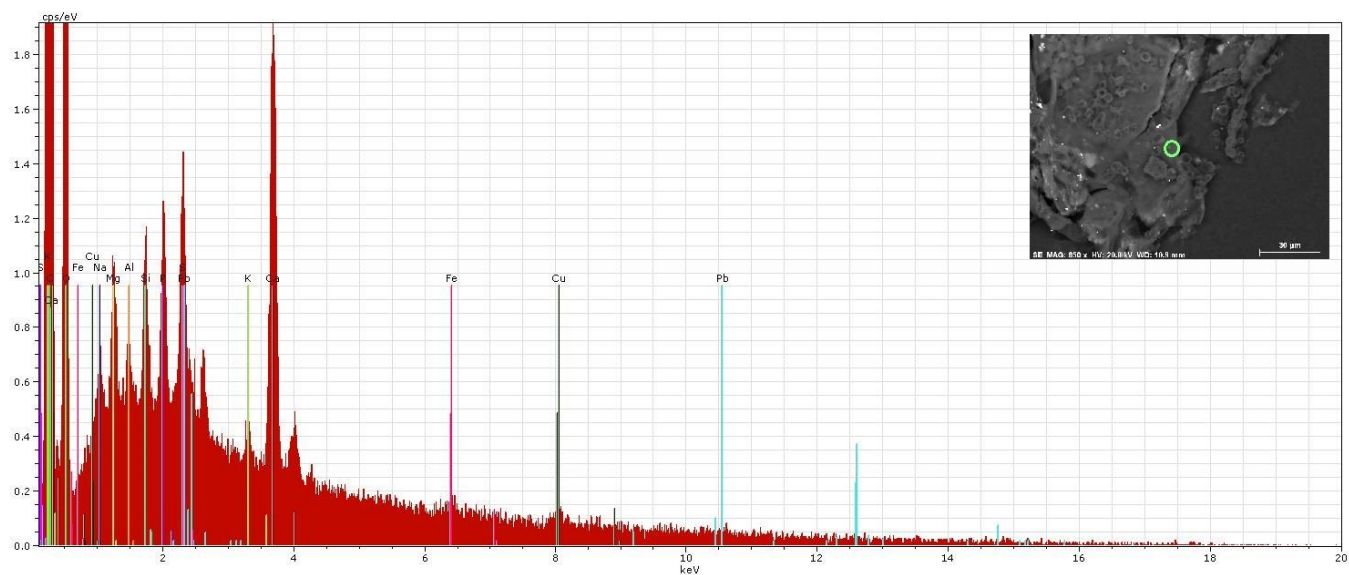
III.10.6: Da.S.1 (paper), point 6



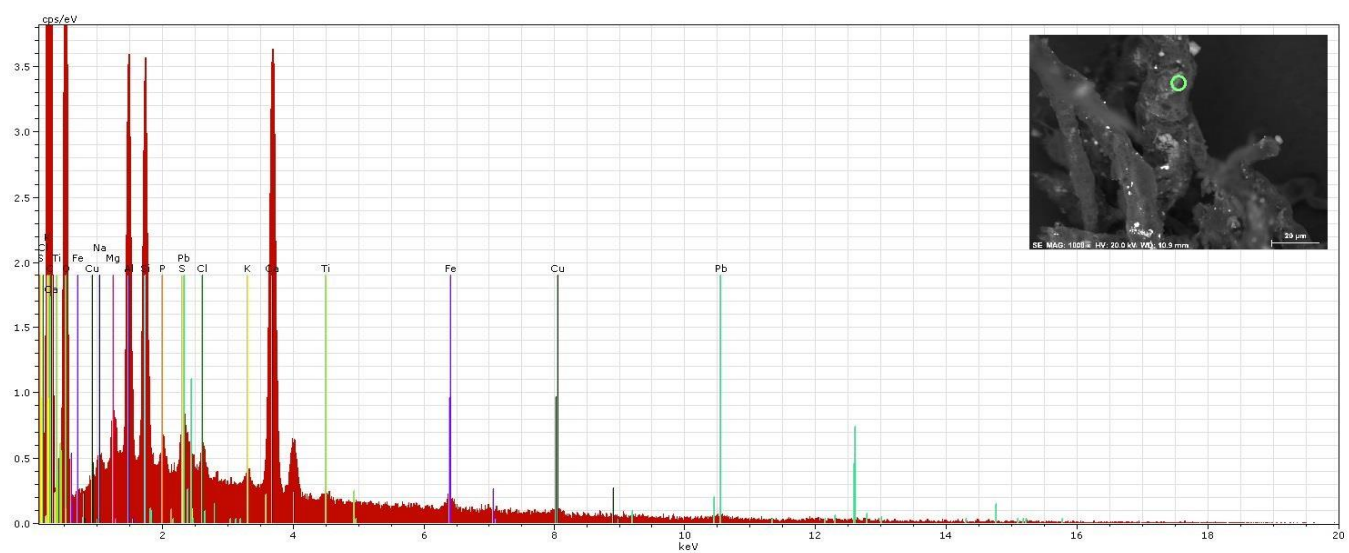
III.10.7: Da.S.1 (paper), point 7



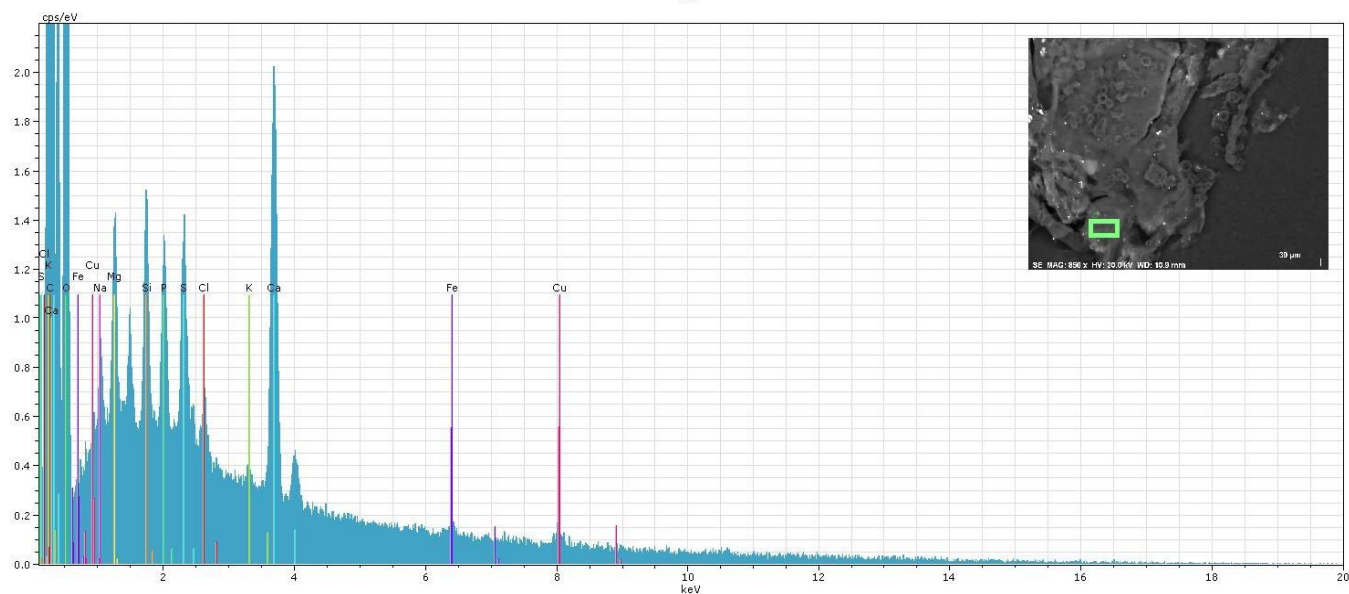
III.10.8: Da.S.1 (paper), point 8



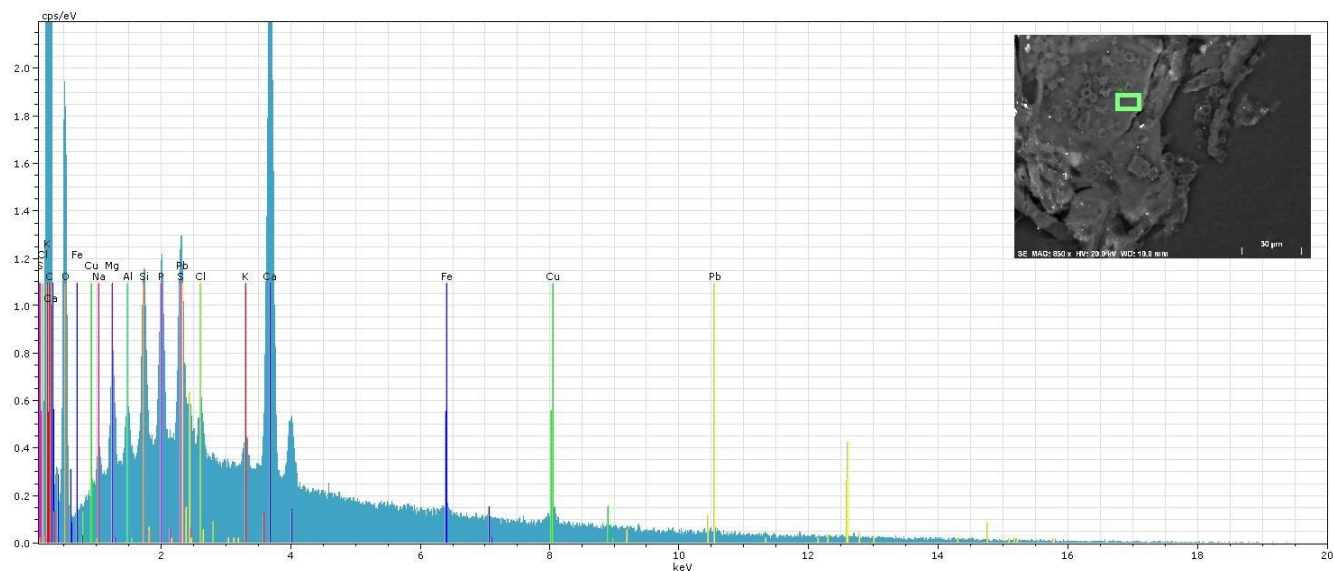
III.10.9: Da.S.1 (paper), point 9



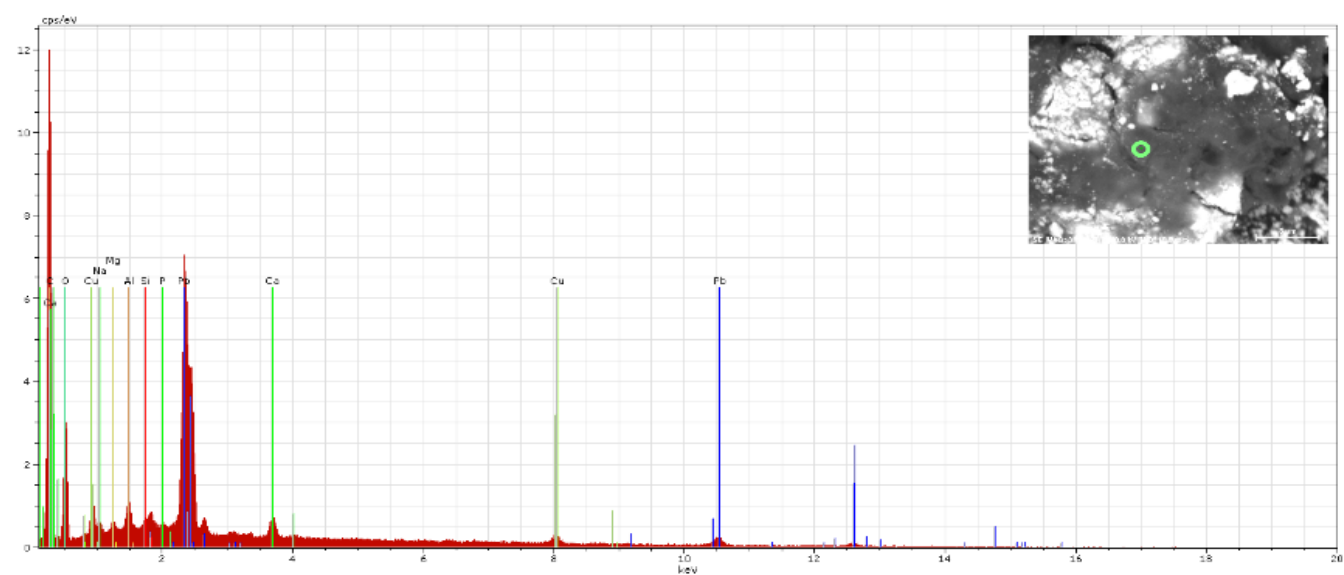
III.10.10: Da.S.1 (paper), area 1



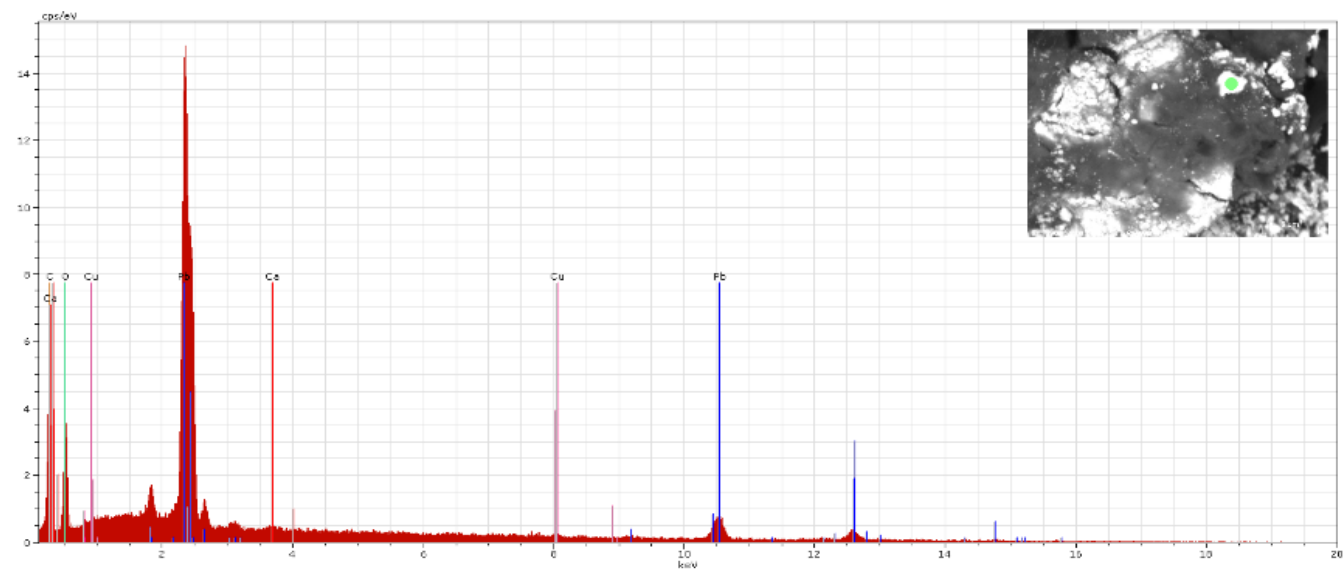
III.10.11: Da.S.1 (paper), area 2



III.10.12: Di.S.5 (pink), point 1

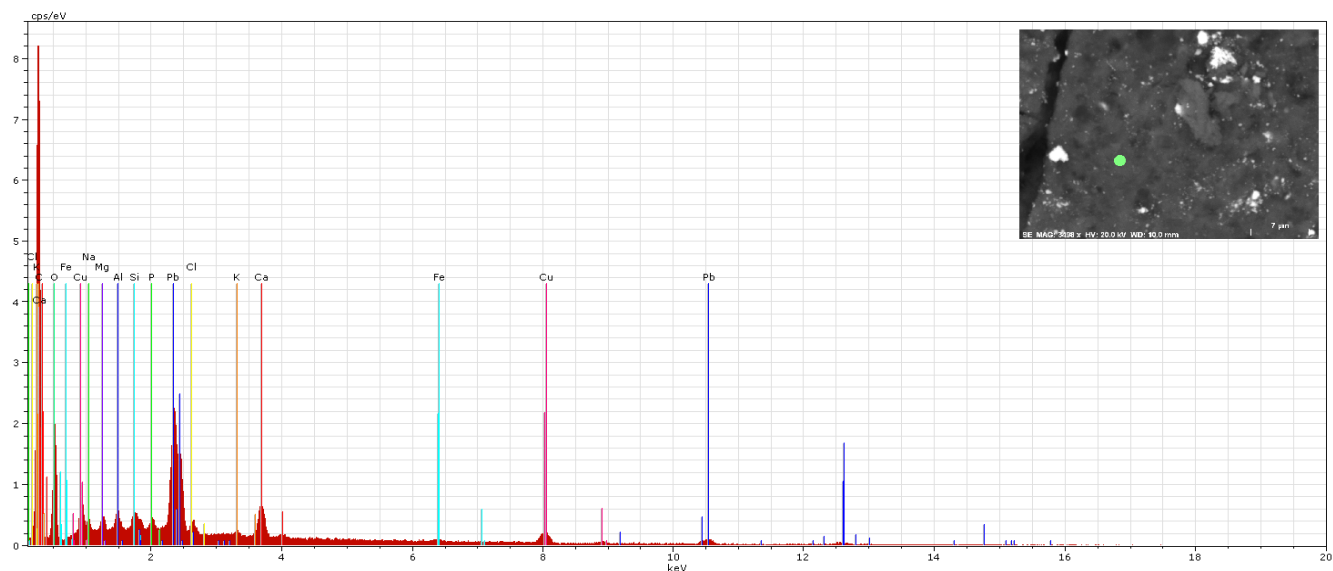


III.10.13: Di.S.5 (pink), point 2

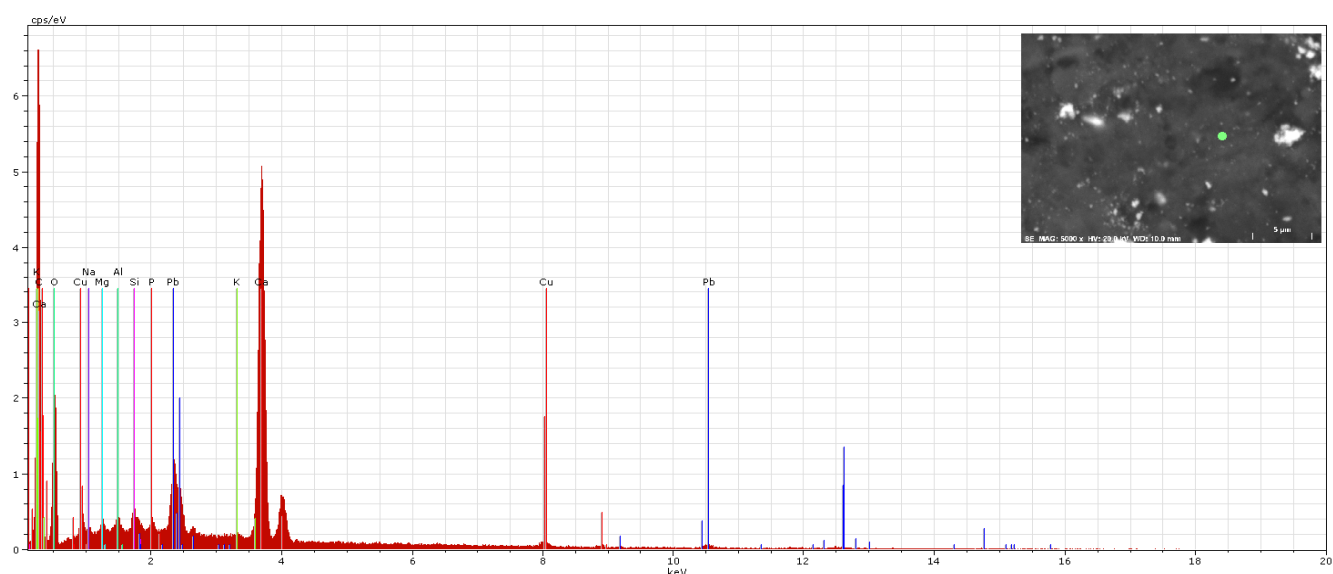




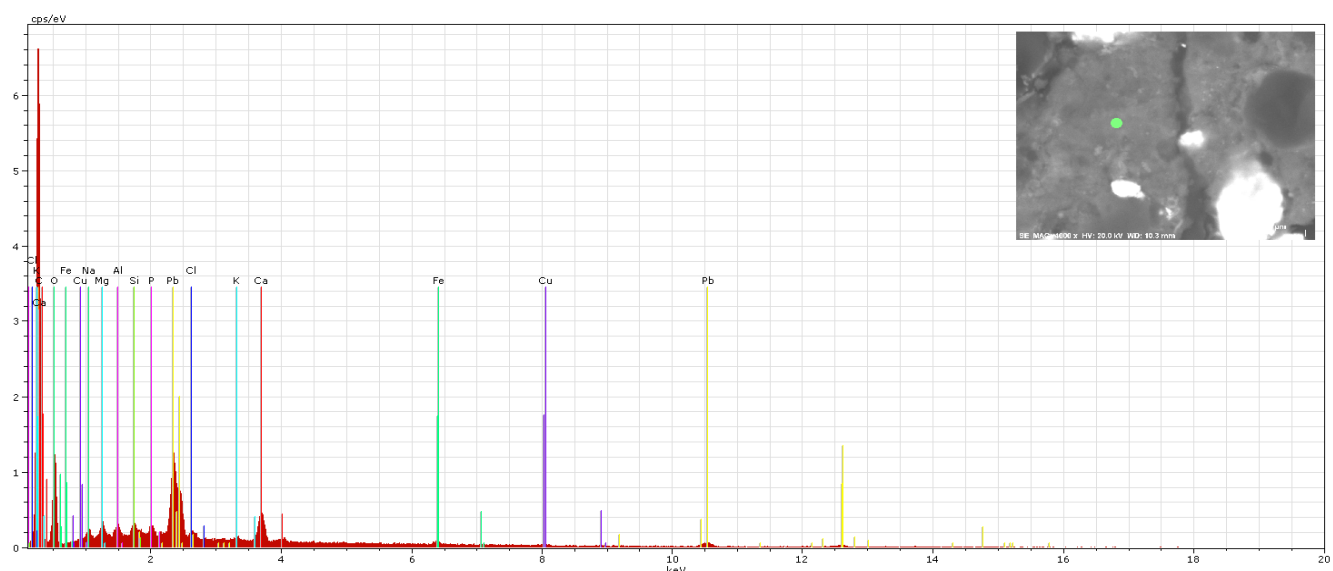
III.10.14: Di.S.5 (pink), point 3



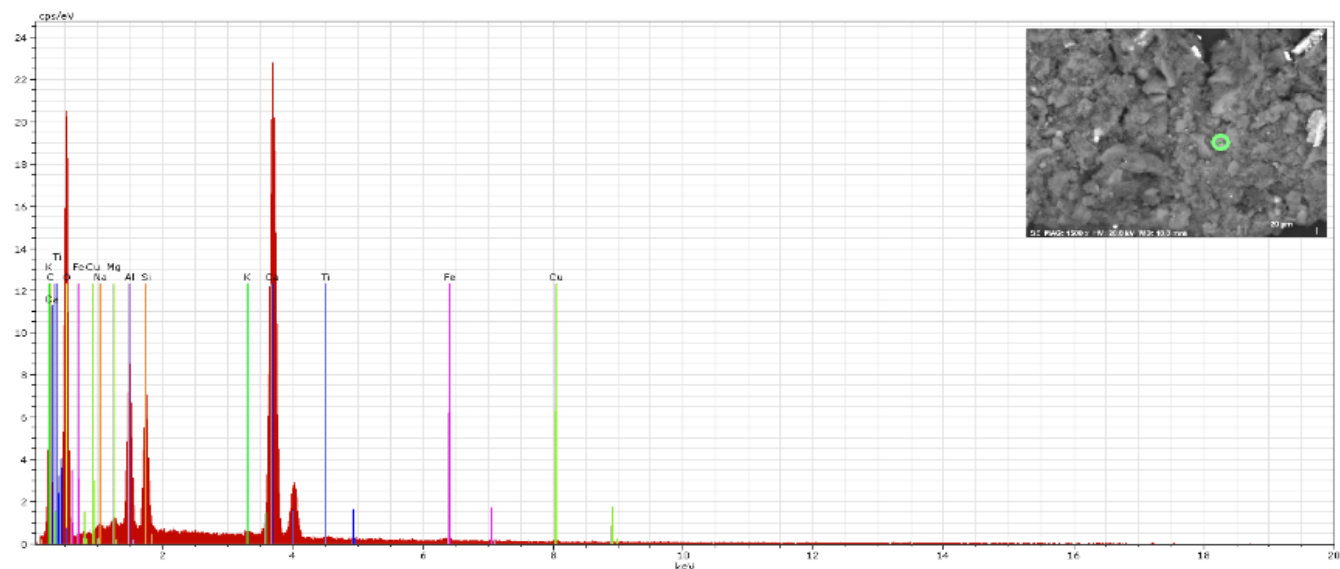
III.10.15: Di.S.5 (pink), point 4



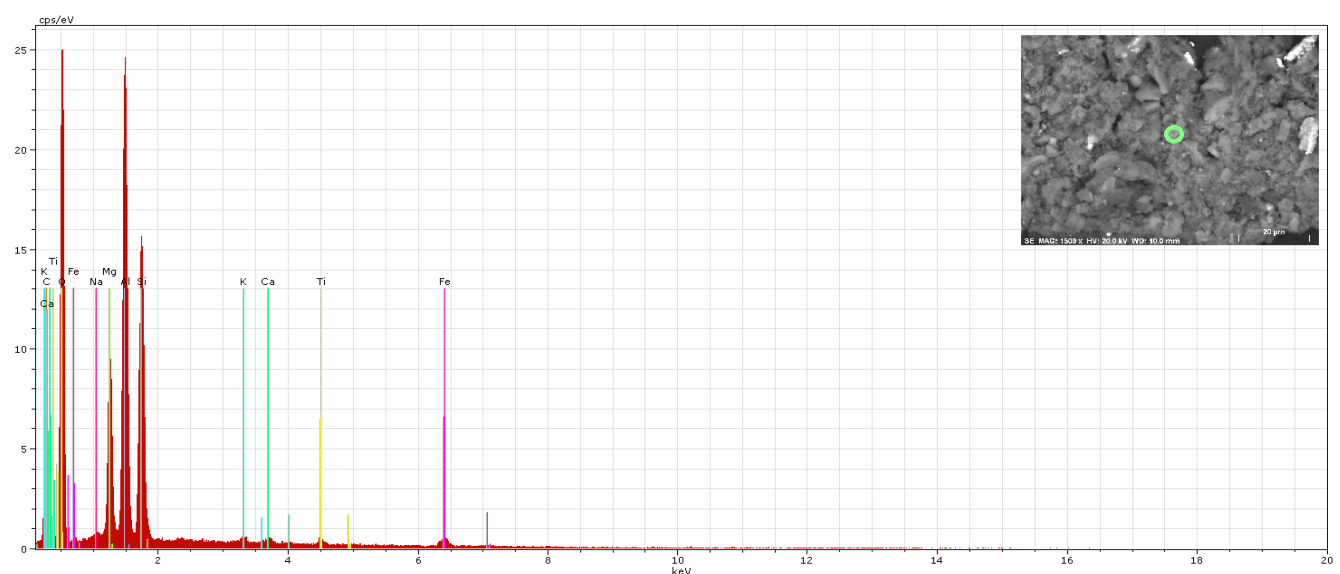
III.10.16: Di.S.5 (pink), point 5



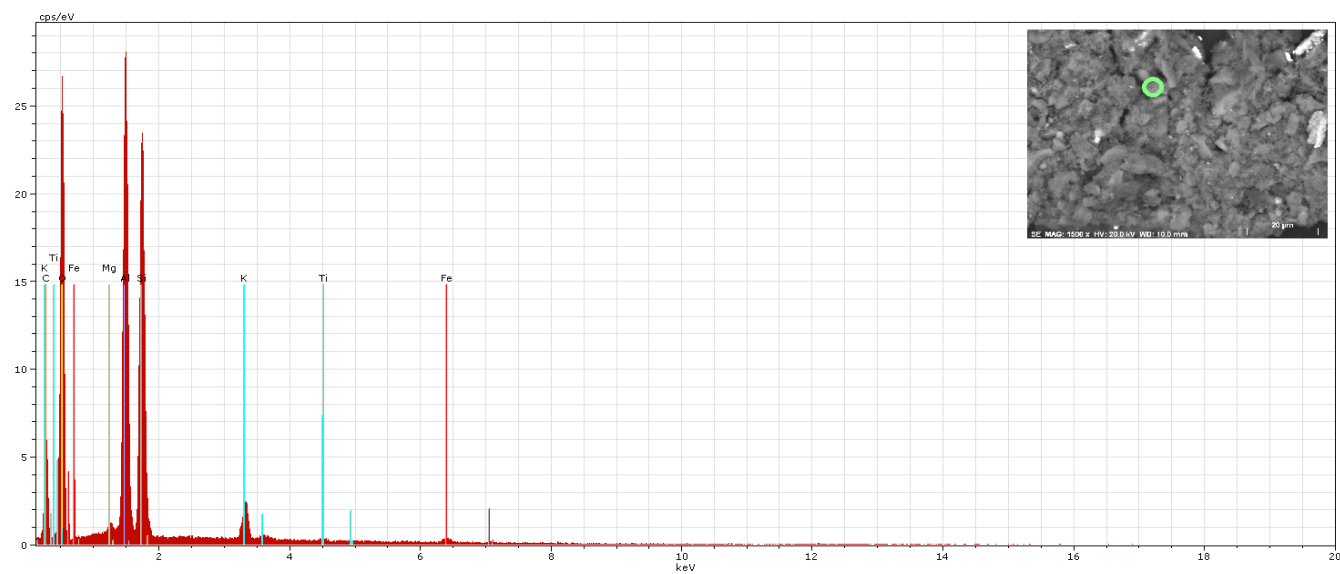
III.10.17: Da.S.2 (blue), point 1



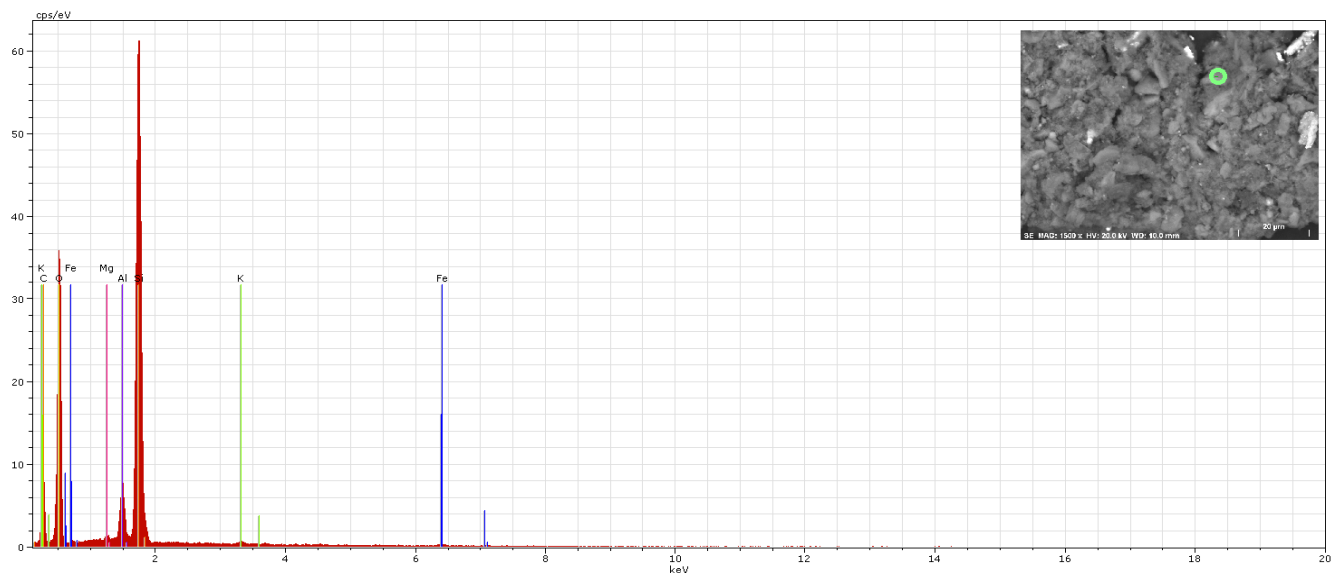
III.10.18: Da.S.2 (blue), point 2



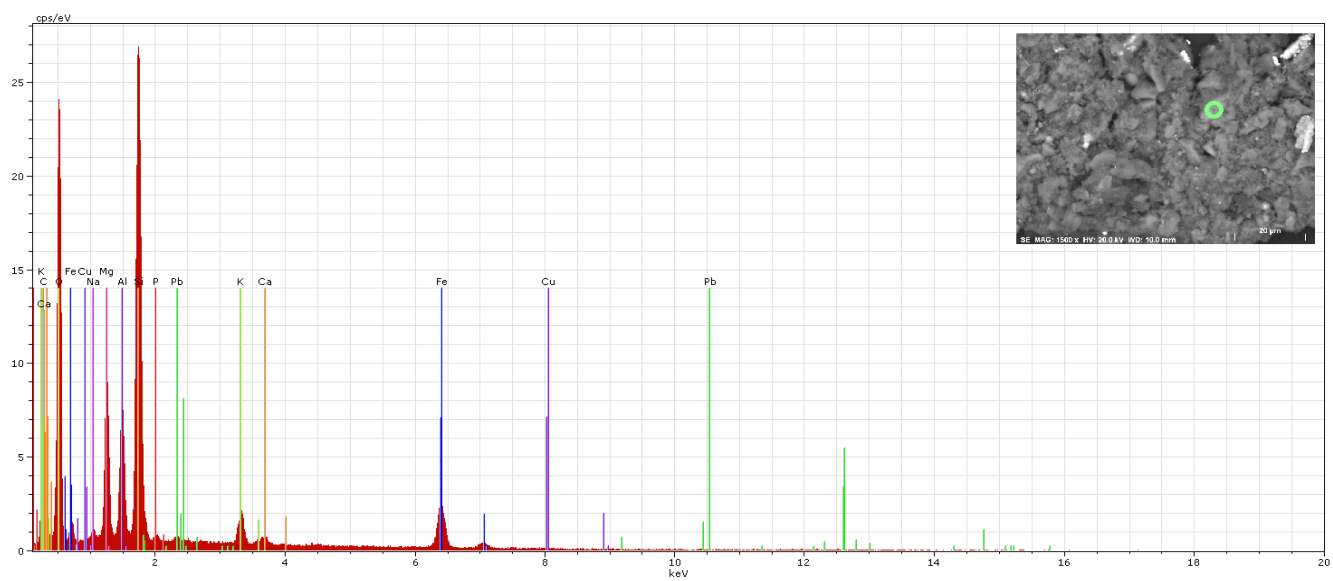
III.10.19: Da.S.2 (blue), point 3



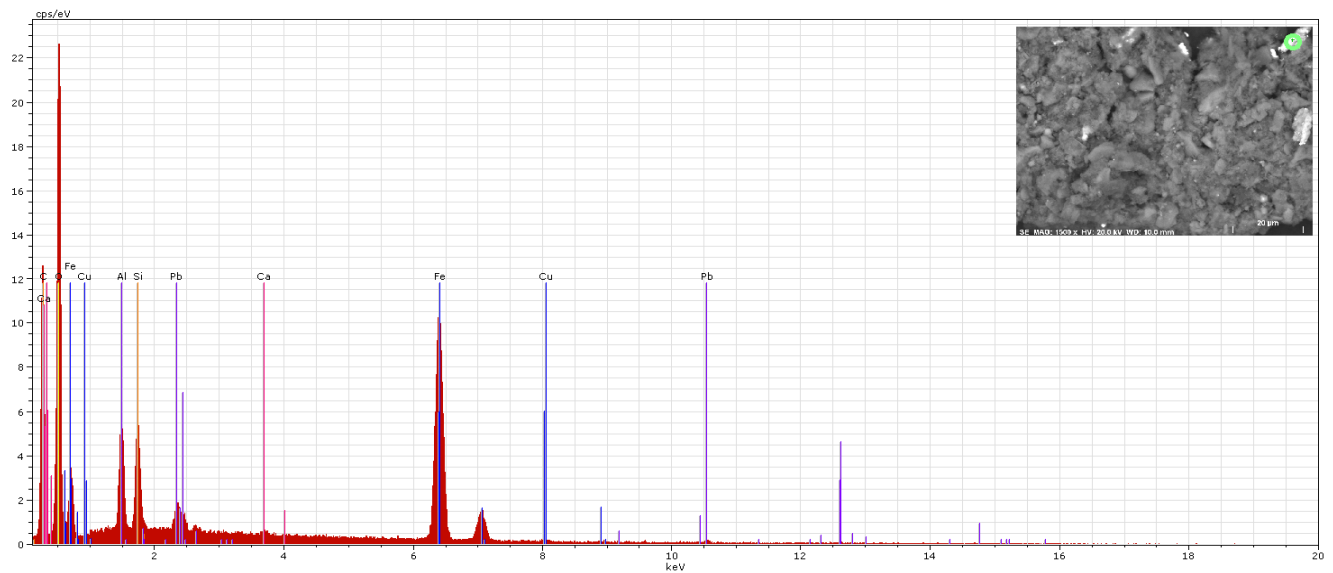
III.10.20: Da.S.2 (blue), point 4



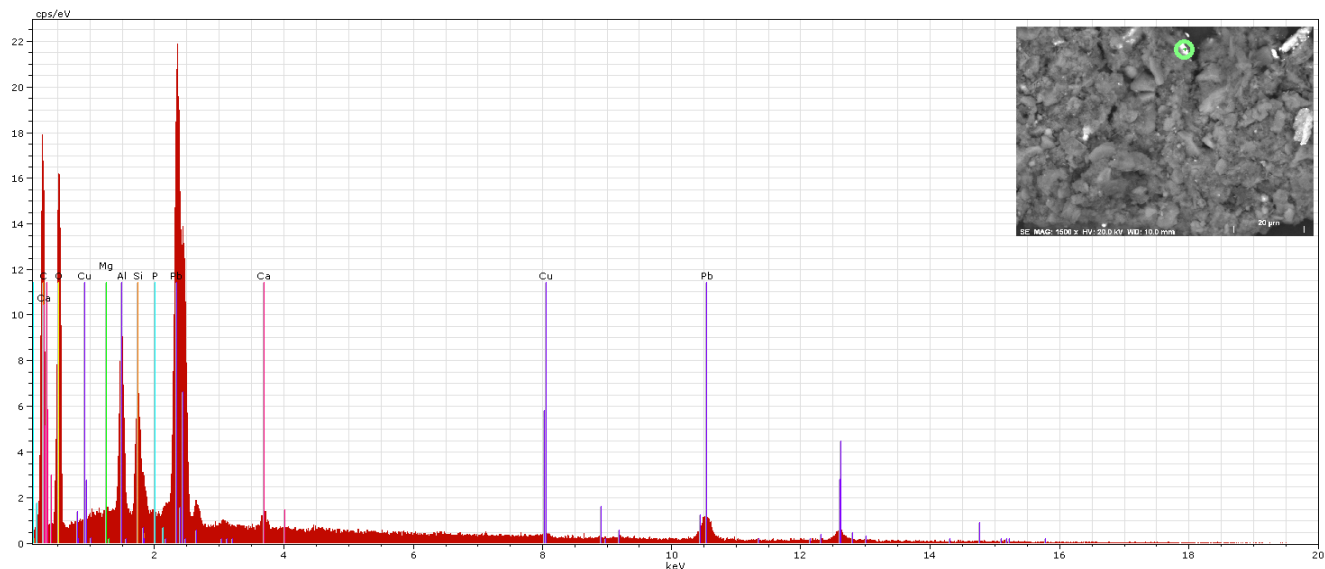
III.10.21: Da.S.2 (blue), point 5



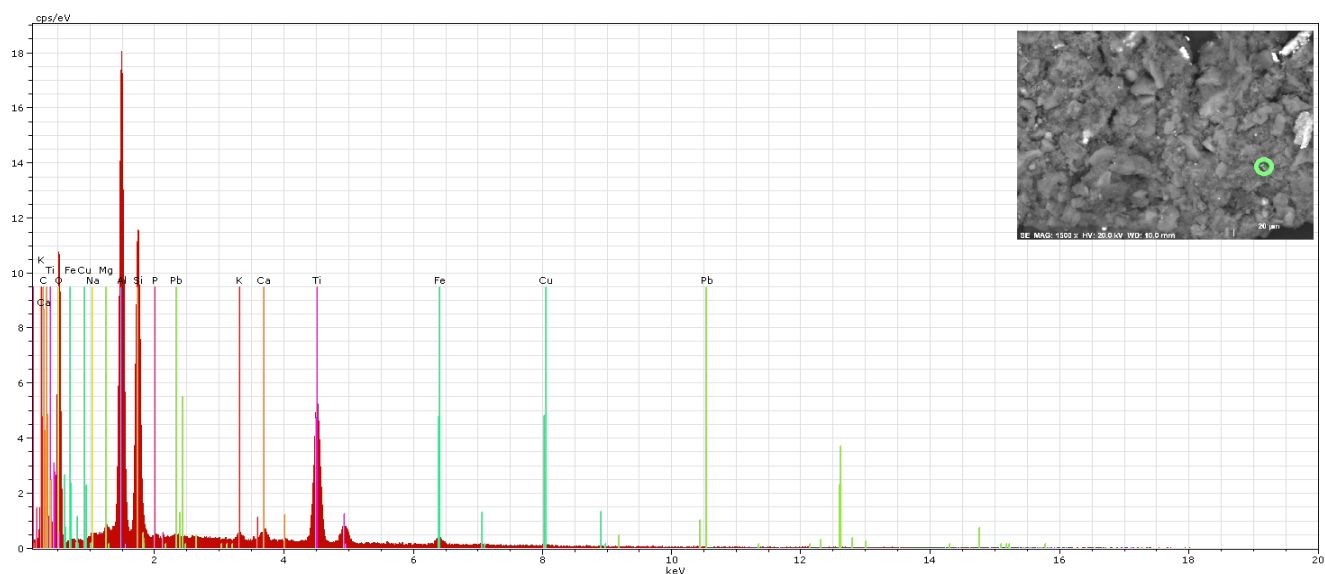
III.10.22: Da.S.2 (blue), point 6



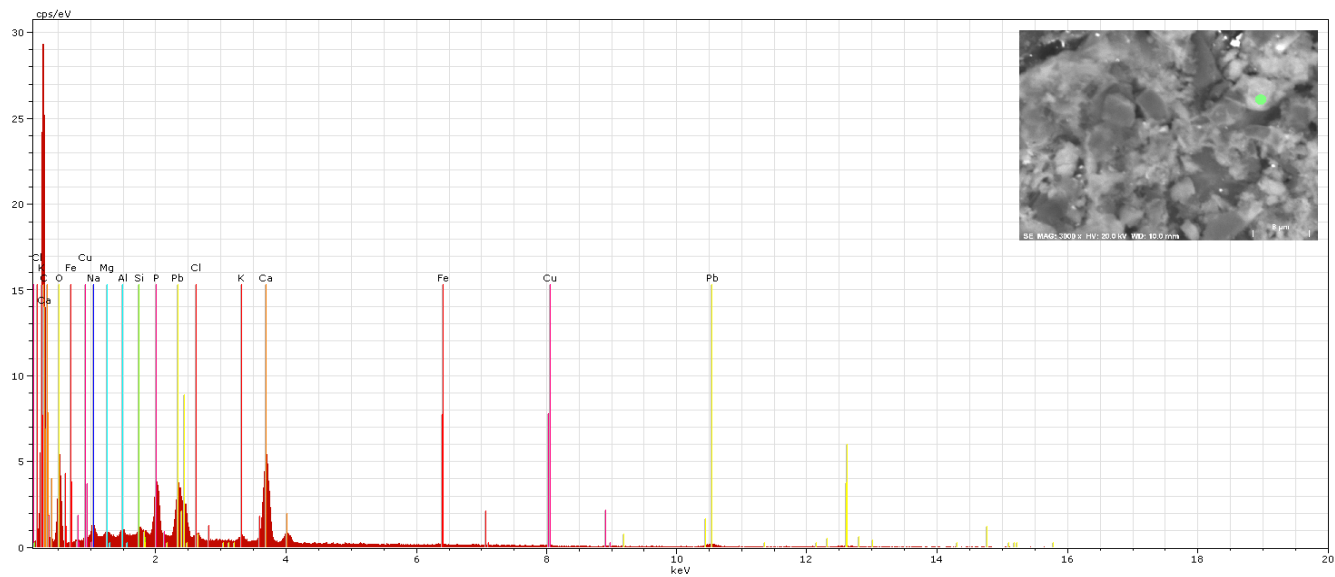
III.10.23: Da.S.2 (blue), point 7



III.10.24: Da.S.2 (blue), point 8

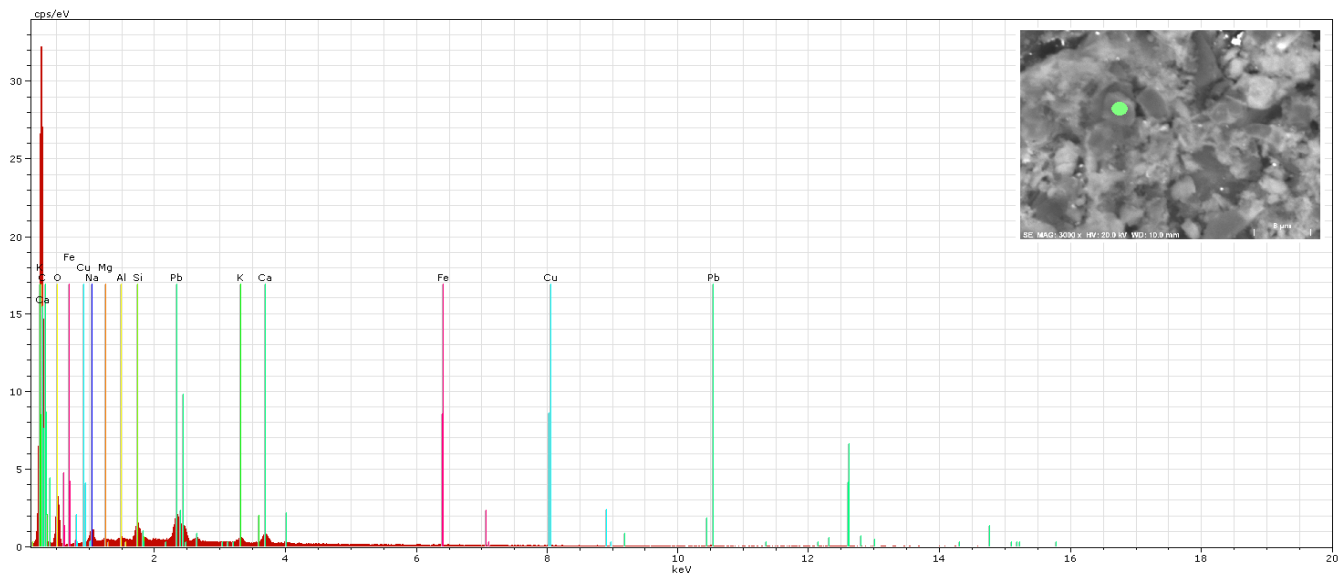


III.10.25: Co.S.4 (black), point 1

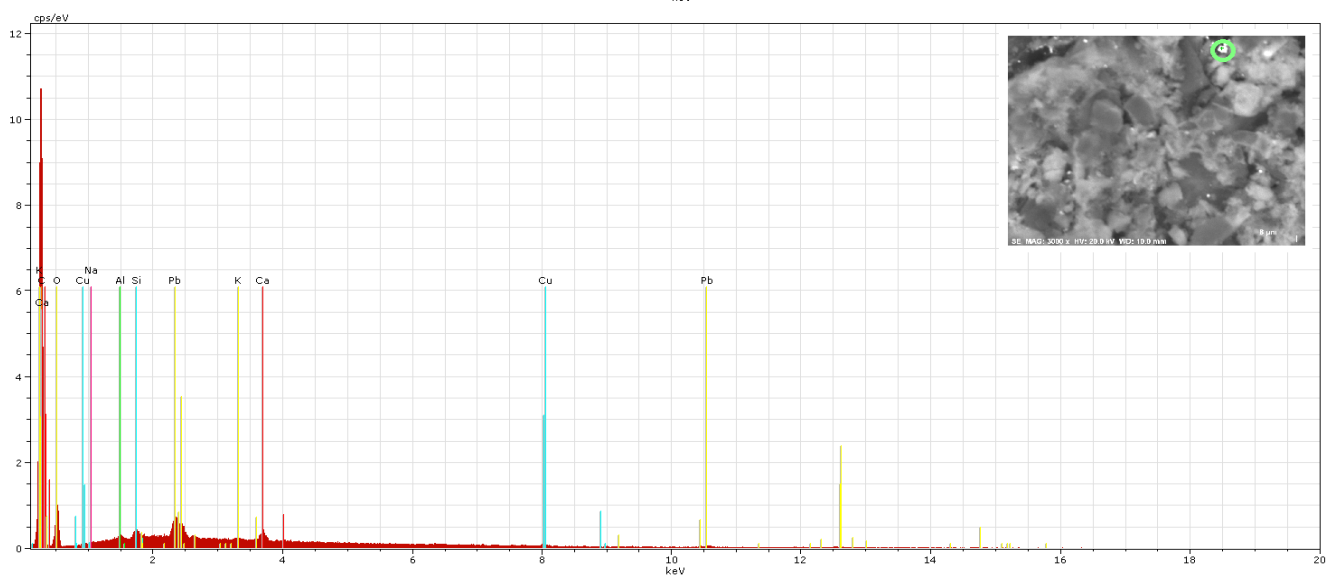




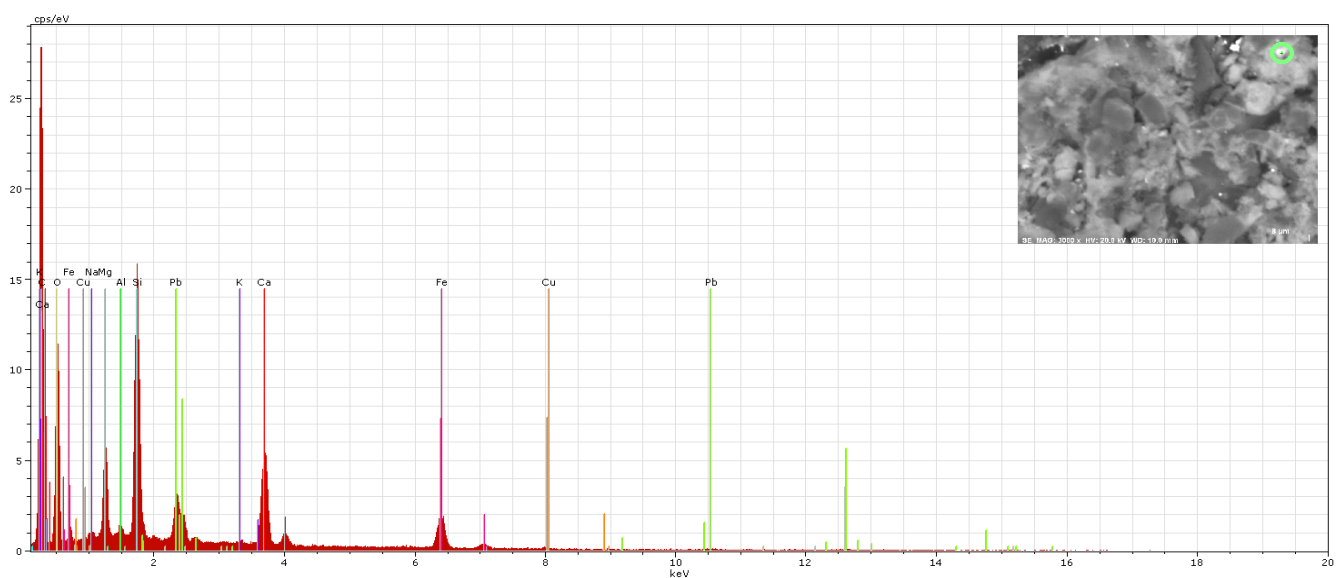
III.10.26: Co.S.4 (black), point 2



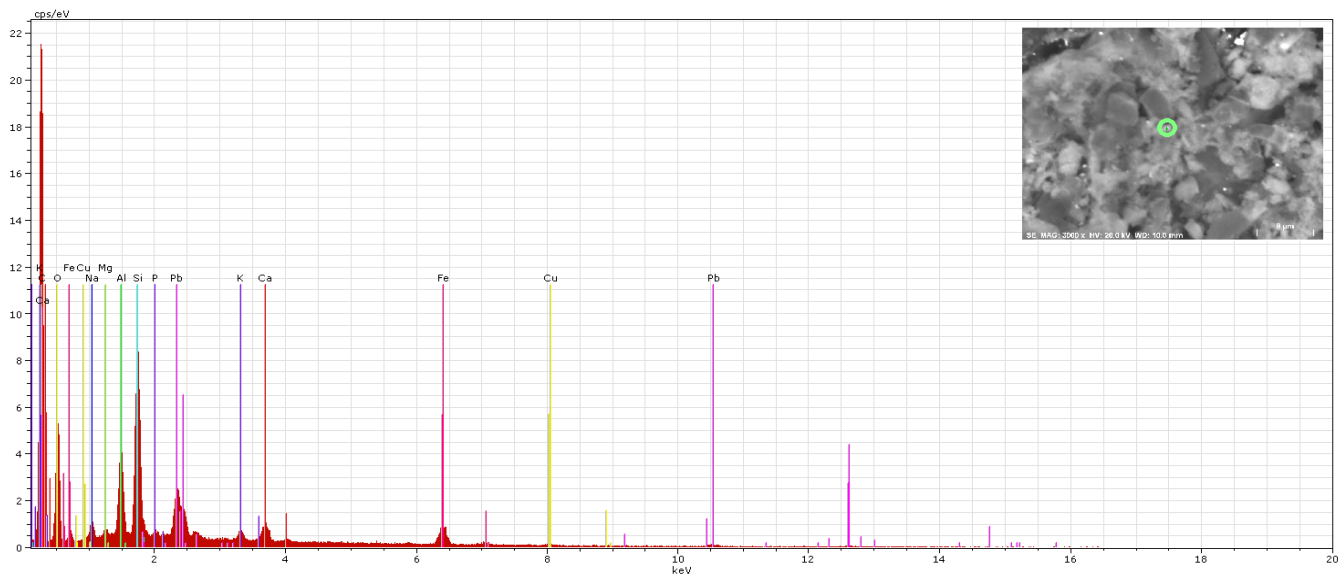
III.10.27: Co.S.4 (black), point 3



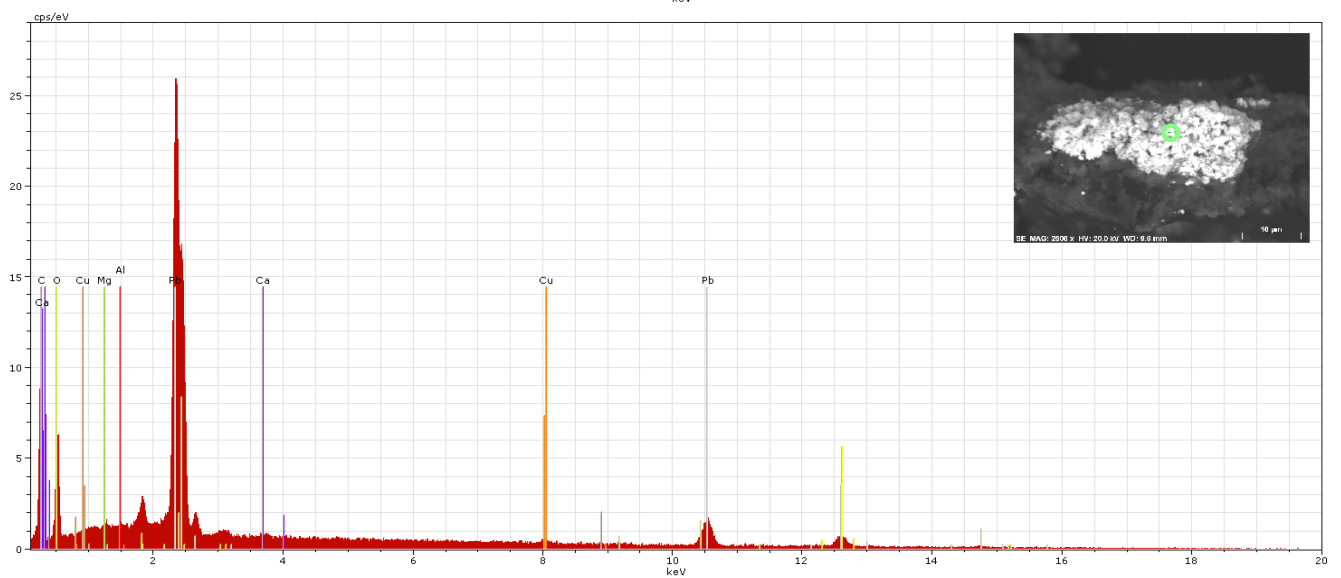
III.10.28: Co.S.4 (black), point 4



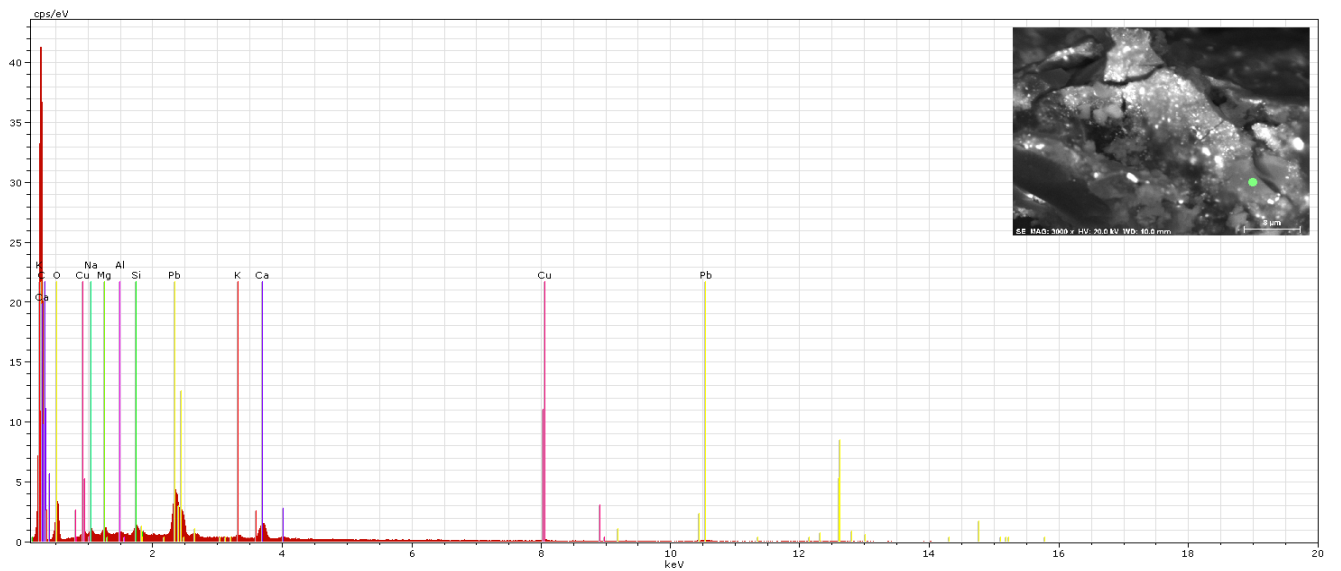
III.10.29: Co.S.4 (black), point 5



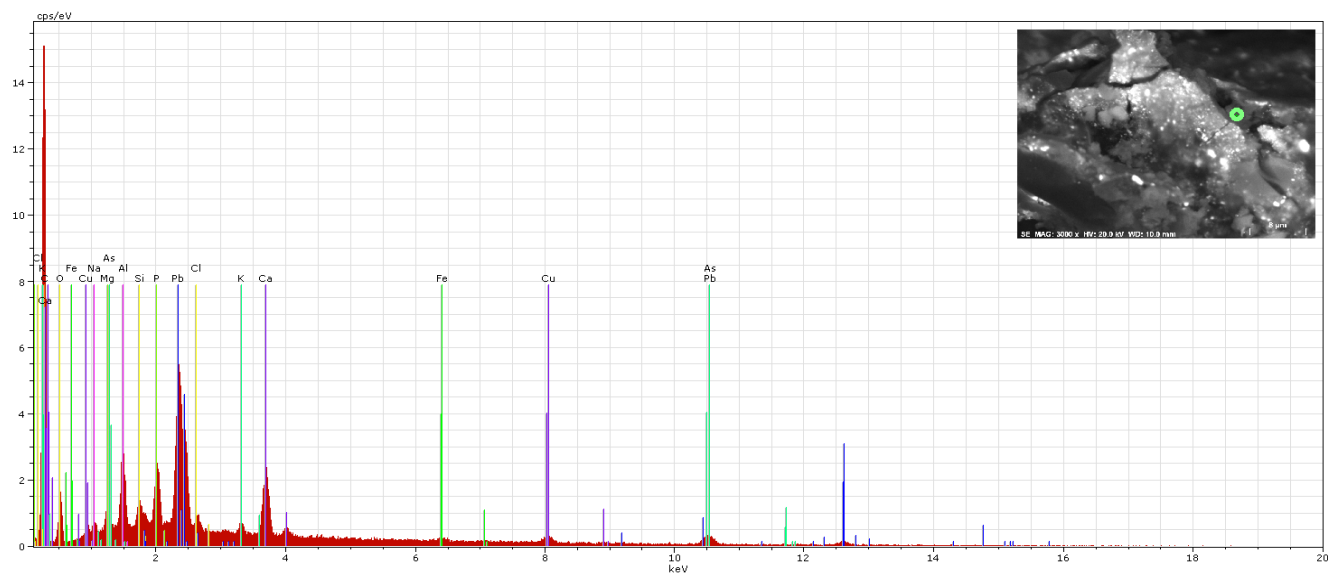
III.10.30: M.S.1 (black), point 1



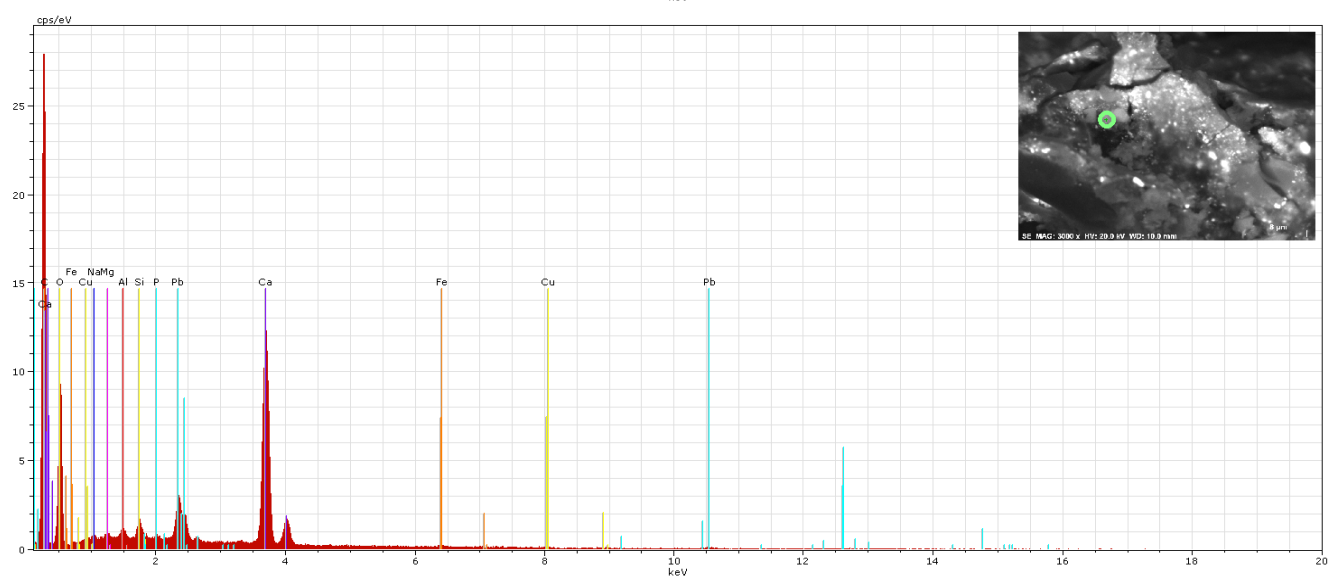
III.10.31: M.S.1 (black), point 2



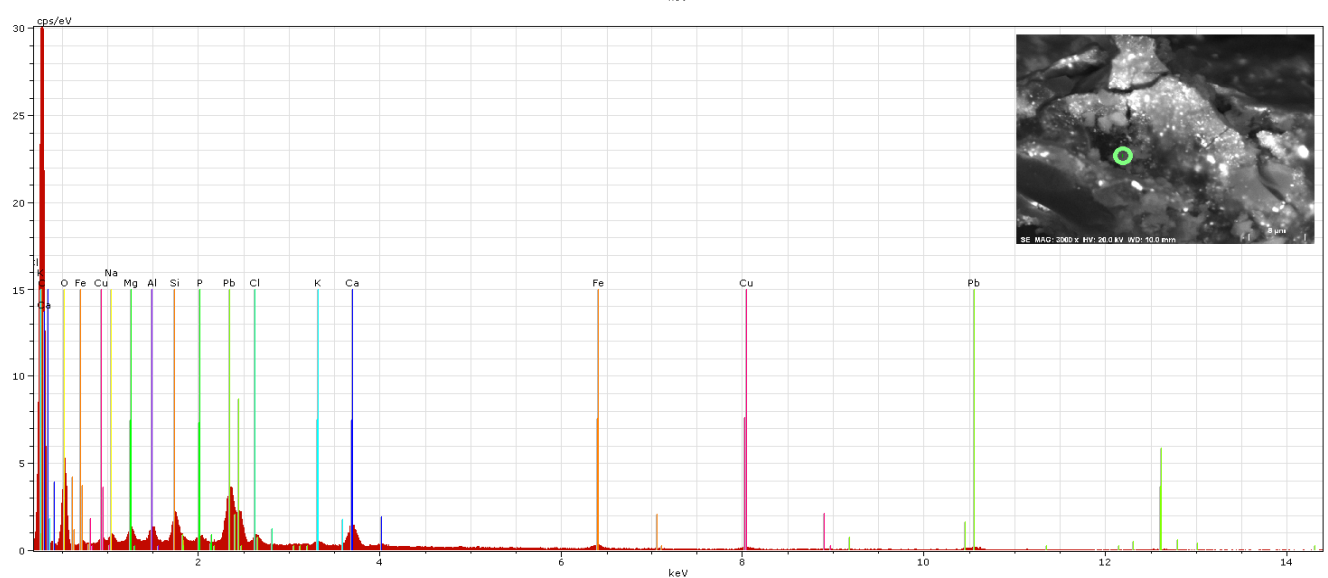
III.10.32: M.S.1 (black), point 3



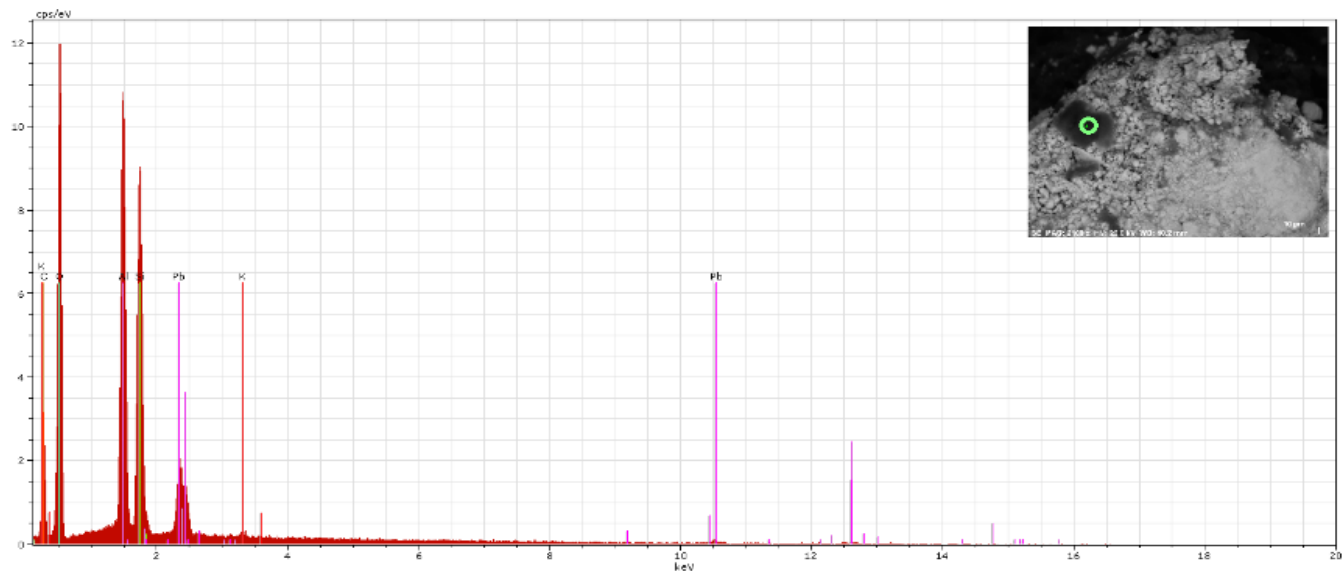
III.10.33: M.S.1 (black), point 4



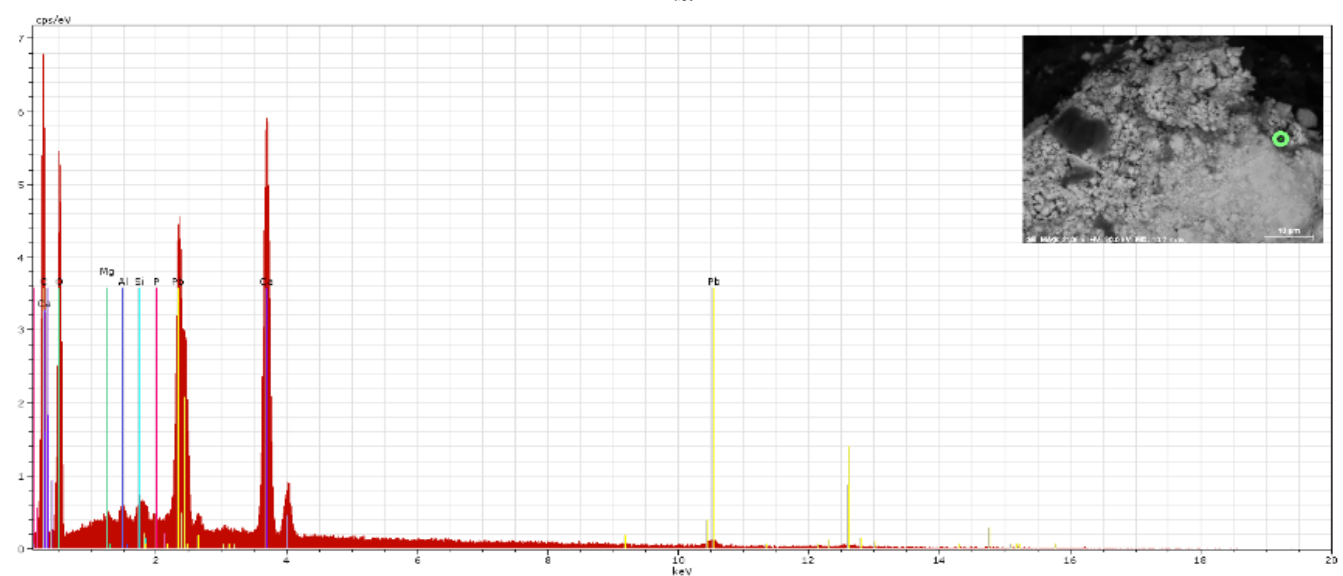
III.10.34: M.S.1 (black), point 5



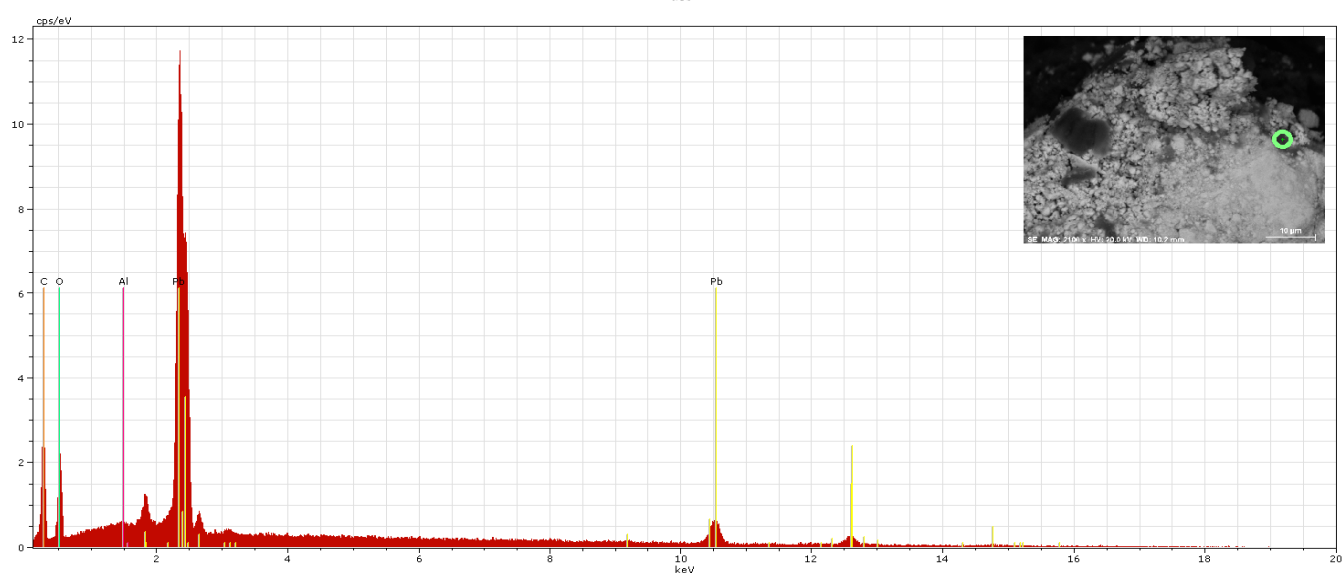
III.10.35: M.S.2 (white), point 1



III.10.36: M.S.2 (white), point 2

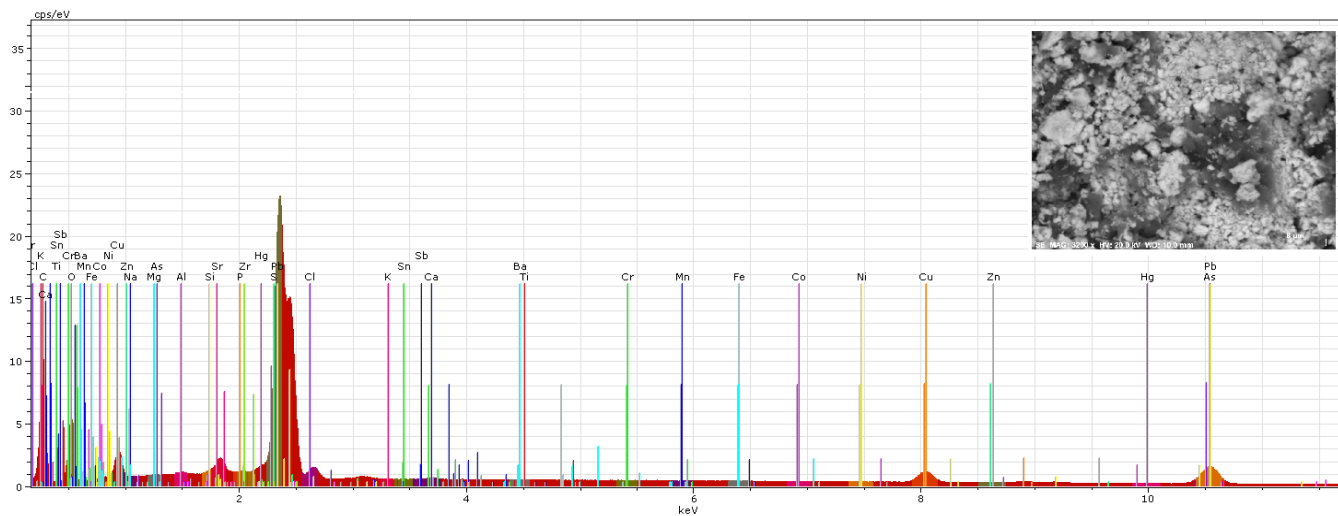


III.10.37: M.S.2 (white), point 3

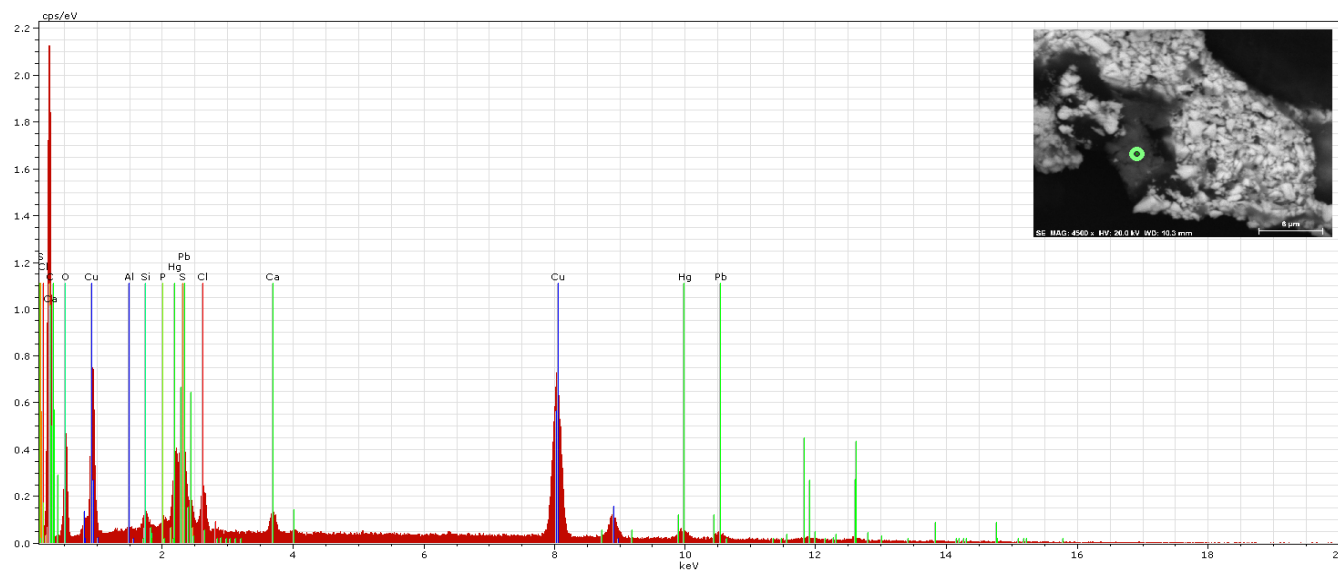




III.10.38: Di.S.2 (white), map



III.10.39: Da.S.3 (red), point 1



III.10.40: Da.S.3 (red), point 2

